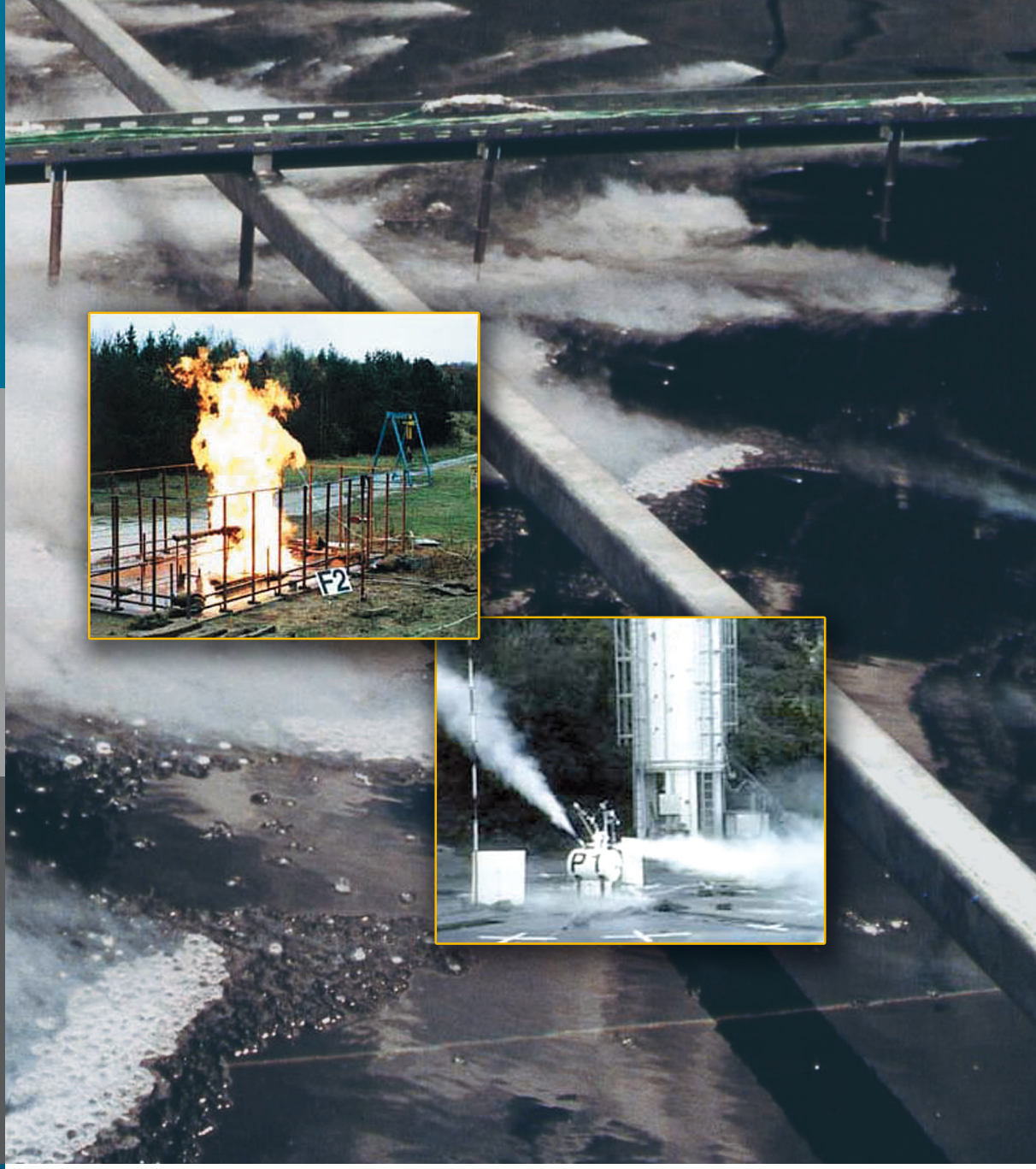

Safety Considerations on Liquid Hydrogen

Karl Verfondern

Mitglied der Helmholtz-Gemeinschaft

JÜLICH
FORSCHUNGSZENTRUM

TABLE OF CONTENTS

Schriften des Forschungszentrums Jülich
Reihe Energie & Umwelt / Energy & Environment Band / Volume 10

Forschungszentrum Jülich GmbH
Institut für Energieforschung (IEF)
Sicherheitsforschung und Reaktortechnik (IEF-6)

Safety Considerations on Liquid Hydrogen

Karl Verfondern

Schriften des Forschungszentrums Jülich
Reihe Energie & Umwelt / Energy & Environment Band / Volume 10

ISSN 1866-1793 ISBN 978-3-89336-530-2

Bibliographic information published by the Deutsche Nationalbibliothek.
The Deutsche Nationalbibliothek lists this publication in the Deutsche Nationalbibliografie; detailed bibliographic data are available in the Internet at http://dnb.d-nb.de.

Publisher and Distributor:	Forschungszentrum Jülich GmbH Zentralbibliothek, Verlag D-52425 Jülich phone:+49 2461 61-5368 · fax:+49 2461 61-6103 e-mail: zb-publikation@fz-juelich.de Internet: http://www.fz-juelich.de/zb
Cover Design:	Grafische Medien, Forschungszentrum Jülich GmbH
Printer:	Grafische Medien, Forschungszentrum Jülich GmbH
Copyright:	Forschungszentrum Jülich 2008

Schriften des Forschungszentrums Jülich
Reihe Energie & Umwelt / Energy & Environment Band / Volume 10

ISSN 1866-1793
ISBN 978-3-89336-530-2

The complete volume is freely available on the Internet on the Jülicher Open Access Server (JUWEL) at http://www.fz-juelich.de/zb/juwel

Abstract

The interest in hydrogen as a clean fuel and energy carrier of the future has grown in many countries and initiated comprehensive research, development, and demonstration activities with the main objective of the transition from a fossil towards a CO_2 emission lean energy structure as the ultimate goal. Reasons for these worldwide incentives towards a change of the energy structure are the obvious indications for a climate change from man-made greenhouse gas emissions, the steadily increasing world energy consumption connected with the finite nature of fossil resources, but also the need of reducing national dependencies on energy imports.

Hydrogen represents an energy carrier with high energy content and a clean, environmentally friendly source of energy to the end-user. The volume-related energy content of gaseous hydrogen, however, is comparatively small. For various applications of hydrogen where volume is an essential issue, it is necessary, e.g., to liquefy the hydrogen for the sake of volume reduction. But there are also other situations where the liquid state represents a reasonable and economic solution for storage and distribution of large amounts of hydrogen depending on the end-user's requirements. Furthermore liquid hydrogen has the advantage of extreme cleanliness making it, apart from its cooling ability, appropriate in many industrial applications. Major drawback is the enormous energy input required to liquefy the hydrogen gas, which has a significant impact on the economy of handling LH_2.

The experimental and theoretical investigation of the characteristics of liquid hydrogen, its favorable and unfavorable properties, as well as the lessons learnt from accidents have led to a set of codes, standards, regulations, and guidelines, which resulted in a high level of safety achieved today. This applies to both LH_2 production and the methods of mobile or stationary LH_2 storage and transportation/distribution, and its application in both science and industries.

The hazards associated with the presence and operation of LH_2 containing systems are subject of safety and risk assessments. Essential part of such accident sequence analyses is the simulation of the physical phenomena, which occur in connection with the inadvertent release of LH_2 into the environment by computation models. The behavior of cryogenic pool propagation and vaporization on either a liquid or a solid ground is principally well understood. Furthermore state-of-the-art computer models have been developed and validated against respective experimental data. There are, however, still open questions which require further efforts to extent the still poor experimental data basis. These efforts should include the examination of the pool propagation from large spills of LH_2, the vaporization on different grounds, and pool fire, but also the atmospheric dispersion behavior of cold vapor clouds evolving from the vaporization of the cryogenic liquid.

Kurzfassung

Weltweit ist das Interesse an Wasserstoff als einem umweltfreundlichen Brennstoff und möglichen Energieträger der Zukunft gestiegen und hat umfassende Forschungs- und Entwicklungsarbeiten ausgelöst. Ziel ist es dabei, den Übergang von einer fossil-gesteuerten hin zu einer weitgehend CO_2-emissionsfreien Energiestruktur zu fördern. Auslöser für diese Anstrengungen sind die offensichtlichen Anzeichen eines Klimawandels infolge erhöhten Ausstoßes von Treibhausgasen, der weltweit stetig wachsende Verbrauch an Energie verbunden mit den allmählich zu Neige gehenden Vorräten an fossilen Energievorräten, aber ebenso die Notwendigkeit vieler Staaten, ihre nationale Abhängigkeit von Energieimporten zu mildern.

Wasserstoff ist ein attraktiver Energieträger mit hohem masse-bezogenen Energiegehalt und stellt eine für den Endverbraucher umweltverträgliche Energiequelle dar. Der volumen-bezogene Energieinhalt gasförmigen Wasserstoffs jedoch ist vergleichsweise gering. Viele Anwendungen, in denen das Volumen eine wichtige Rolle spielt, erfordern daher eine Verflüssigung des Wasserstoffgases aus Gründen der Platzersparnis. Ferner ist Speicherung und Transport von Wasserstoff in flüssiger Form je nach Anforderungen des Verbrauchers oft die wirtschaftlich günstigere Alternative. Zudem besitzt flüssiger Wasserstoff einen extrem hohen Reinheitsgrad, der ebenso wie sein Gebrauch als Kühlmittel in zahlreichen industriellen Anwendungen zum Einsatz kommt. Ein großer Nachteil ist hingegen der enorm hohe Energieaufwand, der für die Verflüssigung erforderlich ist und die Wirtschaftlichkeit der Nutzung flüssigen Wasserstoffs stark beeinträchtigt.

Die experimentelle und theoretische Untersuchung der sicherheitstechnischen Eigenschaften von flüssigem Wasserstoff einerseits sowie die aus Unfällen gewonnenen Erfahrungen andererseits, haben zu einer umfassenden Reihe von Gesetzen, Richtlinien und Regeln geführt, die für einen hohen Sicherheitsstandard beim Umgang mit flüssigem Wasserstoff sorgen. Dies betrifft sowohl die großtechnische Produktion, die Speicherung und den Transport im großen Maßstab, als auch die zahlreichen Anwendungen in Wissenschaft und Industrie.

Die potenziellen Gefahren beim Umgang mit flüssigem Wasserstoff sind Gegenstand von Sicherheits- und Risikostudien. Einen wesentlichen Bestandteil solcher Analysen von Unfallszenarien bildet dabei die Simulation physikalischer Phänomene durch Rechenmodelle, die bei ungeplanter Freisetzung von flüssigem Wasserstoff auftreten. Das Verhalten einer kryogenen Lache bei der Ausbreitung und Verdampfung auf festem oder flüssigem Untergrund ist vom Prinzip her gut verstanden. Entsprechend konnten Rechenmodelle nach dem neuesten Kenntnisstand entwickelt und getestet werden. Allerdings bleiben noch zahlreiche offene Fragen zu klären, die weitere Untersuchungen erfordern hinsichtlich der Ausbreitung und Verdampfung von Lachen großer Mengen an flüssigem Wasserstoff auf verschiedenen Untergründen und deren Verbrennungsverhalten, aber auch der atmosphärischen Ausbreitung aus der Verdampfung tiefkalt verflüssigter Liquide entstandener kalter Gaswolken.

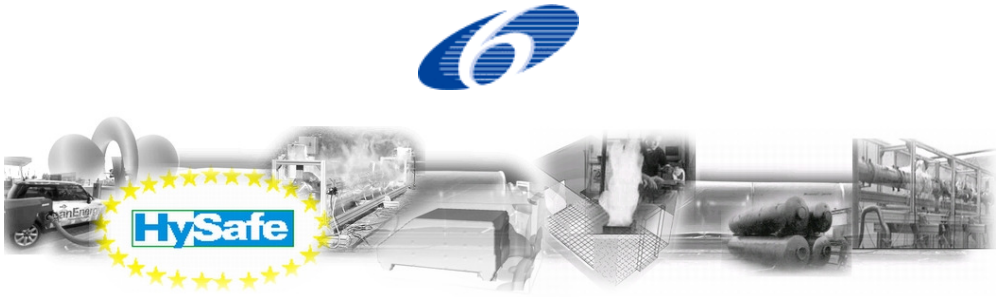

HYSAFE – Network of Excellence

This report is the extended version of a contribution to the

2nd European Summer School on Hydrogen Safety,
held at the University of Ulster (UU) in Belfast, July 31 - August 7, 2007

as a part of the European Union Network of Excellence HYSAFE
"Safety of Hydrogen as an Energy Carrier"
(Contract No SES6-CT-2004-502630).

1. INTRODUCTION

Despite energy saving efforts and improved efficiency of energy production, projections of the World Energy Council [WEC 2007] indicate a significant increase in global energy demand doubling today's level of energy supply at least by 2050 due to a further growing world population and rising prosperity. On the other hand, continuation of the extended use of the fossil natural resources, which presently amount to 80 % in the world's energy consumption, carries the danger of over-stressing the environment. In addition, strongly fluctuating energy prices, the dependence of many countries on energy imports from politically unstable regions, and the uncertainty about how long oil and gas reserves will last, are raising fears concerning the energy supply security. This all urgently calls for political and technological counteractions. The UN Climate Council (IPCC) demands that greenhouse gas emissions must be curbed latest by 2020 and reduced to 50 % of the 1990 level by 2050. "Business as usual" is no model for the future, a transformation of the world's energy economy is demanded.

The interest in hydrogen as a clean fuel and energy carrier of the future has grown in many countries and initiated comprehensive research, development, and demonstration activities. As a matter of fact, a major hydrogen economy exists already today. Significant amounts of hydrogen are currently used as a raw material in the fertilizer and steel industries as well as in the chemical and petrochemical industries, where the available crude stocks are becoming progressively heavier and the hydrogen is needed for the refining of the petroleum products. Total demand for hydrogen corresponds to about 2 % of the world's primary energy consumption, and this is anticipated to further increase. The European Commission High Level Group estimates growth rates of 4 - 10 % per year until, after 2025, a decrease in these areas could coincide with the market introduction of new hydrogen applications such as in the transportation sector or as a distributed electrical energy source through the use of fuel cells [EC 2003].

Hydrogen represents an energy carrier with high energy content and a clean, environmentally benign source of energy to the end-user. The volume-related energy content of NTP (normal temperature and pressure: 293 K, 101,325 Pa) hydrogen gas (GH_2) is low with 2.78 kWh/m^3 (based on the Higher Heating Value), whereas the mass-related content is with 39.3 kWh/kg comparatively high. For various applications of hydrogen where volume is an essential issue, it is necessary to liquefy the hydrogen for the sake of volume reduction. A well known example is the use of liquid hydrogen (LH_2) as fuel in space and long-range supersonic aviation considered ideal because of its high energy-to-weight ratio, its high heating value and its good cooling capacity compared to other fluids. But there are also other situations where the liquid state represents a reasonable and economic solution for storage and distribution of large amounts of hydrogen. Furthermore liquid hydrogen has the advantage of extreme cleanliness making it appropriate in many industrial applications. Major drawback is the enormous energy input required to liquefy the hydrogen gas, which has a significant impact on the economy of handling LH_2.

Still back in the 1950s, liquid hydrogen or "SF-1", as it was code-named at that time, was considered by many experts an "impractical fluid and only a laboratory curiosity" [Sloop 1978], because it was so dangerous to store and handle and connected with high cost and low availability. But the increasing interest for using LH_2 as a fuel for rocket or jet engines also raised the demand for larger quantities. The first major safety issue recognized was that LH_2 is a powerful fuel that must be handled carefully to minimize the risk of explosion. This

image of an exotic and extremely dangerous matter, however, changed with the accumulation of experience in its safe handling and with widening the application range of liquid hydrogen beyond space industries representing today a well established technology on a large scale.

The application of hydrogen as a fuel at a larger scale is anticipated in transportation sector. Markets with high priority would be public transportation with city buses or companies operating large car fleets with the advantages of permanent operation, centralized refuelling systems and, last but not least, a significant reduction of local emissions of pollutants. Present fuel storage concepts for hydrogen-driven vehicles include both the high-pressure gaseous storage and the cryogenic liquid storage, which requires an appropriate infrastructure including refueling devices for both modes.

From the beginning, people were aware of the hazardous potential of LH_2, and its handling was accompanied by safety measures in compliance with a permanently reviewed and updated set of national and international codes, standards, and regulations. This has to be particularly looked at if considering the gradual penetration of the every day's life, e.g., by having hydrogen refueling stations or repair shops incorporated into a "conventional" neighborhood or having more and more people dealing as not explicitely trained personnel with hydrogen.

Prerequisite of the implementation of systems containing large amounts of hydrogen (or other hazardous materials) is a thorough evaluation of their safety and risk to the people and environment. With regard to accident scenarios where liquid hydrogen is involved, the precise simulation of the initial phase, i.e., the release from the LH_2 containing system, plays an important role as it has a strong influence on the further accident sequence. Conditions and configuration of the source determine the features of the evolving vapor cloud such as cloud composition and dimension changing with time, or energy balance, which again significantly determine the consequences following the potential ignition and explosion of the flammable vapor cloud.

Such safety and risk analyses are typically characterized by methods to identify initiating events for conceivable accident scenarios, to construct and classify event sequences. For events dominating the risk, deterministic methods are applied to simulate the physical phenomena during an accident sequence by applying state-of-the-art calculation models, and to assess quantitatively the risk and the consequences on health and environment. The development of computer models allowing predictive calculations goes hand in hand with their verification and validation against experiments.

2. PROPERTIES OF LIQUID HYDROGEN

2.1. Physical and Chemical Characteristics

2.1.1. Physical Properties

Hydrogen is the lightest and most abundant element in the universe (ranking #10 on Earth). At standard temperature and pressure conditions, hydrogen is a colorless, odorless, tasteless, non-toxic, non-acid, non-metallic diatomic gas, which is in principle physiologically not dangerous. The energy density of hydrogen is very high; 1 kg of hydrogen contains approximately 2.5 times more energy than 1 kg of natural gas. One of the most important characteristics is its low density which makes it necessary for any practical applications to either compress the hydrogen or liquefy it.

Hydrogen can be considered an ideal gas over a wide range of (not too low) temperatures and (not too high, up to 10 MPa) pressures. At some point, however, like any other substance that is sufficiently cooled or compressed, hydrogen will act like a real gas. This behavior when departing from an ideal gas can be described, e.g., by the Redlich-Kwong-Soave equation [Wikipedia 2007]:

$$p = \frac{RT}{V_m - b} - \frac{a\alpha}{V_m(V_m + b)} \tag{2-1}$$

with $a = 0.42747\frac{R^2 T_c^2}{p_c}$ and $b = 0.08664\frac{RT_c}{p_c}$

and for hydrogen: $\alpha = \alpha(T_r) = 1.202 \exp\{-0.30288 T_r\}$ with $T_r = \frac{T}{T_c}$

where p – pressure, Pa; T – temperature, K; V_m – molar volume, m^3/mol; R – universal gas constant, = 8.3145 J/(mol K); T_r – reduced temperature; T_c – critical temperature, = 33.25 K; p_c – critical pressure, = 1.297 MPa.

Hydrogen gas is highly diffusive and highly buoyant. It is lighter than air above a temperature of 22 K, i.e., over (almost) the whole temperature range of its gaseous state at atmospheric pressure. Due to its high diffusivity, it rapidly mixes with the ambient air upon release. The diffusion velocity is proportional to the diffusion coefficient and varies with temperature according to T^n with n in the range of 1.72 - 1.8. Because of its small molecular weight and its low viscosity, hydrogen can cause a problem with respect to the propensity of the gas to leak. Diffusion in small amounts is even possible through intact materials, in particular organic materials. Leakage rates are by a factor of 50 higher compared to water and by a factor of 10 compared to nitrogen. Unlike invisible "normal" gaseous leakages, the release of liquid hydrogen (LH_2) or gaseous hydrogen at cryogenic temperature will usually produce a visible water vapor fog. The addition of an odorant or colorant would ease the detection of small leaks; however, this is not feasible in most situations due to freezing-out of the substances added.

When handling LH_2 in confined areas, a hazard is given by the fact that due to the volume increase by a factor of 845, when LH_2 is heated up from its boiling point (20.369 K) to ambient conditions, the composition of the local atmosphere may change drastically. In a

completely filled enclosed space, final pressure after warm-up to 300 K may rise to 172 MPa which certainly overpressurizes systems to bursting [Edeskuty 1996].

A further temperature decrease below the boiling point eventually results in the generation of solid hydrogen. Mixtures of coexisting liquid and solid hydrogen or slush hydrogen (SLH_2) offer the advantages of a higher density by up to 16 %, a higher heat capacity by up to 18 %, and a prolongation of the storage time of the cryogen as the solid melts and absorbs heat. There it is of particular interest to use slush as a rocket fuel in space missions. Due to the fact that the hydrogen vapor pressure is strongly reduced with decreasing temperatures, from 98 kPa (which is about atmospheric pressure) at 20 K down to 13 kPa at 13 K, SLH_2 systems must be designed to safely operate far below atmospheric pressure. A safety risk is arising from such a low pressure demanding protection against air ingress into the system.

The triple point of hydrogen is the temperature (13.8 K) and pressure (7.2 kPa), at which all three phases can exist in equilibrium (Fig. 2-1). The boiling point increases with pressure to the critical point which is given by T_c = 33.15 K, p_c = 1.296 MPa with a critical density of γ_c = 31.4 kg/m³. A pressure increase beyond the critical point has no further influence.

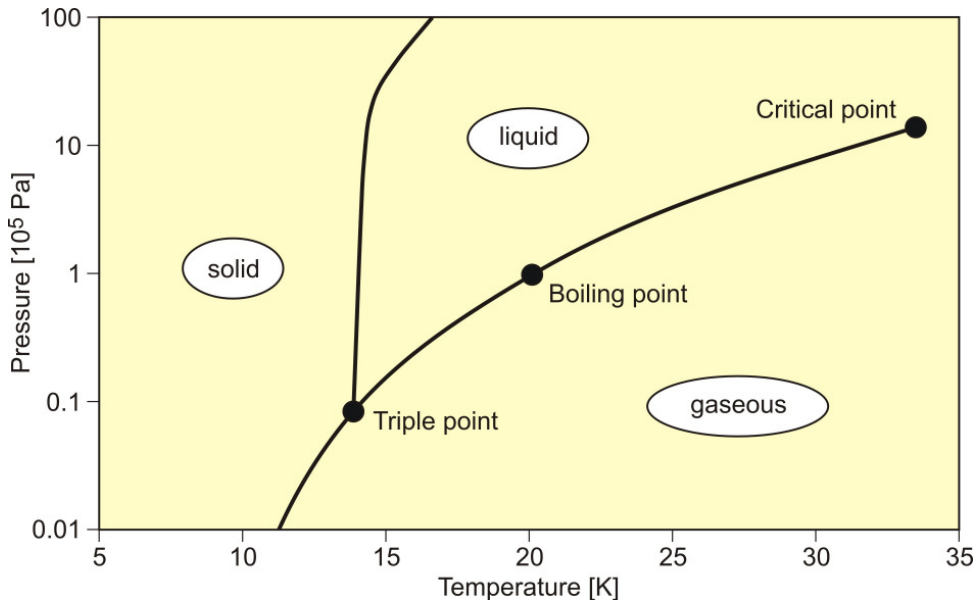

Figure 2-1. Phase diagram of hydrogen

There is no liquid phase of hydrogen existing above its critical temperature. If a fluid is heated and maintained above its critical temperature, it becomes impossible to liquefy it with pressure. When pressure is applied, a single phase "supercritical fluid" forms which is characterized by T_c and p_c.

“Supercritical” generally refers to conditions above the critical temperature and close to the critical pressure. It has characteristics similar to a gas and a liquid without changing its chemical structure. It is gas-like in that it is compressible and easily diffuses through materials; it is liquid-like in that it has a comparable density and may dissolve materials. And there are some transition states in between characterized by strong structural fluctuations causing the unusual behavior of fluids near the critical point covering all scales from microscopic to macroscopic.

Due to the strong dependence on temperature and pressure in the supercritical state, the thermo-physical properties of cryogenic hydrogen vary strongly especially in the near-critical region. By proper control of pressure and temperature, one can access a significant range of physico-chemical properties, i.e., density, viscosity, diffusivity, without passing through a phase boundary. The specific heat capacity has a maximum at the temperature called the pseudo-critical temperature. Also the isothermal compressibility is particularly large just above the critical temperature; at the critical point, it tends to infinity. For a highly compressible fluid, a small temperature gradient implies a large density gradient. It exhibits higher flow rates as compared with liquids. An important factor may be that the coolant might undergo a turbulent-to-laminar transition due to the dependence of viscosity on temperature. Heat transfer coefficients are unpredictable in the transition regime, and are much lower in the laminar regime. Thermodynamic data can be obtained from the chemistry database of the National Institute of Standards and Technology [NIST 2005].

Hydrogen at extreme, but accessible pressures (2 - $3*10^5$ MPa) and temperatures (~4400 K) will make a phase transition to (liquid) metallic hydrogen which may be superconducting at room temperature. This effect predicted in 1935 was eventually proven in a shock compression test in 1996 [Nellis 1996]. Metallic hydrogen is said to exist in the interior of the planets Saturn and Jupiter, but has no practical application on Earth so far.

Hydrogen coexists in two isomeric forms, ortho and para hydrogen. A small energetic difference is given, if the spins of the two protons of a hydrogen molecule are either aligned parallel (ortho) or anti-parallel (para). The existence of the two forms was proven experimentally in 1929 by K. F. Bonhoeffer and P. Harteck using charcoal as catalyst for the separation. The partition is dependent on the temperature. Normal hydrogen at room temperature is a mixture of 75 % ortho and 25 % para hydrogen. In the lower temperature range < 80 K, para hydrogen is the more stable form. At 20 K, in thermal equilibrium, the concentrations are 99.825 % para and 0.175 % ortho. The rate of conversion between ortho and para states is with 0.0114 h^{-1} slow in the gas phase. The proton spin state has to flip from 1 to 0, which is intrinsically triggered by the collision between two ortho molecules. The non-catalyzed transition takes place over a longer period (about 3 - 4 days), until a new equilibrium state is reached. However, magnetic impurities and also small oxygen concentrations are able to accelerate ortho-para conversions raising the rate by several orders of magnitude (very good: $Fe(OH)_3$) to the order of hours. The conversion from ortho to para is an exothermal reaction with a conversion energy of 270 kJ/kg at room temperature which increases with decreasing temperature. At temperatures below 77 K, it is almost constant at 523 kJ/kg. The liberated heat of ortho-para conversion is larger than the latent heat of vaporization/condensation (446 kJ/kg at the same temperature), which means that normal liquid hydrogen is able to vaporize completely even in a perfectly insulated vessel. It therefore represents a safety issue requiring a design of the LH_2 containing systems to be able to remove the heat of conversion in a safe manner.

For any given pressure, a real gas has an inversion temperature T_I. The so-called Thomson-Joule effect arising from the forces between the gas molecules means that the temperature of a real gas decreases ($T < T_I$) or increases ($T > T_I$) upon expansion (depressurization) at constant enthalpy. It is "internal work" against the van der Waals forces acting among the molecules, which is used to cool or heat the gas.

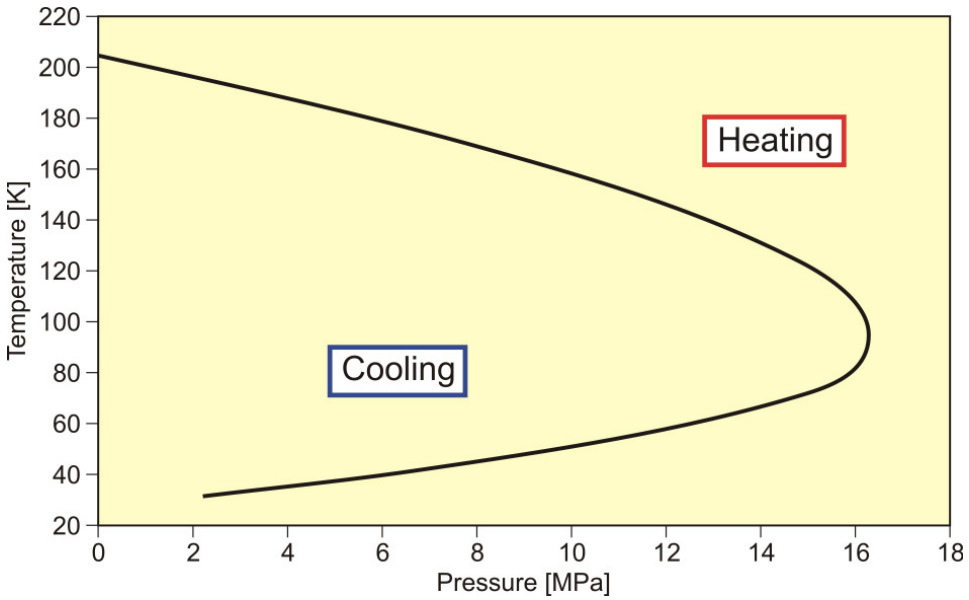

Figure 2-2. Inversion temperature of hydrogen

The Thomson-Joule coefficient at constant enthalpy

$$\mu_{TJ} = \left(\frac{dT}{dp}\right)_H \tag{2-2}$$

is negative, if the temperature is decreasing, and positive for an increasing temperature. It is zero for an ideal gas. All locations where there is no temperature change are forming the so-called inversion curve (Fig. 2-2). Unlike most other gases, the inversion temperature of H_2 gas is with 193 K at atmospheric pressure much lower than ambient temperature. A safety concern is that the sudden depressurization of a GH_2 storage vessel may lead to an ignition. For example, the temperature increase is 6 K, if a sudden pressure drop from 20 MPa to ambient pressure takes place. The chance of a spontaneous ignition just by that effect, however, is small. An explosion is more likely to occur because of electrostatic charging of dust particles during the depressurization or auto-ignition at high temperatures or other mechanisms such as spark discharges from isolated conductors, brush discharges, corona discharges [Astbury 2005].

Hydrogen is both in the gaseous and liquid phase essentially an insulator. Only above some critical "breakdown" voltage (~300 V), where ionization occurs, it becomes an electrical conductor.

2.1.2. Chemical Properties

Hydrogen is able to react chemically with most other elements. In connection with oxygen, hydrogen is highly flammable over a wide range of concentrations. It burns in a non-luminous hot flame to water vapor liberating the chemically bound energy as heat (gross heat of combustion: 286 kJ/mol). A stoichiometric hydrogen-air mixture contains 29.5 vol% of hydrogen. The flammability range is between 4 and 75 vol% of concentration in air and up to 95 vol% in oxygen and widens with increasing temperatures. The lower flammability limit (LFL) as the minimum amount of fuel that supports combustion, is usually the more important limit for low-rate releases, since it will be reached first in a continuous leakage. The influence of the temperature is expressed in the modified Burgess-Wheeler equation for the LFL, which is for hydrogen (at ambient pressure) [Zabetakis 1967]:

$$c_{LFL} = c_{LFL}(300\,K) - \frac{3.14}{\Delta H_c}(T - 300) = 4.0 - 0.013\,(T - 300) \quad [vol\,\%] \tag{2-3}$$

where ΔH_c – net heat of combustion, = 242 kJ/mol; T – temperature, K.

For just vaporized hydrogen at the boiling point, the LFL is 7.7 %. The respective equation for the upper flammability limit (UFL) is [Eichert 1992]:

$$c_{UFL} = 74.0 + 0.026\,(T - 300) \quad [vol\,\%] \tag{2-4}$$

valid for the temperature range 150 - 300 K.

The auto-ignition temperature of 858 K is relatively high, but can be lowered by catalytic surfaces. The minimum ignition energy at stoichiometric mixture is with 0.02 mJ very low, much lower than for hydrocarbon-air mixtures. A weak spark or the electrostatic discharge by a human body, which is in the range of 10 mJ, would suffice for an ignition; this is, however, no different from other burnable gases. The minimum ignition energy is even further decreasing with increasing temperature, pressure, or oxygen contents.

The thermal radiation emitted from hydrogen combustion in narrow infra-red bands essentially originates from the water vapor within the hydrogen flame. The emissivity factor of water vapor, however, is comparatively low ($\varepsilon < 0.1$). Therefore, despite its potentially high flame temperature (adiabatic temperature of 2318 K in air), the radiation hazard from a hydrogen flame is small compared to other fuels. It also results in the non-visibility of hydrogen flames even in a dark room (unless impurities in the air are present), and therefore a hydrogen fire is difficult to recognize and localize. This is a major problem with regard to the detection of hydrogen fire accidents. In contrast, other gases containing carbon generate – in addition to water vapor and carbon dioxide – also soot within the flame. Soot is an efficient infrared emitter, leading to a strong thermal radiation and visible flames.

It is known from the experience that a hydrogen-air gas cloud evolving from the inadvertent release of hydrogen upon the failure of a storage tank or a pipeline liberates only a small portion of its thermal energy contents in case of an explosion, which is in the range between 0.1 and 10 %, in most cases < 1 % [Lind 1975].

The laminar burning velocity in a flammable gas mixture, defined as the speed with which a smooth plane combustion wave advances into a stationary flammable mixture, is a pertinent property of the gas depending on temperature, pressure, and concentration. The burning velocity of hydrogen in air at stoichiometric ambient conditions is 2.37 m/s reaching a maximum of 3.46 m/s at a concentration of 42.5 %. Compared to other hydrocarbon fuel-air mixtures (e.g., methane: 0.43 m/s), it is highest for hydrogen because of its fast chemical kinetics and high diffusivity.

The flame front velocity is defined as the product of laminar burning velocity and the expansion ration for constant pressure burning leading to a value of up to ~24 m/s for hydrogen. The turbulent burning velocity is significantly higher and reaches the order of several hundreds of m/s resulting from small-scale turbulence and flame instabilities which increase both energy transfer and flame surface. Most realistic flames are turbulent.

This comparatively high burning velocity results in a greater chance for a transition from deflagration to detonation (DDT). The detonability range is usually given to be 18 - 59 vol% of hydrogen concentration, however, the range was found to be depending on the system size. In the Russian detonation test facility RUT, the largest of its kind, a lower detonability limit of as low as 12.5 vol% has been observed [Breitung 1995]. The detonation velocity reaches values in the range of 2000 m/s.

For open LH_2 pools, it needs to be considered that cold hydrogen gas is less volatile compared to ambient gas and thus more prone to the formation of a flammable mixture with air. Furthermore LH_2 in direct contact with the ambient air quickly contaminates itself due to condensation and solidification of air constituents. Solid particles may lead to plugging of pressure relief valves, vents or filters. In addition, due to the different boiling points of nitrogen (77.3 K) and oxygen (90.2 K), the oxygen condenses first upon cooling down or vaporizes last upon warming up, both situations always connected with an oxygen-enriched condensate forming shock-explosive mixtures. Also liquid or solid oxygen in combination with another combustible material, even if solid and thus not “flammable”, may form highly explosive mixtures with drastically decreased ignition energies. Examples are LH_2 plus solid air having an O_2 fraction of > 40 %, or liquid oxygen spilled onto asphalt [Zabetakis 1967]. The ignition of premixed LH_2 with condensed air significantly enhances burning rates with a large variation. The flame will become wider and taller, and the radiated energy increases [Urano 1986].

The safety-relevant characteristic data of hydrogen are summarized in the table given in the Appendix.

2.2. Influence of Cryogenic Hydrogen on Materials

The stress which a structural material is able to withstand is determined by its ductility (Fig. 2-3). A material is elastic if, after being elongated under stress, it returns to its original shape and volume as soon as the stress is removed. At a certain strain, it departs from linearity, i.e., the material will retain a permanent elongation. The applied stress is the so-called "yield stress". A further increase of the strain eventually reaches the "ultimate or tensile stress" beyond which the stress steadily decreases until rupture. In contrast, a brittle material does not exhibit a permanent elongation phase and rather breaks abruptly without any warning as soon as it is exposed to its tensile stress [Edeskuty 1996].

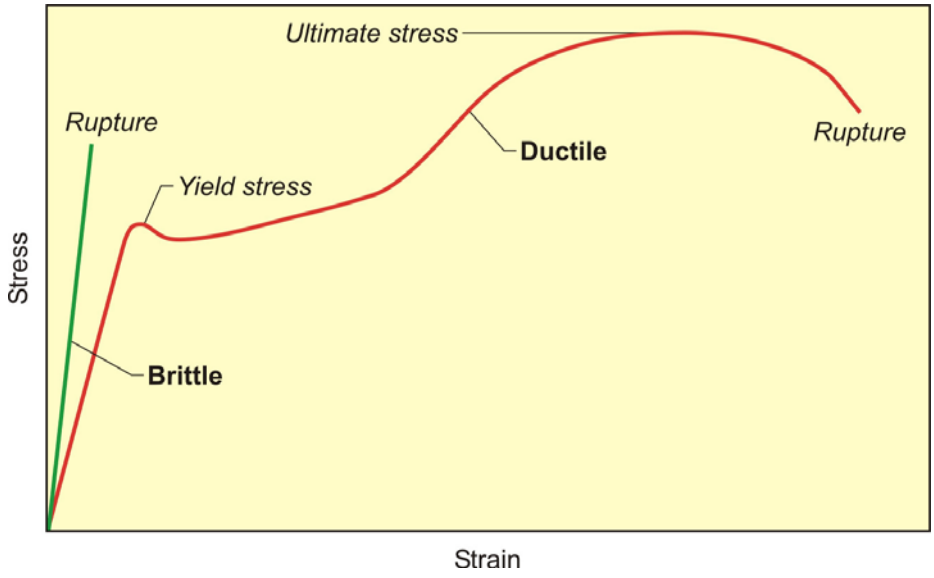

Figure 2-3. Ductile and brittle behavior of materials [Edeskuty 1996]

Hydrogen has long been recognized to have a deleterious effect on some metals by changing their physical properties. It is basically due to the presence of hydrogen atoms dissolved in the metal grid and accumulating in disturbed lattice regions. Apart from this "environmental" embrittlement effect, there is an additional influence on structural materials at cryogenic temperatures, which account for most service failures of brittle-type materials. With decreasing temperature, the yield stress and ultimate stress increase for most metals, generally connected with a corresponding drop in fracture toughness which is a measure of the ability of materials to resist crack propagation. The lower the toughness, the smaller is the tolerable crack length.

A material can change from ductile to brittle behavior as soon as the temperature falls below its so-called "nil-ductility temperature". This temperature is not a fixed value, but may vary as a function of prior heat or mechanical treatment and of the alloy composition and impurities, respectively. It is, in principle, the minimum temperature, at which a structural material is

considered useful and can sometimes be significantly higher than the temperature of the cryogen. For some materials at cryogenic temperature, little stress is sufficient to break it, and it can occur very rapidly resulting in an almost instantaneous failure. This effect is a particular problem in cryogenic equipment exposed to periodic changes and was found in several accidents to have caused the failure of a cryogenic storage vessel, e.g., the rupture of a 4250 m^3 LNG tank in Cleveland, USA, in 1944 [Zabetakis 1967].

The components of a cryogenic system usually undergo a thermal gradient, some only during cool-down or warm-up phases, others even at steady state operation. Strong gradients, particularly if non-linear, result in stresses which may lead to rupture. Thermal gradients are of significance in systems with stratified two-phase flows of cryogens.

Low temperatures can also affect materials by thermal contraction causing large thermal stresses, if the system cannot accommodate the differential thermal contraction of the materials. The thermal expansion coefficient is a function of the temperature. For many materials which are cooled down to cryogenic temperatures, more than 90 % of the total contraction will have already taken place until 77 K. The coefficient is in the range of 0.3 % in iron-based alloys, 0.4 % in aluminum, or more than 1 % in many plastics [Edeskuty 1996, NASA 1997]. Cryogenic vessels or piping must account for this contraction to avoid large thermal stresses.

Materials with sufficiently high strength and high ductility, working successfully at low temperatures, include aluminum and most of its alloys, copper and its alloys, nickel and some of its alloys, as well as austenitic stainless steels and should be used in cryogen containing systems. EN (European Standards) and ISO (International Organization for Standardization) standards cover the requirements for selecting appropriate materials resisting to cold embrittlement.

For many materials, specific heat exhibits a strong temperature dependence below 200 K showing that at cryogenic temperatures, much less heat is required to raise the temperature of a body than at ambient temperatures. An example: heat capacity of aluminium is reduced from about 950 J/(kg K) at ambient temperature to less than 10 J/(kg K) at 20 K.

2.3. Physiological Problems in Connection with Liquid Hydrogen

Hydrogen is classified as non-toxic and non-acid, non-carcinogenous, being a simple asphyxiant with no threshold limit value (TLV) or LD50 (lethal dose 50 %) value established [NASA 1997].

Vaporization of released liquid hydrogen affects the composition of the atmosphere, particularly in (partially) confined areas, carrying the risk of asphyxiation. The enormous liquid/ambient expansion ratio combined with condensation of O_2 from the ambient air and burning of flammable H_2-air mixtures leads to a significant dilution of the local atmosphere. An oxygen volume fraction of less than 19.5 % is considered by NASA to be dangerous to humans; less than 8 % will be lethal within minutes (Table 2-1). Alarm levels are generally set at 19 % of oxygen.

Table 2-1. Impact on humans by an atmosphere with decreasing oxygen contents

Oxygen contents in air [%]	Symptoms
~ 21 - 19	None
~ 19 - 15	Reduced reaction times, no visible effects
~ 15 - 12	Heavy breathing, rapid heart beat, impaired attention or coordination
~ 12 - 10	Dizziness, faulty judgement, poor muscular coordination, rapid fatigue, lips slightly bluish
~ 10 - 8	Nausea, vomiting, inability to move, loss of consciousness followed by death
~ 8 - 6	Brain damage after 4-8 min, death within 8 min
< 6	Coma after 40 s, respiratory failure, death

Direct contact with liquid hydrogen or with surfaces at very low temperature causes cryogenic "burns" similar to thermal burns. Living tissue will freeze except for very brief contact periods where the temperature difference between cryogen and skin is still high (film boiling regime) and heat transfer small. The freezing of skin onto a cold surface can lead to severe damage upon removal. Prolonged skin exposure to cold hydrogen may result in frostbite. A symptom is short-lived local pain. Frozen tissues are painless and appear waxy, with a pale whitish or yellowish color. Thawing of the frozen tissue can cause intense pain. Shock may also occur. Prolonged inhalation of cold vapor or gas may cause serious lung damage. Particularly eyes are sensitive to cold. A longer exposure to cold temperatures after a large spill lowers the body temperature resulting in hypothermia, organ dysfunction, and respiratory depression [Edeskuty 1996].

There are no significant environmental hazards associated with the accidental discharge of liquid hydrogen due to its non-toxic character.

3. PRODUCTION OF LIQUID HYDROGEN AND SLUSH HYDROGEN

The liquefaction of hydrogen is usually conducted in several separate, energy-intensive steps of multi-stage compression and expansion (cooling). During the cooling process, additional energy is needed to remove the heat generated from both the condensation process (446 kJ/kg) and from the conversion of normal H_2 (75 % ortho, 25 % para) to para-H_2 (523 kJ/kg).

3.1. Liquid Hydrogen Production Methods

3.1.1. Energy Requirement

As is shown in Fig. 3-1, different pathways are possible to cool the H_2 gas down to its boiling point, but all require the same minimum specific exergy. The type of process selected is depending on different parameters such as the real energy demand determined by the efficiencies of the single compressing and cooling steps, the amounts of irreversible losses, and last but not least, the availability of respective systems and their costs.

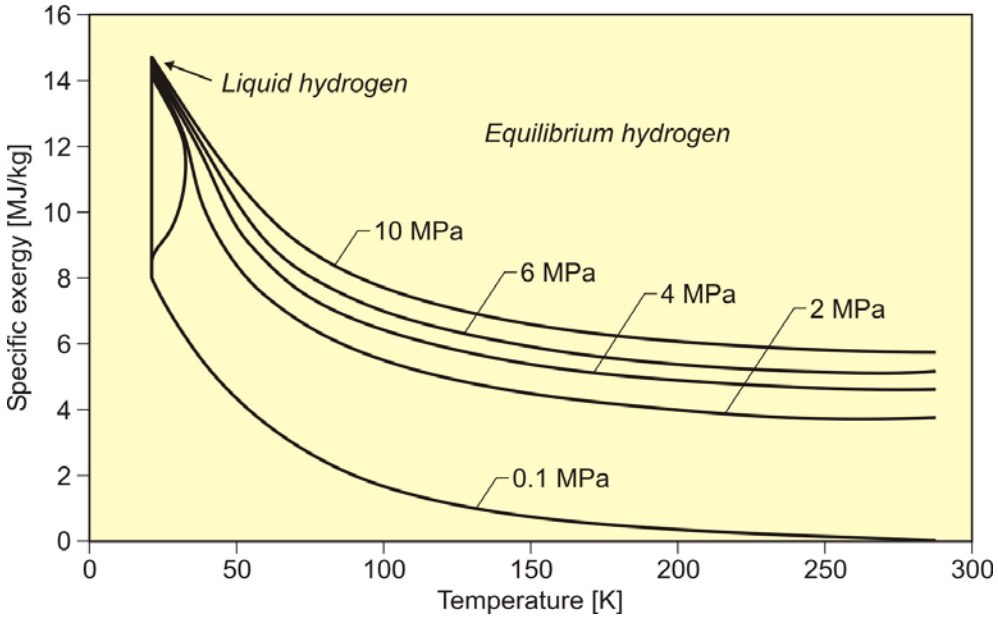

Figure 3-1. Specific exergy required for the liquefaction of hydrogen [Quack 2002]

There is a minimum specific work (exergy), A_{min}, required for the liquefaction of hydrogen at ambient conditions. It is composed of [Vander Arend 1964]

I. the work for cooling the gas to the boiling point determined by the Carnot cycle $A = (T_o - T_s) * \Delta s = (T_o - T_s)/T_s * \Delta Q$, with $\Delta Q = T_s \Delta s$ the heat withdrawn at T_s,

II. the work for condensation of the gas, and

III. an additional amount of work necessary for the temperature dependent ortho-para conversion.

$$A_{\min} = \int_{T_o}^{T_s} \frac{T_o - T}{T} c_p dT + \frac{T_o - T_s}{T_s} \Delta H_v + \int_{C_1}^{C_2} \frac{T_o - T_s}{T_s} C_{o \to p} dC \qquad (3\text{-}1)$$

$$= 1.58 + 1.70 + 0.62 = 3.90 \quad kWh/kg$$

where T_o – ambient temperature, K; T_s – boiling point, K; c_p – specific heat capacity (temperature dependent), J/(kg K); ΔH_v – heat of vaporization, J/kg; C – concentration of ortho hydrogen; $C_{o \to p}$ – conversion energy from ortho to para hydrogen, J/kg.

Table 3-1 shows a comparison of the minimum liquefaction work and its single contributions for some other gases. The total minimum energy required for liquefying hydrogen quoted in [Peschka 1992] is 3.92 kWh/kg or 14.1 MJ/kg. Values for "Condensation" and "Total" in the table are slightly different from the Peschka data. The comparison of hydrogen with the other fluids shows that for helium, due to the lower boiling point, the contribution from cooling to the liquefaction work is dominant, whereas condensation work is small. In contrast, for methane and nitrogen with much higher boiling points, the cooling work is small compared to the condensation work. But for both, total liquefaction energy required is smaller than that for hydrogen and helium.

Table 3-1. Minimum liquefaction energy for different gases [Peschka 1992]

Gas	Boiling Point [K]	Heat of vaporization [kJ/kg]	Minimum Work [kWh/kg]		
			Cooling NTP → BP	Condensation	Total
Hydrogen	20.268	445.59	2.242*	1.666	3.91
Methane	111.632	509.88	0.077	0.230	0.31
Nitrogen	77.34	201.	0.055	0.156	0.21
Helium	4.216	20.9	1.917	0.398	2.32

* includes ortho-para conversion

First step in the liquefaction process is the pre-cooling of the hydrogen, usually done with liquid nitrogen. This pre-cooling step is necessary, because if a gas is to cool down upon expansion, its temperature must be below the inversion temperature which is 193 K for hydrogen at ambient pressure.

Soon after the first experimental experience with LH_2 recognizing the fact that it rapidly disappears by vaporization mainly due to the heat released from the ortho-para conversion, it was proposed to have this process step performed already at the site of liquefaction by applying a catalyst. Ortho-para conversion can be done adiabatically, simply using a catalyst bed, however, on the expense of a temperature increase of the flowing hydrogen. There is also an isothermal method (Fig. 3-2), putting the catalyst into LN_2 or LH_2 at boiling point with temperature remaining constant [Stang 2006].

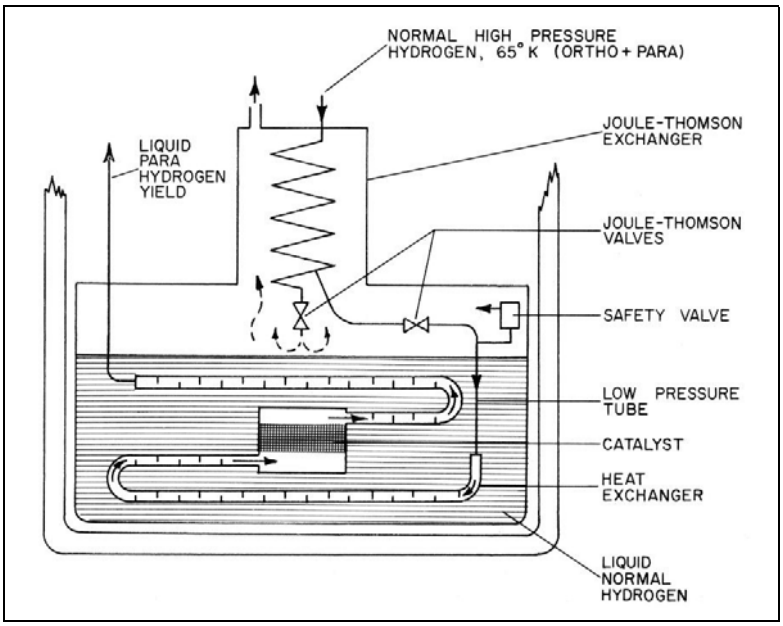

Figure 3-2. Schematic of the ortho-para conversion process with the isothermal method [Sittig 1963]

3.1.2. Linde Hampson Process

Most liquefaction processes in practice use thermodynamic gas cycles with compression, heat exchange and expansion. The Linde-Hampson method is the most simple one using a single thermodynamic process. Its efficiency, however, is not very high. Under optimized conditions, liquefaction energy requirement would be 13.12 kWh/kg of LH_2 plus 6.7 kg of LN_2 per kg of LH_2 for pre-cooling [Vander Arend 1964]. William Hampson applied the process in 1896 for the liquefaction of air using air at ~20 MPa to be expanded to atmospheric pressure and passing the cooled air through a heat exchanger. A power of 3.7 kW was necessary to produce 1 l/h of liquid air.

Carl von Linde's approach at the same time was more efficient, but also somewhat more complex by employing a pre-cooling step for the H_2 gas, a two-stage isothermal gas compression and an insulated coiled-tube heat exchanger for regenerative cooling (meaning that the fluid involved in the process is used at the same time as a coolant for the incoming gas before expansion). His liquefaction device had a capacity of 8 l/h of liquid air [Sloop 1978]. Pre-cooled hydrogen gas is first isothermally compressed followed by a cooling step down to 80 K along an isobar done in a counter-flow heat exchanger using LN_2. Finally isenthalpic Joule-Thomson expansion through a throttle valve or a mechanical expander to ambient pressure is used as the refrigeration process takes place to liquefy a part of the gas. After separating the liquid, the cool gas returns to the compressor. This process was first successfully demonstrated by Linde in 1895.

The first to liquefy hydrogen was the Scottish physicist James Dewar on May 10, 1898. The hydrogen gas compressed ~18 MPa was pre-cooled with LN_2 and expanded in a vacuum-insulated vessel, later known as a "Dewar". In this process, he obtained a conversion of 1 % of the incoming H_2 gas into a liquid. Despite its simplicity and reliability, this method is usually not applied to liquefy hydrogen because of its low efficiency.

3.1.3. Claude Process

A major step in the further improvement of the process was suggested by Georges Claude in 1902 with the use of an expansion engine, a cylinder with a moving piston, i.e., applying "external work" to produce low temperatures. Heat is removed as mechanical energy. Later expansion engines were substituted for expansion turbines, first introduced by P. Kapitsa in 1936. The Claude process has become since the commonly applied method in large-scale liquefaction plants. Refrigeration is conducted in four principal steps (Fig. 3-3):

I. Compression of hydrogen gas at ambient temperature, removal of compression heat;

II. Cooling with liquid nitrogen (~80 K);

III. Expansion of a part of the hydrogen in an expansion turbine resulting in a further cooling of the residual hydrogen (80 → ~30 K);

IV. Expansion of the residual hydrogen in a Joule-Thomson valve until liquid state is reached.

The first expansion step would already be sufficient for liquefaction. But the Joule-Thomson expansion is applied for the final step to avoid two-phase flow in the expander. Variations of the dual-pressure Claude process as a large-scale liquefaction method have proven to be the optimal solution. Maximum impurity level in re-gasified H_2 is in the order of 1 ppm.

The final cooling stage from 80 to 30 K represents the most energy-intensive step. Possible solutions are either the "classical" cascade refrigeration with cycles using different coolants (as was demonstrated by Dewar) or, a more economic method, the Brayton cycle with just one gaseous coolant which is sequentially expanded, before it cools down the hydrogen in a counter-current heat exchanger.

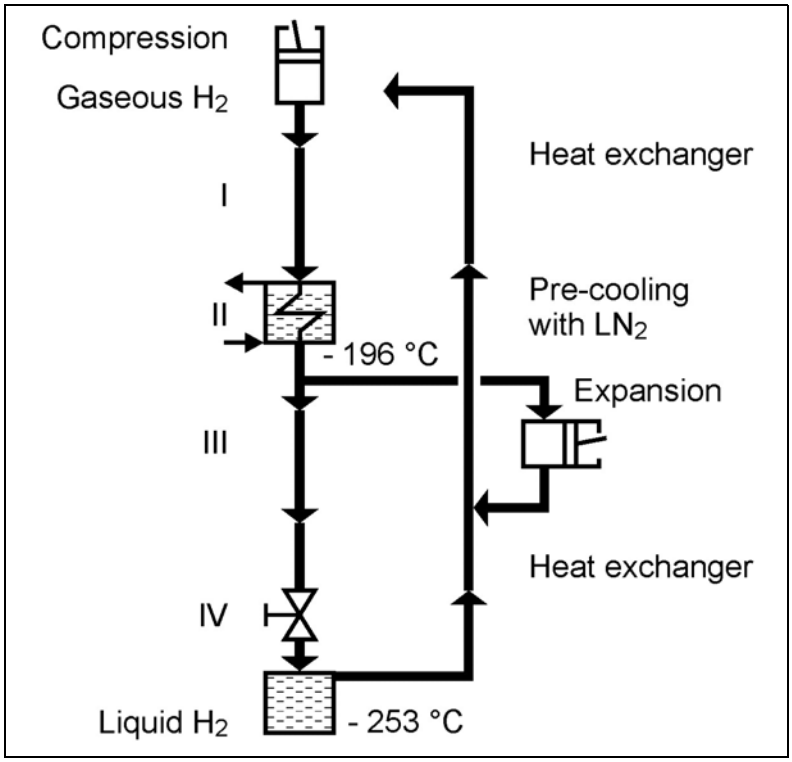

Figure 3-3. Schematic of Claude process for hydrogen liquefaction

Herrick L. Johnston from the Ohio State University constructed in 1946 a hydrogen liquefier for a 25 l/h (~0.04 t/d) production capacity [Sloop 1978]. As shown in Fig. 3-4, it consisted of a series of heat exchangers through which the hydrogen gas, initially at room temperature and ~12.5 MPa, was passing until close to the boiling point. Final step was an expansion valve, "H", where 20 % of the cold H_2 gas were liquefied. An over-sized version of the Johnston liquefier was constructed by Aerojet General Corporation in California in 1948 for the delivery of LH_2 to the Jet Propulsion Laboratory (JPL) for rocket tests increasing liquefaction capacity to 80 l/h (0.14 t/d).

In 1952, the largest LH_2 plant operated at the NBS-AEC Cryogenic Engineering Laboratory at Boulder had a liquefaction capacity of not more than 350 l/h (0.6 t/d) of normal H_2 and 480 l of LN_2, and with storage capacities of 4.5 m^3 of LH_2 and 22 m^3 of LN_2, respectively. But the production capacity was sharply increasing from the mid 1950s when development work for LH_2 driven jet and rocket engines was beginning (see also section 7.2). For the "304" engine testing series by Pratt&Whitney, the "Three Bears" LH_2 production plants were fabricated by Air Products, "Baby Bear" with 0.8 t/d capacity, "Mama Bear" with 3.4 t/d, and "Papa Bear" with 27.2 t/d. By middle of the 1960s, a 62.5 t/d capacity plant was in operation. The catalysts used in the early years of large-scale plants were chromium oxide on an Al support or iron hydroxide [Vander Arend 1964].

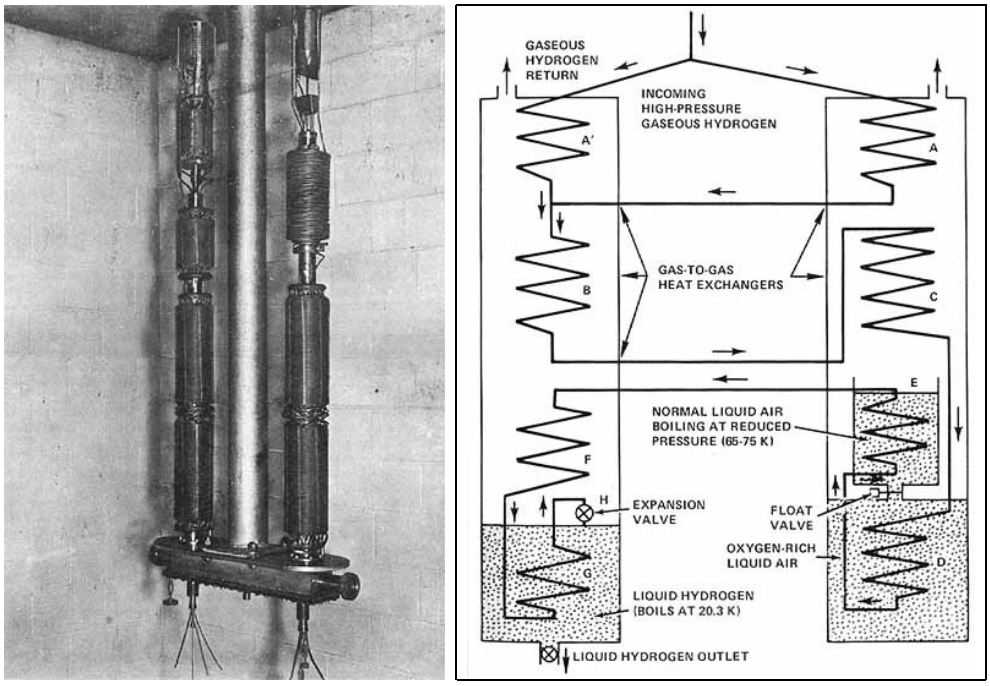

Figure 3-4. Hydrogen liquefaction facility of 1945 at the Ohio State University [Sloop 1978] (Courtesy of NASA)

Today's large-scale plants usually operate with six heat exchanging stages, first of which is the LN_2 stage. Principle of the heat exchanger is to use the adiabatic expansion with smaller temperature drops per expansion step. The cooled gas is taken to pre-cool the incoming gas, which then starts expansion at a lower temperature level ("progressive cooling"). Heat exchangers are typically operated at pressures up to 6 MPa. They are compact to minimize heat input from outside and made of aluminum or chromium alloy steels with sufficiently high thermal conductivity and sufficiently low thermal expansion and resistant against H_2 embrittlement. Respective efficiencies are in the range of 60 % [Tzimas 2003]. The ortho-para conversion is also done in several stages at different temperature levels achieving a para fraction of > 95 %.

According to research activities at the Technical University of Dresden, Germany, the employment of a helium-neon coolant (compromise between the good heat transfer characteristics of helium and the more economic compressibility of neon) in a suggested mixture of 4:1 has been assessed to lead to a further improvement. The estimated 7 kWh/kg of such a liquefaction plant compared to the minimum specific exergy would correspond to a total efficiency of 60 %. This value does not include yet the savings potential of a liquefaction plant directly connected to high-pressure electrolysis [Quack 2002].

Another improvement could be made by replacing the pre-cooling medium LN_2 by a multi-component refrigerant (MCR) promising a higher efficiency and lower capital cost [Stang 2006]. It is boiling over a wide range and does not freeze until down to 75 K. MCR is being used already for the liquefaction of natural gas. Based on this approach, a small-scale liquefier

has been designed and constructed. The principle applied here is to use liquid helium at a temperature of 4.5 K and cool down hydrogen gas in a series of heat exchangers. The tubes of the heat exchangers also contain the catalyst for the ortho-para conversion. The vaporized helium is captured and re-liquefied.

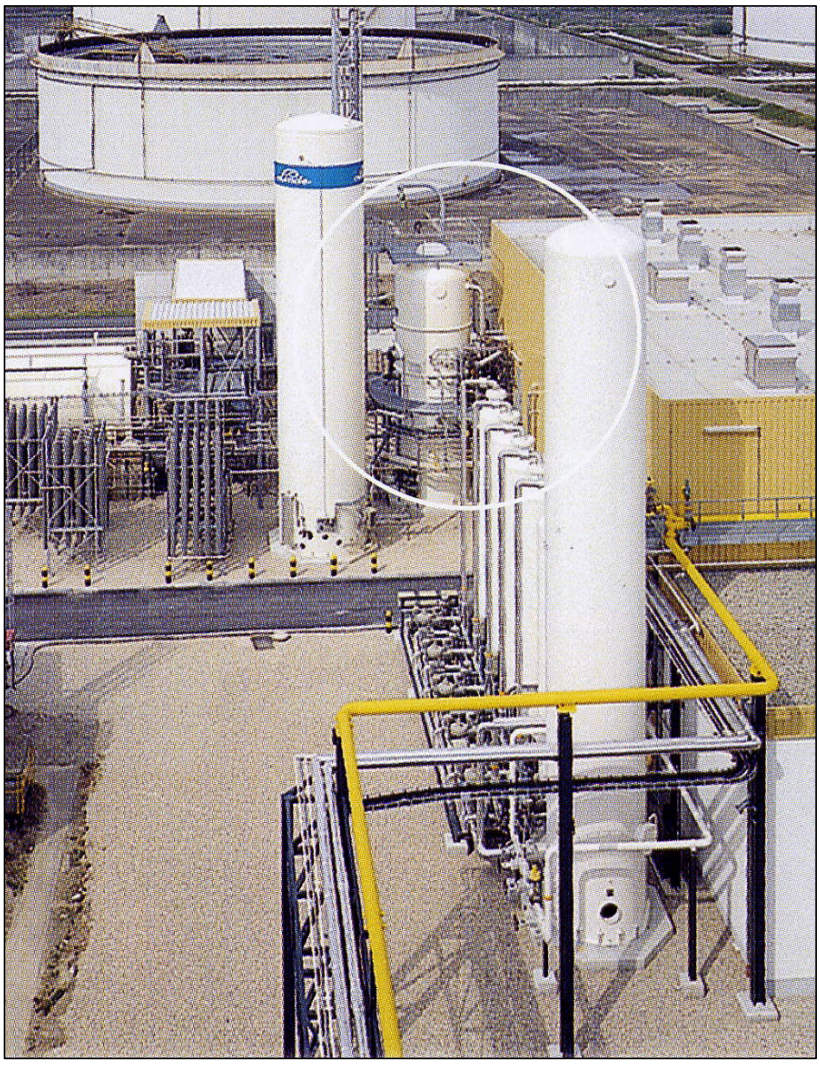

Figure 3-5. LH_2 liquefaction plant in Ingolstadt, Germany, with 4.4 t/d capacity (Courtesy of Linde AG)

LH_2 Liquefaction Process Details

for the 4.4 t/d production plant in Ingolstadt, Germany [Bracha 1994]:

- feed stock: H_2-rich raw gas from a refinery;
- cold box (white circle in Fig. 3-5) has 3.5 m diameter, 11.3 m height, and 300 - 1000 Pa vacuum pressure;
- H_2 entering cold box at 2.02 MPa and 308 K;
- purification by pressure swing adsorption (PSA) to ~4 ppm;
- Claude process liquefaction with refrigeration at three levels
  (a) pre-cooling with LN_2 (80 K)
  (b) expansion turbines (30 K)
  (c) Joule-Thomson valve (21 K);
- expansion turbines operating in the pressure range 2.2 - 0.3 MPa;
- ortho-para conversion at 4 temperature levels using $Fe(OH)_3$ catalyst, $p \geq 95$ %;
- further purification by low-temperature adsorber at 80 K to ~1 ppm;
- LH_2 exiting cold box at 0.13 MPa and 21 K;
- LN_2 flow is 1750 kg/h or 2.2 m^3/h with the gas vented;
- thermodynamic efficiency 33 %.

3.1.4. Magnetic Refrigeration Process

A magnetic type of cooling was proposed by P. J. W. Debye and W. F. Giauque in 1926. The magnetic refrigeration method takes advantage of the magneto-caloric effect, i.e., the adiabatic temperature increase in the presence of a magnetic field in the working material, and decrease, if the magnetic field is removed. It uses isentropic demagnetization of a ferromagnetic material as cooling process. Materials are magnetized slowly at the higher temperature, before they are suddenly demagnetized and return to the initial state. The magnetic refrigeration cycle consists of the steps (Fig. 3-6):

I. Adiabatic magnetization in an external magnetic field causing order of the magnetic dipoles (thus reducing entropy, thus increasing temperature);

II. Transfer of the heat to a fluid (water, helium) at the same magnetic field strength;

III. Adiabatic demagnetization with removal of the magnetic field at constant entropy, i.e., decreasing the temperature;

IV. Heat transfer from the gas (to be cooled) to the working material (solid).

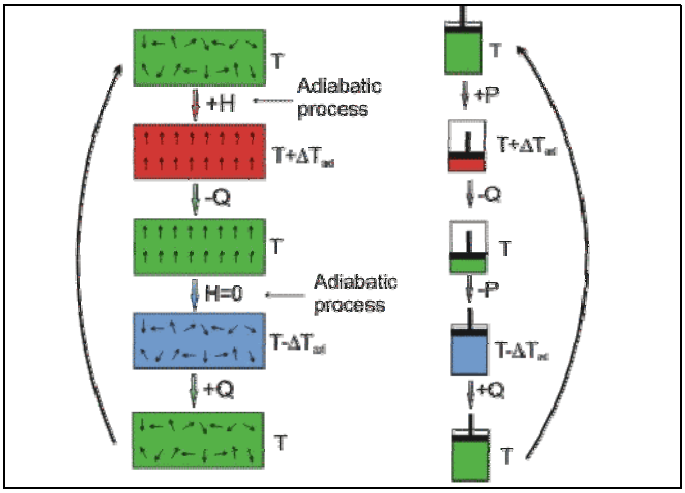

Figure 3-6. Schematic of the magnetic refrigeration process [Wikipedia 2008]

The temperature can drop by 10 - 15 K depending on the strength of the magnetic field. Temperature change is maximal at the material's Curie point, where it changes from ferromagnetic to paramagnetic. The magneto-caloric effect is significant at ± 25 K around the Curie point. Various candidate materials with reversible transition and significant adiabatic temperature change are available covering the total range between 20 and 300 K. Most appropriate materials to show a high magneto-caloric effect are based on gadolinium and some of its alloys, e.g., $Gd_5Si_2Ge_2$ [Bowman 1998].

This method promises a compact cooling system design with a long lifetime, higher efficiencies and lower capital cost, since neither expanders nor compressors are required. Liquefaction work is estimated to be at the level of 7.3 kWh/kg [Foldeaki 1995]. Magnetic refrigeration, however, is still on R&D level. Within the WE-NET project, a 10 kg/d capacity lab-scale plant was constructed and operated [Iwasaki 2003].

3.2. Safety Issues

A major problem when handling and producing liquid hydrogen is the potential contamination of the hydrogen stream with air or oxygen. The opposite direction, hydrogen leakages to the outside (atmosphere) may cause a hazard in confined or partially confined spaces, but is a comparatively minor problem. Safety measures to assure hydrogen of being separated from oxygen are

- System pressures in cold box and piping above ambient pressures;
- Continuous and precise monitoring of contaminants to avoid their accumulation;
- Filtering of hydrogen streams to remove solid particles;
- Purging of lines with pure nitrogen.

3.3. Liquefaction Efficiency

A realistic unit power value for today's modern large-scale liquefaction plants in the USA comprising the whole process of cooling H_2 from ambient temperature to its liquid state at the boiling point, including all thermal and mechanical losses, is in the order of 12.5 - 15 kWh/kg [Drnevich 2003]. This corresponds to an efficiency of 26 - 32 %. The smaller-scale facility in Ingolstadt requires an energy input of ~15 kWh/kg of H_2 or up to about 38 % (45 %) of the higher (lower) heating value of hydrogen.

From the cost stack for a typical hydrogen liquefaction plant, capital cost are covering with about 63 % most part mainly due to the compressors and brazed aluminum heat exchanger cold boxes. It is followed by power cost (~30 %) and O&M (~7 %). Further cost reduction is seen in the development of improved expanders and compressors, lower cost insulation, more efficient refrigeration, but also in the construction of larger-scale plants with capacities up to 850 t/d and modular type systems with plant repeatability [Drnevich 2003].

Fuel Cell Plant

If an electric power of 500 MW (a typical medium-sized power plant) is to be generated from hydrogen (in a fuel cell plant) assuming a 75 % efficiency, it needs 670 MW of H_2. Based on the lower heating value of 120 MJ/kg or 33.3 kWh/kg, the throughput at the power plant would be ~480 tons of H_2/day, much more than today's world LH_2 production capacity.

3.4. Present Hydrogen Liquefaction Capacity in the World

Starting with the Apollo space program in the USA in the 1960s, hydrogen liquefaction plants have been designed and constructed on a large scale. Their concepts were based on the experience gained from the numerous small-scale plants previously developed in laboratories over the world, and on the requirement of an economic production of LH_2.

Also mobile hydrogen liquefaction stations on a small-capacity scale have been constructed to meet the temporary demands, e.g. at testing sites. In 1952-54, the total equipment for hydrogen liquefaction was mounted on three trucks to produce LH_2 at a rate of 100 l/h with a para-hydrogen share of 45 %. Two trucks carried huge compressors, while the third one carried the liquefaction and purification equipment. The historic and a recent development are shown in Fig. 3-7.

In Europe, it was the Ariane space program that initiated the construction of LH_2 production plants in the 1980s. Liquid hydrogen production in Japan and China (no specific data found), also in India since 1996, is only temporary and dedicated to their respective space rocket developments. Since recently in Japan, smaller-scale production started in Japan as part of the current national hydrogen and fuel cell program. There appears to be a growing market for smaller facilities to serve the needs for LH_2-fueled vehicles. Table 3-2 gives an overview of the worldwide existing liquefaction plants.

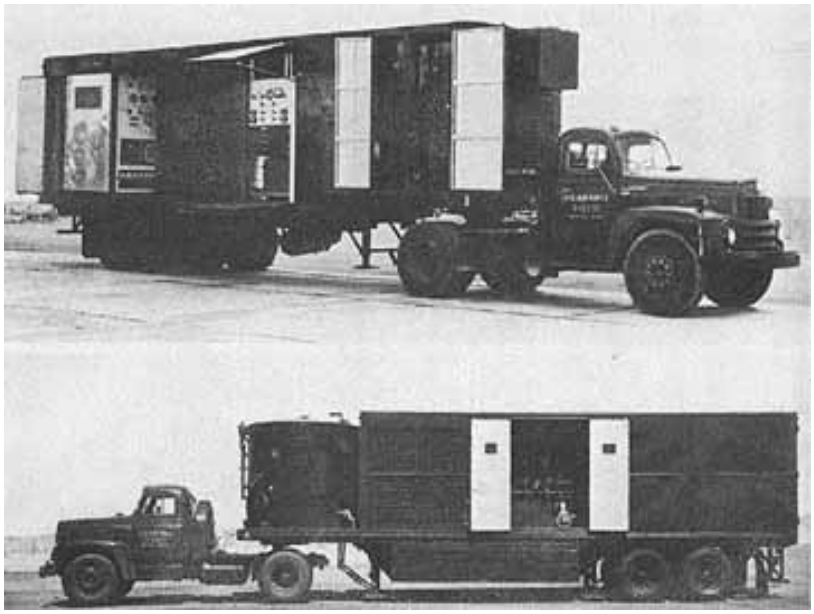

Figure 3-7. Two of the three trucks carrying the mobile 100 l/h capacity liquefier designed and developed by H.L. Johnston in 1952-54 [Sloop 1978]

At present, total world's hydrogen liquefaction capacity amounts to 310 (metric) tons per day. Europe has just three plants with a total capacity of 25 t/d. The latest facility in East Germany started operation in September 2007 adding some 5 t/d to the total production.

3.5. Slush Hydrogen Production Methods

James Dewar was also the first to produce solid hydrogen in 1899. Today most slush hydrogen is being produced by means of the so-called Freeze-Thaw method [Edeskuty 1996]. In this technique, liquid hydrogen near its triple point is continuously injected, and the gaseous phase above the LH_2 surface is pumped away to lower the pressure until the liquid has cooled down below the freezing point (13.8 K) and a film of solid ice forms on the surface. The pumping process is then stopped to allow the solid phase to settle into the liquid. After decreasing the pressure again, the formation of a new solid layer on the surface is initiated. The cycle is repeated until the desired amount of SLH_2 has been produced. A major safety issue is the extremely low vapor pressure even below atmospheric pressure which enhances the chance of air ingress into the system and formation of an explosible or even detonable mixture (LH_2 + LOX).

Some other production methods apply liquid helium for cooling. In the Auger method, a hollow cylinder is placed in liquid hydrogen. An annular interior is then cooled with LHe of 6 - 13 K temperature. The hydrogen freezing on the surface is scraped off by a rotating auger. This method provides a stable, continuous, and clean slush production. Small-scale SLH_2 production facilities were operated in the US since 1990 and Japan mainly for the purpose of testing and process improvement.

Table 3-2. Overview of worldwide existing hydrogen liquefaction plants

Place	Operator	Capacity [t/d]	Operation since
America			
Sarnia, ON, Canada	Air Products, USA	29	1962
New Orleans, LA, USA	Air Products, USA	68	1977
Pace, USA	Air Products, USA	29	1994
Sacramento, CA, USA	Air Products, USA	6	1986
Magog, QU, Canada	BOC, USA	15	1990
Becancour, QU, Canada	HydrogenAl, Canada	11	1986
Kourou, French Guiana	L'Air Liquide, France	5	1990
East Chicago, IN, USA	Praxair	29	1999
McIntosh, AL, USA	Praxair	29	1995
Niagara Falls, NY, USA	Praxair	38	1981 /1989
Ontario, CA, USA	Praxair	22	1962
	Total America	**281**	
Europe			
Rozenburg, Netherlands	Air Products, USA	5.0	1987
Lille, France	L'Air Liquide, France	10.5	1987
Ingolstadt, Germany	Linde, Germany	4.4	1991
Leuna, Germany	Linde, Germany	5.0	2007
	Total Europe	**24.9**	
Asia			
Amagasaki, Japan	Iwatani Gas, Japan	1.2	1978
Ooita, Japan	Pacific Hydrogen Co., Japan	1.4	1986
Kimitsu, Japan	Nippon Steel Corp., Japan	0.2	2004
Sakai, Japan	Iwatani Gas, Japan	1.1	2006
	Total Asia	**3.9**	
	Total World	**309.8**	

4. STORAGE OF LIQUID HYDROGEN

Due to its low volume-related energy density, hydrogen requires a comparatively large volume if stored. While its gravimetric density is three times that of gasoline, the volumetric density is only 25 %. Surprising at the first view is the fact that even 1 m^3 of liquid hydrogen has with 71 kg a lower H_2 mass contents than other chemical hydrogen storage media, e.g., gasoline (84 kg) or ammonia (136 kg) or even water (111 kg) (Table 4-1).

Table 4-1. Hydrogen densities in different forms of storage

Fuel	Formula	Density [kg/m^3]	Energy per mass [kJ/kg]	Energy per vol [GJ/m^3]	H_2 density [kg H_2/m^3]
Hydrogen	H_2	0.09	141,890	0.013	0.09
LH_2	H_2	71	141,890	9.9	71
LNG (methane)	CH_4	423	55,530	~ 20.5	106
LPG (propane)	C_3H_8	581	50,400	25.2	106
Gasoline (octane)	C_8H_{18}	745	47,400	30.4-34.8	118
Methanol	CH_3OH	793	22,700	18.0	99
Ethanol	C_2H_5OH	794	29,900	23.5	104
Methylcyclohexane	C_7H_{14}	862	42,500	26.9	96
Ammonia	NH_3	771	22,500	17.4	136
Water	H_2O	1000	-	-	111

The storage of hydrogen in the liquid phase, however, is beneficial and practical in many applications. Storage of larger amounts as liquid allows for lower central storage cost and provides greater flexibility. More storage capacity leads to a higher utilization rate of a hydrogen consuming plant [Simbeck 2002]. Liquid hydrogen is particularly demanded where the hydrogen is needed at a high purity level and where volume and weight is an issue like in the transportation sector. Drawbacks are special handling requirement, boil-off losses, the need for control of temperature stability to avoid overpressure, and, most important, the liquefaction energy requirement. LH_2 storage technology is commercially available in a wide range; vessels are manufactured in sizes from 0.1 to several thousands of cubic meters.

4.1. Principal Tank Design

Because of its low temperature, liquid hydrogen must be stored in an effectively insulated container, a “dewar” or “cryostat”. The typical design of a storage tank is a double-walled, vacuum-jacketed fluid container (Fig. 4-1). The outer tank serves as protection of the inner tank against impacts from outside as well as of the neighborhood, if the inner tank fails. The

space between the two vessels serves as insulation layer to minimize heat transfer into the inside. Supporting structure and interconnections have to fix the inner shell, but also assure it can freely undergo contraction and expansion due to the numerous temperature cycles (refills) that may occur during the tank's lifetime. Also heat transfer from the outside must be minimized. An even more complex structural design is necessary for large vessels. Ideal shape of the vessel is spherical because of its minimum surface-to-volume ratio and its more uniform distribution of stresses and strains.

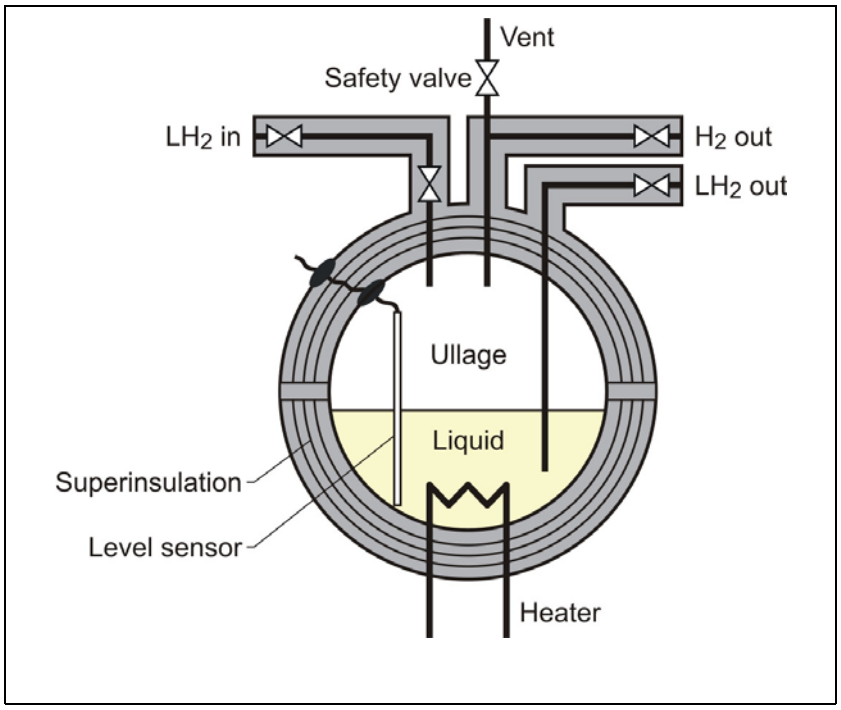

Figure 4-1. Principal schematic of LH_2 tank

A multi-layer foil insulation is usually chosen for tank sizes up to 300 m^3 to minimize the transport of radiation heat. It consists of some 60 - 100 layers of reflective foils fixed on the outside of the inner vessel with a total thickness of at least 20 mm. (The layered type of insulation is usually called superinsulation.) The remaining void volume of the intermediate space serves basically as vacuum jacket to avoid air condensation on the cold surfaces and heat transport by convection or residual gas conduction. Typical pressures are < 0.013 Pa. Appropriate getter materials such as metal hydrides may help maintain the vacuum over longer times and absorbing boil-off losses. Alternatively the void volume can be filled with perlite powder of reflective particles or hollow glass microspheres (15 - 150 µm diameter). They significantly reduce heat convection and thus allow for a less demanding vacuum (< 1.3 Pa). A safety issue that has to be taken care of is a potential shifting of insulation particles during contraction of the inner vessel, which leads to compaction upon re-expansion and may rupture supporting structures [Edeskuty 1996].

Maximum and minimum design temperatures are determined by the loss of strength of the storage walls at the higher end and by loss of ductility (embrittlement) at the lower end. A relief valve should be designed as to handle abnormal operating conditions such as overfilling; it should open at pressures less or equal the design pressure to allow a relief such that the pressure does not rise beyond 110 % of the design pressure.

Depending on the insulation quality and the surface-to-volume ratio, a certain fraction of the stored cryogen is an unavoidable boil-off to keep the rest cold. It is in the order of a few percent per day for a passenger car tank and decreases with increasing volume to 0.4 %/d for a 50 m^3 cryogenic tank and 0.06 %/d, respectively, for a 20,000 m^3 LH_2 tank. Overpressures exceeding specified limits after a certain time, the so-called lock-up time, are relieved via a boil-off valve and a safety valve, respectively, (and a second one, if the first is insufficient to discharge). It is a safety issue, if LH_2 fueled cars are parked in closed or partially closed garages.

Boil-offs rates can be further reduced by (re-)cooling the insulation with cold venting gas. For this purpose, metallic shields are installed with the insulation. In smaller containers, also liquid nitrogen can be used for cooling the insulation. But as an additional system, it provides more complexity and needs periodic refilling. A more fundamental approach is the employment of a cryo-cooler to re-liquefy boiled-off gas. For future vehicle tanks, however, some sort of innovative solution might be necessary that avoids boil-off, when the vehicle is not in use.

Some of the liquefaction work can potentially be recovered when the liquid is vaporized, which is a matter of downstream engineering technology. The theoretical maximum is 10 % of the energy invested [Taylor 1986]. The autonomy of the storage system, i.e., the time without any loss of the contents, is typically 30 days. For vehicle tanks, the lock-up time could start at zero again after a short ride.

Typically the liquid hydrogen will be expelled from the container by pressurization. This can be done by either a pressurizing gas from an external source or a vaporizer in form of a heat exchanger which receives liquid from the container by means of a pump or gravity and sends the gas into the ullage space.

Appropriate materials used for a cryogenic tank are carbon steel for the outer vessel and stainless steel or aluminum for the inner vessel. Tubing from the inner vessel to the outside is generally made of stainless steel with vacuum-sealed transition on the cold side [Peschka 1992]. On the longer term, however, state-of-the-art stainless steel tanks for vehicles must be further reduced in weight. Therefore investigations are on-going to take fiber-reinforced (composite) materials, which are used for high pressure tanks, also for cryo-tanks, and with a comparable specific energy storage capacity similar to conventional tanks. The advantages would not only be the higher strength compared with steel and a lower weight, but also, due to the lower pressure, the possibility to adjust the shape of the tank to the vehicle structure. On the other hand, composites are prone to enhanced embrittlement and exhibit an anisotropic thermal expansion, almost none in fiber direction and a high one perpendicular to the fiber direction.

4.2. LH_2 Tanks for Mobile Applications

4.2.1. Passenger Car Tank Design

Cryogen storage tanks for passenger cars are typically cylindrical, double-walled container with capacities up to 10 kg of LH_2 or 170 l of volume. The insulation of 70 layers of foils made of aluminum or aluminized polymer, separated by glass fibers or polymer spacers with a total thickness of ~30 mm allows a boil-off loss of less than 1.5 %/day. A double-walled filling pipe as well as the required safety vent and a safety valve are passing through the insulation. The cryo-tanks are operated at pressures of ~0.4 MPa; the maximum allowable pressure is 0.7 MPa, before the vent line opens. The inside pressure is controlled in most cases by means of an electric heating device. Lock-up times can be up to 12 days [Krainz 2003, Tzimas 2003]. A schematic of an LH_2 tank for a passenger car is shown in Fig. 4-2.

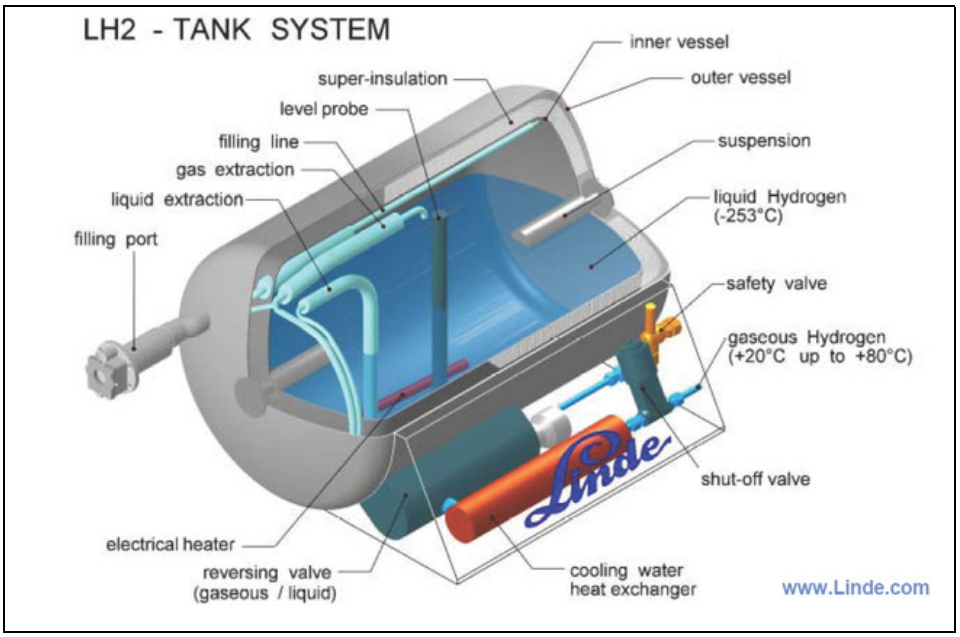

Figure 4-2. LH_2 tank for passenger cars
(Courtesy of Linde AG)

Hot Coffee

The latest LH_2 tank for passenger cars fabricated by the Austrian company Magna Steyr for the BMW Hydrogen 7, consists of a double-walled steel vessel with 2 mm wall thickness each and a 30 mm vacuum superinsulation in between. The pressure in the vacuum jacket is 0.01 Pa @ 20 K. Regarding the tank's insulation capability, if filled with boiling coffee, it would take about 80 days, until it sufficiently cooled down to become drinkable [Müller 2006].

An improved pressure management system compared to electric heating has been suggested in [Michel 2006]. Depending on the pressure measured in the exit line, a part of the gas is heated and routed back inside the tank to transfer its heat (Fig. 4-3). This arrangement has the advantage that some part of the waste heat from the engine can be utilized, and avoids the disadvantages of electricity consumption and cable connections.

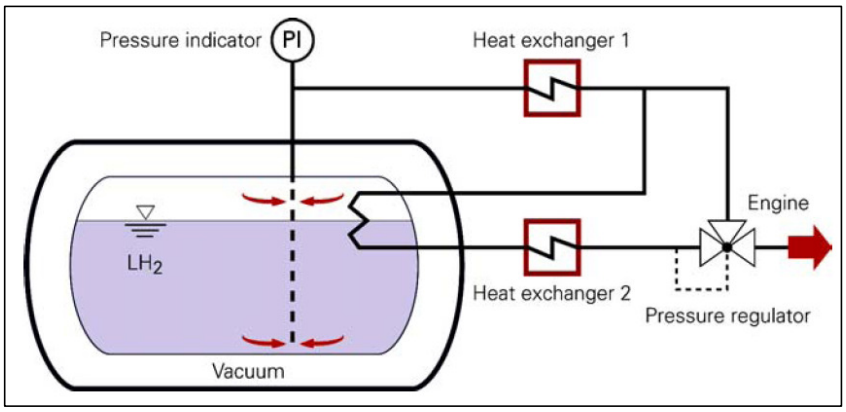

Figure 4-3. Advanced pressure management system developed by Air Liquide [Michel 2006]

While the present generation of passenger car tanks has already successfully demonstrated the requirements with regard to filling time, fatigue strength, crash safety, or recyclability, the development of future cryo-tank designs has already started. The next generation will consist of flat tanks made of light-weight metals, small-series production of components, buttresses inside to accommodate for changed pressure conditions, which are currently under development (Fig. 4-4). Final stage in future, from 2020, will be a more complex shaped tank made of fiber materials to better adjust to the vehicle, and automated mass production at reasonable cost [Krainz 2008].

The combination of cryogenic and high-pressure hydrogen storage in hybrid tank concepts is also currently being investigated. Such systems of cryo-compressed storage that can operate at LH_2 temperature (20 K) and at higher pressures (~25 MPa), are more compact than "normal" pressure vessels, have less weight than hydride storage tanks, and also exhibit a smaller boil-off loss. Due to H_2 delivery at a high pressure, high-pressure pumps are not required. Such insulated, cryo-capable pressure vessels are more flexible in using the hydrogen infrastructure and do not need the full energy demand of liquefaction [Aceves 2002]. Tanks of such design have undergone certification tests and were already used in test vehicles. A tank of the latest generation will be installed in an H_2-driven Toyota Prius [Aceves 2006].

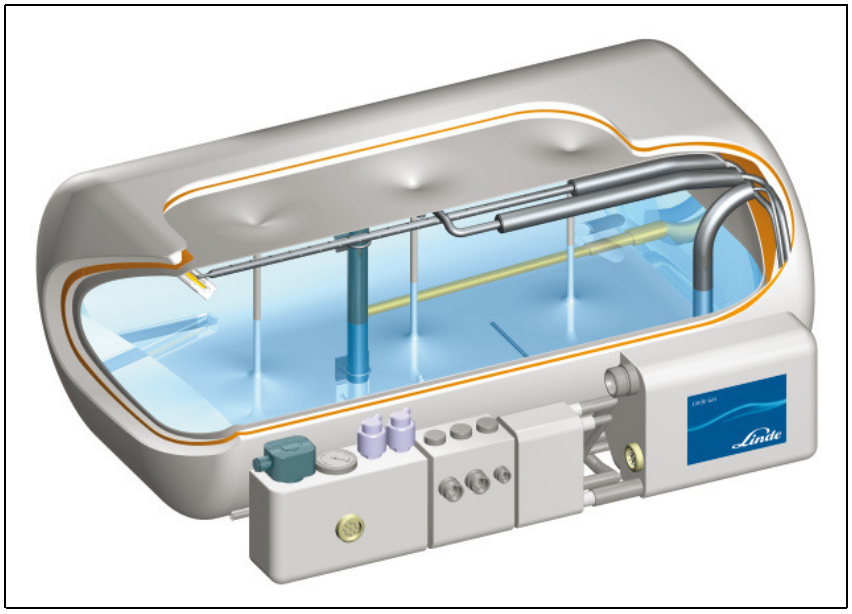

Figure 4-4. Flat tank design for liquid hydrogen
(Courtesy of Linde AG)

4.2.2. Safety Tests with LH_2 Vehicle Tanks

In an extensive experimental study as part of the Euro-Quebec project (see chapter 7), the German car company BMW has investigated from 1992 to 1995 the safety of such cryo-tanks for cars under worst-case conditions [Pehr 1995, Pehr 1996]. Original cryo-tanks filled with either LH_2 or LNG were taken and investigated under conditions of vibration and acceleration, loss of vacuum by air ingress, vessel deformation, and perforation. The aim was to check the stability of the supporting structure and the performance in conceivable traffic accident scenarios (Fig. 4-5). Strong deformation usually resulted in cracks which limited the pressure increase. The enhanced heat transfer from the outside increased the vaporization rate through the safety valves.

Furthermore tests with bursting of the tank due to increased inside pressure were conducted [Pehr 1995] revealing a safety factor of more than 15, i.e., failure pressure was 15 times higher than the maximum allowable inside pressure for the tank with a 2 mm wall thickness. Tanks with wall thicknesses of 1.5 mm and 1 mm still had safety factors of 11 and 7, respectively. These tests demonstrated the fail-safe design (leak-before-rupture principle) of such storage tanks, i.e., a small crack develops first, through which the H_2 could escape, before it would fail in a catastrophic rupture.

The temperature and pressure response of an LH_2 car tank in a bonfire test is depicted in Fig. 4-6. The average temperature of 920°C to which the half-filled tank was exposed, resulted in a rapid pressure increase (solid line in bottom figure). After about 4 min into the test, both safety valves opened and gradually liberated the stored energy. The LH_2 filling level decreased (dotted line), until it has completely vaporized after 14 min, While the pressure in

the vacuum space gradually increased (dashed line) due to the thermal decomposition of the insulating material, the inner Al tank started to melt and eventually failed after 16 min shown by the sharp pressure increase in the vacuum space. The outer tank exhibited almost no change until the vent line opened about 38 min. There was neither an explosion nor the evolution of an H_2 vapor cloud. The tanks have principally demonstrated good-natured behavior during the depressurization phase. Reliability over the whole lifetime, however, still needs to be proven [Pehr 1995].

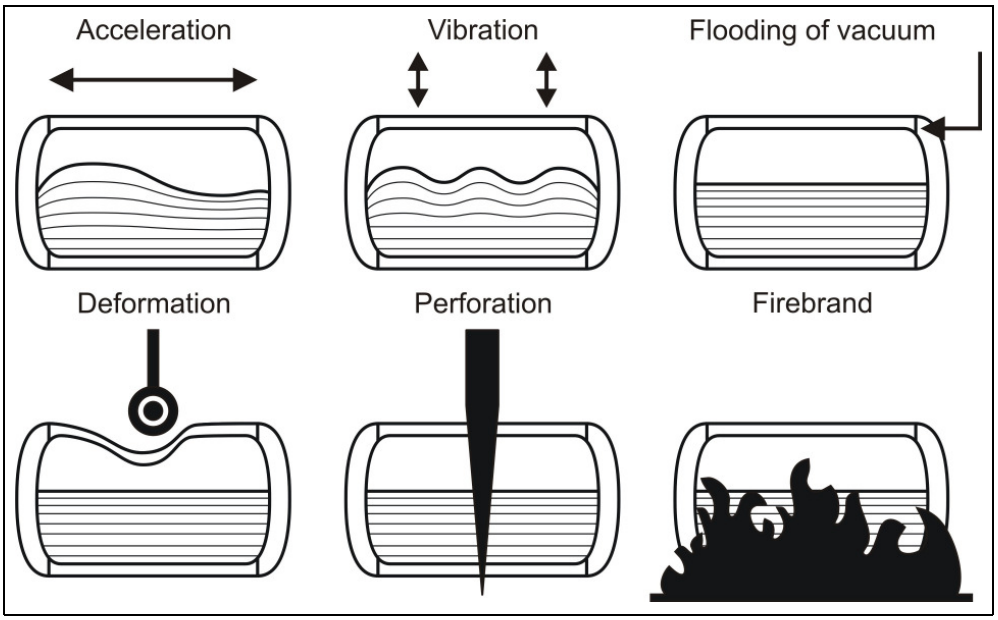

Figure 4-5. Safety tests on LH_2 vehicle tanks conducted by BMW [Pehr 1995, Pehr 1996]

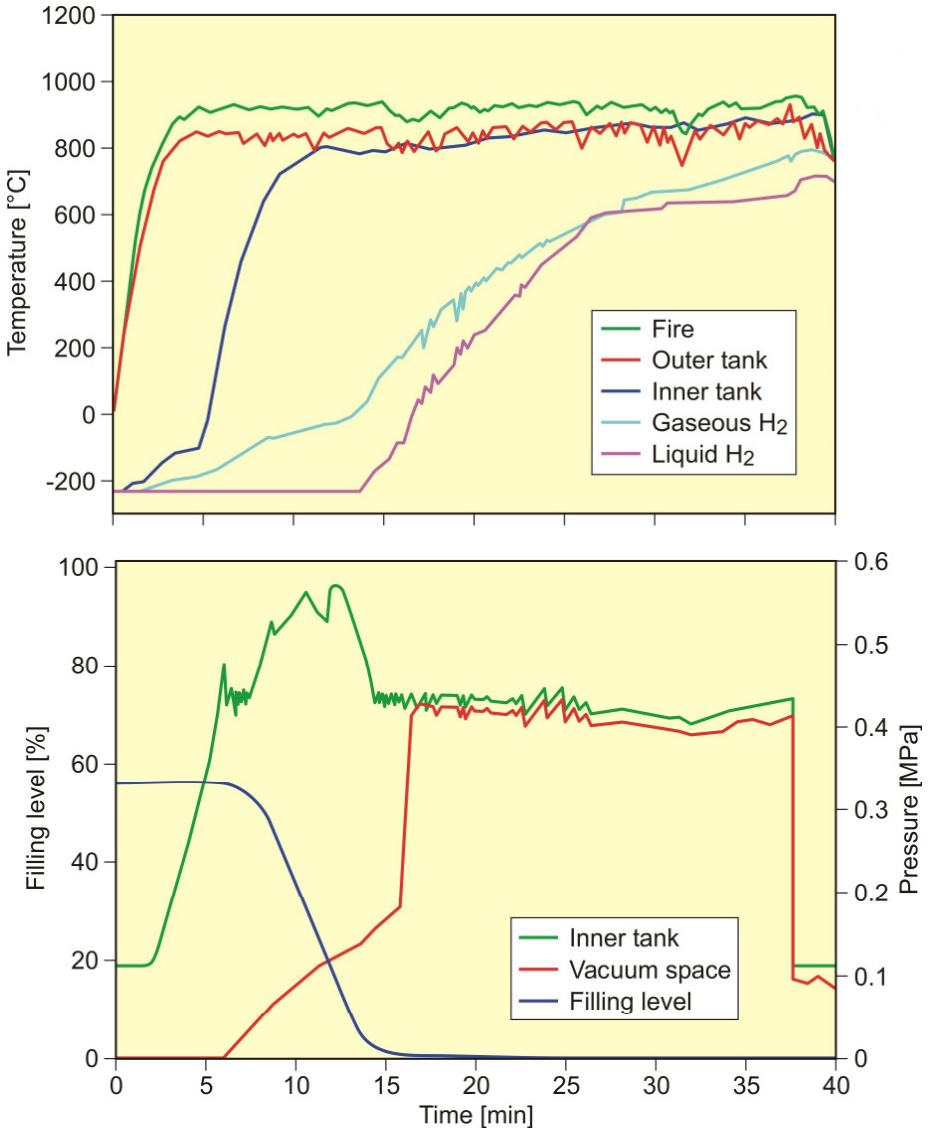

Figure 4-6. Transient temperature and pressure behavior in a half-filled LH_2 tank in a bonfire test [Pehr 1995]

Also GM/Opel conducted safety tests with LH_2 vehicle tanks looking specifically at the situation of accidents in a road tunnel. Release tests with H_2 in a Norwegian tunnel have shown that both an immediate ignition and a 15 min delayed ignition failed [GM 2007].

Safety experiments with an LH_2 storage tank at a larger scale were conducted in Germany by the Federal Institute of Materials Testing and Research (BAM), Berlin, and the Germanischer

Lloyd, Hamburg, using a 61 m^3 LH_2 model tank to simulate a future tank for storage and maritime transportation. Main goal was the investigation of the thermodynamic behavior of the cryogen in the tank. The boil-off rate was measured for the filled open tank to be approx. 1.3 % or about 700 liters per day, while it was decreasing to 0.6 %/d at filling levels below 40 %. The decrease in the boil-off rate can be explained by a stronger uptake of heat from the steel structures at higher temperatures which develop when in contact with the gas phase. A calculation model was developed to enable the simulation of the complex fluid-dynamic processes in such a tank.

With respect to future storage tanks, the LH_2 storage container considered for the Euro-Quebec barge carrier has been designed as a pressure vessel to carry a volume of 3000 m^3 of LH_2. The cylindrical tank consists of two concentric vessels with a length of 22 m and a diameter of 14.7 m for the outside vessel. The inside vessel has a length of 18.7 m and a diameter of 14.0 m. Total tank weight is 1000 t. The net volume of the tank is 3047 m^3 corresponding to a load of 213 t of LH_2 with an ullage of 15 %. The cargo is stored at an initial pressure of 125 kPa; the upper design limit for the tank is 500 kPa. The container is designed to serve both as a transportation vessel and as an onshore vessel, i.e., there is no need for a cargo transfer from one to another vessel. The tank must guarantee a stand-alone period of more than 25 days [Giacomazzi 1993, Petersen 1994].

4.3. Stationary LH_2 Tanks

Large stationary LH_2 tanks usually have an additional outer wall with the space filled with LN_2. Inner vessel walls are preferably thin due to cost and cooling, where the outer walls should be thick for the purpose of stability and stress uptake. Most of the large vessels are of spherical shape. Lock-up times are in the order of 50 hours [Tzimas 2003]. Boil-off losses can also be reduced by making sure that most of the LH_2 to be filled is para-hydrogen.

Large-scale LH_2 tanks at the production site typically have a capacity of more than 100 t (~1400 m^3). The ullage gas carries a large refrigeration potential which is being recovered for the liquefaction process via a vapor return line whenever practical. Tanks at the utilization sites are usually smaller with capacities from 110 up to 2500 kg for vertical tanks or up to 5300 kg for horizontal tanks. The vessels are usually operated at an overpressure of 1.2 MPa.

Some examples: The horizontal tank at the German liquefaction plant in Ingolstadt has a diameter of 4.2 m, a length of 25 m, and a volume capacity of 270 m^3 to contain 19 t of LH_2, i.e., the production of a few days; boil-off rate is 0.3 %/d [Bracha 1994]. The tanks being operated at the Tanegashima space center in Japan, are two spherical vessels with an outer diameter of 12.6 m and a capacity of 540 m^3 each. Storage at liquefier plants is in vacuum-insulated spherical tanks that usually hold about 1500 m^3.

The world's largest LH_2 tanks, that have been constructed so far, are located at the NASA Kennedy Space Center (KSC), Florida, USA, two identical ball-shaped tanks used within the space shuttle program (Fig. 4-7). The tank is a 3800 m^3 double-walled, vacuum perlite insulated spherical storage vessel. The outer sphere is made of carbon steel with an inside diameter of 21.34 m, and the inner sphere is made of austenitic stainless steel with an inside diameter of 18.75 m. The LH_2 contents is 850,000 gal (3218 m^3) corresponding to an ullage of about 15 %. The tank operated at a pressure of 620 kPa has a boil-off rate of 0.025 %/d or about 800 liters/d [Peschka 1992] (a somewhat higher figure is given in [Tzimas 2003]).

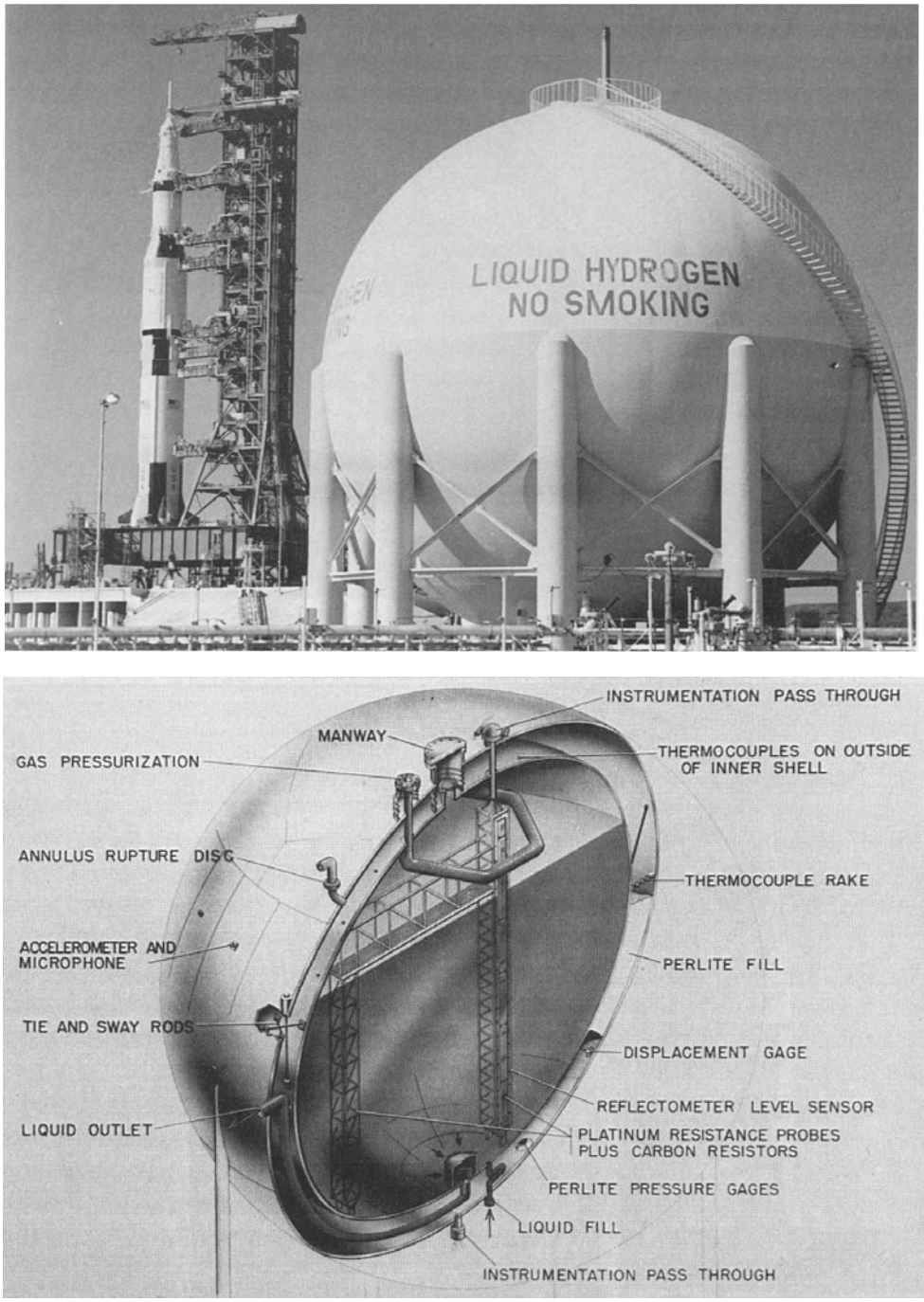

Figure 4-7. Schematic of the 3218 m^3 LH_2 tank at Kennedy Space Center (Courtesy of NASA)

The second KSC tank was found to exhibit a more than double as high boil-off rate. Missing perlite insulation at some spot of the upper part was identified by infrared imaging to be the reason [Gu 2005]. Approximately one half of the LH_2 contents, 1500 m^3 or 106 tons, is needed to fill the tanks inside the External Tank when launching a space shuttle. The LOX tanks at KSC are also ball-shaped dewars with each containing 900,000 gal (3407 m^3) of liquid oxygen at 90 K.

The German company Messer Griesheim has designed and constructed a special high-pressure storage tank (Fig. 4-8) with the inner vessel to contain 12 m^3 of LH_2 at a pressure of up to 40 MPa [Ewald 1987]. It has been operated within the frame of the European Ariane V rocket development. Another example for a high-pressure tank is from the USA used within the Pratt&Whitney reusable rocket engine program to test the 1.1 MN thrust XLR-129 engine. The tank of spherical shape with an inside diameter of 2.6 m and a stainless steel wall of about 300 mm thickness could hold some 9 m^3 of LH_2 at pressures up to 45.5 MPa to be emptied during a 10 s test run [Mulready 2001].

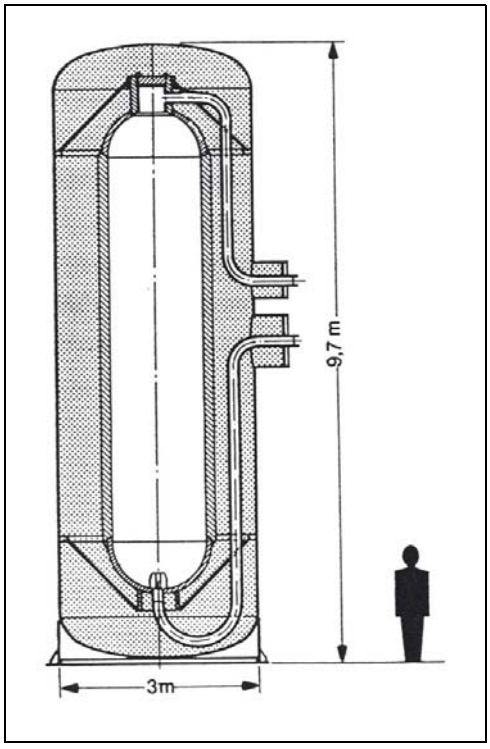

Figure 4-8. Schematic of the high-pressure LH_2 tank used for rocket engine testing in Germany [Ewald 1987]

5. TRANSPORTATION OF LIQUID HYDROGEN

Most of the hydrogen produced today is transported over short distances only, mainly by pipeline, e.g., on-site in refineries. Pipeline distribution is most effective for large flows and amounts today to approximately 240 t/d. Larger grids connecting H_2 producers with H_2 consumers are being operated in Europe and the United States. The transportation over longer distances is primarily by ship or truck in liquefied form or, to a much smaller amount in gaseous form. For distribution closer to the point of end-use, smaller-sized tanks are used. If the application of hydrogen as a fuel will increase in future, the transportation and distribution via tank ship and pipeline might be in most cases the best option.

Design criteria for LH_2 container used in transportation are essentially the same as for LH_2 storage containers. Differences refer, e.g., to the degree of insulation required which is lower in short-term transportation compared to long-term storage. Also, in general, geometry and weight are limited. Only the cryogenic propellant tanks for space vehicles are characterized by a different concept.

5.1. Road Transportation of LH_2

With increasing activities using liquid hydrogen, trailers were developed for LH_2 road transportation. Fig. 5-1 shows the one-axle U-1 semi-trailer used in the 1950s, the first to get permission for hauling LH_2. The tank had a capacity of 26.5 m^3 and an estimated boil-off loss rate of 2 %/d. Main problems were encountered with the truck-weighing officials who were puzzled about the single axle system such that it was later replaced with two-axle trailers, although not necessary for the full-size tanker because of the light weight (but it could not be disclosed to the officials because of the secrecy of the load) [Sloop 1978]. A modern LH_2 truck is shown in Fig. 5-2.

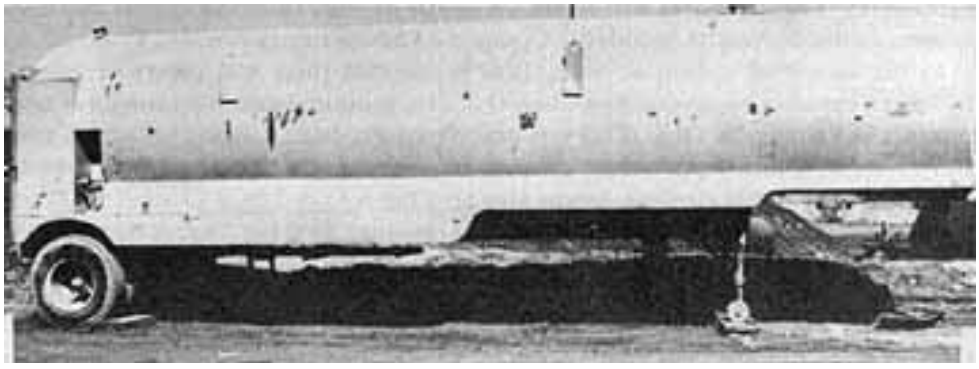

Figure 5-1. One-axle semi-trailer U-1 for LH_2 highway transportation [Sloop 1978] (Courtesy of AF)

"The single-axle is OK while it is unloaded",

said the truck-weighing official to the driver.

"But don't bring it back here when you fill it up." (The trailer was fully loaded!) [Mulready 2001]

Figure 5-2. Modern LH_2 road truck
(Courtesy of Air Products)

As of 1994, road transportation of hydrogen in Europe was about 311 million Nm^3. In Germany, it is 140 million Nm^3 with 10 % as liquid. The number of deliveries is about 50,000 per year, of which ~2300 are LH_2 deliveries. In the USA, LH_2 truck deliveries are estimated to 15,000 per year providing approx. 180 tons of LH_2 to customers [Danieli 1997, Trill 1997]. The hydrogen quantity transported as liquid is with ~2.4 t/d larger by a factor of about 7 compared to the gaseous transport in tube trailers [Simbeck 2002]. A more recent figure is ~250 t of LH_2 per day by truck compared to 470 t or 5 million Nm^3 per day via pipeline [Ogden 2004]. Substituting conventional gasoline fuel by liquid hydrogen would increase the number of tank truck transports by a factor of three.

LH_2 Transportation Activities of Air Products

The US gas company Air Products is [Guthrie 2006]:

- operating 75 LH_2 tank trucks which are
- driving ~13 million km per year;
- transporting ~265,000 Nm^3 of LH_2 per year; and
- have delivered ~91,000 metric tons of LH_2 over 25 years without any significant incident with regard to hydrogen.

Unlike conventional fuels, the transportation of hydrogen by trucks is limited with regard to volume rather than weight. Today's modern liquid hydrogen trucks can carry up to 3.5 - 4 t or more than 50 m^3 of LH_2. Gardner Cryogenics is said to be the first company to operate ~65 m^3 semi-trailers for LH_2 road transportation. Typical pressure in superinsulated tanks with additional LN_2 shield is 0.15 - 0.2 MPa (maximum pressure: 1.11 MPa). The gross weight of a tank truck is ~40 t. The potential hazard of stratification in the tank does not really occur in transportation, because the liquid is stirred by the movement and kept in thermal equilibrium.

In contrast, the amount of gaseous H_2 transported in pressure tube trailers is by at least a factor of 10 smaller, not more than 300 kg per truck load, equivalent to about 3300 Nm^3. LH_2 trucks will be preferably used to meet demands of a growing market in near future.

5.2. Maritime Transportation of LH_2

Barges carrying liquid hydrogen have been used for fuel supply within the US and French space programs. Storage containers with a capacity of 947 m^3 of LH_2 (Fig. 5-3) are being used on the way from Louisiana to Florida since the NASA Apollo project, today serving the space shuttle. The European Ariane project was supplied with LH_2 by maritime transportation from New Orleans to Kourou, French Guiana, in 20 m^3 storage vessels with vapor or LN_2 cooled multilayer insulation [Peschka 1992]. These transports were discontinued with the operation of the 5 t/d capacity, on-site liquefaction plant since 1990.

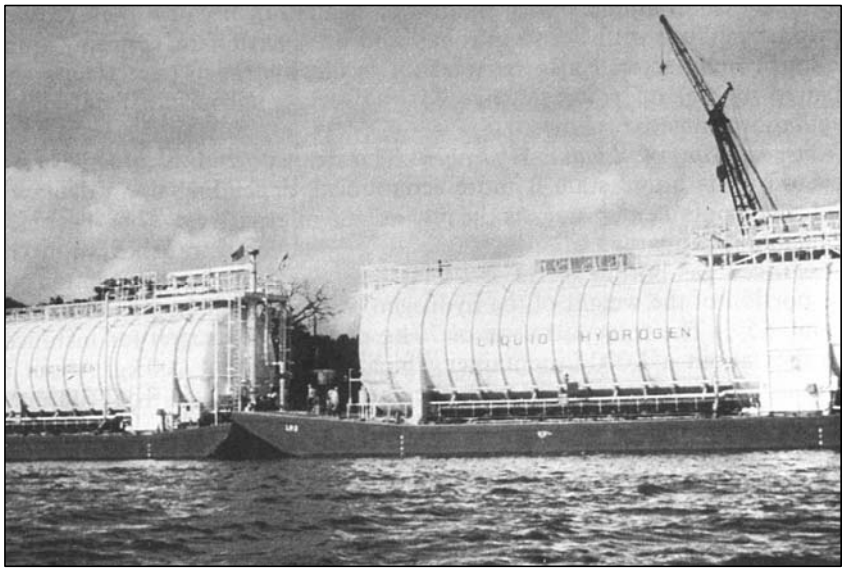

Figure 5-3. NASA LH_2 transportation by barge carrier to the Kennedy Space Center (Courtesy of NASA)

Various ship designs have been developed within the Euro-Quebec project for future maritime transportation (between Canada and Europe) [Giacomazzi 1993, Petersen 1994]. The barge carrier considered is being designed as a dock ship with a total length of 180 m and a width of 29 m carrying five barges (see also previous chapter) to contain a total of 15,000 m^3 of LH_2 (Fig. 5-4). Its safety features are a double-walled hull, a distance of 6.5 m between side shell and barge, and a distance of 11 m between ship bottom and vessel. The ship is powered by 10 MW diesel engines and reaches a speed of ~18 kt (about 33 km/h).

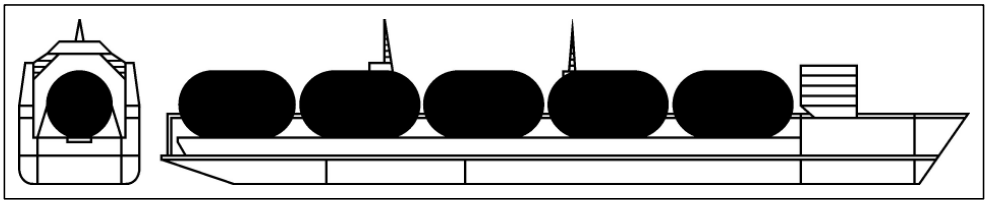

Figure 5-4. Dock ship of 180 m length to carry 15,000 m^3 of LH_2 in five barges

Follow-on LH_2 tank ships are the dock ship and the catamaran-type, so-called SWATH ship (Small Waterplane Area Twin Hull) developed by the German companies Howaldtswerke Deutsche Werft, Noell-LGA Gastechnik, and Germanischer Lloyd [Petersen 1994]. Both are designed for a load capacity of 125,000 m^3 to take up 8150 tons of LH_2. The SWATH ship (Fig. 5-5, left) is superior to the dock ship in that it has a lower weight and lower energy consumption per sea mile. With a length of more than 300 m, it carries four spherical LH_2

tanks. The hydrogen propulsion system proposed, for which the LH_2 as well as the boil-off losses (~0.1 %/d) is to be used, is a gas turbine with steam injection of 41 MW. The system allows to regain a part of the technical work that was introduced during the liquefaction process ("Enhanced Cryogen Exergy Recovery System", ECERS).

A flow diagram of the exergy or technically usable energy (based on relative numbers) for LH_2 transportation with a SWATH ship is given in Fig. 5-6. The gross primary energy input by hydro power, in the figure E_{tot} = 100 arbitrary units, corresponds to 310 MJ/kg of LH_2. The overall efficiency of the system has been assessed to be 42 % translating into an available energy of 130.2 MJ/kg. As indicated on the left side of the figure, a fraction of E_{tr} = 10.4 % of the primary energy input is needed for the hydrogen-fueled propulsion system of the ship. Other major losses are due to the electrolyis step and subsequent liquefaction of the H_2 gas [Petersen 1994].

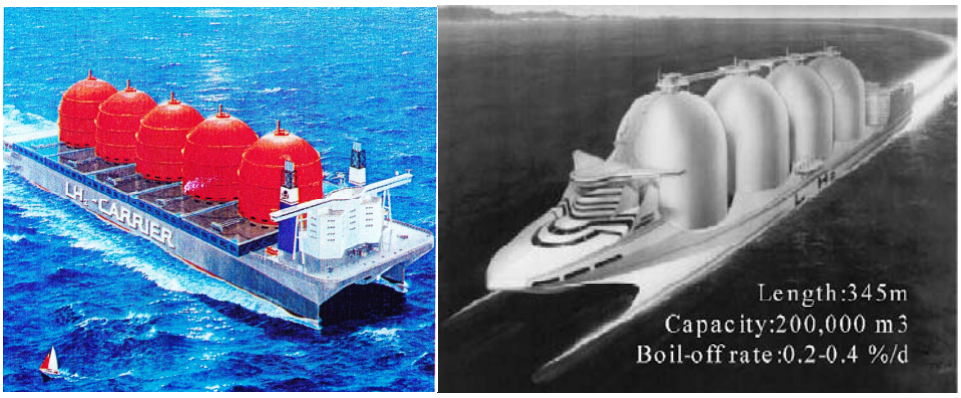

Figure 5-5. Barge carrier concepts for LH_2 transportation from the Euro-Quebec project (left) (Courtesy by Germanischer Lloyd and Howaldtswerke Deutsche Werft AG), and the Japanese WE-NET project (right) [Hijikata 2002]

Studies of LH_2 maritime transportation were also conducted in Japan based on their broad experience of LNG ship construction. Within the former WE-NET ("World Energy Network", see chapter 7) project, ships were concepted at a scale to deliver a 10-days supply of LH_2 as fuel to a 1000 MW(e) gas turbine power plant consuming 1200 t of LH_2 per day (Fig. 5-5, right). With the additional consumption of H_2 for the 6000 sea miles trip (~11,100 km) every 10 days plus estimated losses, one transport with the 345 m long ship was to carry some 200,000 m^3 (or ~14,000 t) of LH_2. Two tank concepts have been suggested: the ISI SPB self-supporting prismatic tank system with a 100,000 m^3 capacity and an estimated boil-off rate of 0.2 - 0.4 % per day, and the MOSS self-supporting spherical tank system with a 50,000 m^3 capacity and a 0.1 %/d boil-off rate. Boil-off losses were to be consumed in the hydrogen ship engines with a power of two times 30 MW allowing a speed of up to ~50 km/h [Abe 1998].

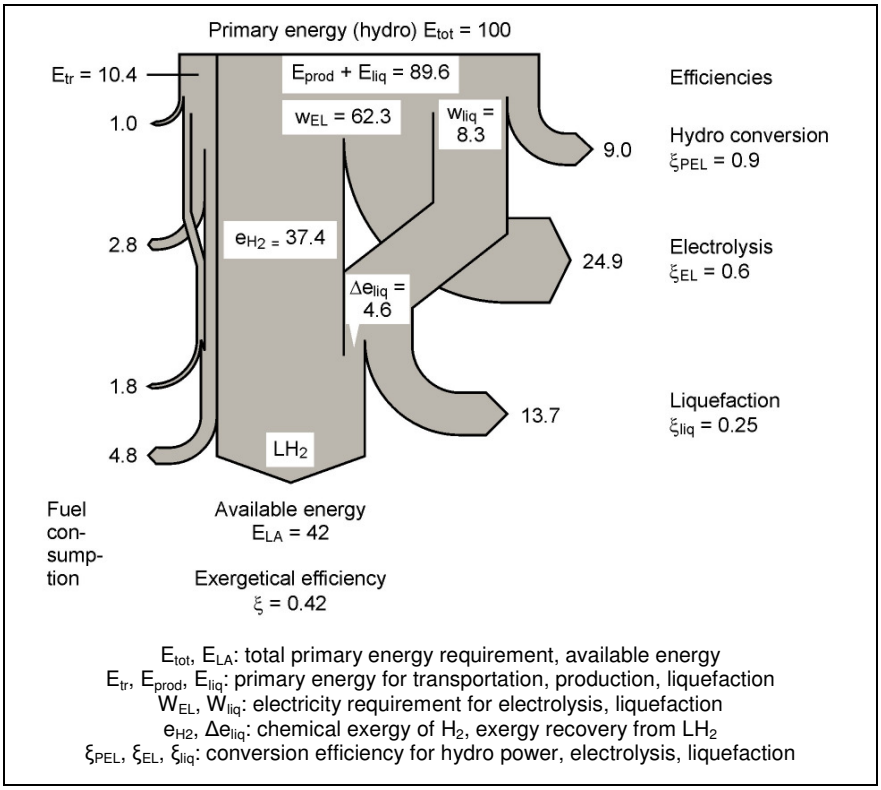

Figure 5-6. Exergy diagram for sea-borne LH_2 transportation [Petersen 1994]

Flow Primary Energy Consumption in Germany

The Euro-Quebec Hydro-Hydrogen pilot project was designed to deliver 14,600 tons of LH_2 per year from Canada to Hamburg. One "reference" barge carrier is able to transport 1065 tons, which translates into 13.7 shipments per year. The amount of LH_2 arriving in Hamburg corresponds to a power of 74 MW or $6.48*10^8$ kWh/yr.

Primary energy consumption in Germany in 2006 was 345 million tons of oil equivalent (TOE) or approx. $4*10^{12}$ kWh. The assumption that just 1 % of this energy be provided in form of hydrogen means a supply of 1 million tons of H_2 or almost 1000 reference ship loads per year, or 3 ship loads per day, arriving at Hamburg harbor. A large-scale hydrogen economy, however, would require the employment of larger tank ships such as SWATH. The above figure of energy to be transported then corresponds to some 125 loaded LH_2 SWATH ships per year arriving at the coast in North Germany.

For comparison: In 2000, every 20 hours, an LNG tank ship entered Tokyo Bay; one LNG cargo per week entered Boston harbor [Bainbridge 2002].

5.3. Rail Transportation of LH_2

The transportation of cryogens in railway tank cars started in the beginning of the 1940s, where LOX was increasingly needed for the steel production. Liquid hydrogen transports in rail cars began in the 1960s by the Linde company using a 107 m^3 tank with a multiple layer insulation. Measured boil-off rate was 0.2 %/d. The US company Praxair is operating a fleet of 16 hydrogen rail cars. They are operated at a working overpressure of 55 kPa with a pressure control system to open the safety relief valve at an overpressure of 117 kPa. The quantities of LH_2 transported in rail cars are approx. 70 tons or about 10 rail car loads per month [Danieli 1997].

5.4. Aircraft Transportation of LH_2

In the 1950s, at a time when liquefaction production in the USA was still scarce and a rapid transport to the test sites required, air-transportable dewars of 750 l capacity were developed with the special aim to sustain rough treatment. They were double-walled with high vacuum in the inner space and the outer wall kept at LN_2 temperature and with the LN_2 container itself surrounded by another vacuum space. With a remaining heat flow into the LH_2 of 4 W, the boil-off rate was with 1 %/d comparatively low [Sloop 1978].

Arthur D. Little Inc. developed a 2 m^3 LH_2 storage and transportation vessel surrounded by a closed-cycle helium refrigerator leading to a virtually zero-boil-off rate. It weighed more than 18 t and needed the space of a full semi-trailer [Sloop 1978].

The transportation of LH_2 as a payload onboard an aircraft has been considered an alternative delivery scheme to the ship transport including the option of a cryo-fueling of the aircraft itself. The advantages of air transportation is the light weight of the LH_2, a reduced boil-off loss, the short traveling duration, the direct accessibility of the production site, and the reduced buffer storage required. Drawback is the large number of deliveries in a large-scale supply connected with an extensive ground infrastructure and last, but not least, the lack of any practical experience [Meratla 1996]. Besides, at present, the transportation of LH_2 in cargo aircraft is prohibited by US legislation.

Also within the Euro-Quebec project, air transportation of LH_2 across the Atlantic Ocean was considered for some time a potential option. The full payload capacity of an Airbus A300-600 would cover the entire daily production of 42.7 t of LH_2. The overall energy yield, however, was estimated to be as low as 35 % compared with 45 % for transportation by ship. Also the fact that the energy demand of transportation in an aircraft was as high as the payload itself, was deemed unacceptable [Dechema 1987]. Within the Japanese WE-NET project, the possibility of LH_2 air transportation was also investigated conceiving two airplanes with a payload of 454 t for a distance of 5000 km at a speed of ~740 km/h to be sufficient for the fuel supply to a 1000 MW(e) H_2 power plant [NEDO 1996].

5.5. Pipeline Transportation of LH_2

Pipeline transportation of liquid hydrogen is realized on a small scale and short range. Similar to LH_2 storage tanks, pipelines are of double-wall design and vacuum-jacketed. Stainless steel is usually taken for the inner line with low heat conduction spacers as a support in the vacuum jacket. Because of the high cost which increase linearly with distance, LH_2 pipelines are economically attractive only for short distances. The transfer is done by pressure difference rather than by pumps. Major concerns, apart from heat leakage, are the mechanical stress imposed on the inner line due to contraction/expansion, pressure oscillations upon cooldown, or two-phase flow. Therefore cryogenic pipes must be sufficiently flexible which can be done by appropriate pipe routing and expansion joints.

In the late 1950s, during the hydrogen engine testing at the Pratt&Whintney test center in Florida, the LH_2 storage tanks of the 4.5 t/d capacity liquefier were connected to the engine and components test site by a double-walled, vacuum-jacketed pipeline. It had a 75 mm inner diameter and a length of 610 m which could provide LH_2 at a rate of up to 1700 l/min. But when becoming aware of the significant quantities lost due to cool-down of the lines, it was considered more efficient to transport the LH_2 in dewars on the road and run the engines directly from the truck [Sloop 1978, Mulready 2001].

The Kennedy Space Center uses today an LH_2 (and LOX) pipeline of ~600 m length with an inner pipe diameter of 150 mm. The flow rates are up to 250 m^3/min of LH_2 and 100 m^3/min of LOX, respectively [Edeskuty 1972].

During the period of chill-down of an LH_2 line, a two-phase flow develops which is stratified for horizontal flows as is schematically shown in Fig. 5-7 [Mei 2006] exhibiting a vapor layer above the liquid due to vaporization and also a thin film underneath the liquid layer. This phenomenon is encountered particularly in refueling lines where chill-down is required before the fueling process itself begins to avoid the gaseous phase to enter the tank.

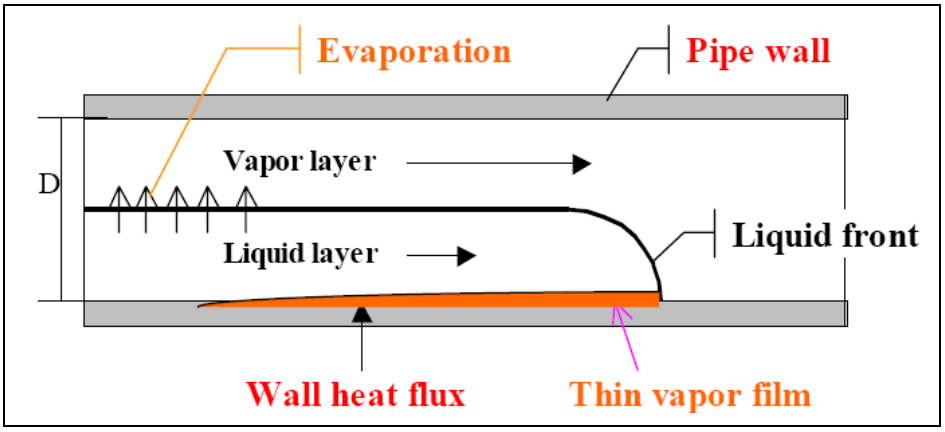

Figure 5-7. Two-phase flow in a horizontal line [Mei 2006]

For still large temperature differences between fluid and wall, a gaseous film develops between liquid and surface (film boiling regime). With decreasing temperature difference, passing the Leidenfrost temperature, the cold liquid is getting into contact with the wall (nucleate boiling regime), before the nucleate boiling is eventually replaced by pure convection.

Apart from pressure drop, also heat transfer in transport pipes is complex. While for single-phase flows, heat transfer is predominantly by convection, there are significant differences in heat transfer between the gaseous or the liquid phase and the wall in two-phase flows. Flow models have been developed at the University of Florida to account for the above phenomena for predicting flow and temperature distribution in both vertical and horizontal flows Fig. 5-8 presents the calculated temperature distribution in the wall of a pipe through which LN_2 is flowing, for different moments during the chill-down phase. It indicates that the cooling process in the wall is much slower in regions with contact to the gaseous phase.

The two-phase solid-liquid slush hydrogen has similar flow characteristics in a pipeline like "normal" liquid hydrogen as long as the mass fraction of the solid phase is less than 50 % [Miyake 1995].

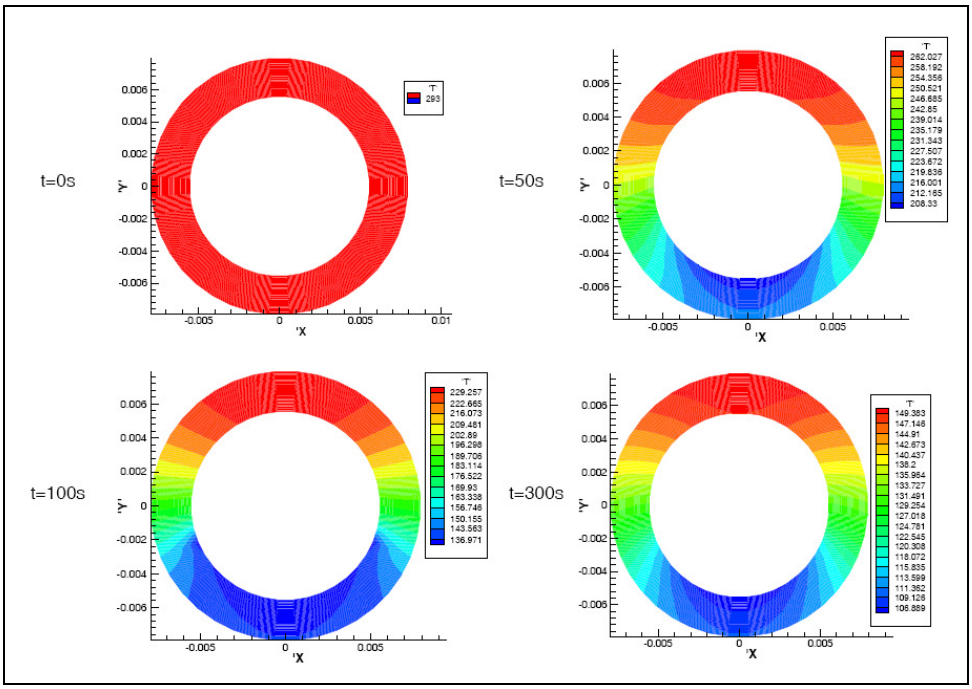

Figure 5-8. Calculated temperature distribution in the pipeline wall (thickness: 4.8 mm) at different times for an LN_2 flow at ~50 mm/s through a concentric tube (Temperature of LN_2: 77 K) [Mei 2006]

A Government-funded project in Germany, named “Integrated Cable Energy for Fuel and Power” or “icefuel” [BMBF 2006], starting in 2006, is aiming at a new, highly efficient energy infrastructure. A system for energy storage and the transportation of both chemical and electric energy as part of a decentralized infrastructure will be developed and tested. The goal is to design a flexible, thermally insulated line for the simultaneous transport of cryogenic liquids (LH_2 or LNG), electricity, and data via high-temperature superconducting material. In a second phase of “icefuel”, it is planned to demonstrate the concept on a pilot-plant scale.

6. SAFETY IN HANDLING LIQUID HYDROGEN

6.1. Safety Aspects of Cryogenic Storage

Many different situations are conceivable which can give rise to the emission of a flammable substance and which have great influence on the evolution of a vapor cloud. Depending on the thermodynamic conditions of the fluid, it can be released as a liquid or a gas or a two-phase mixture. The component, from which the substance is released, may be a tank, a pump, a valve, pipe work or other equipment. The orifice, through which it is leaking, can vary over different shapes and sizes. The leaking fluid can flow into different geometries.

Main safety goal of cryogenic storage tanks is the prevention of damage to the inner container. Mitigation measures to reduce the risk of a tank loss are

- Properly designed pressure relief;
- Minimum pipework and ancillary equipment;
- Backup instrumentation.
- Water spray system;
- Availability of sufficient quantity of water/foam;
- Prevention of overfilling;
- Generous spacing between tanks;

Major sources of hazards for cryogenic tanks are rapid mechanical changes of the system such as pipe ruptures. They may cause blast waves and high exit velocities or catalytic effects at the fracture location; they also may result in a jet fire or an unconfined vapor cloud explosion (UVCE). Also thermal changes such as rapid cooling of connecting elements or heat ingress (loss of isolation vacuum) may lead to mechanical loads on the system and significantly enhanced vaporization rates of the cryogen. At elevated temperatures and pressures, hydrogen attacks mild steels severely, causing decarburization and embrittlement. This is a serious concern in any situation involving storage or transfer of hydrogen gas under pressure. Proper material selection, e.g., special alloy steels, and technology is required to prevent embrittlement.

If the pressure in an LH_2 tank is kept constant, i.e., the vapor boil-off being removed, the temperature also remains constant (auto-refrigeration). If the boil-off is not removed, both temperature and pressure will rise. Thermal expansion of the cryogen also results in a pressure increase. Thermal expansion coefficients are higher for cryogens with lower boiling point. Therefore overfilling must be avoided.

Another hazardous situation is given, if air penetrates the system leading to the formation of condensation products of liquid/solid air or ice with the risk of plugging pipes or valves.

If there is heat input in a confined volume of a cryogen, the pressure will rise. The container will eventually rupture, if no or not sufficient gas can be vented from the system. Therefore a safe and reliable relief system must be provided. At closed valve, the heat input from the

outside initiates a thermal stratification (Fig. 6-1), which makes the pressurization process somewhat faster than in the case of thermal equilibrium. However, the relative heat transfer into the tank is lower, the larger the tank and the better the surface-to-volume ratio and the insulation. The speed of pressurization also depends on the boiling temperature of the cryogen. The lower the boiling point, the stronger is the driving force for heat input.

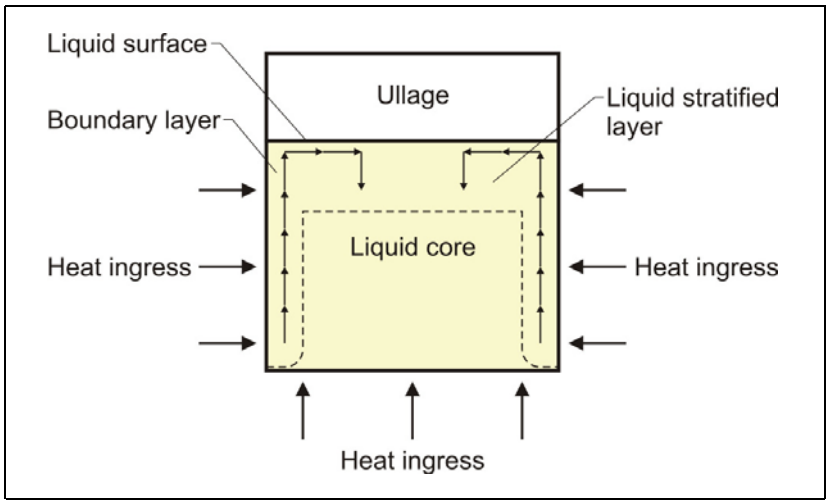

Figure 6-1. Thermal stratification in LH_2 tank [Sherif 2003]

A calculation model to describe thermal stratification has been developed which allows the determination of pressure rise rates and temperature and velocity profiles dependent on the heat input from the bottom or the side walls and the ortho-para conversion [Sherif 2003]. Thermal stratification results in higher temperatures in certain regions of the tank and could lead to cavitation. Pressures and temperatures were found to strongly increase with enhanced heat transfer; also stratification develops faster. For a higher fill level, pressures reach higher values, while the rate of pressure rise remains about the same. Both pressures and temperatures were also found higher for smaller tank sizes.

All liquid hydrogen storage installations should be located in the open air and away from electric power cables. In general, storage tanks for refrigerated liquids, e.g., LNG, require an impoundment area to retain the liquid in case of a leakage, with separate bunds for the single tank units. Main purpose is to limit the vaporization rate and the size of the evolving flammable vapor cloud. For LH_2, however, it may be preferable to use neither dikes nor barricades. In order to maximize the input of ambient heat thus enhancing the buoyancy and reducing the duration of a hazardous condition, artificial slopes or other topographical features should rather be used instead in order to direct the spilled LH_2 away from areas to be protected [NFPA 2005]. Further means to increase the vaporization rate is, e.g., a gravel ground and benefit from the dispersion mechanism supported by the high spill and vaporization induced turbulence.

Undesired events are caused by either human error or component failure or external impact. They can occur during steady-state operation or during the loading/unloading process such as leakage or rupture of the pressure vessel, leakage or rupture of transfer lines, overfilling, vessel failure due to impact from outside, or BLEVE. According to the type of event and according to the state of the fluid, it may exhibit a different physical release behavior, if accidentally released:

- Volatile liquid at ambient conditions showing slow evaporation;
- Flashing liquefied gas under pressure showing immediate large flash-off and slower evaporation of any residue; considered as the most serious case;
- Semi-refrigerated liquefied gas under pressure and at low temperature showing initial flash-off and violent evaporation;
- Refrigerated liquefied gas at low temperature and atmospheric pressure showing initial flash-off and relatively slow evaporation;
- Gas under pressure showing large physical energy release.

Fire protection of storage serves the purpose to minimize hazards to personnel and loss as well as prevent a spreading of initial fire. For atmospheric storage, stationary or mobile water or foam spray systems are employed. In refrigerated storage, it has to be considered that heating and vaporization is much more rapid. Initial protection is given by fire proof insulation to obtain a fire resistance of at least two hours.

Once a fire is established, subsequent failures can occur; for example, pipework fails within approx. 15 minutes, if exposed to fire. The scale of fire/explosion on a storage tank can be very large. Fires can occur in the vapor phase of the tank or outside, when an escaping vapor cloud ignites. Causes for fires are often given due to malfunctions in the operation procedure such as overfilling, failure of instrumentation, or operator error.

If an LH_2 pool fire is extinguished, the remaining pool still continues to vaporize, where the developing vapour cloud could easily re-ignite. For hydrogen on fire, best practice is therefore to cut off or isolate the source and allow the fire to burn, until the hydrogen is consumed [NASA 1997].

6.2. Safety Distance

There is a wide variety of possibilities for the definition of “safety distance” and it is largely depending on country or document [Marangon 2007]. As commonly understood, a safety distance is the required minimum separation distance between a potential hazard source, e.g., the location of a flammable gas leakage, and the vulnerable object to be protected from an external impact. But apart from the difficulty in providing a precise definition, another problem arises with the necessity to select the appropriate method for quantifying a separation distance. Fixing of numerical values could be done by estimations assuming severe accident conditions or the application of probabilistic risk assessment methods taking account of mitigation measures such as, e.g., fire walls. And last but not least, there is a need for harmonization of the various approaches of quantification among the countries.

The separation distance is usually determined as a function of the quantity of hydrogen involved ("quantity-distance relationship"). It may be fixed on the basis of credible events taking account of – if referring to hydrogen – the evolving flammable atmosphere as well as of the heat and pressure wave resulting from a possible ignition. The separation distance can then be defined according to physically defined criteria, e.g., the dose of thermal radiation or the peak overpressure, to have reached a certain threshold value. A particular aspect is the risk of projectiles which may be thrown much further away than the blast pressure based safety distance. A basic prerequisite is the knowledge of the source term which is dependent on leak size and thermal dynamic conditions of the leaking substance. Small, hardly quantifiable leakages, e.g., from cracks in welding seams, will be a safety issue.

Safety distance guidelines approaches are often simplified. They may, however, not be applicable in situations where confinement and congestion could collect gas and influence the flame acceleration. For certain conditions, LH_2 releases may show dense gas behavior, and if such a dense cloud of cold hydrogen-air mixture will enter a partly confined and congested region, one should not expect simplified safety distance guidelines to be valid. In such complex situations, a quantitative risk assessment could be the appropriate tool.

A well established liquefied fuel storage tank design comprises the assessment of the consequences of potential accident scenarios. They should be based on estimated transient release rates or design spill rates as a function of pressure, orifice, detection time, disconnection time including certain safety margins.

In the case of an accidental release of liquefied gases from stationary tanks, plant layout should provide sufficient spacing for a vapor cloud to disperse before it can reach ignition sources and a possible explosion of the storage contents to pose a fire risk to adjoining facilities.

Examples of Quantity-Distance Relationships

As a result of the early testing with LH_2 release and combustion end of the 1950s, the Arthur D. Little company has given a recommendation for separation distances with regard to LH_2 storage tanks as is shown in Table 6-1 [ADL 1960]. It was based on the demand for minimizing the possibility of ignition of a vapour cloud released, eliminating the chance for a fire to travel to another tank site, and offering no confinement that could enhance the risk of DDT. Furthermore all storage tanks of a tank park should have individual diking, but sufficiently low (< 0.9 m), and a vent of at least 9.1 m above ground. Vented hydrogen should be mixed with inert gas, or flared if the continuous flow rate exceeds 0.23 kg/s.

In a study of 1960 [Zabetakis 1960] investigating the vaporization of LH_2 and the ignition of H_2-air vapor clouds above LH_2 pools, a conclusion was made that the quantity-distance relation valid at that time was very conservative. The recommendation as is shown in Fig. 6-2 as a step function is based on the assumption that the total content of an LH_2 storage tank of up to 45 t or 640 m^3 is released, ignited, and burnt (almost) instantaneously. The solid curves represent the estimated distances at which thermal radiation values reach a value of about 84 kJ/m^2. It represents the limit where flesh burns are created and certain combustible materials are expected to ignite. Curves are given for different humidity concentrations in the air where the severest case would be a zero water vapor content meaning that an essential radiation heat sink will be absent.

Table 6-1. Safety distances recommended by Arthur D. Little for LH_2 storage tanks with 4.5 - 45.4 t capacity [ADL 1960]

Minimum safety distance [m]	Item
16.2	Adjacent LH_2 tank for up to 45.4 t or 640 m^3
12.2	Adjacent LH_2 tank for up to 27.2 t or 380 m^3
8.2	Adjacent LH_2 tank for up to 13.6 t or 190 m^3
61	Other operating areas or service roads
152	Public highways

The quantity-distance relationships between a stored LH_2 mass and a safety distance to personnel and residential areas assuming no barricades are given in Figs. 6-3 and 6-4 [Hord 1978]. It is distinguished by means of differently defined threshold values between people and less demanding equipment, e.g., adjacent storage tanks, working buildings, or different with respect to fireballs, shrapnel, structural response, or physiological effects (heat radiation). Fig. 6-3 applies to the protection of personnel and inhabited buildings from hydrogen fire and from shrapnel in explosions. Separation distances may also differ for experimental and LH_2 storage areas (Fig. 6-4).

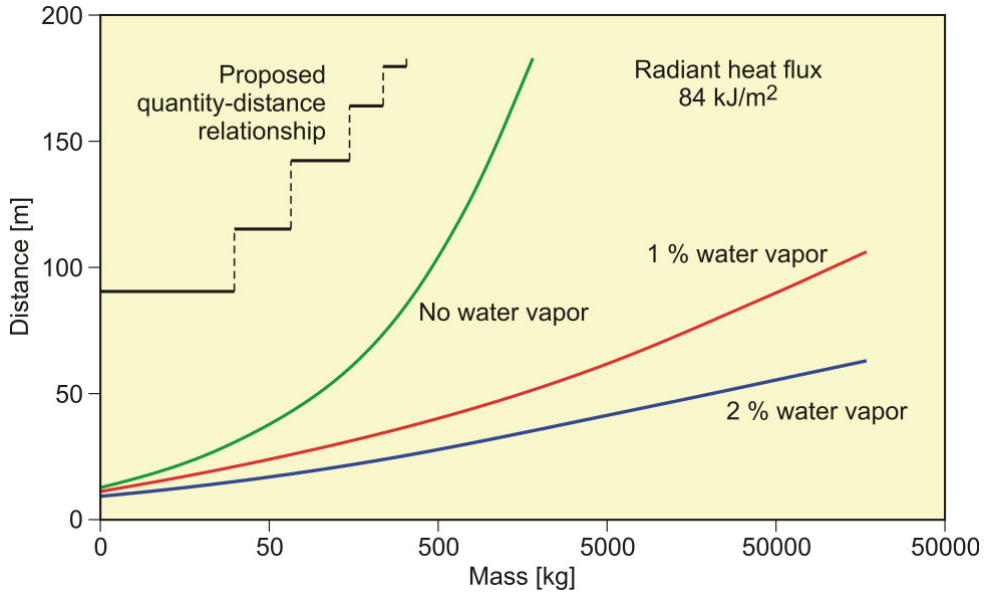

Figure 6-2. Distance at which a radiant flux of 84 kJ/m^2 would be received as a function of LH_2 mass assuming (almost) instantaneous release and combustion compared to recommended safety distance for residential areas [Zabetakis 1960]

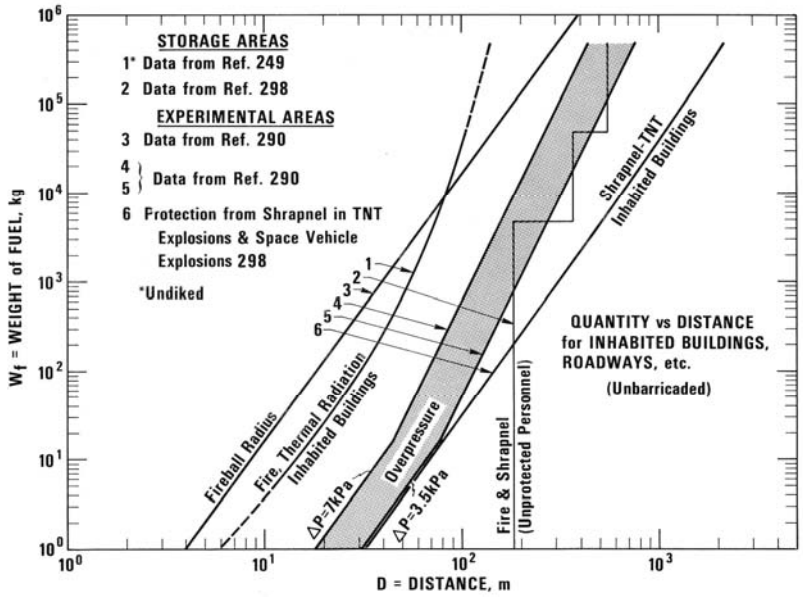

Figure 6-3. Quantity-distance relationship for protection of personnel and inhabited buildings near LH_2 storage containers in the USA [Hord 1978]

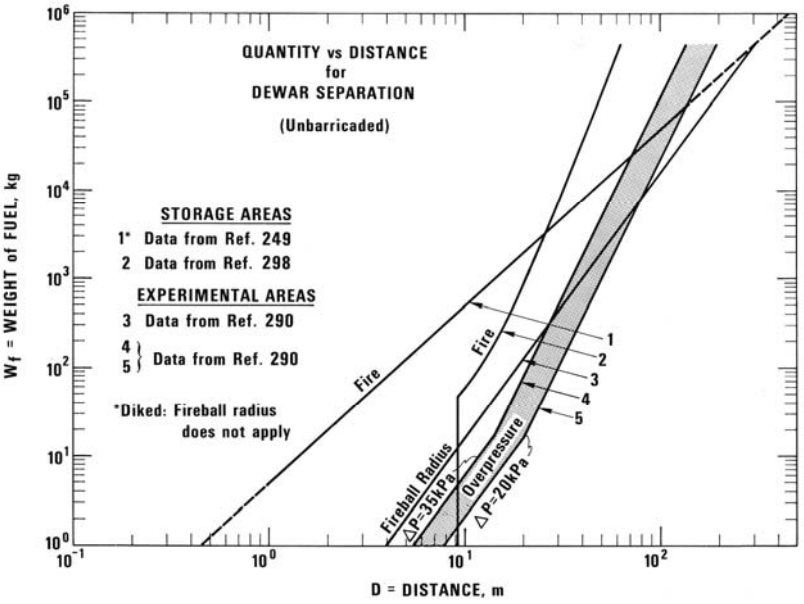

Figure 6-4. Quantity-distance relationship for protection of adjacent LH_2 storage containers in the USA [Hord 1978]

Design and operation of GH_2 and LH_2 storage installations in the USA today is regulated under the US OSHA (Occupational Safety and Health Administration) regulations as part of 29 CFR (Code of Federal Regulations). Here the minimum safety distance to be provided between the installation and people or property is defined as 15.3 m (50 ft) for gaseous H_2 amounts > 425 Nm^3. For LH_2 tanks containing more than 2.27 m^3 (600 gal), the respective distance must be at least 23 m [US-DOT 1997].

For hydrogen stored at US refueling stations, existing ASME pressure vessel standards apply requiring various distances between the pressurized tanks and public facilities depending on the amount of fuel stored. Current safety distance restrictions are significant. If reduced separation distances are desired, respective safety implications need to be investigated. On-board hydrogen storage tanks are being covered by US-DOT regulations. They appear to be reasonable in their present form [Bevilaqua 2001].

For customers' LH_2 storage installations in Europe, recommendations are given by the European Industrial Gases Association for minimum safety distances [EIGA 2002]. Some examples are listed in Table 6-2.

Table 6-2. Recommended safety distances in Europe for LH_2 storage at customer site [EIGA 2002]

Minimum safety distance [m]	Item
2.5	90 min fire resistant walls
6	Liquid oxygen storage
8	Flammable gas storage
10	Combustible liquids / solids road, railroad overhead power lines technical buildings
20	Occupied buildings air compression intake, air conditioning places of public assembly

Fig. 6-5 shows a few examples among the numerous efforts to determine quantity-distance-relationships between LH_2 storage systems and inhabited buildings as a function of LH_2 mass as were fixed in codes and standards from different institutions and countries, respectively. The wide variety is due to different assumptions made illustrating the variation in conservatism of these institutions that generate safety criteria.

In Japan, respective safety distances rules have to meet the "High Pressure Gas Safety Law" (Fig. 6-5). It prescribes at present the H_2 pressure at filling stations to be not higher than 40 MPa. The respective upper limit for vehicle tanks is 35 MPa. There are activities ongoing to shorten the presently valid safety distances for H_2 refueling stations. The corresponding investigation includes H_2 gas leakage experiments plus respective simulation calculations for demonstration purposes and also tests with ignition of the escaping gas as well as the effect of barriers.

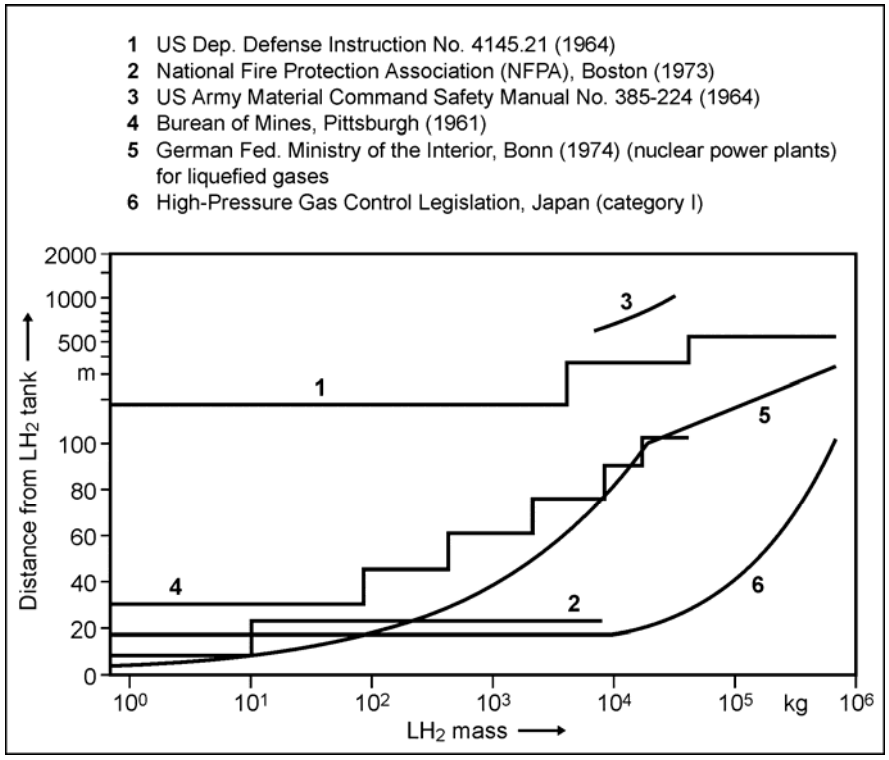

Figure 6-5. Safety distances (please note scale change on the ordinate) [Verfondern 1999]

A formula for the safety distance is generally acknowledged to have the form

$$R = k * M^{1/3} \tag{6-1}$$

where R – safety distance, m; M – mass of the flammable substance, kg.

The k-factor depends on the building to be protected (German recommendations: 2.5 - 8 for working building, 22 for residential building, 200 for no damage) and on the type of substance. The relation may be modified by damping parameters, if some sort of protective measure is applied, e.g., wall or earth coverage.

The above mass-distance relation applying a k-factor of 8 (green curve in Fig. 6-6) in combination with an overpressure history to be sustained is being used in the German legislation on the protection of nuclear power plants against external explosions [BMI 1976], which was the consequence from experimental activities within vapor cloud explosion programs. It applies to explosive substances which are handled in the neighborhood like production sites, waterways, railways, roads. Explosive substances which are required for the plant operation, are not included. In this guideline, a distinction is also made for flammable substances in different thermodynamic states.

The distance between nuclear plants and locations where explosive substances are stored or transported, shall be calculated according to the following mass - distance relation:

$$R = 8 * L^{1/3} \qquad (6\text{-}2)$$

If M is the maximum possible explosive inventory of a production facility or a storage tank or the biggest pipeline section between isolating equipment or transportation container in kg, then L is defined as the TNT equivalent in kg for explosive substances with

L = 1 * M for unsaturated hydrocarbons and non-liquefied gases;
L = 0.5 * M for gases liquefied under pressure;
L = 0.1 * M for gases liquefied at low temperatures;
L = 0.003 * M for combustible liquids with a flash point < 21 °C.

In terms of hydrogen, this is equivalent to a reduction of the k-factor from 8 m/kg$^{1/3}$ for pressurized gases down to 3.7 m/kg$^{1/3}$ for cryogenic liquids, respectively. It means in particular that for the same amount of hydrogen, the minimum safety distance can be cut to less than half, if the H_2 is present in liquid form. Or for the same safety distance, the allowable mass of H_2 as a liquid is 10 times as much as that of gaseous H_2. According to the guideline, the safety distance has to obey a minimum of 100 m [BMI 1976].

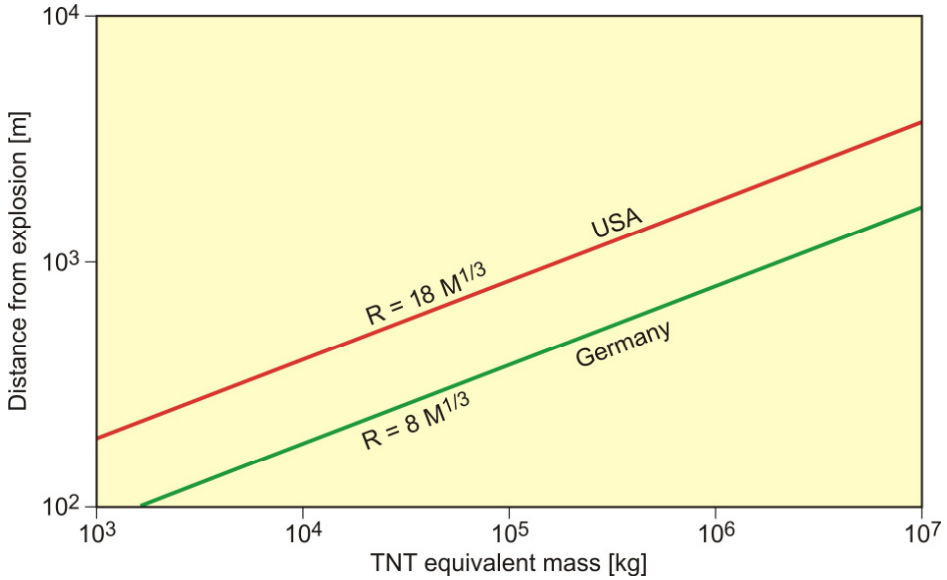

Figure 6-6. Safety distance as a function of the quantity of released liquefied gas according to the BMI guideline and the US regulatory guide 1.91 [Verfondern 2007]

In the USA, it is judged according to the US-AEC Regulatory Guide 1.91 [US-NRC 1978] that structures, systems, and components important to safety and designed for high wind loads are also capable of withstanding pressure peaks of at least 7 kPa resulting from explosions. No additional measures need to be taken, if the above equation with a k-factor of 18 is met

(red line in Fig. 6-6). The 1.91 guideline, however, offers additional options such as risk analysis for further reduction of the safety distance.

Safety distance guidelines approaches are often simplified. They may, however, not be applicable in situations where confinement or congestion may lead to flame acceleration. Also non-quantifiable leakages, e.g., from cracks in welding seams, cannot be applied. Another aspect is the risk of projectiles. Even if the blast pressure hazard is acceptable at a certain safety distance, dangerous projectiles may be thrown much further away.

6.3. Accidental Occurrences with Liquid Hydrogen

Numerous accidents have occurred in the past with the combustion or explosion of a flammable vapor cloud, the majority in the chemical process industries. According to UNEP (United Nations Environmental Programme) statistics, about 180 severe industrial accidents occurred worldwide between 1970 and 1990. These accidents were mainly caused by fires, explosions, or collision during transport, and killed about 8000 people, injured more than 20,000, and led to evacuations involving hundreds of thousands of people. Among the largest losses in the hydrocarbon process industries, vapor cloud explosions represent a significant portion and accounting for an even higher share in terms of the financial loss they have caused. Fig. 6-7 summarizes the type of accident for the 100 largest losses (out of ~5400 records, excluding off-shore events) in the hydrocarbon chemical industries during the 30-years period between 1972 and 2001 [Marsh 2003].

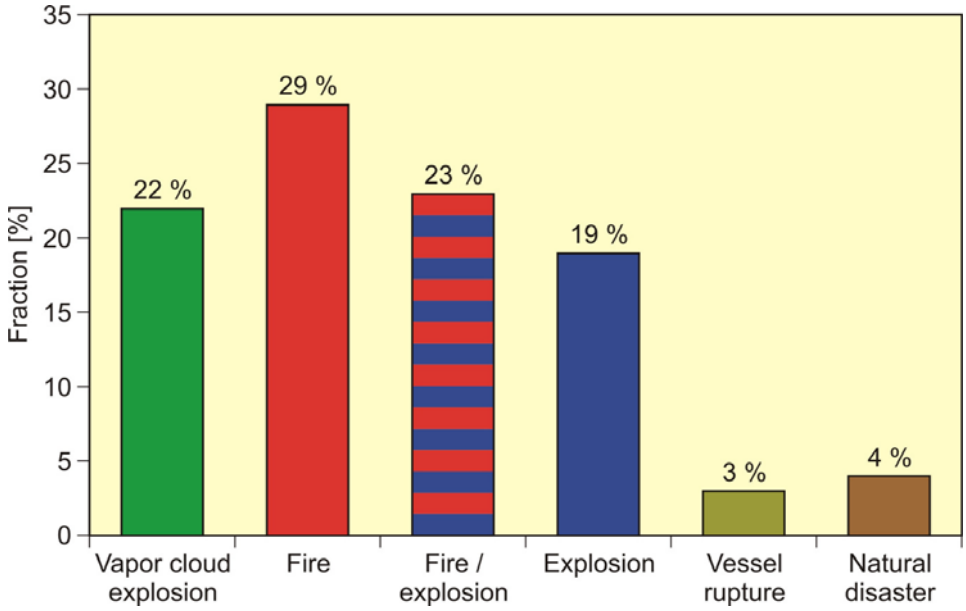

Figure 6-7. Type of loss for the 100 largest losses in the hydrocarbon industry between 1972 and 2001 [Marsh 2003]

6.3.1. Hydrogen Accident Statistics

During the first approximate 50 years of handling liquid hydrogen in small (lab-scale) quantities only, numerous inadvertent explosions occurred, fortunately not disastrous due to the small amounts. With increasing quantities handled and the need for larger storage devices, experimenters aware of its hazards used testing facilities which were equipped with safety devices. Initial difficulties in handling LH_2 were often caused by leakages from lines due to insufficient tightness of plumbing connections. Some incidents occurred in liquefaction plants resulting from the accumulation of solid air.

An evaluation of reports and statistics of accidents with hydrogen in industrial facilities in the period 1965-1977 covers a total of 409 accidents investigated with 78.5 % related to gaseous H_2, 20.8 % related to liquid H_2, and 0.7 % related to hydrides [Zalosh 1978]. Major findings were that accidents were mainly caused by leakage or insufficient purging or venting, and that most releases eventually led to ignition. Also spontaneous ignition was observed from jets escaping from a burst disk or a safety valve. In partially obstructed areas, most explosions resulted in a fast deflagration or even detonation. The average damage per accident was independent of the state of the H_2.

Foggy

From the Lockheed Aircraft "Skunk Works" test site in California, it was reported that within a three years period (in the 1950s) not a single accident occurred caused by the hydrogen. There was, however, one remarkable event during a test to simulate the temperature condition of a supersonic flight. A wooden-framed furnace which was put over the fuselage model to heat it up above 180°C, caught fire. Trying in vain to put out the fire with fire extinguishers, it was decided – as a precaution measure – that a nearby tank with 2000 l of LH_2 be dumped on the ground. Following the release was a 1.5 m thick layer of fog developing near the ground. Fortunate to all people standing right in the middle of the vapor cloud was that the hydrogen did not ignite. Fire fighters were wearing gas masks since they were not informed that the fog was caused by the LH_2 (due to the secrecy of the project) and eventually extinguished the fire [Rich 1995].

NASA statistics on 96 accidents during hydrogen operations revealed that ignition occurred in all cases with release into confined spaces, and in 60 % of the cases with release into the open atmosphere. Improper system purging was the cause in 25 % of the mishaps. Some cases were due to air entrainment into LH_2 systems. H_2 leaks were discovered to be mainly due to personnel not following prescribed procedures [Ordin 1974]. Considering accidents during transportation, in 71 % of the inadvertent H_2 release cases recorded, no ignition was observed, a trend that is also confirmed by NASA experience [Schödel 1978].

A description of the evaluation of 287 occurrences, of which 86 were with cryogenic H_2, is given in [Kreiser 1994]. Main conclusions from this analysis were:

- There is a high probability of an explosion of accidentally released gaseous hydrogen (96 %), whereas only about half of the occurrences with cyrogenic H_2 were leading to an ignition (Fig. 6-8).

- The perception of an LH_2 occurrence as an accident with its good visibility (condensation of moisture in the air) appears to be much stronger than with gaseous H_2 (hardly visible and rapidly diffusing away).

- The tendency of (partial) confinement to favor the formation of flammable H_2-air mixtures, flame acceleration, and overpressures is obvious for accidents with gaseous H_2, but can also be recognized for LH_2 (although the statistical basis is less strong).

- In most cases, hot surfaces or open fire represent the ignition source (21 % for gaseous H_2, 10 % for liquid H_2);

- With regard to injuries of humans: from 201 accidents with gaseous H_2, there were 56 with a total of 199 injuries corresponding to a ratio of ~1 injury per accident; from the 86 accidents with liquid H_2, there were 8 with person damage and a total of 10 injuries corresponding to a ratio of ~0.12 injuries per accident.

Excellent Safety Record

Incidents reported by Air Products [Ringland 1994]: From the approximately 6000 fills and 14,000 unloadings of LH_2 from truck per year, there were just five incidents reported between 1970 and 1993:

- Hose rupture during loading, no fire;
- Weld failure on truck while unloading, small fire;
- Trailer pull-away with filling hose attached, no fire;
- Customer station overfill, small fire;
- Valve leakage, small fire.

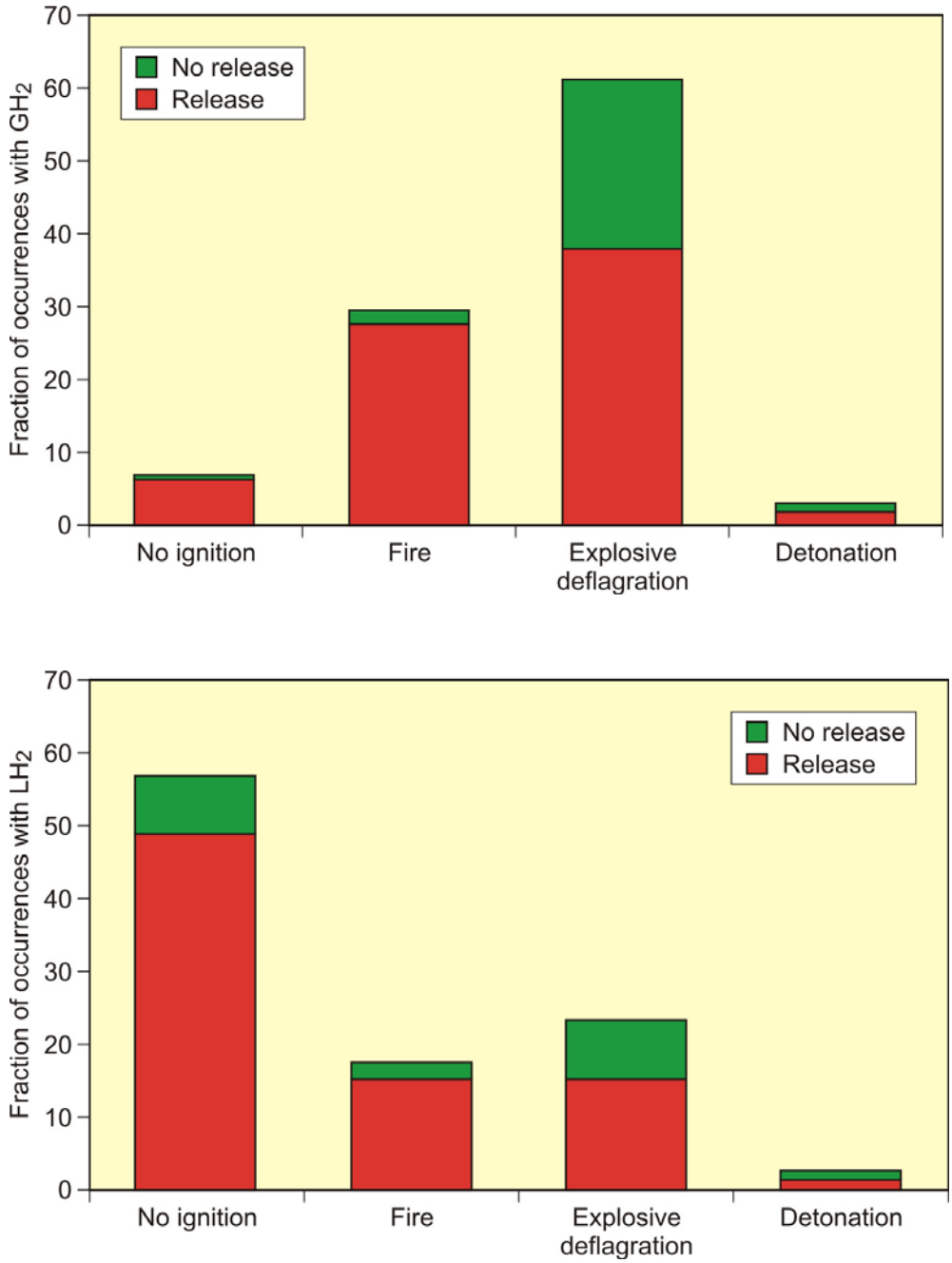

Figure 6-8. Statistics of investigated accidents with gaseous H_2 (top) and cryogenic H_2 (bottom) [Kreiser 1994]

6.3.2. Examples of Major Accidental Occurrences

In the following, various accidental occurrences with hydrogen or natural gas are listed to give an idea about the variety of causes and consequences that one can encounter at the presence of flammable gas mixtures. They all taught lessons to be learnt and contributed more or less to a subsequent modification, improvement, extension of the existing set of codes and standards which provides the basis for a safe handling of flammable hazardous substances. An extended list of accidents, where mostly hydrocarbons were involved, is given in [Gugan 1978].

1785 The first severe accident with hydrogen occurred in 1785, when two Frenchman were flying a balloon filled with hydrogen in an attempt to cross the Channel to England. It was also carrying a small hot-air balloon to control the altitude. This eventually ignited the hydrogen gas demonstrating its extremely high flammability. Both pilots were killed in this accident [Sloop 1978].

1937 The spectacular disaster at Lakehurst with the 'Hindenburg', the largest airship ever built, has set a sudden end to this type of transportation system. The airship (Zeppelin) filled with 200,000 Nm^3 of hydrogen gas caught fire during the docking procedure and was destroyed by fire within 32 s. The flame speed was assessed to be 50 m/s. One of various theories for the cause of the ignition assumes that it was the outside protective paint on the skin of the airship, which was later found to contain highly flammable substances such as iron oxide and aluminum and, in the case of the Hindenburg, caught fire during a thunderstorm [Baines 2000].

1944 An LNG liquefaction, storage and regasification plant at Cleveland was involved in a severe accident, when a new larger storage tank of 4500 m^3 capacity failed shortly after the installation. The steel of the tank contained only a low amount of nickel which made the tank brittle at cryogenic temperatures, and the tank ruptured. Approx. 2000 m^3 of LNG were spilled. The tank did not have an impoundment area. The LNG penetrated a sewer system and eventually ignited. This accident claiming the life of 128 people, stopped virtually all LNG activities for a long time.

1964 In a test for a rocket nozzle, the Los Alamos National Laboratory at Jackass Flat has conducted an intentional venting of 1000 kg of hydrogen at 23 MPa within 30 s, when unintentionally a spontaneous ignition occurred after 26 s. The burning gas cloud of approx. 9 m diameter and 45 m height contained about 9 kg of H_2. The flame speed reached about 35 m/s, the overpressure an estimated 3.5 kPa at buildings in a distance of about 60 m.

1972 In an LNG liquefaction and peak shaving plant in Montreal, a back flow of natural gas from the compressor to the nitrogen line occurred during defrosting operations. The valves on the nitrogen line were mistakenly not closed after completing the operation, causing overpressurization of the compressor. Natural gas could enter the control room and was ignited by smoking operators.

1973 A construction accident occurred at Staten Island in an LNG peak-shaving plant, when the roof of a storage tank collapsed. During liner repair works, the liner and later the thick, so-called self-extinguishing polyurethane foam insulation inside the

tank were accidentally ignited. The increase in temperature and pressure was so fast that the concrete dome of the tank was lifted and then collapsed down burying 40 construction workers. The ignition was made possible by the use of non-explosion-proof equipment.

1973 After a natural gas liquids pipeline rupture in Austin due to an improper weld, a flash fire occurred with the vapor cloud traveling approx. 800 m before it ignited after about 15 min. Six people were killed.

1979 The Cove Point LNG terminal in Maryland, USA, experienced an unexpected explosion. LNG was leaking through an inadequately tightened LNG pump electrical penetration seal, vaporized, passed through a 60 m underground electrical conduit, and entered an electrical substation where it finally ignited. One operator in the building was killed. Codes and standards which all were met at the time of the accident, were changed afterwards with particular consideration of equipment and systems downstream of pump seals.

1983 In Bontang, Indonesia, an LNG explosion occurred, when a heat exchanger failed due to overpressurization. It was caused by an inadvertently closed valve on a blow-down line, to which all relief systems were connected.

1986 The catastrophic accident of the Challenger Space Shuttle shortly after launching was said by NASA officials to have been caused by the failure of an O-ring rubber seal in one of the two solid rocket boosters due to erosion by hot gases. A steady flame developed which was directed towards the surface of the External Tank containing the LH_2 and LOX tanks. The flame eventually breached the tank resulting in an explosive combustion of the hydrogen and oxygen. This official NASA theory was questioned in another study assuming so-called "phantom" fires which resulted from undetected LH_2 leakages (< 1.4 kg/s) from the External Tank and their early ignition at low altitude by plumes from the adjacent rocket booster causing a quick deterioration of the tank structure [NASA 1997, Chirivella 1997].

1987 In a tank truck accident near Columbus, Ohio, the truck overturned and the cryo-tank lost its vacuum. The vaporizing hydrogen was vented, but did not ignite, and therefore no significant damage was observed [Ringland 1994].

1989 An explosion of a 9000 gal (34 m^3) LH_2 storage tank took place, when – due to repair work on the vent stack – the vessel was purged with N_2 gas to boil away the LH_2. Pressure inside the vacuum jacket increased despite opening the vacuum valve eventually leading to a catastrophic tank rupture where one end of the tank blew off [Lodhi 1989].

1991 In a spectacular accident at an industrial site in Hanau, Germany, the catastrophic failure of a tank with pressurized hydrogen occurred. The 100 m^3 cylindrical pressure vessel with a total height of 16 m, a diameter of 2.8 m and a wall thickness of 22 mm was operated with a cyclic change of the inner pressure between 1.5 ("empty") and 4.5 ("full") MPa. At the time of the accident, the tank was filled with with 370 kg of H_2. The failure of the vessel was caused by a fatigue rupture near a longitudinal welding seam due to accelerated crack growth from H_2 embrittlement. The explosion resulted in severe damage within a radius of 1 km [Behrend 1993].

Although hydrogen has the reputation as a particularly dangerous fuel, the overall statement was made that the technology of handling H_2 as high-pressure gas or as liquid is successful and safe [Edeskuty 1996]. The excellent safety record, however, should not be extrapolated to a large-scale use in a hydrogen economy, since experience so far is mainly based on the existence of well-trained personnel and extreme concern about system reliability. Hazards of hydrogen are generally recognized to be different than those of petroleum fuels, but not necessarily greater [Lipman 1996]. A similar conclusion was made in [Eichert 1992] saying that, if considering all processes of spillage, vaporization, vapor cloud spreading, and fire, liquid hydrogen has significant safety advantages versus conventional fuels due to shortest vaporization times, shortest combustion duration, and lowest thermal impact.

7. APPLICATIONS OF LIQUID HYDROGEN

After hydrogen has been first liquefied in 1898, liquid hydrogen was mainly applied in research for the production of low temperatures. A strong increase in the demand for LH_2 was given with the developing space aviation program in the USA. Some 40 years ago, almost all produced LH_2 was consumed in the various space programs. Although this share decreased to about 25 % by today, the space industry still is one of the main customers for liquid hydrogen. There is a wide variety of industrial customers for hydrogen which require, depending on the application area, different quantities and purities of hydrogen. Largest consumer is the chemical industry presently with a demand for hydrogen at an annual growth rate of 7 - 10 % [Wolf 2003]. Also the delivery of liquid hydrogen is strongly customer-dependent. Besides those who need the liquid directly (e.g., NASA), there are other customers who utilize gaseous H_2, but – for convenience and economic reasons – request delivery and storage as liquid. Furthermore sudden fluctuations are possible such like a demand increase after the (accidental) shutdown of an on-site H_2 production plant compensated by the purchase of LH_2, or a drop in the demand, if some customer starts to operate its own H_2 production line. Apart from the space industries, the primary commercial markets for LH_2 are in the chemical, metals, electronics, fats and oils, and glass industries [SRI 1990].

7.1. Liquid Hydrogen Use in the Industries

7.1.1. Chemical and Petrochemical Industries

By far the largest amount of hydrogen is consumed in the chemical and petrochemical industries. A non-energetic utilization of hydrogen is mainly given as raw material in the synthesis of ammonia (NH_3) for fertilizer and plastic production, methanol, polymers, or solvents. It is required in the direct reduction process of iron to iron sponge or raw iron and in the production of alcohols via oxo-synthesis. An indirect energetic utilization is given in refineries where the H_2 is used in catalytic cracking operations or hydro-treating to upgrade heavy and unsaturated compounds into lighter and more stable species. It is also needed in the production of synthetic fuels via Fischer-Tropsch synthesis, of methanol, or of synthetic natural gas. Furthermore it is used in the hydrogenation of coal and heavy crude oil.

Hydrogen is also taken to remove sulfur from crude oil and gasoline, and to purify gases, e.g., by capture of oxygen traces in argon. In power plants, LH_2 can be used for the cooling of large electric generators. Sites where no H_2 production plant is available, delivery is preferably in form of liquid hydrogen.

7.1.2. Metal Industry

In the metal industries, LH_2 is used in the metal production process directly (e.g., tungsten, tungsten carbide, molybdenum metal powder), and also, if mixed with inert gases, in secondary processes to act as reducing atmosphere in heat treating, sintering, copper brazing.

7.1.3. Electronic Industry

Highly pure hydrogen is mainly needed as a carrier gas for active elements as arsine and phosphine in the manufacture of integrated circuits, polycrystalline silicon for semiconductors, optical fibers for communication, or fused quartz. Pure water vapor required is generated from mixing oxygen with vaporized LH_2. The hydrogen is either used as atmosphere or as a clean burning fuel.

7.1.4. Food Industry

The properties of fats and oils are changing through hydrogenation of organic intermediate products like amines and fatty acids making food less susceptible to oxidation and spoilage.

7.1.5. Glass Industry

In the production process of glass, the hydrogen is used as an oxygen scavenging atmosphere (~6 % of H_2 and ~94 % of N_2), and to prevent oxidation of the large tin bath in the float glass process. Polishing and melting of high-quality optical glasses is done by means of a soot-free hydrogen flame.

7.2. Liquid Hydrogen as a Fuel

7.2.1. Space Rockets

The application of liquid hydrogen as a fuel in space rockets was suggested as early as 1903 by the Russian Konstantin E. Tsiolkovsky (Fig. 7-1), only a few years after hydrogen was first liquefied. In 1910, it was Robert H. Goddard who pointed out the advantages of LH_2, and in the 1920s, the German rocket pioneer Hermann Oberth argued for its use in the upper stage of space vehicles. All three rocket pioneers, however, never worked experimentally with liquid hydrogen.

The LH_2-LOX bipropellant system has an extremely high specific impulse performance, but drawbacks were seen in the low density leading to large tanks which would add to weight and drag. As can be seen from Table 7-1, liquid hydrogen shows extreme behavior in desired and undesired features.

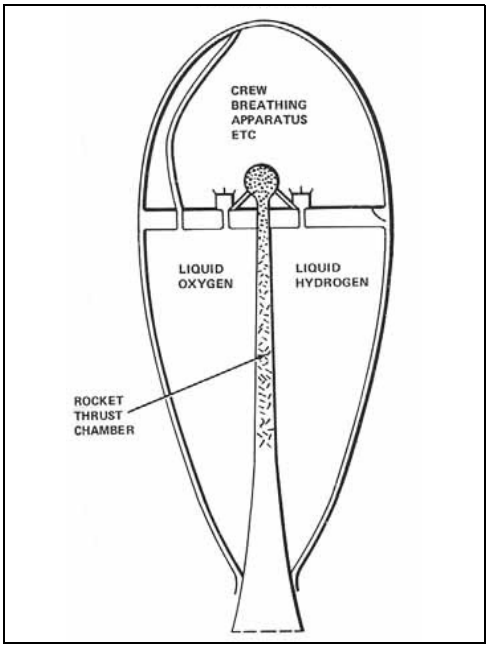

Figure 7-1. Tsiolkovsky manned rocket concept of 1903 with integral propellant tanks and thrust chamber in the rear [Sloop 1978]
(Courtesy of NASA)

Table 7-1. Pros and cons of liquid hydrogen as a rocket fuel

Characteristic	Requirement	Pro / Contra LH_2
High exhaust velocity	High heating value Low molecular mass	+ +
High fuel density	Smaller tanks Reduced drag forces Large payload capacity	– –
Cooling capacity	Low combustion temperature High thermal stability High heat capacity Low vapor pressure Low critical pressure	+
High reaction rate	Rapid conversion of energy to heat	+ +
Easy handling and storage	Low vapor pressure High shock stability High ignition energy Non-toxic, non-corrosive	–
Availability	Liquefaction capacity	o

LH_2 Tank Design

Also the cryogenic fuel tank design is completely different from those previously described designs (Chapter 4) due to the need of saving weight on the one hand and very short lifetimes on the other hand. LH_2 tanks in rockets or space ships are usually filled short before launch and emptied within minutes. According to the fuel tank design of the Centaur upper stage mounted on top of an Atlas rocket, the LH_2 is contained in thin-walled stainless steel tank structures. Rather than internal buttressing, an internal pressure is used to maintain shape of the tank and keep it rigid. The major safety concern here is that it has to sustain high aerodynamic loads and, in case of an unintended depressurization, tank and vehicle might collapse under their own weight.

The two propellants are separated by a double-walled bulkhead, two thin metal skins with a 6 mm fiberglass insulation in between. The hollow bulkhead interspace is filled with nitrogen which freezes out, if the LH_2 is given to the tank, creating a near perfect vacuum as additional thermal barrier against heat transfer from the LOX to the LH_2 tank. Furthermore, on the outside of the LH_2 vessel, fiberglass insulation panels are fixed to reduce boil-off from aerodynamic heating. An outer seal coating is applied to prevent air from contaminating the insulation. These panels are jettisoned in space. In later versions, the jettisonable panels were replaced by a fixed foam insulation system glued to the outside of the LH_2 tank reducing both weight and complexity and cost, and rather increased reliability [Dawson 2004].

The LH_2 tank of the Centaur combined with the more powerful Titan first stage rocket was additionally protected by a radiation shield which allowed a longer coasting period in space of 5 h compared to only 30 min before. In the follow-on Saturn-Centaur system, the LH_2 tank of Centaur was designed much larger with a bulkhead consisting of a two-layer foam blanket and a three-layer radiation shield. This system, however, was never operated in space due to cancellation of the project [Dawson 2004].

US Space Program

The first experiments with LH_2 in a small rocket engine were conducted in the late 1930s by the German Walter Thiel, who fought with various technical and other difficulties and eventually discontinued these activities. Wernher von Braun was once observing test operation of the Thiel engine and was mainly impressed by the numerous line leaks and difficulties of handling the LH_2. Later during his years involved in the US space program, he always remained an opponent of using LH_2 as rocket propellant.

First systematic experimental investigations in the USA to investigate hydrogen as a fuel for aircraft and to study the properties of LH_2 and the low-temperature impact on materials started at the Aerojet General Corporation in California (1945-49), the Ohio State University (1947-50), and the Jet Propulsion Laboratory in California (1948-49).

In August 1958, development began on the first large launch vehicle, later called Saturn, for lunar and deep space missions, i.e., the requirement of carrying a payload of some 4.5 tons. In 1958/59, it was decided in the USA to use LH_2 and LOX in the upper stages of Centaur and Saturn, both successful programs of unmanned space missions and manned moon voyages, respectively, using for the first time this high-energy propellant combination in practical applications.

Short-Lived

On Sept 21, 1948, the first delivery of 75 l of LH_2 to the Jet Propulsion Laboratory was made and used the same day in a rocket test. Surprising to the experimenters was the small fraction of LH_2 left available to testing. From the 75 liters,

- 21 % were lost by cooling the transport dewar;
- 16 % were lost by vaporization;
- 26 % were lost by cooling the already (LN_2) pre-cooled propellant tank;
- 37 % only were burnt in the rocket engine.

From the production of 7.5 m^3 in the first four months of testing, only 30 % of the LH_2 were consumed in the tests, while most was lost during storage and test delays. Production cost at that time were 45 US$/kg or about 3 US$/l of LH_2 [Sloop 1978].

Based on the experience with the LH_2-driven "304" jet engine (see section 7.2.3.), the Pratt&Whitney company began works in October 1958 on the development of RL-10, the first LH_2 fueled rocket engine. One of its innovative features was that the liquid hydrogen flowed through tubes inside the jacket of the combustion chamber for cooling as is illustrated in the bottom part of Fig. 7-7. A textured surface consisting of a special aluminum mesh, "Rigi-Mesh", was added to facilitate cooling. The LH_2 was gasified and expanded ("expander cycle") providing sufficient energy to drive the turbine and turbopumps. The hydrogen gas reached a temperature of 163 K at the turbine inlet. The exhaust gas from the pump is routed to the main combustion chamber (stage 2) where the remaining fuel is burnt at a very high efficiency. The engine design applying this expander cycle turned out to be much simpler than a conventional version [Mulready 2001]. Both innovative features of expander cycle and double-walled bulkhead were direct benefits from the properties of liquid hydrogen.

The RL-10 engine was first tested in 1959 on the company's test site in West Palm Beach in Florida. It could be started, stopped, and restarted with surprising reliability. The original engine had a height of 1.73 m, a diameter of 0.99 m, and a weight of 135 kg. With a propellant flow rate of 16 kg/s, it could achieve a thrust (at altitude) of 66.7 kN for a burn time of 470 s. Three years later, the engine successfully performed a "Preliminary Flight Rating Test". Subsequent testing was done on upgraded versions. By September 1963, the RL-10 counted 3300 firings on test stands; in space, there were more than 550 firings with just three failures associated with the engine. During the RL-10 engine development and testing, in total more than 100,000 m^3 of liquid hydrogen were consumed provided by the nearby large-scale liquefaction plant in West Palm Beach. No injury to any personnel due to hydrogen was reported in that period [Sloop 1978].

Safety Measure Broom

A safety measure for the operation staff at Cape Canaveral in the early days was to carry a broom when walking near a hydrogen line, since burning H_2 itself would not produce visible flames. It was considered safe to proceed, if the broom did not burst into flames [Dawson 2004].

The first rocket to operate with the cryogen propellants LH_2 and LOX was the Atlas-Centaur (Fig. 7-2) based on the idea of the German-US rocket technician Krafft A. Ehricke. Pushed by an Atlas rocket as the first stage to an altitude of about 240 km, Centaur represented the high-energy upper stage with its approximately 10 minutes of lifetime between booster shutdown and payload release. It used two RL-10 engines with a thrust of 65 kN (at altitude) and an exhaust velocity of 4245 m/s. One of the main objectives of the first Centaur tests was to prove the feasibility of cryogenic rocket fuels.

The first start of a Centaur rocket in May 1962, however, was a failure when 54 s into the mission, the missile blew up. Aerodynamic pressure had caused the cover protecting the insulation to burst. Internal pressure increase from enhanced boil-off eventually ruptured the tank and released the LH_2 which was ignited by engine sparks [Dawson 2004].

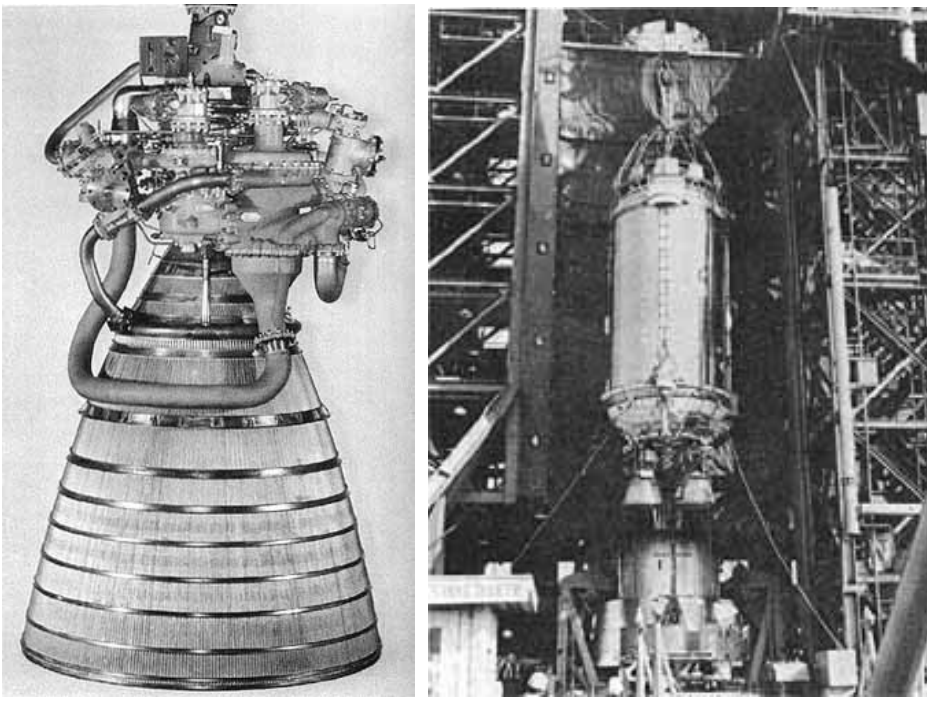

Figure 7-2. LH_2-LOX driven rocket engine RL-10 by Pratt&Whitney (left), with two of those engines used in the Centaur upper stage (right) [Sloop 1978] (Courtesy of NASA)

The first successful launch of an LH_2/LOX propulsion system in the upper stage of a NASA Atlas-Centaur rocket finally took place on November 27, 1963, proving that the LH_2 engines could be fired in space. The RL-10 engines used had a thrust of 0.07 MN each. In the 1970s, the Atlas-Centaur was replaced by the more powerful Titan-Centaur launch vehicle, where the "Centaur D-1T" represented the 3rd stage with a length of 7 m and a weight of 17.7 t (including the LH_2-LOX fuels). Despite successful flights such as for the Voyager missions to the outer planets, the Titan-Centaur expendable system was terminated to be replaced by the reusable shuttle system.

The subsequent NASA programs Apollo and Space Shuttle then applied LH_2 at a large scale. The first Saturn flight in January 1964 used six RL-10A-3 engines. Saturn-V rockets used for the Apollo moon flights (1967-72) Rocketdyne J-2 LH_2/LOX engines in their second (five J-2 engines) and third stages (one J-2 engine) reaching a thrust of ~1 MN each (and with a lifetime of one hour under normal operating conditions). A special feature of J-2 was that it could be ignited twice. The first ignition at start was to bring Apollo into the Earth orbit, while the re-ignition was made to bring the spaceship on moon course. A total of 12,000 m^3 of LH_2 was necessary to fill up the tanks of the Saturn carrier rockets.

The Space Shuttle or Space Transportation System (STS) for manned missions is the combined system of external tank with the LH_2/LOX fuel (Fig. 7-3), two rocket boosters with solid fuel, and a winged spaceplane as the orbiter and payload carrier. It is the first system that is designed for the partial re-use of components. The three main engines, SSME, also a product of Pratt&Whitney's Rocketdyne, are running on LH_2/LOX fuel reaching a thrust of ~1.8 MN each and designed for a burning time of about 9 min. Low-pressure and high-pressure turbo pumps pressurize the fluids to 30 MPa (oxygen) and 45 MPa (hydrogen), respectively, before injected at rates of 424 kg/s and 70.3 kg/s, respectively, into the combustion chamber and spark-ignited.

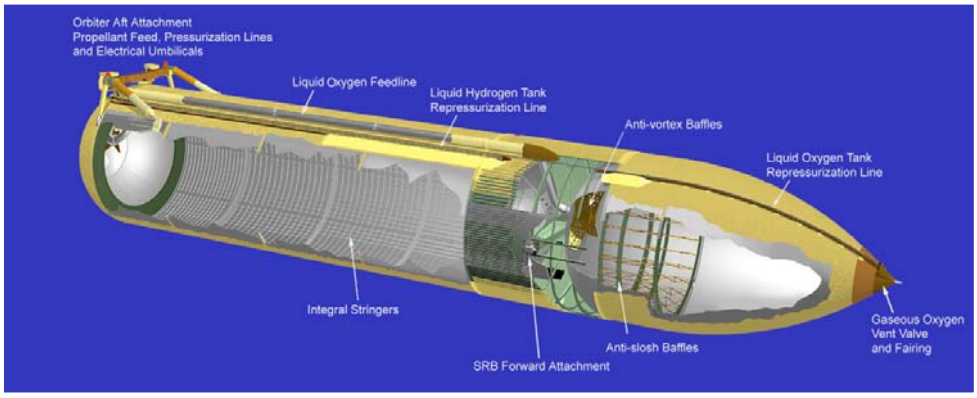

Figure 7-3. External Tank of the Space Shuttle (Courtesy of NASA)

Cryogens needed at the Kennedy Space Center for a launch-countdown of a Space Shuttle [NASA 2006]

LH_2	2380 m^3, of which 1454 m^3 for loading the External Tank with the remainder used for pre-chill of fuel lines, for the "Power Reactant Storage and Distribution System" (PRSDR) or lost as boil-off; shipped to KSC in 49 m^3 tank trucks.
LOX	946 m^3, of which 537 m^3 for loading the External Tank; small quantities used on-board to provide breathable atmosphere; 3 m^3 with a higher purity used in the PRSDS; shipped to KSC in 23 m^3 tank trucks.
LHe	~32 m^3, of which about 1 m^3 is used on-board, all remainder used for purging fuel lines and pressurization; shipped to KSC in 49 m^3 tank trucks.
LN_2	as part of the total 1220 m^3 of N_2 needed, only for ease for transportation; no LN_2 is used on-board; shipped to KSC in 23 m^3 tank trucks.

While the space shuttle will be retired by 2010, the follow-on system, Orion with its launch vehicle Ares, is planned to resume manned flights to the moon by 2020. Respective rocket engines have been suggested to be based again on the Apollo J-2 engine design.

European Space Program

Resulting from the USA's decision to abandon their expendable launch vehicle programs, the European counterpart, Ariane, has emerged as a strong competitor gaining a significant market share of launching satellites. Initially intending to buy RL-10 engines from the USA, a request which was declined by the US Government, Europe started its own engine development as part of the Ariane rocket program. Since 1988, Vulcain has been developed as a first-stage main engine (Fig. 7-4). A prototype rocket engine with a 1 MN thrust was tested as early as 1964 progressing to a 1.35 MN thrust Vulcain-2 engine (since 2002) for the Ariane-V rocket. The Vulcain engine is 3 m high, has a diameter of 1.76 m, and a weight of 1.8 tons. The liquid hydrogen, prior to entering the combustion chamber, cools the chamber wall down to about 500°C to prevent its deterioration. Powerful turbopumps with speeds of 13,000 rpm (for LOX) and 34,000 rpm (for LH_2) drive the cryogenic propellants at a rate of 235 kg/s (with 41.2 kg/s of LH_2) into the combustion chamber to be ignited reaching a temperature of ~3000°C at ~11.5 MPa.

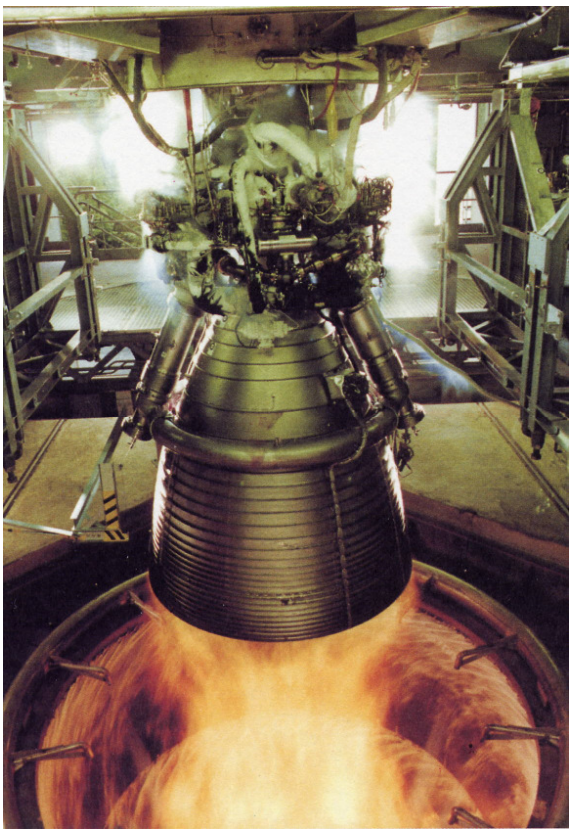

Figure 7-4. Testing of the Vulcain engine for the Ariane rocket (Courtesy of DLR)

In Stuttgart, Germany, a test facility has been operated to investigate cryogenic rocket propulsion for the Ariane V transportation system. The aim is to provide key technologies for future cryogenic rocket engines. The research work is focused on the injector, combustor, and nozzle technology.

More powerful engines are needed to meet the increasing demands for payloads. The version Ariane-VESC-A (with the "C" standing for "cryo-technique") employs a hydrogen-driven engine also in the upper stage and allows the transportation of a 10 t payload.

7.2.2. Spaceplanes

Also for supersonic and hypersonic transportation, liquid hydrogen is being considered the ideal fuel. Because of the enormous fuel consumption at very high speed, a light-weight fuel is of major importance. In addition, a supersonic aircraft requires cooling of the aerodynamic surfaces which would otherwise become overheated by friction of the air. Here the cryo-hydrogen is used to cool these surfaces while vaporized, before it is introduced into the combustion engine.

The X-33 spaceplane designed in 1986 in the United States (Fig. 7-5), was the sub-scale prototype version of the single-stage-to-orbit “VentureStar”. It was designed to take off vertically, to cruise at a speed faster than Mach 13, and to land horizontally. The X-33 was to use linear aerospike rocket engines and to employ light-weight graphite composite internal structures supporting the three large propellant tanks. The light-weight components and fuel tanks comprising most of its interior were designed to conform to the vehicle's outer shape. Work on the X-33 concept, however, was discontinued in 2001.

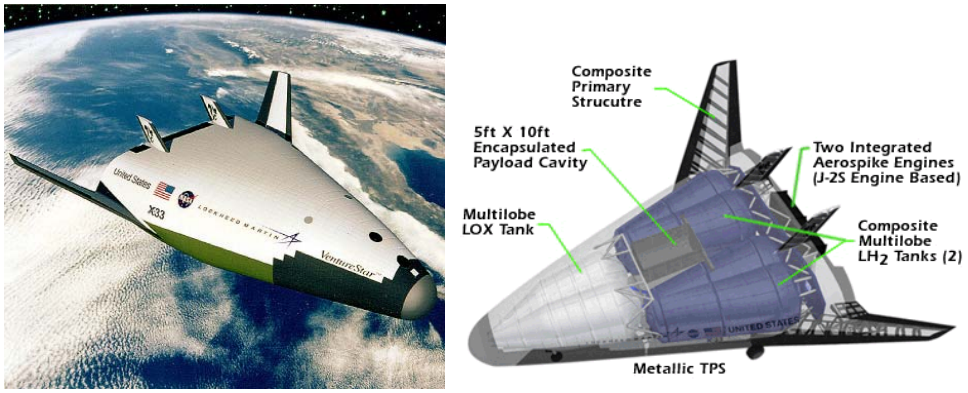

Figure 7-5. US spaceplane X-33 design of 1986
(Courtesy of NASA Marshall Space Flight Center)

Within the German Hypersonics Programme, the “Saenger” spaceplane was proposed as a two-stage-to-orbit vehicle with horizontal take-off. The Saenger-II reference design of the late 1980s and early 1990s was comprised of a large hypersonic booster aircraft and a small rocket-powered delta winged manned orbiter ("Horus") or unmanned cargo module ("Cargus"). The booster aircraft would cruise on turboramjets with LH_2/air fuel at Mach 4.4 to the launch area (stage 1), then accelerate to Mach 6 and release the upper stage running on LH_2/LOX propellants. Design specifications were a lift-off thrust of 4.5 MN, a total mass of 750 t, and a total length of 101 m with a core diameter of 14 m. Europe's first turboramjet engine beginning ground run at MBB in 1991. The Saenger development was eventually discontinued in 1994 for reasons of cost being only 10 - 30 % below that of the Ariane 5 expendable vehicle.

Japan launched in 1986 the first H-I rocket with the LE-5 engine running on LH_2. Further engine developments leading to the LE-7 first stage engine and the LE-5A second stage engine were used in the H-II rockets (Fig. 7-6), whose first successful flight was in 1994 [Fukushima 1995]. The LE-7 engine and a schematic of its LH_2/LOX fuel system are shown in Fig. 7-7.

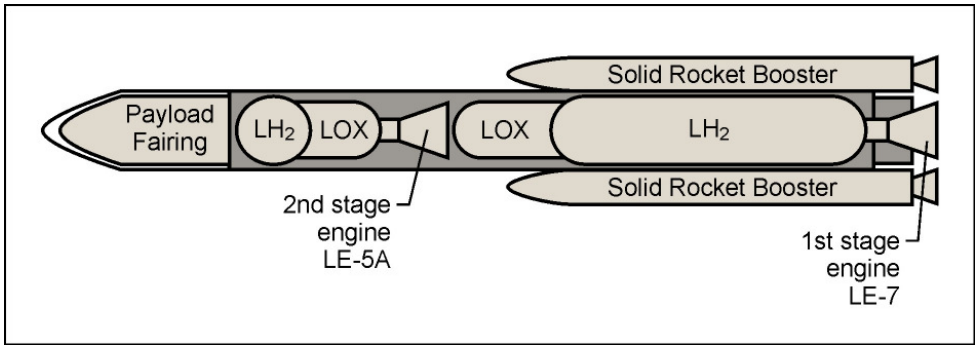

Figure 7-6. Schematic of Japan's two-stage rocket H-II

The present generation launch vehicle, H-IIA, is an upgrade in that – in addition to the two or four rocket boosters – two or four smaller "solid strap-on boosters" can be attached to increase launch capability. The H-IIA is 53 m long and has a weight of 285 t (without payload). The LOX and LH_2 cylindrical tanks have a diameter of ~4 m and a length of 4 and 17 m, respectively, for the first-stage engine, and 2.3 and 4 m, respectively, for the second-stage engine.

Since 1991, also the use of slush hydrogen as rocket fuel has been investigated. The concept spaceplane, Hope-X-Prototype, was developed as a single-stage-to-orbit version designed for 10 passengers. Propulsion system was a scramjet engine which runs on liquid air/SLH_2 propellants and allows a speed of > Mach 14. The project was cancelled in 1997 due to budget cuts.

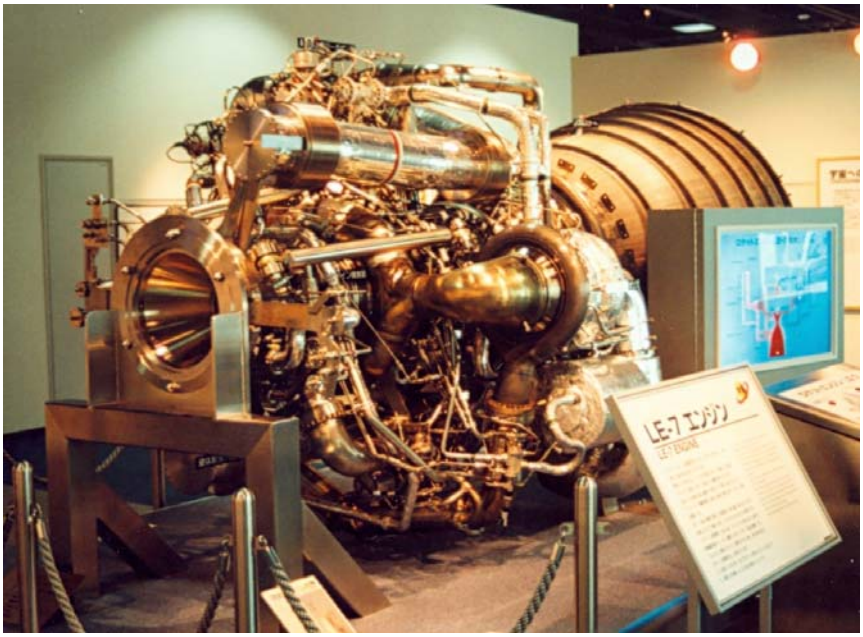

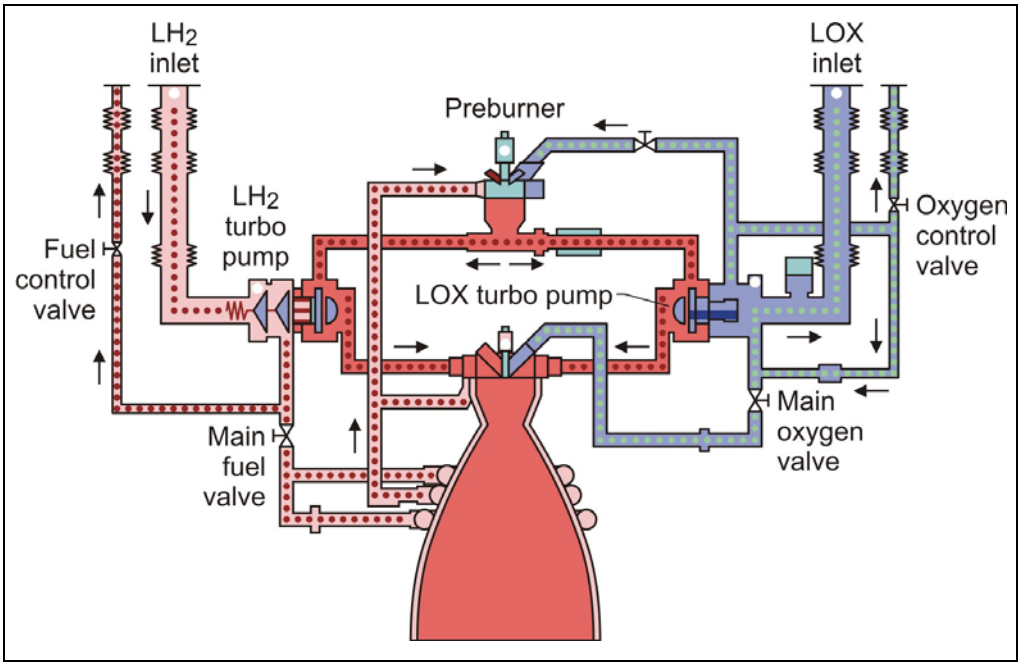

Figure 7-7. Japanese rocket engine LE-7 (top) and its LH_2/LOX fuel system (bottom)

7.2.3. Airplanes

The idea to use LH_2 as aircraft fuel was considered as early as 1918 stressing that H_2 had a greater heat content than any other fuel. A detailed proposal was made by Igor I. Sikorski, a Russian-American aviation pioneer, in 1938 promising not only a doubling of fuel flight efficiency, but also a lighter weight, less noise, and reduced pollution. The wide range of flammability of H_2 in air enables a stable combustion chamber operation far beyond the limits of hydrocarbons. Also in terms of safety, LH_2 is expected to be safer than the conventional kerosene due to smaller endangered areas and shorter fire duration. But it was not until the 1950s, when the attractiveness of LH_2 gradually became evident, despite its low availability and handling hazards. This was due to incentives for the development of airplanes at very high altitude, advances in LH_2 technology, and experiments that H_2 could combust readily at low pressures.

An early concept of a liquid hydrogen driven airplane designed by Abe Silverstein and Eldon Hall of 1955 is shown in Fig. 7-8. Plans were developed for both a subsonic and a supersonic version with the latter to be lighter and faster, but having a smaller cruising range. Four turbojet engines were foreseen. Light-weight, insulated LH_2 fuel tanks were to be mounted underneath the wings with an option for additional drop tanks to enlarge the range [Sloop 1978].

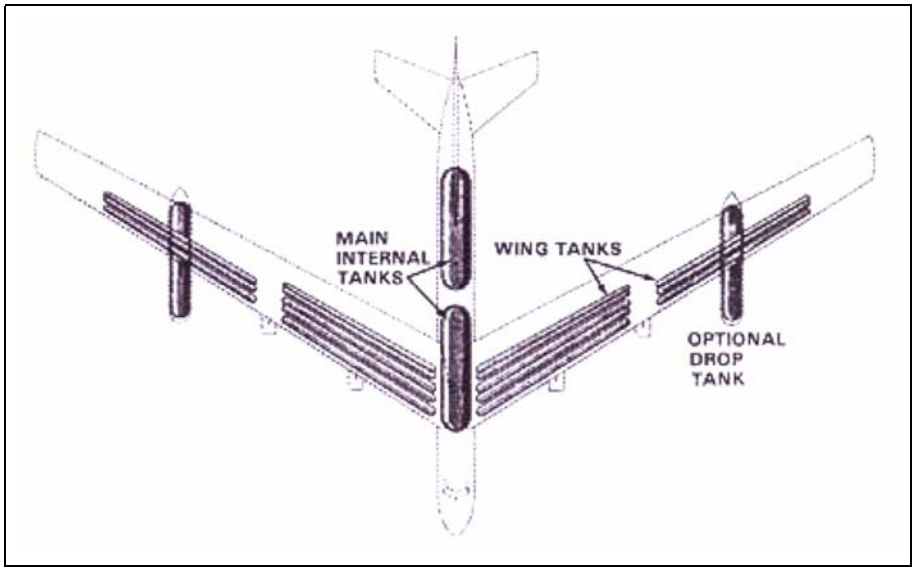

Figure 7-8. Design of an LH_2-driven, high-altitude reconnaissance aircraft of 1955 developed by Silverstein and Hall [Sloop 1978]
(Courtesy of NASA)

Suntan Project

The Lockheed "Skunk Works" (formal name: Lockheed's Advanced Development Projects Unit; today: Lockheed Martin Aeronautics) at Burbank, California, under the direction of Clarence "Kelly" Johnson was contracted to design and build a hydrogen-fueled, supersonic high-altitude reconnaissance aircraft as the ultimate flying machine. It was actually resulting from a secret project, named Suntan, starting in 1956.

Loose Screws

"When I told him that I wanted to learn how to make liquid hydrogen and store it in the hundreds of gallons, the professor shook his head solemnly. 'With all due respect, Sir, I think you've got a screw loose.' "

(Skunk Worker B. Rich in a discussion in 1956 with Nobel laureate (of 1949) William F. Giauque) [Rich 1995].

The aircraft, designated CL-400, (Fig. 7-9) intended to fly with Mach 2.5 speed at 27,400 m altitude [Rich 1973, Rich 1995] was designed with a stunning length of 90 m, but a light weight of 32 t (without fuel). The CL-400 was to be equipped with three tanks, a front tank with 67 m^3, a rear tank with 54 m^3, both at 230 kPa, and a central 15 m^3 working tank for a total of 9.7 t of LH_2 fuel to supply the two air-breathing jet engines allowing for a cruising range of 4800 km.

A major problem turned out to be the question of materials. Due to estimated maximum temperatures of 427°C at the aircraft nose, 327°C around the windscreen and some 180°C at the rest of the fuselage, the material of choice to sustain such temperatures was stainless steel, but would have made the aircraft unacceptably heavy. The material finally chosen was titanium, very expensive and extremely difficult to machine [Mulready 2001].

From April 1956, the Pratt&Whitley Aircraft division in Connecticut was set to develop an LH_2 driven engine. First step was the modification of an existing engine, the "J57" to run on hydrogen. This was realized within six months with the experience that the operation of the converted J57 with LH_2 was better than it had ever been with jet fuel [Mulready 2001]. The second step was the construction and testing of an Air-Turbo-Ramjet (ATR) demonstration engine for supersonic speed which became known as "model 304". The first complete test of such a Suntan engine was made in September 1957 on a new test area in Florida. In a series of 10 tests in 1958 and a total of 25 hours of operation, the predicted performance was confirmed [Sloop 1978].

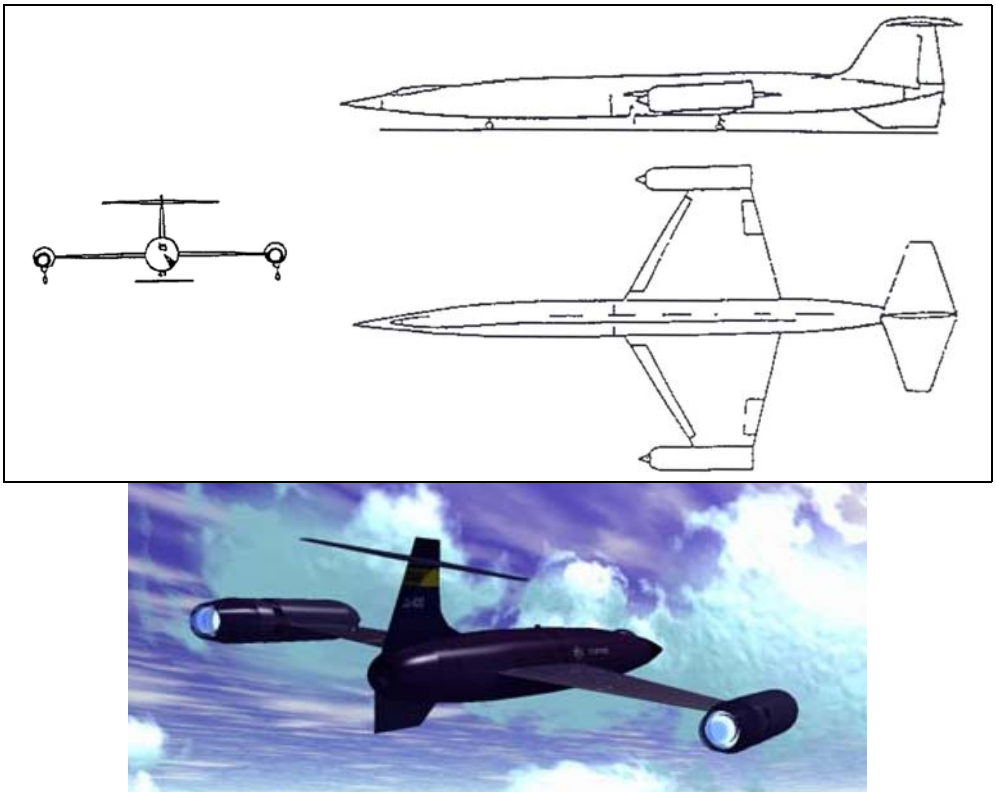

Figure 7-9. Schematic of the Suntan aircraft concept CL-400 [Sloop 1978]
(Courtesy of NASA, Image:Suntan-aircraft.jpg - Wikipedia, the free encyclopedia)

Pratt&Whitney had fabricated five prototype "304-2" turbojet engines and the Skunk Works nearly completed the first airplane, when the Suntan project gradually died away and eventually cancelled in February 1959. While the engines were running perfectly on LH_2, all difficulties remained with the aircraft which had become an immensely complex and costly development, and still did not meet the expectations for an aircraft to be superior, i.e., faster and farther, to a kerosene-driven airplane within the foreseeable future. It added to the major drawback of a need to construct LH_2 production and storage plants everywhere in the world to maintain reconnaissance duties. The existence of the Suntan project was kept secret for almost 20 years.

The achievements made in LH_2 technology and equipment, however, were enormous (Skunk Works had become at that time the world's largest producer of LH_2 with ~750 l/day) and deemed highly valuable in the rapidly developing space program. It was spurred by the world's first successful launch of the – then Soviet – space vehicle Sputnik I on October 4, 1957.

Project Bee

The first successful in-flight test of an experimental hydrogen-propelled aircraft was made in the USA after E. Silverstein received funding for an LH2 test program at the NACA Lewis Laboratory. Starting 1955, the "Project Bee", classified secret, a B-57B twin-engine aircraft was taken powered by two Curtiss Wright J-65 turbojet engines and converted one engine to run on both JP-4 and hydrogen fuel (Fig. 7-10). A heat exchanger was employed to gasify the LH_2 by air. The stainless steel tank for the LH_2 on the left wing tip was 6.2 m long, had a volume of 1.7 m^3 and a 50 mm plastic foam insulation. The design pressure was ~340 kPa. The aircraft was supposed to start with the conventional JP-4 fuel, be switched to H_2 fuel at an altitude of ~16,400 m, before switched back to JP-4 and return to the ground under normal operational conditions [Sloop 1978]. Due to the significant loss of LH_2 fuel during chill-down of all LH_2-lines, it was considered wise to have the chill-down process made with liquid helium on ground prior to the flight [Dawson 2004].

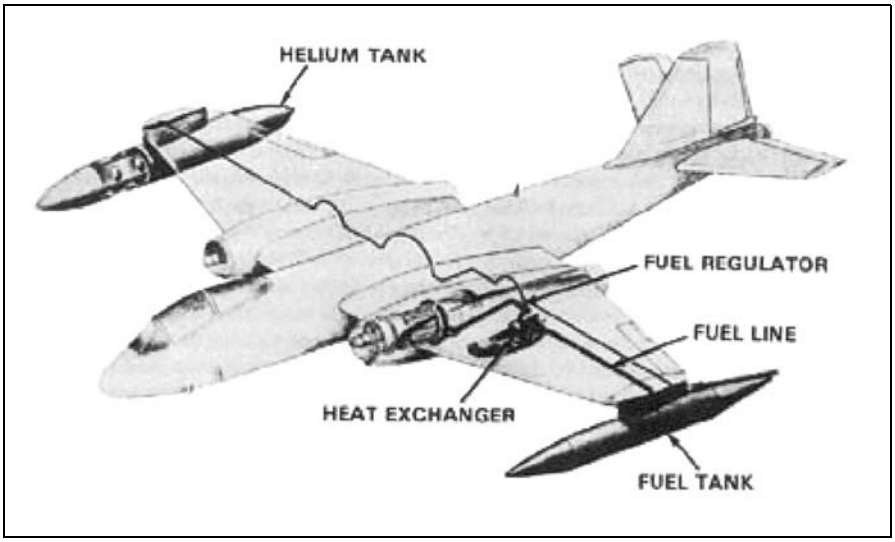

Figure 7-10. B-57B twin-engine aircraft with one engine fueled by LH_2 successfully operated first in 1956 [Sloop 1978] (Courtesy of NASA)

The first two flight tests failed, but demonstrated at least that the LH_2 fuel could be safely jettisoned. The tank was emptied within about 3 minutes forming a dense plume which disappeared approximately 6 m behind the tank. On Feb. 13, 1957, finally the first of three successful flights took place. The one engine operated on H_2 for about 20 min at a speed of Mach 0.72 before the fuel tank was running empty. In contrast to JP-4 fuel, the H_2 consumption caused the formation of a dense and persistent condensation trail [Sloop 1978].

The First Flight

The first test flight with the modified B-57 took place on Dec. 23, 1956. The tank filled with 94 kg (1.3 m^3) of LH_2 was estimated to reach its designed pressure limit due to boil-off within about 5 min. It therefore had to be vented eight times (manually by the co-pilot), thus loosing 16 % of the H_2 fuel, before the final cruising height was reached to begin the test [Sloop 1978].

In 1988, a four-seater Grumman Cheetah with an LH_2 fueled internal combustion engine became the first and sole, so far, airplane to take off, cruise, and land by means of hydrogen power only [Peschka 1992], although it was a 36 s flight only.

Tupolev Flying Laboratory

In the same year, the Russian company ANTK-Tupolev has operated the "Flying Laboratory" Tu-155 (Fig. 7-11), which is a hybrid version of the Tu-154 airplane [DASA 1992]. One of the three engines ("NK-88") could be fueled with either hydrogen or natural gas stored in a 17.5 m^3 capacity tank. The maiden flight on April 15, 1988, lasted 21 min; total operating experience with LH_2 accumulated to 10 h. Major efforts, however, are concentrating on LNG as fuel because of the enormous domestic resources of natural gas in Russia and the low LNG price, respectively, which is only 40 % of the kerosene price [Tupolev 2008]. The freight aircraft Tu-156LNG was built designed for an optimized airborne cryogenic fuel system during long-term operation for distances up to 2600 km, if LNG is used, and 3300 km, if LNG plus kerosene is used. The cryogenic tank system consists of the main tank with a capacity of 31 m^3 (13 t) and an active tank composed of two horizontal communicating vessels. Currently under development is a passenger version, Tu-204LNG, designed for 210 passengers, a cruising range of 5200 km, 22.5 t of LNG plus a reserve of 5.5 t of kerosene [Tupolev 2008].

CRYOPLANE Project

The project CRYOPLANE was launched in 1990 by a joint German-Russian consortium (DASA as the lead with main partners MBB, MTU, Tupulev, Kuznetsov), and later as an EU activity with 35 partners from 11 countries and coordinated by EADS Airbus GmbH. Its objective was to study the feasibility of an aircraft propelled by cryogenic fuels [DASA 1992]. The aim was to find out whether the use of liquefied natural gas (mainly on the Russian side) or liquid hydrogen (on both sides) as an aircraft fuel was technically possible and reasonable in terms of ecology and economy. Topics covered by the project were scenarios for the transition to an alternative aviation fuel, infrastructure, aircraft design, fuel system layout, engine modifications, and ecological issues (e.g., water vapor and NOX emissions). The transition of short/medium range aircraft serving routes in or between leading industrial nations was seen as an introduction phase, followed by the development of the appropriate infrastructure and the operation of a demonstrator airplane.

Figure 7-11. Tupolev 155 "Flying Laboratory" of 1988 with the central engine fueled by LH_2 or LNG
(Courtesy of PSC Tupolev)

An Airbus A310-300 was selected as the baseline aircraft to be converted to LH_2 propulsion. For the new fuel tank concept, the most favorable design was seen in the top-mounted tank configuration with four tanks, two active ones with 40 m^3 each for either engine, and two passive ones with 80 m^3 each to refill the active tanks (Fig. 7-12).

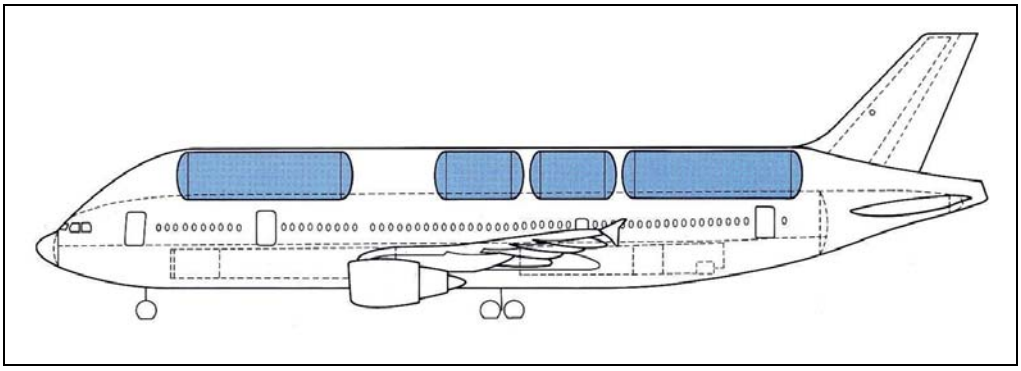

Figure 7-12. Schematic of the Cryoplane demonstrator based on an Airbus A310-300 with the top-mounted LH_2 tank arragement [DASA 1992]
(Courtesy of Airbus Deutschland GmbH)

Total fuel weight for the cryoplane Airbus was estimated to be 15.6 tons of LH_2 (compared to 27 tons of kerosene for the same flight range). Due to the environmental impact on the stratosphere by the formation of long-lived ice cloud condensation trails, the typical cruising height of ~12 km would be lowered to ~10 km. Cruising range of the cryoplane was estimated to be 2700 nautic miles (5000 km).

At a later stage in the project, a smaller airplane was chosen to precede the Airbus as LH_2 demonstrator, a 30 passenger regional airplane of type Fairchild-Dornier 328 with one of the two engines to be converted to H_2 fuel. The fuel capacity is 420 kg (6 m^3) of LH_2 stored in two cylindrical tanks underneath the wings (plus 1150 kg of kerosene for the second engine). Advantages of this intermediate step are the availability of the hydrogen engine, lower investment in infrastructure, and the earlier introduction of a series aircraft [Pohl 1996].

A technological development program for the fuel system components began in 1993 including the selection of materials for tanks and piping, control system and sensors for hydrogen leak detection, fuel pumps, LH_2 gasifier, combustion chamber. The first generation of LH_2 aviation was foreseen to require a fleet of 400-500 airplanes and the respective modification of ~70 European airports. The fuel consumption was assessed to be about 2 million t/yr of LH_2 or ~170 t/d for an average airport.

HALE Concept

Most recent concept of an aircraft with hydrogen propulsion is HALE, “High Altitude Long Endurance”, developed by Boeing (Fig. 7-13). It is designed as a propeller-driven, unmanned surveillance and reconnaissance airplane and will be equipped with a modified Ford engine to stay for at least 7 days in the air and carry a payload of up to some 900 kg. The engine, a multi-stage turbo-charged internal combustion engine, was recently tested in a special climate chamber over 4 days, with 3 days under simulated high-altitude (~20 km) conditions proving the technical maturity of the H_2 propulsion system [Boeing 2007].

Figure 7-13. HALE, concept of an unmanned aircraft with a Ford internal combustion engine running on hydrogen
(Courtesy of Boeing - Chuck Schroeder)

Airport Conversion to LH_2 Fuel

With regard to the conversion of airports to LH_2, no major change of the overall layout is required. Only the interface between fuel supply and fuel tanks needs to be modified. Liquefaction of the hydrogen should be made in the immediate vicinity to avoid truck delivery and minimize cryogenic pipeline grids. Tanks need to be purged by an inert gas prior to refilling, therefore respective helium (or other appropriate fluids) handling facilities must be provided. Also the refueling process itself is different with regard to the larger volumes and longer times involved. Recovery lines are necessary to collect boil-off losses. The H_2 gas could be used to operate fuel cell buses and/or other airport ground support activities.

A number of conceptual design studies for airport conversion to LH_2 has been conducted. Investigations were made for the airports San Francisco, Chicago, and Zurich in terms of installations and investment required. According to the baseline concept for the O'Hare International Airport in Chicago [Boeing 1976], gaseous H_2 is delivered to a liquefaction plant consisting of three modules with a total capacity of 726 t/d with 86 % for aircraft fuel, 11 % demand variation and the remainder ground system losses. The LH_2 is stored in four spherical tanks to take up a two-days production. Defueling of the aircrafts is done into tank trucks which transfer the LH_2 to the storage tanks. As a safety distance, 305 m between runway, storage, and liquefaction plant was considered an adequate spacing. For LH_2 distribution to the aircraft refueling devices, a three-line system was selected for the purpose of redundancy, where one is filled with liquid, another one with vent gas and the third one to be used for either liquid or gas. The supply line with 400 mm diameter allows a flow rate of 227 t/h at 0.3 MPa pressure. The refueling rate is < 14.3 t/h to keep the inner diameter of the aircraft fuel pipe below 180 mm.

Aviation Fuel LH_2

Consumption of aviation fuel in Germany in 2002 was estimated to be 5.8 million tons of kerosene. In case of a complete introduction of LH_2 aviation, this would translate into about 2.1 million tons of LH_2 (same energy contents) per year or ~5800 t/d. The production of this amount requires 100 liquefaction plants (of the largest unit size presently existing). Respective energy requirements would be $1.1*10^{11}$ kWh/yr for H_2 production (assuming 4.5 kWh/Nm^3 for electrolysis) plus $2.6*10^{10}$ kWh/yr for liquefaction (assuming 12.5 kWh/kg) corresponding to a total power need of some 15,000 MW(e) or, e.g., twelve nuclear power plants of the 1300 MW(e) class.

Safety considerations are related to the separation of the LH_2 containing facilities from roads, buildings, or runways, the ventilation for enclosed areas, the preclusion of air ingress, automated system shutdowns, confinement and control of large-scale spills, or the use of non-sparking electric devices. Particularly numerous LH_2 refueling processes increase the possibility of a potential accumulation of impurities, solid N_2 or O_2, which enhance the risk of fuel system component damage and explosion. Conventional warm-up in order to vaporize impurities is not practicable for frequently used tanks.

7.2.4. Road Vehicles

There are numerous projects worldwide going on to design and construct all kinds of vehicles and demonstrate their ability to run on hydrogen fuel. The applications with regard to liquid hydrogen refer to the type of storage of the fuel which is gasified before used as feed to a fuel cell (FC) or an internal combustion engine. A fuel cell vehicle combined with an LH_2 tank has the advantage that the H_2 is supplied with the required purity for low-temperature fuel cells. A complete description cannot be given here, only a few typical examples should provide an idea on past and current activities. An actual overview is available on the internet [LBST 2008a].

The Perris Smogless Automotive Association in the USA is said to have converted in 1971 a Ford F250 pickup into the world's first LH_2/LOX fueled car. Two LH_2 tanks with 150 l each and a LOX tank with 110 l were installed on the truck. The car was operated for 25 hours and 160 km, respectively [Stewart 1980].

In a cooperation between the German DFVLR (today: DLR) and the US Los Alamos National Laboratory, research on a baseline LH_2-fueled vehicle and refueling technology was conducted between 1979 and 1981. The DFVLR provided the on-board LH_2 tank and later an improved version and the refueling device (see also Fig. 7-19). The car, a Buick Century 4-door Sedan, was running for 133 h, driving 3540 km and was refueld at least 60 times [Stewart 1984].

GM and Opel started fuel cell vehicle activities some 40 years ago with the construction of a prototype fuel cell vehicle in 1967, an electro van (Fig. 7-14) which was equipped with cryo-tanks for both LH_2 and LOX [Arnold 2005].

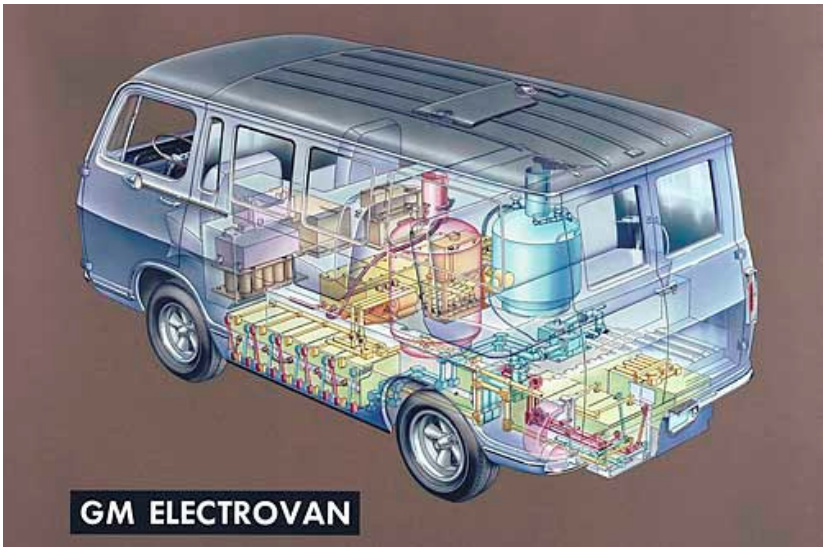

Figure 7-14. GM Electrovan from 1966 equipped with LH_2 and LOX tank (Courtesy of Adam Opel GmbH)

GM presented in 2000 the HydroGen1 car based on the Opel Zafira. The third-generation version, HydroGen3, (also a Zafira) can be equipped with either a GH_2 or an LH_2 tank system to power a 60 kW electric engine. In the "gaseous" version, 3.1 kg or 77.4 l of H_2 at 70 MPa are stored in two tanks (total weight: 95 kg) to allow a cruising range of 270 km. In the liquid tank (weight: 90 kg), there is space for 4.6 kg or 68 l of LH_2 sufficient for a 400 km drive. The maximum speed is 160 km/h. The HydroGen3 was the first car to get permission to operate on Japan's public roads [GM 2007].

The German car company BMW started as early as 1978 its research on H_2 driven cars with a prototype internal combustion engine (ICE). The DFVLR presented in 1979 a BMW 518 which was operated on both hydrogen and gasoline. BMW is pursuing the concept of storing the hydrogen fuel in liquefied form. The car development was therefore accompanied by a steadily improving design of the LH_2 storage system. The 4th generation of 1988 was a BMW 735i converted to hydrogen and equipped with a 120 l LH_2 tank; cruising range was ~200 km [Regar 1989]. In 2000, a fleet of 15 cars, BMW 750hL, was introduced with a cryo-tank for 8 kg of LH_2 on board [Pehr 2002]. Two of these cars were equipped with a 5 kW low-temperature PEM fuel cell to power an air conditioning system during standstill of the combustion engine.

Latest generation is the BMW Hydrogen 7 (basis: BMW 760iL) of 2006, the first H_2 driven car for which series development process has been applied. It is equipped with an 8 kg LH_2 tank for a cruising range of about 200 km and an average H_2 fuel consumption of 3.6 kg per 100 km. Acceleration is 9.5 s to reach a speed of 100 km/h, as would a consumer expect from a car of that power class. By switching the 191 kW engine to the conventional gasoline, the range can be extended by additional 500 km. The maximum speed is 230 km/h in both modes. Refueling time of the LH_2 tank is < 8 min. For a half-filled tank, the lock-up time, i.e., the time when the boil-off valve will be activated, is 17 h; the holding time, i.e., the time by which all liquid has disappeared, is 9 days. Fig. 7-15 shows the arrangement of the main hydrogen components. By September 2007, approximately 100 "Hydrogen 7" cars have been built and are currently tested having accumulated up to now some 2.7 million kilometers.

The BMW H2R concept racing car (Fig. 7-16) constructed in 2004 was equipped with an LH_2 powered 210 kW engine for hydrogen fuel only. Acceleration to a speed of 100 km/h can be done within 6 s; its maximum speed is over 300 km/h. A special 11 kg capacity LH_2 tank for this racing car was constructed. Additional to the "normal" requirements were a short refueling time of $\leq$ 5 min and a rapid change of flow rates from minimum to maximum within 1 s [Michel 2006]. Operating pressure is 0.3 MPa. Part of the safety concept of the tank is the employment of a boil-off valve plus two safety valves.

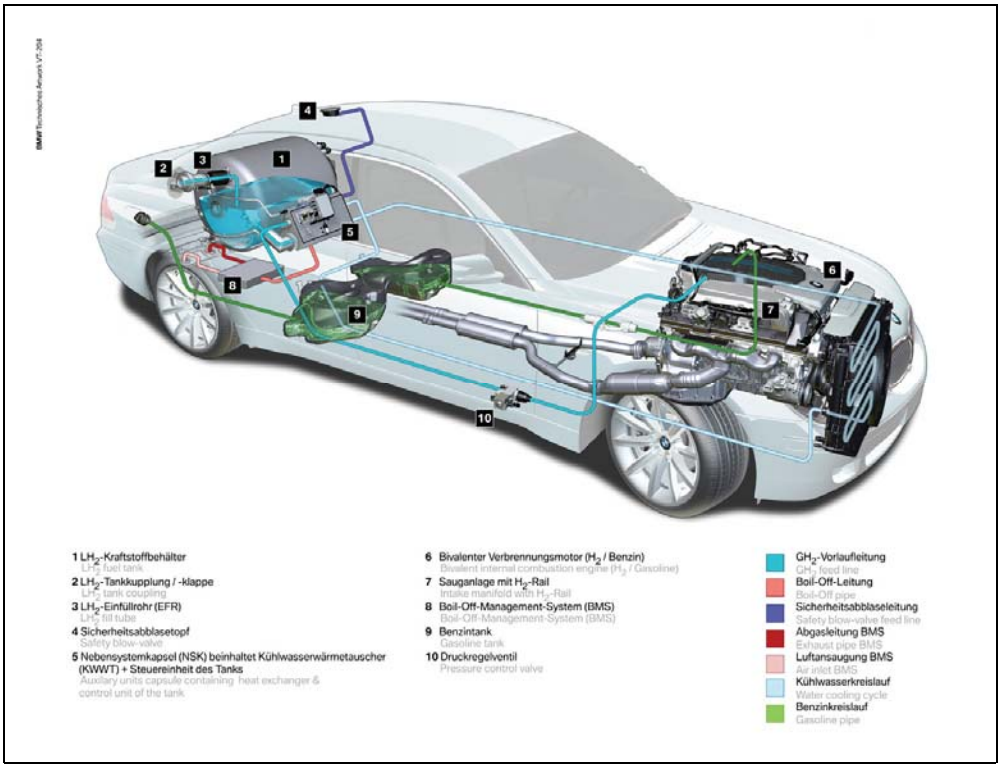

Figure 7-15. LH_2 systems in the BMW Hydrogen 7
(Courtesy of BMW CleanEnergy)

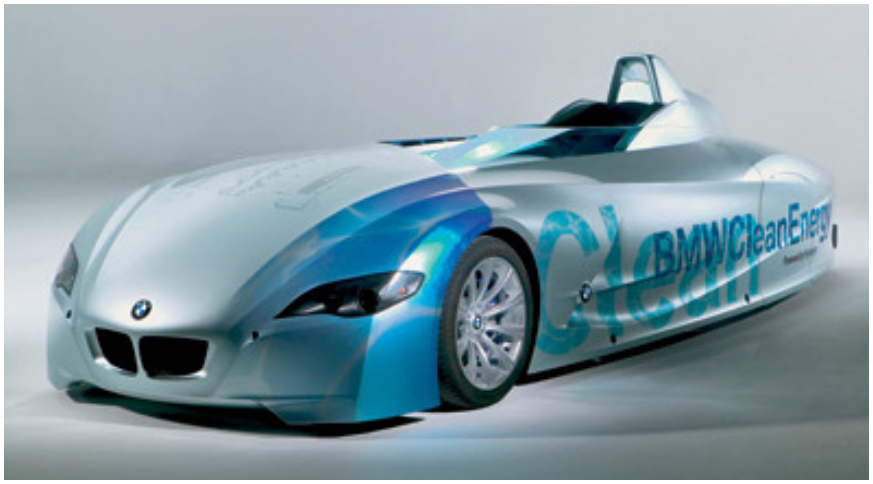

Figure 7-16. BMW H2R racing car of 2004
(Courtesy of BMW CleanEnergy)

The Daimler/Chrysler activities on hydrogen-driven vehicles (passenger cars, light-duty cars, buses) began in the mid 1980s with H_2 and gasoline driven ICE cars. Since the 1990s, focus was on fuel cell vehicles with an electric engine. On-board storage of the H_2 fuel is in form of compressed gas. In the series of experimental cars NECAR (New Electric Car), there was, however, one example, NECAR-4 of 1999, where LH_2 storage was used to supply the 70 kW fuel cell system with hydrogen. Cruising range was 450 km at a maximum speed of 145 km/h.

In Japan, the Musashi Institute of Technology is conducting engine research on hydrogen-driven vehicles with internal combustion engine since more than 30 years. Musashi-1 introduced in 1974 was the first H_2-fueled vehicle in Japan. Except for the first car, all following converted cars or light-duty trucks had on-board storage of liquid hydrogen. Musashi-9 was a 4-ton refrigerator truck, where the LH_2 was used, apart from operating the ICE, also to keep the refrigerated goods at sufficiently low temperatures, thus demonstrating the practical recovery of the potential of cold energy. Latest generation is Musashi-10 of 1997.

Similar to passenger cars, also buses with hydrogen propulsion have been developed and test-operated worldwide, both fuel cell vehicles and H_2-fueled internal combustion engines. Most buses carry the hydrogen as compressed gas. There are, however, a few examples. From the three city buses tested within the Euro-Quebec project in the period 1995-1997, two were based on ICEs using gasified LH_2 as fuel. One was a MAN bus with three superinsulated elliptical cryo-tanks with 200 l geometrical volume each to contain a total of 570 l of LH_2 in an underfloor arrangement allowing a cruising range of 250 km. The bus was operated in Erlangen, Germany, since 1996. The other bus was of the Van Hool type equipped with two 200 l roof-top-mounted LH_2 tanks as fuel supply system. As part of the EU project EUREKA, a hydrogen bus demonstrator was operated since 1995 using a 700 l LH_2 tank in the rear of the bus to operate a 78 kW fuel cell power system for a 200 km cruising range. Refueling was made from a 12 m^3 LH_2 stationary storage tank with a specially developed manifold.

7.2.5. Hydrogen Filling Stations

With increasing number of H_2-fueled vehicles on the road, a respective infrastructure must be established as well. Plans for the establishment of a "Hydrogen Highway" are currently pursued in various countries like in the USA, Canada, Japan, Germany, or the Scandinavian countries, with the objective to construct a sufficiently dense grid of hydrogen stations along major traffic routes to make H_2 vehicles attractive for the consumers. Numerous H_2 filling stations have been erected worldwide in the meantime with public and private funding. In Europe, demonstration projects such as CUTE ("Clean Urban Transport for Europe"), CEP ("Clean Energy Partnership"), or ECTOS, a bus project in Iceland, have been initiated. Their main goal is to gather experience both in the form of the fuel, LH_2 or gaseous H_2 at 35 or 70 MPa, and in the way of providing the hydrogen (e.g., on-site steam reforming or electrolysis or truck delivery).

A liquid hydrogen supply system has the advantage of being capable to dispense the H_2 either as liquid or as high-pressure gas avoiding space consuming GH_2 storage. A schematic of a joint GH_2 and LH_2 refueling system is shown in Fig. 7-17 [Arnold 2005]. There is only one LH_2 storage tank located underground with several tens of tons capacity to serve both modes. Advantages are that separate storage devices for gaseous and liquid H_2 can be avoided as well as separate truck delivery for both modes. Another aim is to reduce filling time. High-pressure

gas (70 MPa) is obtained by using newly developed cryogenic pumps which push the liquid into a heat exchanger where it heats up to ambient temperature. This key component is more compact, less noisy and needs less maintenance than a compressor which would be necessary in the case of gas delivery.

The first refueling station employing an underground LH_2 storage tank has been constructed in Washington D.C. serving both an LH_2 dispenser and, by means of a 3-stage compressor system, a gaseous H_2 dispenser for 35 and 70 MPa. The tank has a capacity of 5.7 m^3 at a nominal working pressure of 1.3 MPa. The vent line opens at 1.8 MPa leading to a stack at a height of 7.6 m above ground. The first in Europe was built in Hornchurch, UK. The LH_2 tank with a capacity of 55 m^3 and a weight of 3.2 t was delivering fuel to the three London buses of the EU-funded CUTE project, before it was demolished in June 2007 after 3 years of test operation.

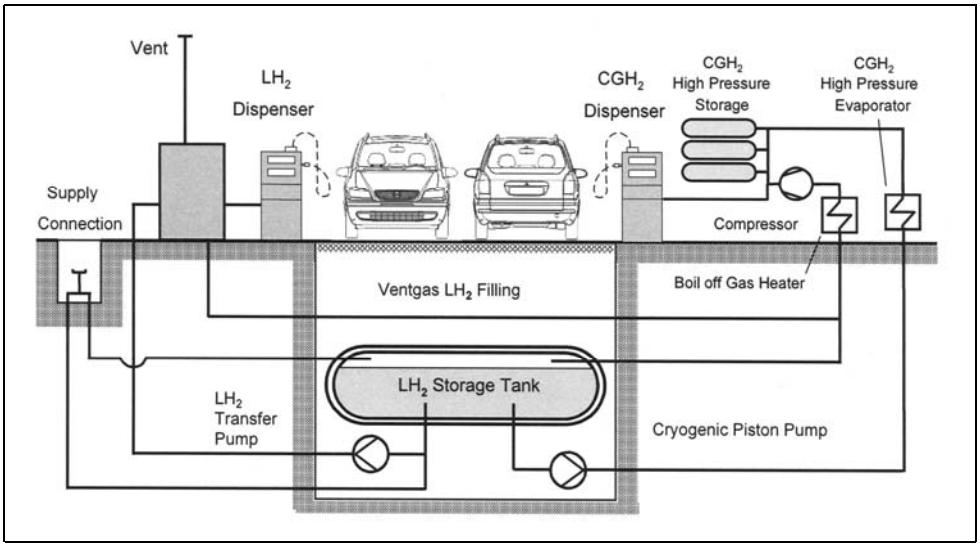

Figure 7-17. Schematic of a hydrogen refueling station [Arnold 2005] (Courtesy of Linde AG)

"Weakest link" in the transfer lines between car tank and dispenser, i.e., the location with the maximum H_2 loss, is the cryogenic coupling. As the tank, it must have a double wall and vacuum insulation. Special constructions are necessary to transfer the cryogenic fuel and making sure that air ingress is avoided. Today's couplings are working with a floodgate which is purged and purified with helium to remove all air, before the valves on either end open at the same time. The refueling is made through an insulated pipe ("cold finger") inside the dispenser, which is pushed pneumatically into the filling line of the tank (Fig. 7-18). The gaseous H_2 is removed from the tank and could be – as is the case in the Berlin filling station – routed to a fuel cell plant for electricity generation.

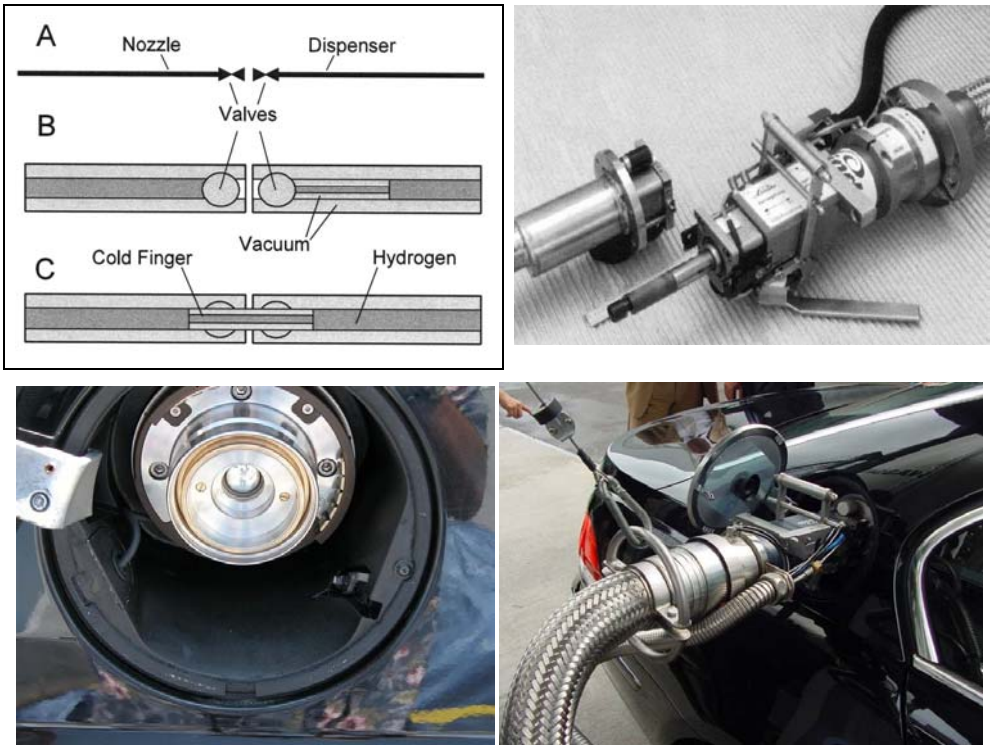

Figure 7-18. LH_2 refueling coupling [Arnold 2005]
(Courtesy of Linde AG (top) and BMW CleanEnergy (bottom))

There are two ways to transfer the LH_2 from the source tank into the vehicle tank, either using a pressure difference or employing an LH_2 circulation pump. In both cases, some part of the LH_2 is gasified to cool down the lines. This gas could be sent back for re-liquefaction, vented, or forwarded to a gaseous H_2 dispenser system. Fore the transfer by pressure difference, the employment of a buffer tank is reasonable because only a limited amount of LH_2 will be heated (and gasified) upon its pressurization.

As of 2006, there were 139 H_2 filling stations being operated and 98 more planned worldwide, with 60 in North America, 43 in Europe (20 in Germany), and 36 in Asia (21 in Japan). For a general introduction of H_2 vehicles on the market, it needs approx. 1500 filling stations in Germany. Only a small number of hydrogen stations, however, offer LH_2 fuel so far. The total number of filling stations for LH_2 worldwide is 21. An actual overview of worldwide available hydrogen refuelling stations is given in [LBST 2008b].

One of the first was in the 1980s a self-service LH_2 pump (Fig. 7-19, left) used in a joint project of the Los Alamos National Laboratory and the German DFVLR (DLR) to refuel their H_2 research car, a modified 1979 Buick [Stewart 1984, Peschka 1992]. Within the time of the German SWB (Solar-Wasserstoff-Bayern) project between 1986 and 1999, the refueling

process for a BMW 735i equipped with a 120 l LH_2 tank was tested. The time of refueling the tank could be decreased from originally ~1 hour down to ~10 min.

The first public station to offer liquid and gaseous hydrogen was opened in 1999 at the airport Munich in Germany and operated until 2006 (when the "ARGEMUC" project was terminated). The LH_2 delivered by truck was filled into a 12 m^3 storage vessel. Refueling of the vehicle was done automatically by a robot system. In the first two years, ~49 m^3 of LH_2 in more than 4000 refueling processes have been transferred into vehicle tanks. A new public filling station for LH_2 was opened in Munich in 2007 with the storage tank located underground. This station is one of the three mainly dedicated to the BMW Hydrogen 7 fleet.

Figure 7-19. LH_2 dispensers 1979 and 2007 (Courtesy of DLR (left), Linde AG (right))

In 2004, GH_2 and LH_2 dispensers have been fully integrated into a conventional service station in Berlin utilized by 17 H_2 driven vehicles (as of May 2007), but with a total capacity of 100 vehicles per day. While the gaseous H_2 is generated on-site by electrolysis, the liquid H_2 is delivered by tank truck. This H_2 filling station is operated by the CEP, a 5-years project of public and private partners to demonstrate production, storage, and distribution of H_2 and the operation, refuelling, and maintenance of H_2 vehicles.

As part of the EU project "ZeroRegio", a new H_2 station for both gaseous and liquid hydrogen is being operated in Frankfurt, Germany. It opened in 2006 and is fully integrated into a conventional gas station. While the LH_2 is delivered by truck, the gaseous hydrogen is generated as a by-product from chlorine production is routed through a 1.7 km long high-pressure pipeline (18/33.7 mm inner/outer diameter, ~90 MPa applying a new ionic liquid compressor technology) with the world's first compressor system for 70 MPa. Another new hydrogen station offering both gaseous and liquid hydrogen started operation in 2006 near Munich to serve, at the beginning, about 10 cars and buses per day; its LH_2 dispenser is shown on the right-hand side of Fig. 7-19.

As part of the ZEMShips project, a hydrogen refueling station with LH_2 storage tank will be employed for filling the 35 MPa pressure tanks of the first ship with fuel cell propulsion (2 x 50 kW) to be operated in Hamburg from 2008. An ionic compressor is used to produce 45 MPa H2 gas. The estimated boil-off loss is 0.95 %/d [Stolper 2008].

Among the 10 H_2 stations which opened in the Tokyo area in the last few years, the Ariake station offers liquid hydrogen since 2003. The LH_2 is produced at Nippon Steel Kimitsu Works, where a 200 kg/d liquefaction plant is being operated extracting the hydrogen from the waste gas stream of a coke furnace.

For the purpose of serving hydrogen-fueled road vehicles in areas with a still insufficiently dense grid of H_2 refueling stations and complementing stationary systems, trailer-mounted mobile mini-fuelers have been developed and constructed. One recent example is shown in Fig. 7-20 delivering both liquid and gaseous hydrogen fuel. While the LH_2 is fueled directly into the car tank, gaseous H_2 will first pass through a buffer storage tank.

Figure 7-20. Linde trailer-mounted filling station for GH_2 and LH_2 fuel

For the example of a refueling station serving LH_2, the methodology of safety-barrier diagrams was applied [Duijm 2007]. It is a tool that can be used in support of the hazardous analysis of a system giving an overview of precaution measures and the consequences in case of their failure. As an easily understandable technique, it is recommended to be used when communicating with authorities or stakeholders during the permitting process. Fig. 7-21 shows the resulting safety-barrier diagrams for the truck unloading process (top) and the LH_2 storage system (bottom). The barriers depicted include both active, like inspections, H_2 sensors, pressure relief valves, and passive systems, such as temporary obstruction.

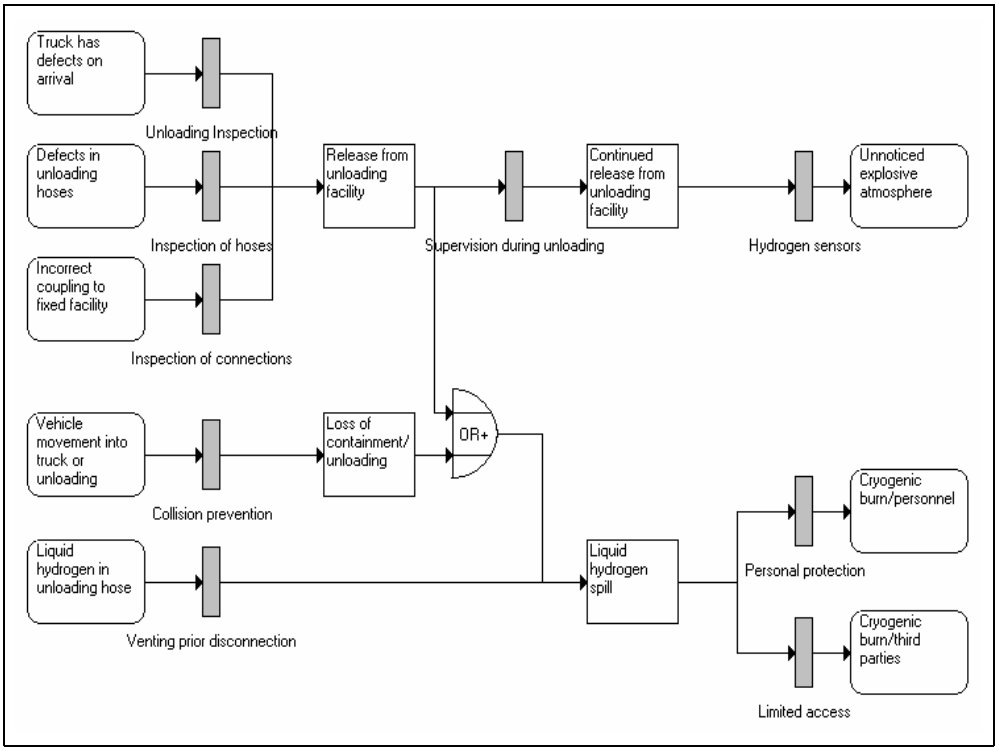

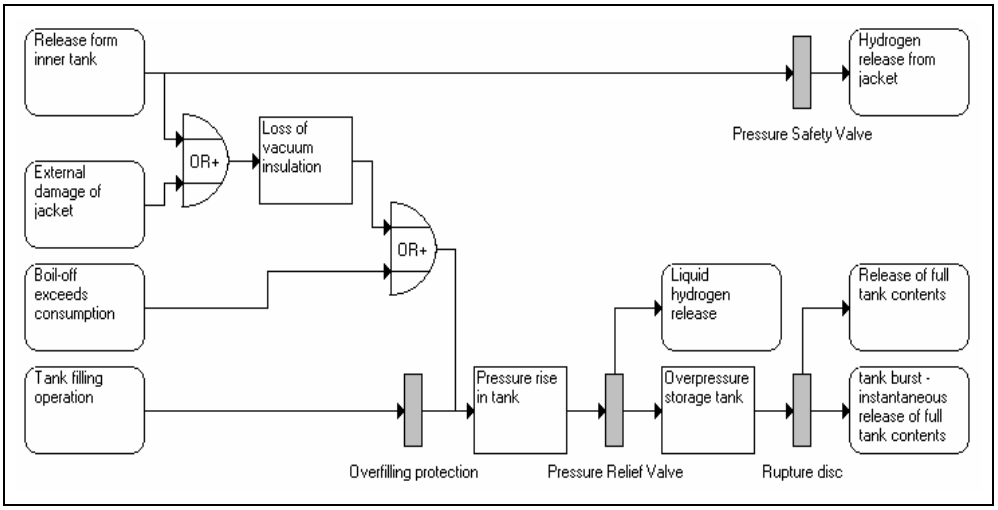

Figure 7-21. Safety barrier diagrams for the unloading process of an LH_2 truck (top) and for the LH_2 storage tank at a refueling station [Duijm 2007]

7.2.6. Fuel Cell CHP Plant Pilot Project

As part of the Euro-Quebec project, a fuel cell CHP (Combined Heat and Power) plant was operated in Hamburg, Germany [Newi 1995]. The PAFC (phosphoric acid fuel cell) based facility started operation in 1995 with one 200 kW(e) unit fueled by natural gas followed two years later by a second unit of the same power size running on hydrogen. The H_2 was stored as liquid in a stationary tank. Overall efficiency was 85 %. The demonstration project for the H_2-fueled plant unit was terminated in May 2000 after a comparatively reliable operation.

The operation of this first-in-the-world H_2-based energy system to meet district heat demand in the middle of a residential area in Hamburg also required first-of-its-kind legal permission procedures. A safety audit has been conducted by the German Federal Institute for Materials Research and Testing, BAM, for an LH_2 storage and vaporization facility to be installed inside a residential area [BAM 1994]. With a storage capacity of more than 3 t, but less than 50 t of hydrogen, the simplified licensing procedure according to the Federal Immission Control Act (BImSchG) without a safety analysis is required.

The LH_2 storage vessel was a cylindrical, standing tank with a net capacity of 60 m^3. The tank was designed to sustain a maximum pressure of 1.2 MPa. The operating pressure was ranging between 0.6 and 1.05 MPa with a nominal value of 0.75 MPa. The typical boil-off rate of a 75 m^3 tank was 0.7 %/day. Both storage tank and vaporizer were designed to withstand a (wind) pressure of 5 kPa corresponding to a wind speed of 150 km/h.

The operation of the 200 kW PAFC plant with hydrogen required a throughput of approximately 6 kg/h. The refueling at the LH_2 storage tank was done every 2 - 3 weeks from a tank truck. Fig. 7-22 shows a diagram of the arrangement of the tank facility and its connections to the refueling truck (left-hand side) and to the fuel cell unit (right-hand side). Pneumatic valves are being operated by pressurized helium or air. The main refueling valve is controlled from the tank truck. The truck driver stops the refueling process when a filling level of 95 % is reached. The hydrogen is withdrawn from the liquid phase inside the tank and routed to the vaporizer.

The storage tank is protected against overpressure by a consecutive series of relief arrangements as shown in the figure. If the pressure exceeds 0.8 MPa, hydrogen from the vapor phase will be discharged to the vaporizer. At a pressure of 1.0 MPa, the H_2 will be vented via PC3 to the stack a2. Upon further increase of the pressure to 1.2 MPa, the safety valves SV1 and SV2 will open and release gaseous H_2 through stack a1. At still increasing pressure, rupture disks BD1 and BD2 will be activated at 1.69 MPa. Safety valves and rupture disks, however, are required only in case of a severe accident with a failure of the outer container. For an intact tank in a closed state, it needs in the order of several days until the pressure has reached a level where the first safety measure would be initiated.

Measures in connection with the refueling procedure are such that the process is automatically interrupted, if the tank driver continues to fill the tank beyond 95 %, if the grounding of the tank truck is insufficient, if the storage tank pressure is too high or too low, or if the helium pressure for valve control is too low. The failure of piping usually will soon be detected due to a significant change in the operational parameters such that the withdrawal of LH_2 from the tank will be disconnected immediately. Furthermore H_2 detection devices and warning systems are installed in areas where hydrogen can leak and accumulate.

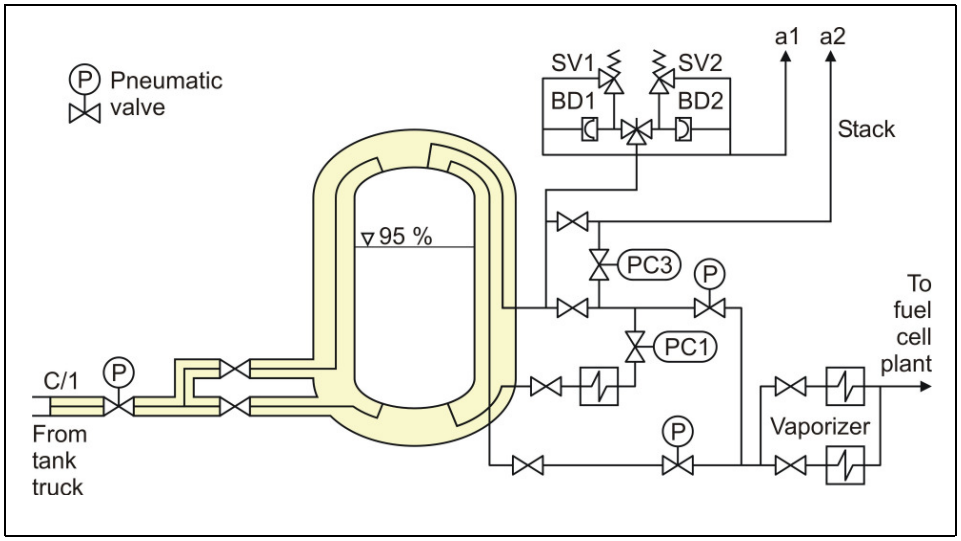

Figure 7-22. Schematic of the LH_2 storage tank system with connection to truck (left) and fuel cell plant (right) [BAM 1994]

A spill of LH_2 is conceivable during the refueling procedure which usually takes about 1 - 2 h, e.g., by a moving tank truck while still connected to the tank. In such a case, the helium line and the grounding connection would fail first and disconnect the LH_2 line. The maximum quantity of LH_2 spilled is estimated to be not more than 0.2 l, too small to cause a major explosion hazard.

In case of a failure of the insulation between the inner and outer container, hydrogen is estimated to vaporize at a rate of 55 kg/h and to be released through the two symmetrically arranged venting stacks. Worst case would be a release in wind direction, when a widely extended plume develops. In a no-wind situation, two symmetrical plumes spreading in opposite directions will be created. Because of its lighter-than-air specific weight, hydrogen will always have the tendency to rise and thus will remain far away from the ground.

According to the German “Technical Rule Pressure Vessel” (TRB), the double-walled storage tank is treated the same as an earth-covered tank with respect to the safety distance. The minimum distance from the outer tank to adjacent buildings or facilities is 5 m. The recommendations of the “International Gas Carrier Code” (IGC) which are partly stricter than the TRB rules, mention safety distances of 10 m to roads and technical (non-residential) buildings and 20 m to residential buildings (which are met here). The protection area, i.e., the zone in which the formation of flammable gas clouds is possible, has a 5 m horizontal and 2 m vertical extension. For the LH_2 storage tank with a height of 14 m and venting lines ending 4 m above the vessel, the protection area thus reaches a total height of 20 m.

7.2.7. H_2/O_2 Steam Generator

In a cooperation between the DLR (today: Deutsches Zentrum für Luft- und Raumfahrt) and other German companies from 1989 to 1993, the concept of a hydrogen and oxygen fueled steam generator has been developed. This component is actually the re-configuration of an H_2/O_2 rocket engine which allows the instantaneous provision of steam of any desired quality. H_2 and O_2 are compressed and injected in a combustion chamber. A schematic of the facility is shown in Fig. 7-23 [Haidn 1996].

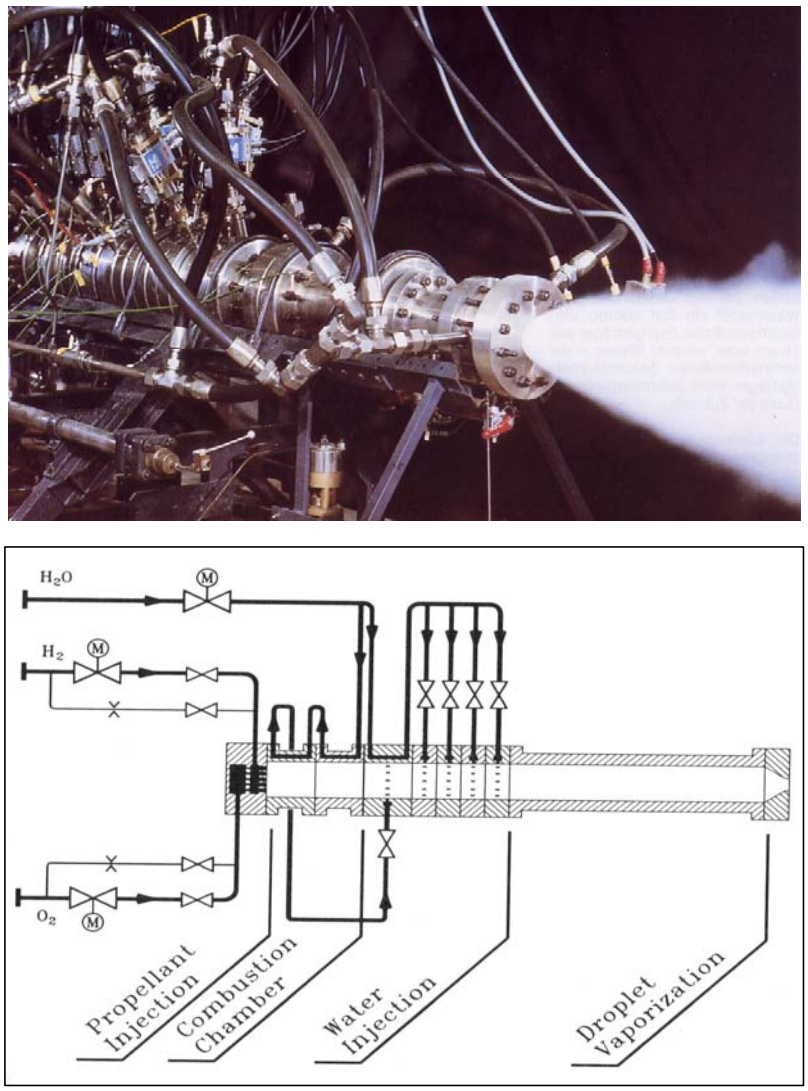

Figure 7-23. Schematic of the DLR LH_2-LOX steam generator [Haidn 1996] (Courtesy of DLR)

Stoichiometric mixture is necessary to generate superheated steam of high quality without any side products. The combustion gas with a temperature of 3000°C can be cooled by adding water to achieve exactly the desired steam condition for injection into the power plant process. Startup time of such a steam generator is in the order of 1 - 2 s with a combustion efficiency of greater 99 %. It can act as a backup system for fast power-up of steam generation plants to serve as a cold stand-by spinning reserve in decentralized power production.

In a first step, totally 285 combustion tests were conducted in 1991/92 with a prototype operated in the power output range between 25 and 70 MW. The second step was the construction of the demonstration facility for H_2/O_2 instant reserve, HYDROSS, consisting of a modified H_2/O_2 steam generator of 2 m length and 0.4 m outer diameter plus storage and supply system [Kusterer 1995]. Full power was obtained after 1 s, and after 3 - 5 s, there was stable steam production. The experimental version of the steam generator produced steam of 560 - 950°C at 4 - 9 MPa. This compact, soot-free, and low-cost component is principally ready for the market.

7.3. Large-Scale Projects

7.3.1. Euro-Quebec Hydro-Hydrogen Pilot Project

In 1987, the concept of a clean energy system based on hydrogen as a transportable medium was presented. It was the result of the cooperation of more than 20 companies and the starting point of the so-called “Euro-Quebec Hydro-Hydrogen Pilot Project”, EQHHPP [GQ-CEC 1991]. The idea of this project, as is depicted in Fig. 7-24, was to use 100 MW of hydro electric power, of which is plenty available in Canada, for the production of hydrogen via electrolysis. The gaseous H_2 would then be liquefied (requiring another 30 MW(e) input) and transported by barge carrier across the ocean to Europe (Hamburg harbor) for being distributed and consumed in various applications. The annual transportation of 14,600 t of LH_2 corresponds to an estimated equivalent power output of 74 MW(e) plus some 7 MW of “cold” energy recovery. The main objective of the EQHHPP was the demonstration of the possibilities of safe transport, storage, and distribution of hydrogen.

Originally three alternative vectors for the seaborne transport of H_2 were investigated: (i) ammonia, (ii) methylcyclohexane (MCH)/toluene, and (iii) liquid hydrogen. The LH_2 vector was finally deemed the best option. For the maritime transportation of the LH_2, concepts of barge carrier ships have been developed with the barge-mounted mobile tanks to be also used for on-shore storage in order to minimize transfer losses (see chapters 4 and 5).

The proposed LH_2 terminal in the harbor of Hamburg comprised the port for loading and unloading operations, a lifting platform to transfer the tanks after being floated out of the barge carrier ship to the shore, and the on-shore storage and distribution devices. The further distribution was planned to be done by tank trucks. Potential consumers were seen in the local transportation system, as fuel for aircrafts, residential heating from fuel cell power plants, gas turbine power plants, or mixing with natural gas to “Hythane” and introduce into the grid.

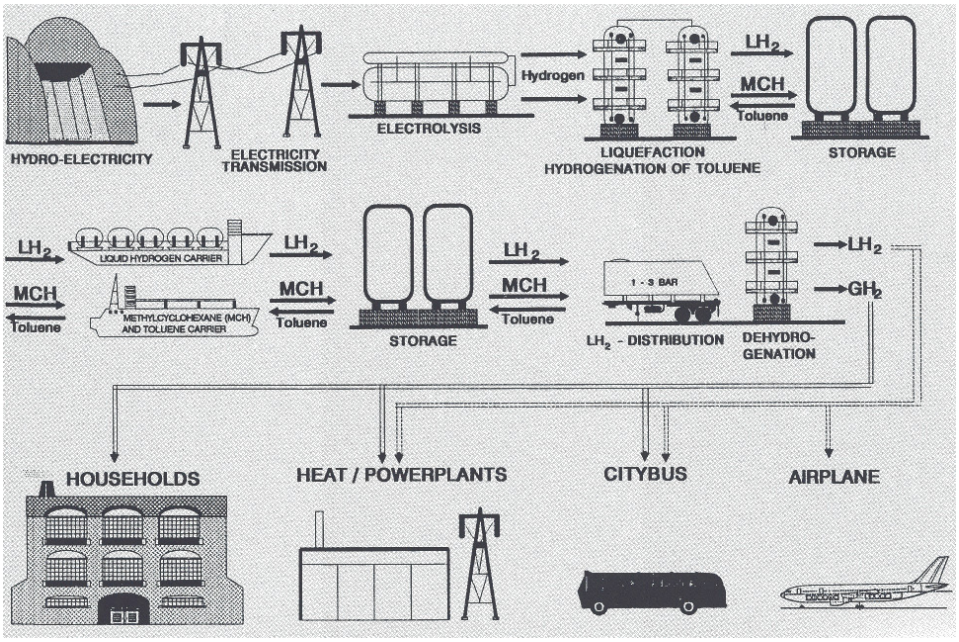

Figure 7-24. Concept of the Euro-Quebec Hydro-Hydrogen Pilot Project

The Euro-Quebec project itself was finally terminated in 1992, but continued to live in form of various single sub-projects of a hydrogen demonstration program such as city buses, a H_2 refueling station in Hamburg, a fuel cell driven boat in Italy, the manufacturing and (safety) testing of a 60 m^3 LH_2 model tank for maritime transportation, a 5 MW(e) H_2 fuel cell plant with an 80 m^3 LH_2 stationary storage vessel, and many others.

7.3.2. WE-NET Project

One of the worldwide most ambitious hydrogen energy research projects pursued in Japan was the "International Clean Energy Network Using Hydrogen Conversion", short: World Energy Network or WE-NET, operating under the wider frame of the New Sunshine Project. Its main objective was the establishment of a large-scale energy system based on hydrogen from renewable energy sources. The project was directed by NEDO (New Energy and Industrial Technology Development Organization), an implementing agency of the Japanese government. Starting in 1993, WE-NET was scheduled to run over 28 years in three distinct phases. Phase I (1993-98) was dealing with the survey on key technologies and elemental research and system studies under various subtasks. Phase II (1999-2005) was dedicated to the development of prototype systems in the order of 50 MW, while in the final phase III, the hydrogen technologies were to be demonstrated in sub and full systems [Murase 1995]. Main hydrogen production method was considered to be solid polymer electrolyte water electrolysis. Long-distance maritime transportation of the hydrogen was foreseen to be done as LH_2, alternatively H_2 carrier liquids like methanol or ammonia. On the demand side, the H_2 was to be used as a fuel in the transportation sector, in fuel cell power plants, in combustion

turbines, in households, and as chemical feedstock. Originally based on renewable energies, the later Phase II considered also fossil fuels to allow the introduction of large amounts of H_2 on a short term.

While in Phase I, both the conceptual design of the total system and the energy balance and the electricity cost were verified, Phase II was used to continue the development of fundamental technologies and, in particular, to prepare distributed energy technologies. Studies were conducted on stand-alone refueling stations (steam reforming or electrolysis), metal hydride vehicle tank systems, low-temperature fuel cells, and also LH_2 (magnetic) liquefaction [Hijikata 2002]. The WE-NET project, originally planned as a long-term program, was eventually discontinued at the end of Fiscal Year 2002, and replaced with a more specific hydrogen and fuel cell program to promote commercialization of fuel cells in mobile and stationary applications.

Investigation and research in the field of safety within the WE-NET project was the establishment of a comprehensive "System Safety Design" including a concept of safety measures for prevention of accidental LH_2 release or the mitigation of accident consequences. These activities included the risk analysis of hydrogen subsystems, a collection of data on accidents with handling hydrogen, and the review and systematization of existing safety standards. The computer code CHAMPAGNE, a multi-phase, multi-component thermodynamics model originally used in the nuclear field was modified to also treat the atmospheric dispersion of hydrogen gas clouds, and was successfully applied to the NASA LH_2 spill experiments of 1980 [Chitose 1996].

7.3.3. PORSHE Project

Another long-distance H_2 transportation system project in Japan was the so-called "Plan of Ocean Raft system for Hydrogen Economy", PORSHE, active during 1974-1998. The concept was based on solar hydrogen generated by means of photovoltaic cells with a total surface of 12,000 km^2 deployed on 12,000 overseas ocean rafts in the South Pacific Ocean. After liquefaction, LH_2 at an amount of 25 million t/yr was then to be transported by tank ships to 20 import bases in Japan for further distribution [Hiraoka 1991].

7.4. LH_2 Applications in Science

The main purpose of liquid hydrogen when used in research is the investigation of the behavior of materials at low temperatures. Also its extreme cleanliness is an important feature widely used. Condensation processes are used to extract trace gases at high purity. Rectification leads to precise isotope separation. LH_2 is also used for cooling purposes, if the more expensive liquid helium could be saved.

7.4.1. Liquid Hydrogen in Bubble Chambers

The bubble chamber was invented in 1952 by Donald A. Glaser, the later Nobel prize winner, as an instrument to detect and visualize moving electrically charged elementary particles. It is a cylindrical vessel filled with a transparent liquid which is a little bit below its boiling point.

A piston is used to suddenly decrease pressure, by which the liquid goes into a superheated metastable phase (Fig. 7-25). When a particle passes through the liquid, it is warmed up to the boiling point along the track of ions created. In the wake remains a trail of microscopic bubbles that can be photographed. Bubble density around a track is proportional to the particle's energy loss. The resolution achieved is down to a few micrometers. Also the recovery time is short; bubble chambers could be operated at 20 pulses/s. Liquid hydrogen is used because it offers the possibility of simple particle interactions, as hydrogen nuclei consist only of single protons. The magnetic field applied serves to curve the tracks of charged particles to ease their identification.

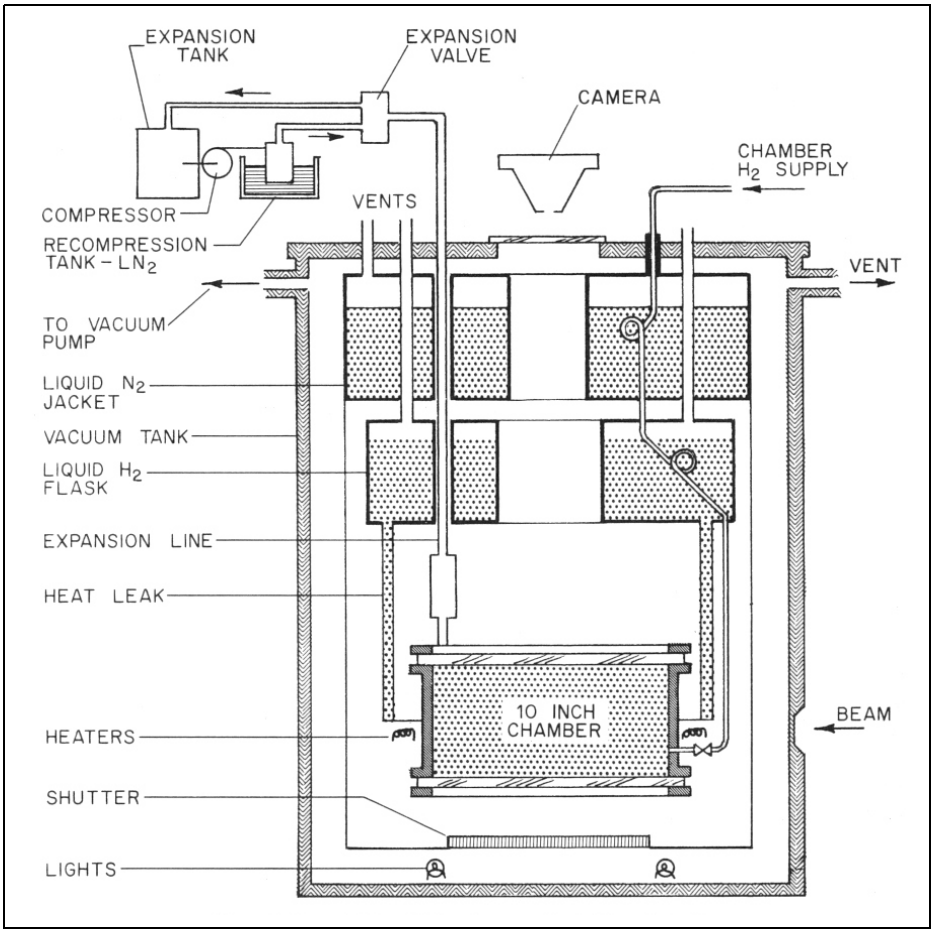

Figure 7-25. Schematic of a bubble chamber [Sittig 1963]

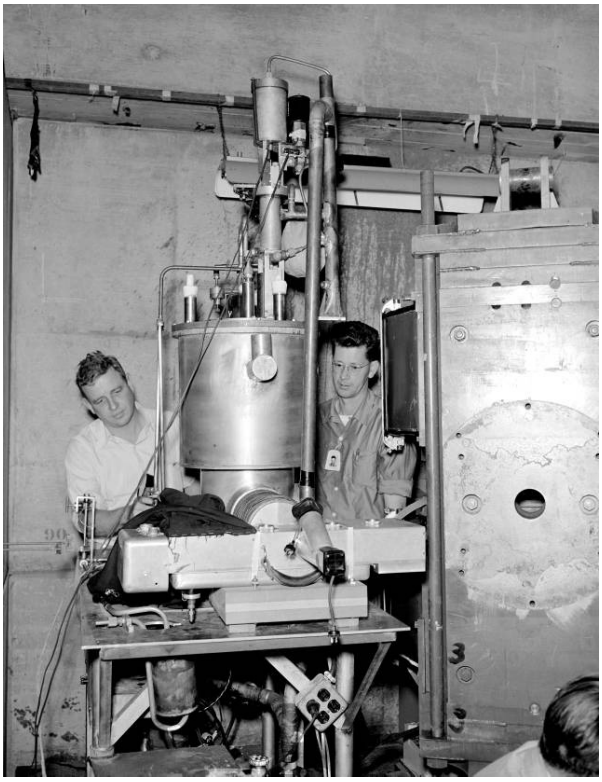

Figure 7-26. First LH_2 chamber by Alvarez (right)
(Courtesy of Ernest Orlando Lawrence Berkeley National Laboratory)

The early bubble chambers were very small. The first fabricated by Glaser was a 100 mm long glass tube of 0.25 mm diameter filled with diethyl ether. Luis W. Alvarez built in 1954 the first device to work with LH_2 at the Lawrence Berkeley National Laboratory (Fig. 7-26). The chamber, 37 mm in diameter, successfully demonstrated the formation of particle tracks. Successor models were rapidly growing in size. A 100 mm chamber filled with 0.4 l of LH_2 was in operation in 1954, two years later a 254 mm chamber with 9 l of LH_2. In 1959, a 180 cm long bubble chamber filled with 500 l of LH_2 (also LD_2) was erected in Berkeley, where the liquid was kept at a temperature of 26 K and at an overpressure of about 0.4 MPa. More than 100 bubble chambers were built throughout the world operating on liquid hydrogen or deuterium, but also propane, argon, or helium were used as working fluids. Among the largest chambers were the 0.8 m Saclay bubble chamber of the European Organization for Nuclear Research (CERN), the 2 m CERN bubble chamber to hold 1080 l of LH_2, the NAL 15 ft (~4.6 m) bubble chamber at Fermilab in Chicago, and the Big European Bubble Chamber (BEBC) also at CERN in Geneva, Switzerland.

Big European Bubbles

The stainless-steel vessel of the Big European Bubble Chamber (BEBC) installed in the early 1970s was measuring 3.7 m in diameter and 4 m in height, and was filled with 35 m^3 of liquid hydrogen (or deuterium or a neon-hydrogen mixture). Its sensitivity was regulated by means of a huge piston weighing 2 t. The first images were recorded when BEBC equipped with the largest superconducting magnet in service at the time to provide a 3.5 Tesla magnetic field started operation in 1973. BEBC operation ended its active life in 1984.

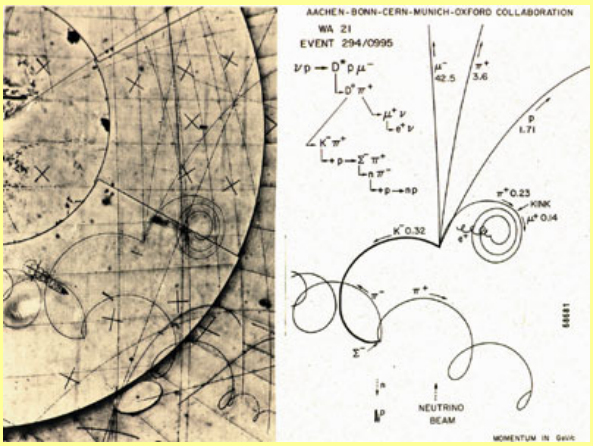

BEBC bubble chamber image (Courtesy of CERN)

Bubble chambers were shielded against thermal radiation by being placed in a vacuum tank. The pumping capacity required is low during normal operation, but may be high in case of hydrogen or helium leaks which happen once in a while, since the chamber remains filled over longer periods of up to 1 year. In case of too high pressures, a safety relief valve is activated to dump the leaking gas into a large sphere. A critical issue is the tight sealing of the glass window in larger bubble chambers due to different shrinkage rates of the glass and metal materials. The vacuum tank is placed in a copper tank cooled with liquid nitrogen as additional thermal insulation.

After a 30 year long bubble chamber epoque, this detection technique came to an end and was gradually replaced with spark chambers, where in a stack of metal plates or wire grids high voltage is maintained between alternate layers and sparks develop as charged elementary particle are traversing.

7.4.2. Hydrogen as Cold Moderator Material

Hydrogen is one of the most attractive materials for cold moderators in steady or pulsed neutron sources. These are devices to generate slow neutrons with energies < 0.005 eV and respective wavelengths in the order of inter-atomic distances, an ideal investigation tool for scattering experiments in material sciences. In most cases, nuclear material test reactors (MTR) are used as neutron sources based on the fission of uranium. The lower the temperature of the moderator, in which the generated neutrons are slowed down, the higher is the yield of slow neutrons. LH_2 or LD_2 is in use as cold moderator material in such MTRs since 1957, when the first system was installed in the BEPO reactor in Harwell, UK.

An alternative neutron source to MTRs is a specifically designed, so-called spallation source with the advantage of a much higher neutron production resulting from the excitation of heavy elements (such as mercury). Parallel to the design and construction of large-scale spallation sources in Oak Ridge, USA, and in Tokai, Japan, the European countries were planning the so-called "European Spallation Source", ESS. It was designed as a 10 MW facility with a 1.334 GeV linear accelerator producing a proton beam to serve two target systems [ESS 2002]. The type of the target was flowing mercury. Cold moderator systems (two for each target) are employed to slow down the liberated neutrons to a desired energy spectrum, before they are routed into the instruments of the users.

Supercritical hydrogen and liquid hydrogen are ideal moderators in that they offer a high cross section and large energy transfer per collision. The hydrogen also remains stable in high radiation fields and, as a liquid, allows easy heat removal. (Methane would be even the better moderator material because of its higher H_2 density, but exhibits other decisive drawbacks.) The advantage of supercritical hydrogen over sub-cooled liquid is the total absence of problems with two-phase flow especially during cool-down, warm-up, stand-by, or other transient conditions. Also it eliminates local supercritical boiling inside the moderator chamber allowing a greater flexibility of operating temperatures. Ortho H_2 is the stronger neutron scatter than para H_2 and is ideal to maximize the production of cold neutrons showing the higher integrated intensity. The ideal ortho-para composition for a given moderator depends strongly on its size and geometry and mode of coupling/poisoning. The dependence of the ortho-para ratio on the source power and the conversion rates make the moderator properties a function of time.

An advanced cold moderator system which was foreseen for the European Spallation Source (ESS) project is shown in Fig. 7-27 [ESS 2004]. Dimensions of the chamber are 120 mm in length, 150 mm in height, and 50 mm in thickness. Moderating material is here a flow of supercritical H_2 at 1.5 MPa (i.e., 0.2 MPa above the critical pressure) with inlet/outlet temperatures of 25 K and 28 K, respectively, to remove the power of maximum 7.5 kW produced in the chamber resulting from nuclear heating of the wall material and the LH_2 from fast neutrons or γ-radiation.

Due to the need of permanent heat removal, a self-sustained, closed-cycle refrigeration system is required. The cryo-system including moderator is cooled down by helium which is brought to low temperatures by means of expander turbines. Insulation of the cold helium and hydrogen systems is made by a vacuum containment. All H_2 containing systems including transfer lines are surrounded by a helium blanket to serve the purpose of detecting leakages in the vacuum containment and preventing air ingress.

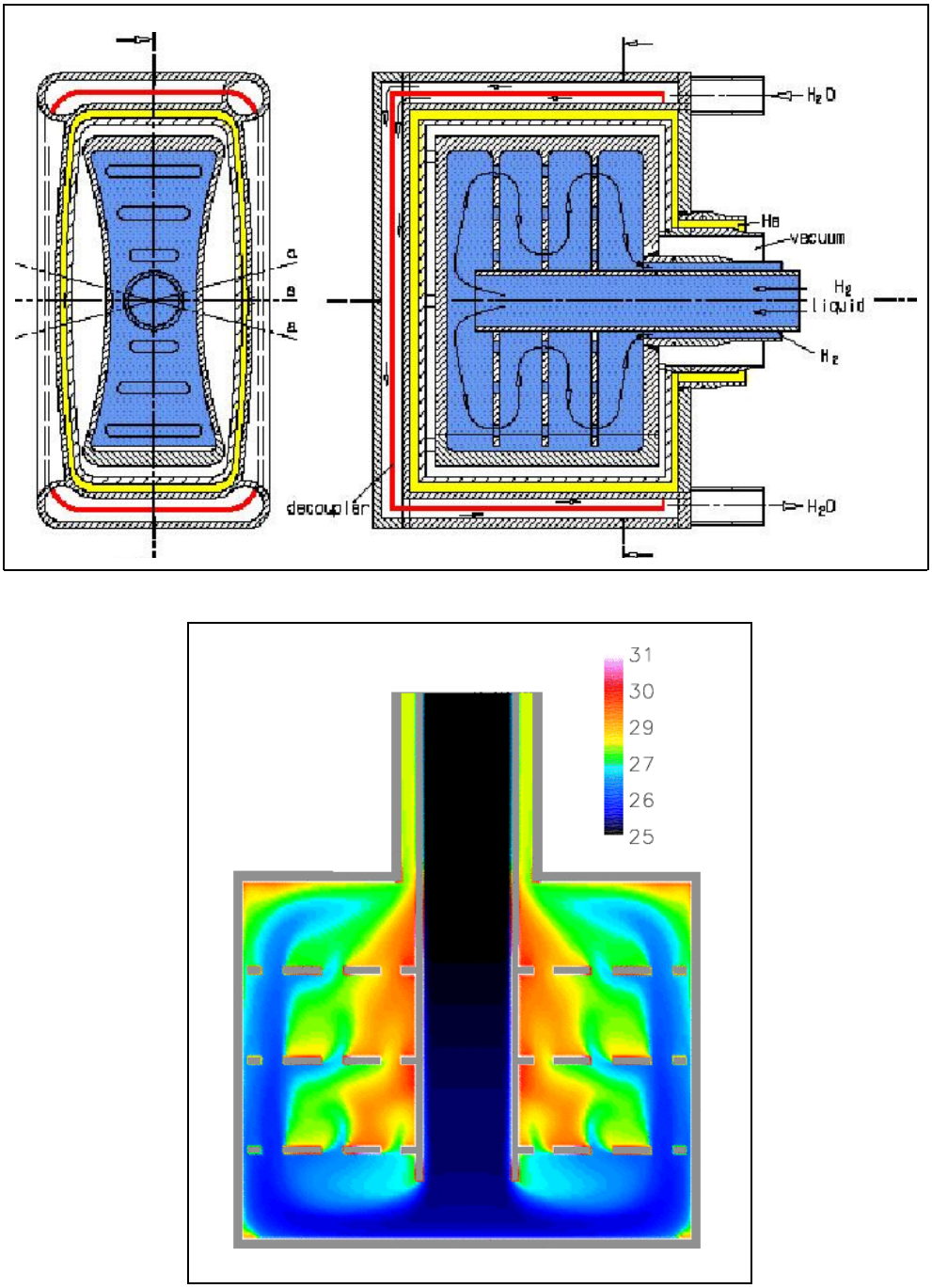

Figure 7-27. Supercritical hydrogen moderator system of the European Spallation Source
Top: horizontal and vertical cut through chamber (walls and gaps enlarged)
Bottom: fluid temperature distribution in chamber during normal operation

This safety concept corresponds to a “triple containment” system to avoid pumping of air and thus oxygen to the cold surface in the case of a small leak in the outer shell. The triple containment is a characteristic – and crucial – feature of all cold moderator systems.

In Fig. 7-28, the cryogenic system is shown as was foreseen for the ESS. Moderator vessel and immediately following coaxial pipes are made of Al, the other parts are made of stainless steel. Fig. 7-29 shows a cross section of the LH_2 transfer lines indicating parallel rather than concentric pipes. The parallel arrangement was deemed superior with regard to thermal and nuclear heating near the target.

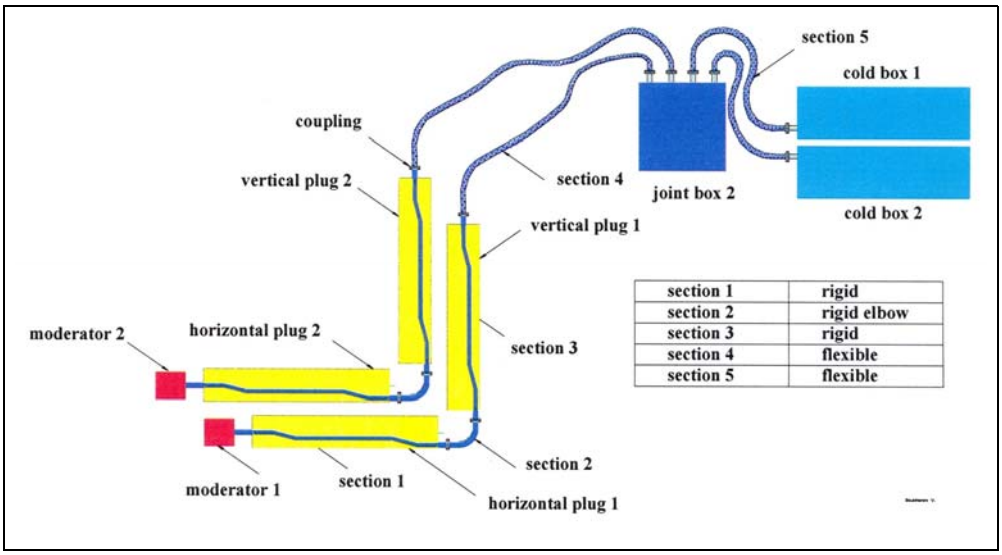

Figure 7-28. General layout of the cryogenic transfer lines for horizontal and vertical moderator plugs [ESS 2004]

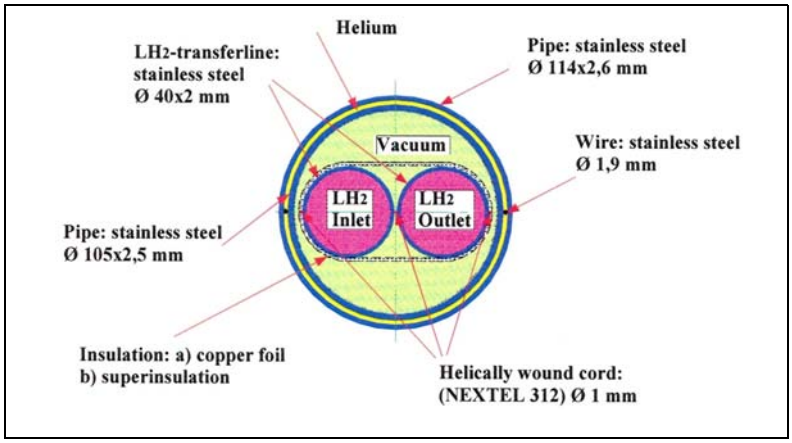

Figure 7-29. Cross section of the hydrogen transfer lines (rigid sections) [ESS 2004]

7.4.3. Heavy Water Production from Distillation of Liquid Hydrogen

Heavy water (D_2O) is an ideal neutron moderator (and cooling) material that can be used in the operation of thermal nuclear reactors as is done in the Canadian type reactor CANDU (Canadian Deuterium Uranium). It has the advantage that due to its low absorption cross section, unlike light water (H_2O), the uranium fuel does not need to be enriched in its fissile U-235 isotope. It is for this reason that production and export of heavy water is controlled under IAEA safeguards.

The production of deuterium, whose natural contents in hydrogen is not more than 0.014 %, can be done on a large scale in various, both physical and chemical processes. Their suitability can be valuated by comparing criteria such as feed, separation factor, natural exchange rate, or the energy demand. There is no economically ideal process; each has its strong and weak points.

One of them is the fractional distillation of liquid hydrogen and subsequent conversion of the deuterium to heavy water. It is an efficient method based on the fact that boiling points are different for H_2 (20.3 K) and D_2 (23.5 K) and HD (22.1 K), respectively, which means that the hydrogen gas above the liquid is slightly depleted in deuterium. Thus deuterium can be gathered by simple vaporization of liquid hydrogen. In principle, the use of water with its boiling points of 100°C (H_2O) and 101.4°C (D_2O) would also be possible, but it is less efficient method. The separation process is conducted in several subsequent stages (Fig. 7-30) until the desired HD concentration is obtained. In a separate unit, reactions of the form

$$2\,HD \rightarrow H_2 + D_2$$

result in a ternary mixture with fractions in the order of 25 % each for H_2 and D_2, with still 50 % remaining HD. In a separate column, the pure D_2 is extracted from the mixture.

Advantages of the refrigeration process are a separation factor (ratio of D_2 concentration in the liquid over concentration in the vapor) of ~1.5 and a moderate energy demand. Major drawback is the need for a highly pure H_2 feed [Miller 2001].

Harold C. Urey proved the existence of deuterium in 1931 (and was awarded the Nobel prize for his studies in 1934) when condensing 5 l of LH_2 down to 1 cm^3 and measured the atomic spectra. The former Soviet Union was successful in the construction of an industrial-scale plant for D_2 production in 1958, a schematic of which is shown in Fig. 7-30 [Malkov 1958]. The distillation columns have typical sizes of up to 10 m in height and 1 - 2 m in diameter. The columns are insulated by a vacuum jacket and an LN_2-cooled heat barrier or installed inside an LN_2-cooled vacuum cold box. Operating conditions are in the ranges of < 35 K and 0.5 - 5 MPa. An important safety-related aspect is again the necessary removal of impurities (N_2, O_2) which may plug lines upon freezing.

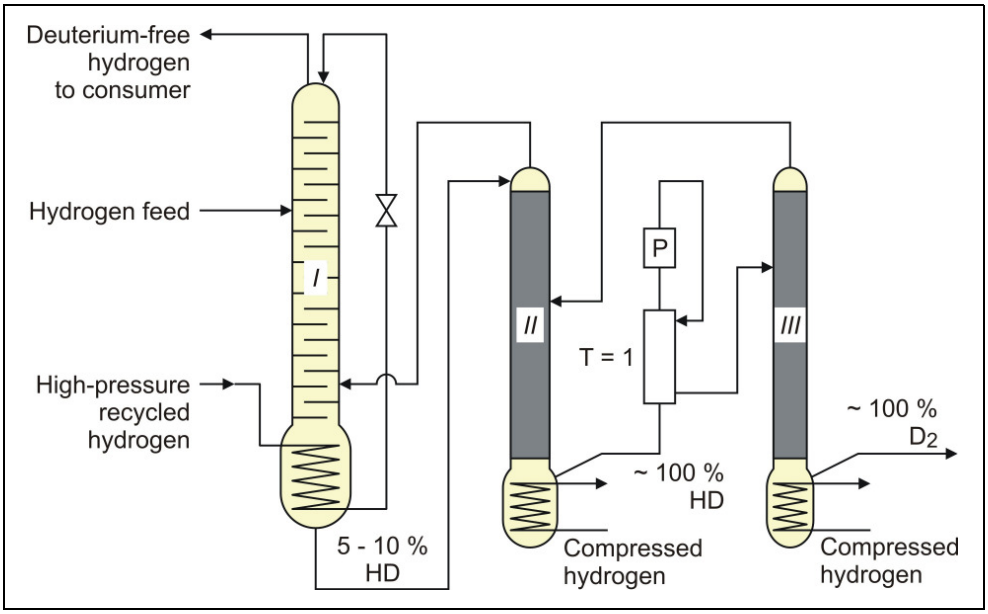

Figure 7-30. Schematic of the refrigeration method for deuterium separation [Malkov 1958]

8. LIQUID HYDROGEN BEHAVIOR UNDER ACCIDENTAL CONDITIONS

8.1. Phenomenology of Cryogenic Release

8.1.1. Accident Scenarios

As a result of the different types of hydrogen storage, various accident scenarios are conceivable for a storage tank to release its contents into the environment:

- Formation of a liquid hydrogen pool on the ground and vaporization of the liquid;
- Release of a jet stream of liquid or gas or a two-phase mixture through a small opening in a pressurized system;
- Catastrophic failure of the tank resulting from high internal pressure with the instantaneous, explosive-like release of the whole content.

Liquefied gases are characterized by a boiling point well below the ambient temperature. If released from a pressure vessel, the pressure relief from system to atmospheric pressure results in spontaneous (flash) vaporization of a certain fraction of the liquid. Depending on leak location and thermodynamic state of the cryogen (pressure expelling the cryogen through the leak is equal to the saturation vapor pressure), a two-phase flow will develop, significantly reducing the mass released. It is connected with the formation of aerosols which vaporize in the air without touching the ground. Conditions and configuration of the source determine the features of the evolving vapor cloud such as cloud composition, release height, initial plume distribution, time-dependent dimensions, or energy balance. The phenomena that may occur after a cryogen release into the environment are shown in Fig. 8-1.

Spillage into the impoundment area may form a vapor cloud that ignites and flashes back to the pool causing a pool fire; to be more precise: it is the flammable vapor-air mixture above the pool that is burning.

8.1.2. Vaporization of Cryogenic Liquids

The release as a liquefied gas usually results in the accumulation and formation of a liquid pool on the ground which expands, depending on the volume spilled and the release rate, radially away from the releasing point, and which also immediately starts to vaporize. The equilibrium state of the pool is determined by the heat input from the outside, i.e., from the ground, the ambient atmosphere (wind, insolation from the sun), and in case of a burning pool, radiation heat from the flame. The respective shares of heat input are depending on the cryogen considered. Table 8-1 compares the data for the cryogens LH_2, LN_2, and LNG assuming a pool of 1 m^2 on a water surface and a wind speed of 5 m/s [Dienhart 1995].

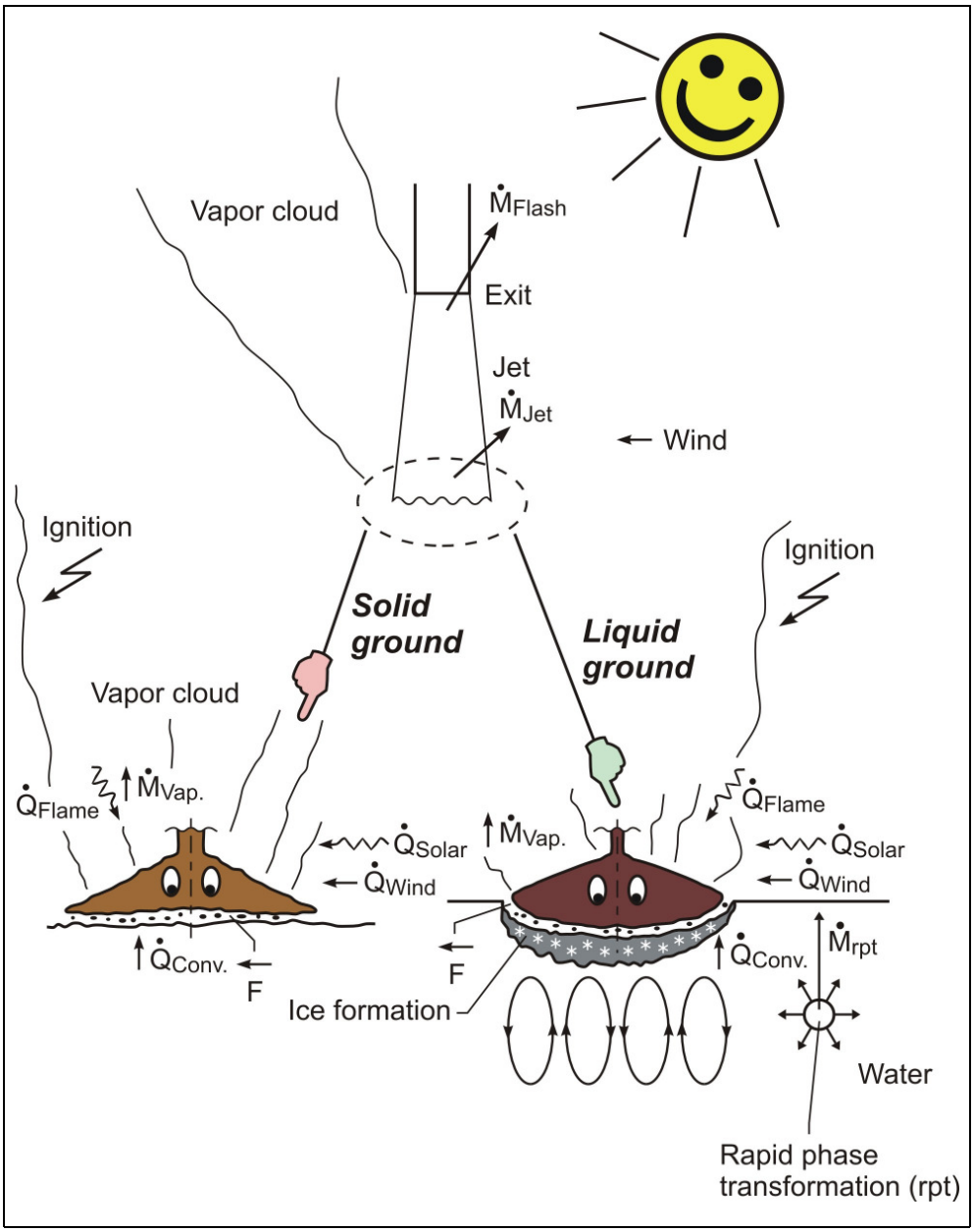

Figure 8-1. Physical phenomena occurring upon the release of a cryogenic liquid

Table 8-1. Sources of heat input into a vaporizing cryogenic liquid pool

Heat input by	Heat Source [kW/m^2]		
	LH_2	LN_2	LNG
Atmospheric Convection	0.8	1.8	1.1
Radiation from flame	12	-	100 - 200
Radiation from ambient	1.6	1.6	1.6
Conduction from ground	100	25	92

As can be seen from the table, the most dominant heat source for all cryogens is heat transport from the ground. This is particularly true for LH_2, where a neglection of all other heat sources would result in an estimated error of 10 - 20 %. For a burning pool, also the radiation heat from the flame provides a contribution. This is significant, e.g., for a burning LNG pool due to its much larger emissivity resulting from soot formation. An additional heat source for the extremely cold LH_2 is from condensation of air (liquefied at 90 K (O_2) and 77 K (N_2), respectively) falling into the pool.

Heat transfer depends, apart from the thermo-physical properties of the LH_2, also on the type of boiling which is classically subdivided into three regimes, film boiling at larger temperature differences between fluid and ground, nucleate boiling at small differences, and some transitional stage in between. The functional relationship is described by the so-called Nukiyama curve as is qualitatively shown in Fig. 8-2.

If liquid hydrogen gets into contact with the ground, the temperature difference between liquid (always at boiling point) and ground is largest. Vaporizing liquid immediately generates a vapor cushion between the “hot” ground and the liquid (film boiling). The vapor film usually hinders the heat transfer into the liquid and the vaporization rate is comparatively low. Realistically the vapor bubbles formed bounce against the lower surface of the liquid which leads to a periodic movement (bubble-driven turbulence). With increasing coverage of the surface, the temperature difference is decreasing until at some point (Leidenfrost temperature), the film layer becomes instable and collapses. The result is an improved heat transfer through direct contact (nucleate boiling). The increase in heat transport is limited by the so-called “critical heat flux” or “boiling crisis”. The transition phase between film and nucleate boiling is of very short duration and hardly experimentally investigated.

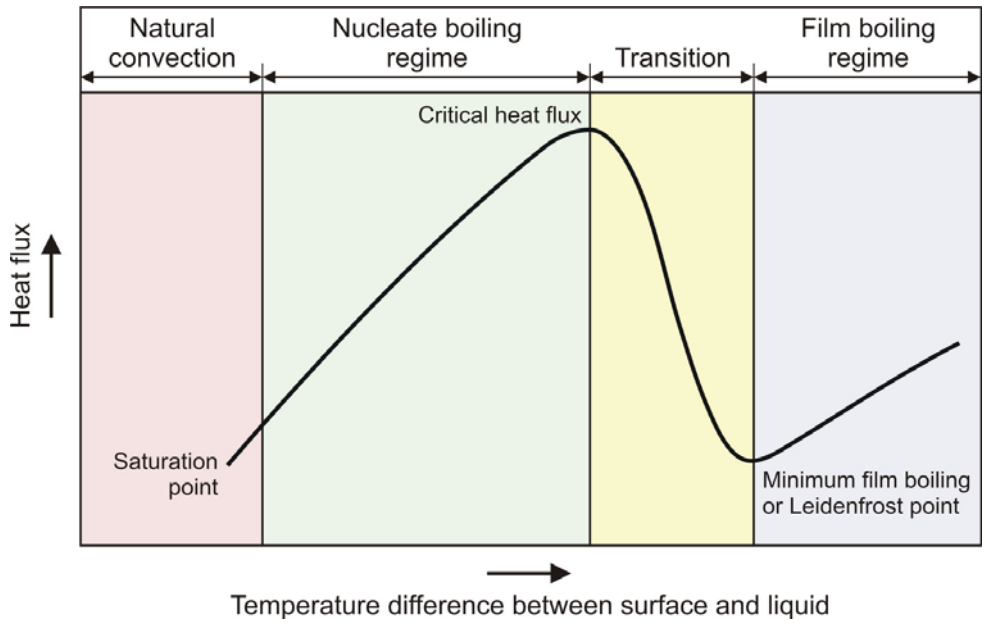

Figure 8-2. Heat flux vs. temperature difference between fluid and ground

The heat conduction in a homogeneous medium can be described by the Fourier differential equation:

$$\frac{\partial T}{\partial t} = a * \nabla^2 T + \frac{\Phi}{\rho c_p} \tag{8-1}$$

where a – thermal diffusivity, m^2/s; Φ – volume-related heat production rate in the ground, kW/m^2; ρ – density of the ground, kg/m^3; c_p – specific heat capacity, J/(kg K); T – temperature, K; t – time, s.

A simple 1D solution of the above equation is the heat flux density [Carslaw 1959]:

$$\dot{q}(z,t) = -\lambda \frac{\partial T}{\partial z} = -\sqrt{\frac{\lambda \rho c_p}{\pi t}} * \Delta T * \exp\left\{-\frac{z^2}{4at}\right\} \tag{8-2}$$

where ΔT – difference between boiling point of the cryogen and the initial ground temperature, K; λ – thermal conductivity, W/(m K); z – coordinate in depth.

Various authors have been investigating theoretically and experimentally the heat flux density for LH_2 (and other cryogens) at the surface. For the film boiling regime, heat flux density can be determined according to [Brentari 1965] by the following relationship:

$$\dot{q}_{FB} = 4.95 \frac{(\Delta\rho)^{0.375}}{\sigma^{0.125}} * \left[\frac{\lambda_g^3 \Delta H_{v,eff} \rho_g}{\eta_g} \right]^{0.25} * (\Delta T)^{0.75} \quad (8\text{-}3)$$

with the effective heat of vaporization $\Delta H_{v,eff} = \frac{\left(\Delta H_v + 0.34 c_p \Delta T\right)^2}{\Delta H_v}$

where σ – surface tension, N/m; λ_g – thermal conductivity of gas, W/(m K); ρ_g – density of gas, kg/m^3; η – dynamic viscosity, N s/m^2.

With decreasing temperature difference, a limit is given by the minimum film boiling heat flux density described by a correlation according to [Zuber 1959]:

$$\dot{q}_{MFB} = \frac{\pi^2}{60} * \left(\frac{4}{3}\right)^{0.25} * \rho_g * \Delta H_v * \left[\sigma \frac{\rho_l - \rho_g}{(\rho_l + \rho_g)^2} \right]^{0.25} \quad (8\text{-}4)$$

where index l – liquid; index g – gas.

For the nucleate boiling regime, Kutateladze has deduced the following relationship [Brentari 1965]:

$$\dot{q}_{NB} = 4.87 * 10^{-11} \frac{c_{p,l}^{1.5} \lambda_l \rho_l^{1.282} p_o^{1.75}}{(\Delta H_v \rho_g)^{1.5} \sigma^{0.906} \eta_l^{0.626}} * (\Delta T)^{2.5} \quad (8\text{-}5)$$

where p_o – ambient pressure, Pa.

The critical heat flux density or “departure of nucleate boiling”, DNB, describes the point where the space between the bubbles is filled with just as much liquid as is needed to form new bubbles:

$$\dot{q}_{DNB} = 15.7 * \Delta H_v * \rho_g^{0.5} * (\sigma \Delta\rho)^{0.25} \quad (8\text{-}6)$$

The areas shown in Fig. 8-3 represent the experimentally determined heat flux densities of LH_2 covering both nucleate boiling and film boiling regimes. The solid lines (in blue) indicate the curves calculated according to the above equations (8-3) and (8-5).

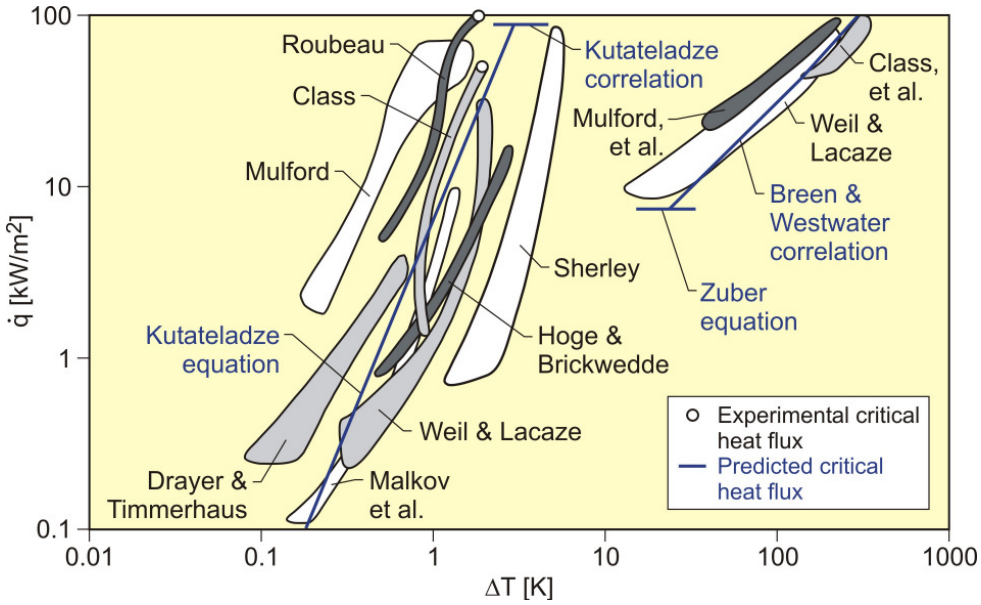

Figure 8-3. Measurements of heat flux for liquid hydrogen [Brentari 1965]
(Differently shaded areas are only used for distinction of the various contributions)

The vaporization behavior is principally different for solid and liquid grounds. On solid grounds, the vaporization rate decreases due to cooling of the ground causing a reduced heat input. For a constant spill rate, this will lead to a gradually increasing pool size. A growing pool surface area implies an enhanced vaporization rate. After an initial phase, a state is reached which is characterized by the incoming mass to equal the vaporized mass. A cut-off of the mass input eventually results in a break-up of the pool from the central release point creating an inner pool front. The ring-shaped pool then recedes from both sides until it has completely died away. Factors influencing the heat transport, i.e., the vaporization rate, are surface roughness, porosity, penetration or percolation in case of a sand ground, or a surface with moisture.

On liquid grounds, the vaporization rate of the cryogen remains approximately constant due to natural convection processes initiated in the liquid resulting in an (almost) constant, large temperature difference between surface and cryogen indicating stable film boiling. On water, there is the chance of ice formation depending on the amount of mass released. It will be hindered due to the violent boiling of the cryogen causing turbulence in the surface layer, particularly if the momentum with which the cryogen hits the water surface is large. Unlike lab-scale testing (confined), ice formation was not often observed in field trials with LNG spills (unconfined). [Prince 1985].

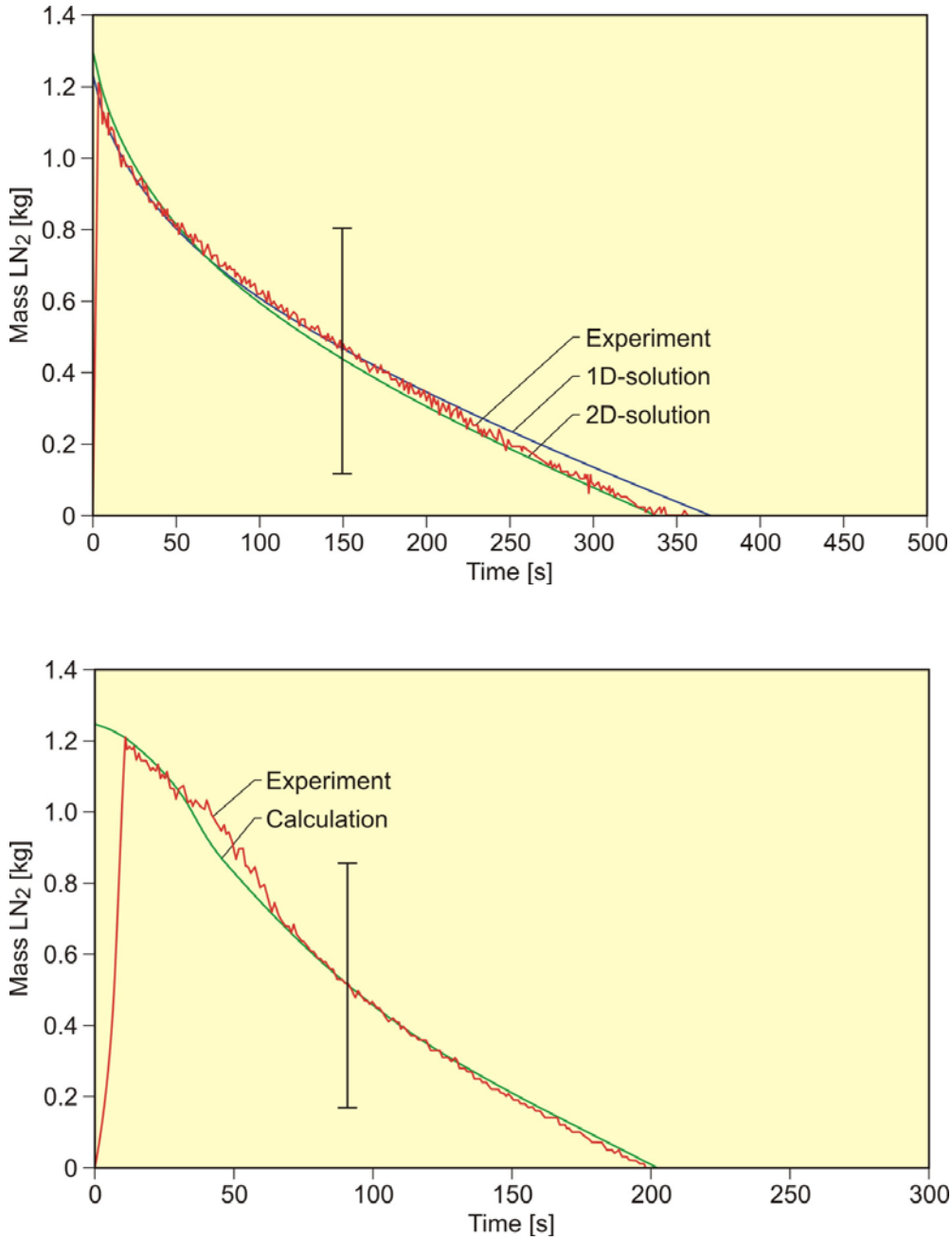

Figure 8-4. Mass loss after LN_2 spillage on a dry (top) and wet (bottom) concrete surface [Dienhart 1995]

An additional significant influence on the pool spreading and vaporization behavior is given, if the pool propagation is limited due to obstruction, e.g., the walls of an impoundment area. A smaller surface area results in a reduced vapor production rate. The general relationship between the mass vaporization rate per unit area of surface, $\dot{m}$, and the time from initial contact, t, is given by:

$$\dot{m} = B * \Delta T * t^{-1/2} \tag{8-7}$$

where B – factor comprising the effective thermal properties of the surface, e.g., the impoundment area of a storage, kg/(m^2 $s^{1/2}$ K); ΔT – difference between initial temperature of the ground and the boiling point of the cryogen, K. Some examples for B values – referring to LNG – are 0.6 for soil, 0.58 for standard concrete, 0.14 for light-weight concrete, 0.07 for super-insulating concrete. The maximum LNG vaporization rate on concrete is 0.5 kg/(m^2 s) or 1.2 mm/min which is reduced to about 3 % of its value after 20 min [Moorhouse 1988].

Tests were conducted at FZJ using liquid nitrogen to be given onto isolated bodies. The specimens investigated were made of bitumen (a piece of original road surface), and of dry or moist concrete. The heat transport was analyzed by measuring the transient mass loss of the fluid. Differences were observed for the vaporization behavior on dry and wet concrete as indicated in Fig. 8-4. The two plots describe the mass loss due to vaporization following the spillage of equal quantities of LN_2.showing that the vaporization rate for dry concrete (and bitumen) was initially large and then decreased with time. A different behavior was found for wet concrete in that the vaporization rate was smaller at the beginning, then increased and eventually decreased again; also the total vaporization time was shorter by 30 % compared to the dry ground under the same conditions. This behavior can be explained by the liberation of the solidification enthalpy of the water in the ground surface layer representing an additional heat source in the ground. A 3 mm water layer on the concrete leads again to a longer vaporization time due to an insulation effect of the – then – ice layer, but the time was still shorter than in the “dry” case [Dienhart 1995].

8.1.3. Cryogenic Pool Spreading

Above a certain amount of cryogen released, a pool on the ground is formed. Both diameter and thickness of the pool are increasing with time until an equilibrium state is reached. After termination of the release phase, the pool is decaying from its boundaries. It breaks up in floe-like islands when the thickness drops below a certain value. This minimum thickness is determined by the surface tension of the cryogen and is typically in the range of 1 - 2 mm. The development of a hydraulic gradient results in a decreasing thickness towards the outside.

The spreading of a cryogenic pool is influenced by the type of ground, solid or liquid, and by the release mode, instantaneous or continuous. In an instantaneous release, the release time is theoretically zero (or release rate is infinite), but practically short compared to the vaporization time. Furthermore the cryogen spreading on the surface penetrates the water to a certain degree, thus reducing the effective height responsible for the spreading and also requiring additional displacement energy at the leading edge of the pool below the water surface.

The reduction factor, δ, is given by the density ratio of both liquids:

$$\delta = 1 - \frac{\rho_{liquid}}{\rho_{water}} \tag{8-8}$$

telling that only 7 % of a liquid hydrogen pool will be below the water surface level compared to, e.g., more than 40 % of LNG or even 81 % of LN_2. δ is 1 for a solid ground.

During the initial release phase, the surface area of the pool is growing which implies an enhanced vaporization rate. Eventually a state is reached which is characterized by the incoming mass to equal the vaporized mass. This equilibrium state, however, does not necessarily mean a constant surface area of the pool. For a solid ground, the cooling results in a decrease of the heat input which, for a constant spill rate, will lead to a gradually increasing pool size. In contrast, for a water surface, pool area and vaporization rate are maximal and remain principally constant despite ice formation as was concluded from lab-scale testing.

A special effect was identified for a continuous release particularly on a water surface. The equilibrium state is not being reached in a gradually increasing pool size. Before reaching the equilibrium state, the pool sometimes forms a detaching annular-shaped region which propagates outwards ahead of the main pool (Fig. 8-5, left) [Brandeis 1983].

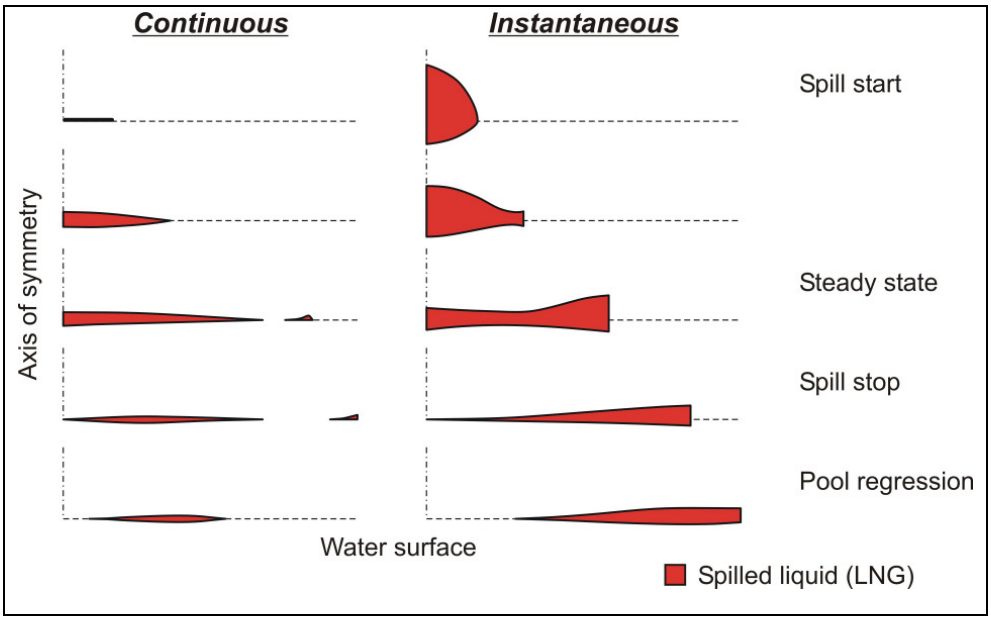

Figure 8-5. Comparison of the transient pool shape of a continuous (left) and instantaneous (right) release on a water surface [Brandeis 1983]

This phenomenon, for which there is hardly any experimental evidence because of its short lifetime, can be explained by the fact that in the first seconds more of the high-momentum liquid is released than can vaporize from the actual pool surface; it becomes thicker like a shock wave at its leading edge while displacing the ground liquid. It results in a stretching of the pool behind the leading edge, where the thickness becomes very small, until the leading edge wavelet eventually separates. Realistically the ring pool will certainly break up soon in smaller single pools drifting away as has been observed in release tests. Whether the ring pool indeed separates or only shortly enlarges the main pool radius, is depending on the cryogen properties of density and vaporization enthalpy and on the source rate.

Another widely observed phenomenon for cryogenic spills on a water surface is the so-called "rapid phase transition" (RPT). RPTs are physical ("thermal"), non-combustive vapor explosions resulting from a spontaneous and violent phase change of the fragmented liquid gas at such a high rate that shock waves may be formed. Although the energy release is small compared with a chemical explosion, it was observed for LNG that RPTs with observed overpressures of up to 5 kPa were able to cause structural damage.

An additional significant influence on the pool spreading and vaporization behavior is given, if the pool propagation is limited due to obstruction or walls, e.g., of an impoundment area. Smaller surface areas result in reduced vapor production rates.

8.1.4. Evolution of a Flammable Vapor Cloud

The processes of release and subsequent distribution of a gas are strongly dependent on its thermodynamic state during storage. Pressurized gases form a free jet or will be flash-released, if there is a complete failure of the storage vessel. For cryogenic storage, the substance will be liberated - depending on the leak location - as saturated vapor or as a liquid which starts to vaporize immediately. Parameters of concern are the expansion of a flammable vapor cloud, the height that it could attain, the time until it becomes sufficiently diluted below the flammability limits, and the total quantity of fuel in the cloud.

The spreading and dispersion behavior of a gas is significantly influenced by the density difference to the ambient air. In case of the release of a neutral or negatively buoyant gas, mixing with air is poor and slow, such that only a part of the gas cloud is within the flammability range. The cloud must be picked up by the ambient flow before it can be carried downstream and diluted. If the source rate is larger than the removal rate, a vapor blanket can accumulate on the ground until a certain size is reached with steady-state conditions.

The initial phase after release of a heavy gas is characterized by a slumping of the gas cloud under gravitation with a behavior similar to a liquid. It shows a spreading behavior which is – at least in the initial phase – independent of the wind direction. It forms a shallow pancake-shaped plume with resistance to vertical dispersion. The spreading of the gas cloud is further influenced by factors such as surface area, type of ground, thermal effects from the interaction with the ambient atmosphere which can either enhance or dampen the turbulence by buoyancy. Air entrainment from the upper surface and the edges due to atmospheric turbulence eventually results in dilution to effectively neutral density. Top entrainment of air into heavy gases is significantly smaller than for neutral gases.

Hydrogen at its boiling point is slightly heavier than air. Small quantities of LH_2 released tend to rise almost immediately. In case of the release of a large amount of LH_2, however, the vaporized gas will remain near the ground for a longer time because of only gradual air entrainment from the outside into the vapor cloud.

Gas at cryogenic temperatures causes the moisture in the air to condense and make the vapor cloud visible which is of advantage in case of accidental releases. The presence of droplets, either liquefied gas resulting from the release process or water from the moisture, result in vaporization and condensation processes with removal of heat from or addition of heat to the gas. Low moisture content thus means a longer lifetime of a heavy gas cloud.

8.1.5. LH_2 Pool Burning

Regarding open burning pools of flammable liquids, the essential parameters are the burning rate and the temperature or heat flux distribution. For a burning gas cloud above a ground pool or tank, heat transport from the burning cloud to the pool is given by conduction, convection, and radiation enhancing the vaporization rate and the pool regression rate, respectively. The fire of a burning vapor cloud may also be able to travel back to the spill point and continue to burn as a pool fire. Hazards associated with pool fires are strongly depending on pool size and shape, burning rate, flame geometry, and heat radiation.

Two regimes for the regression rate have been identified depending on the pool dimension [Zabetakis 1967]. For small diameters ($D < 0.2$ m), heat transport by conduction is dominant, and the regression rate decreases with increasing radius (see also section 8.5.).

Liquid hydrogen pool fires are observed to be dynamic and non-homogeneous with a highly intermittent pulsing structure of the flame. This cyclic changing of flame height is mainly due to the turbulent mixing of air and subsequent combustion and has an influence on the flame temperature. The height of the flame indicates the radiation hazard imposed by the fire, since it directly relates to the heat transfer from the flame into the surroundings. Usually the flame height is defined as the height at which flame is present at least 50 % of the time.

Effects of wind on the flame length are complex. For smaller pools, enhanced ventilation may improve air entrainment and thus allows for a more efficient combustion. Wind also tilts the flame expanding the flame base area and also changing the distribution of radiant heat flux distribution. This influence may even enhance the regression rate [Babrauskas 1983, Rew 1995]. For larger pools, measurements indicate enhanced burning rates. There is, however, a slight decrease for very large pools ($D > 5$-10 m) which could be explained by having several separate burning cells rather than one big pool fire. Complexity is further increased, if there is confinement around the fire, e.g., a tunnel [Kurioka 2003].

It was found from experiments that pools of LH_2 were difficult to ignite, and only accelerated flames were observed with hardly any tendency to detonation. A factor contributing to this effect is the inhibiting influence of the condensing moisture in the open atmosphere [Kreiser 1994].

Another observation from LNG pool fires is that burning rates and flame heights of pools on water are by a factor of 2 higher than those of pools on solid ground [Luketa-Hanlin 2006]. This is explained by the higher heat transfer from the water into the pool due to the rapid

interaction with the water and fragmentation of the pool increasing the heat transfer area. This effect tends to produce smaller pool diameters, but taller flames. The total radiation area is reduced, since a larger fraction of the vapor produced may escape unburnt from the plume.

8.2. Experimental Work with Liquid Hydrogen Release

Most experimental work to investigate the safety of cryogenic liquefied gaseous fuels began in the 1970s concentrating mainly on LNG and LPG, commodities which were shipped around the world to a tremendously increasing extend. Main goal of these works was the investigation of accidental spill scenarios during maritime transportation. A respective experimental program for liquid hydrogen was conducted on a much smaller scale, initially by those who considered and handled LH_2 in larger quantities (space programs). Main focus was on the combustion behavior of the LH_2 and the atmospheric dispersion of the evolving vapor cloud after an LH_2 spill. Only little work was concentrating on the cryogenic pool itself, whereby vaporization and spreading never were examined simultaneously. In 1994, the first (and only up to now) spill tests with LH_2 were conducted in Germany, where pool spreading was investigated in further detail.

8.2.1. Early Liquefied Hydrogen Spill Testing

Experimental activities with the release of liquid hydrogen started in the late 1950s [Cassut 1960, Zabetakis 1961, Rich 1973]. They were mainly concentrating on a visual recording of the evolving H_2 vapor clouds and a few H_2 concentration measurements at different heights above the spillage site. Variations in the translucence of the visible clouds were assumed to result from strong concentration variations presuming incomplete mixing and/or wind influence. The Lockheed Skunk Works in the USA investigated in a series of tests the detonability of LH_2 by subjecting small amounts of the liquid to various impacts.

Vaporized H_2 forms a trail or visible cloud in the open atmosphere as it leaves the liquid. This trail does not necessarily coincide with the flammable zones of the hydrogen vapor cloud. Non-uniform clouds could develop leading to a series of fireballs if ignited. Two separate flammable areas and the height of the visible cloud after spilling 3 l of LH_2 onto a dry macadam surface at 15°C ambient temperature and no-wind condition were identified from the motion pictures as is shown in Fig. 8-6. After ignition of the lower flammable mixture, its fireball ignited then the second one [Zabetakis 1967].

Spill experiments with LH_2 amounts ranging between 5 l and 19 m^3 were conducted by Arthur D. Little Inc. [ADL 1960] simulating the conditions of storage and transport with the objectives to test safe handling, to observe the dispersion behavior, to establish quantity-distance relationships, and to compare with hydrocarbon fuels. The vaporized, still cold hydrogen was found to remain close to the ground for a few seconds and then gradually rise. It also showed the tendency of horizontal spreading in all directions in a semi-spherical shape. Tests with continuous LH_2 release of ~2 l/s over 16 min or 16 l/s over 1 min at wind speeds between 1.8 and 7.6 m/s revealed a dense visible cloud up to 200 m distance. LH_2 pool vaporization rates were measured to be initially 130 - 180 mm/min before decreasing rapidly to a steady state value of ~38 mm/min [Cassut 1960]. There was, however, no instrumentation employed for measurements of the LH_2 pool itself.

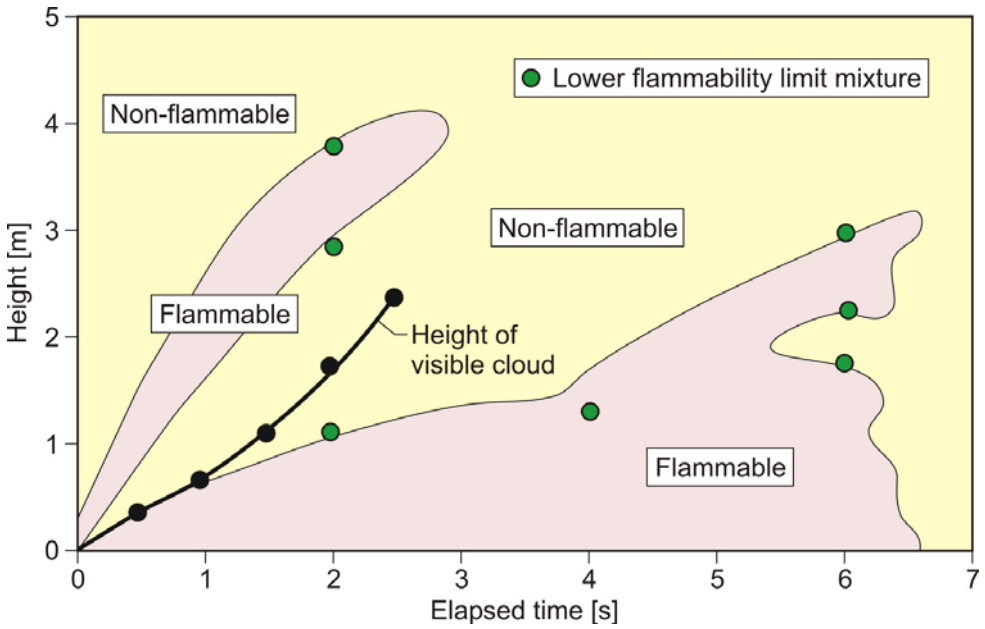

Figure 8-6. Observed flammable areas and visible gas cloud after the instantaneous release of 3 liters of LH_2 at 15°C ambient temperature and quiescent air as a function of time after spillage [Zabetakis 1960]

Zabetakis examined on a lab-scale the LH_2 vaporization behavior due to heat transfer using a 65 mm diameter glass dewar and a block of paraffin wax as "hot" surface. Fig. 8-7 compares the experimental data by measuring the rates of gas evolution with a dry gas meter to the theoretically derived pool regression rate. Good agreement with the long-term behavior was achieved, if disregarding the initial spill-induced thermohydraulic processes and shifting the time scale by 20 s. The solid curve assumes the heat influx rate to be conduction limited, whereas the initial flash vaporization rates are probably film and nucleate boiling limited. Measurements for the "quiet vaporization" resulted in a value of 16 mm/min [Zabetakis 1960].

According to the IAEA recommended cryogenic pool vaporization rates [IAEA 1981], 10 % of the liquid flash-vaporizes upon release, while for the remainder, the rates are set at 10 mm during the first minute and 0.5 mm/min afterwards. For liquid hydrogen, however, this approach appears to provide too low regression rates.

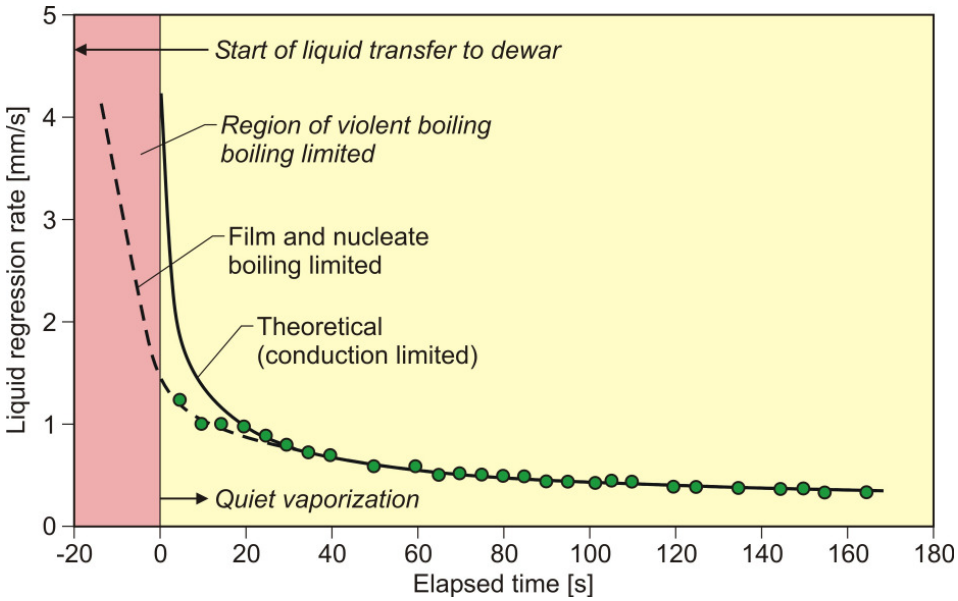

Figure 8-7. Regression rate of liquid hydrogen on a paraffin wax ground [Zabetakis 1960]

LH_2 Vaporization from Open Underground Tank

Considering a future large-scale hydrogen production plant with subsequent liquefaction and assuming an underground storage vessel (where a catastrophic failure of the vessel can be excluded) to take up the day's production of, say, 100 t of hydrogen as LH_2, the tank could have the approximate dimensions of 15 m diameter and 10 m height. For the regression rate due to (quiet) vaporization according to [Zabetakis 1960], such a vessel if open at the top would vaporize empty within about 9 hours. This is an extremely long time in terms of the atmospheric dispersion process for hydrogen, particularly with regard to its extremely strong positive buoyancy, meaning that it will be impossible to have all hydrogen available involved in a potential vapor cloud explosion. Taking the IAEA figures as a basis, vaporization time would be as long as 300 hours.

8.2.2. NASA LH_2 Release Experiments

The NASA LH_2 trials conducted between August and December of 1980 [Witcofski 1984, Chirivella 1986] were initiated when trying to analyze the scenario of a bursting of the 3000 m^3 LH_2 storage tank at the Kennedy Space Center at Cape Canaveral and to study the propagation of a large-scale hydrogen gas cloud in the open atmosphere. The spill experiments consisted of a series of seven trials, in five of which a volume of 5.1 m^3 of LH_2 was released near-ground within a time span of 35 - 85 s. Table 8-2 lists further details of these spill tests.

The liquid hydrogen was released from a 5.7 m^3 dewar, passing a 152 mm inner diameter foam insulated horizontal spill line of about 30 m length, which was curved at its end vertically towards the ground (Fig. 8-8). Prior to the spill test, dewar and line were filled with LH_2. Gaseous helium was used to pressurize the dewar to ~0.7 MPa, before the valve at the end of the spill line was opened. A 1.2 x 1.2 m^2 steel plate was located directly under the line exit to prevent earth erosion. The spill line dumped the LH_2 into a 9.1 m diameter spill pond with compacted sand as ground. The pond had an earthen side, about 60 cm in height.

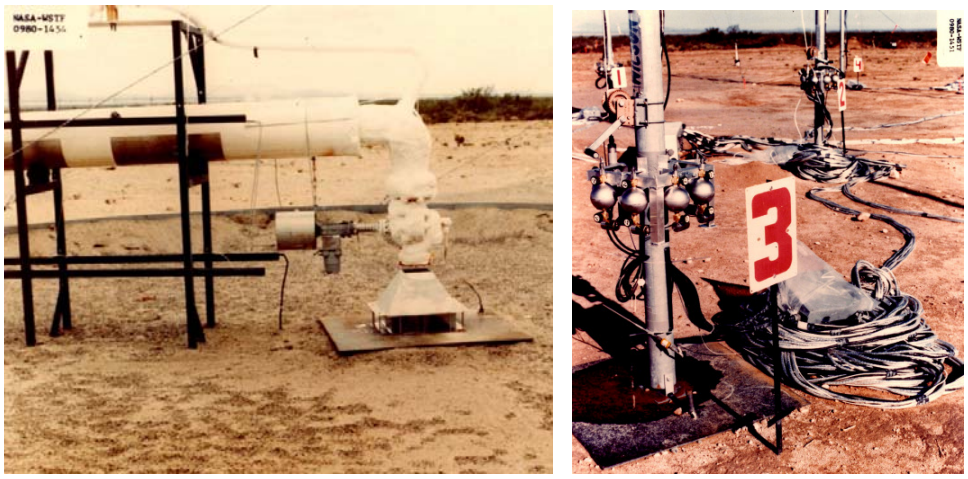

Figure 8-8. Test site (left) and instrumentation (right) for NASA LH2 spill experiments (Courtesy of NASA)

The instrumentation for analyzing the dispersing vapor cloud included 8 concentration measurements (for 8 different points in time) at 27 different positions (Fig. 8-8, right). Pool spreading on the “compacted sand” ground was not a major objective, therefore only scanty data from just one test (#6) are available. From the thermocouples deployed at 1, 2, and 3 m distance from the spill point, only the inner two were found to have gotten contact with the cold liquid, which would mean a maximum pool radius not exceeding 3 m. Visual recordings, however, seem to indicate full coverage of the prepared diked area (radius 4.6 m) during the spill.

Table 8-2. Characteristic parameters of the LH_2 field trials by NASA conducted in 1980 [Chirivella 1986]

Parameter	Test 1	Test 2	Test 3	Test 4	Test 5	Test 6	Test 7
LH_2 spill quantity [m^3]	5110	5110	5110	5110	2270 - 2650	5110	2840
Spill time [s]	63	39	85	35	15 - 20	38	120
Time to total vaporization [s]	102	57	94	42	29.5	43	-
Visible cloud duration [s]	116	80	-	90	50	90	-
Downwind dist. to flammable cloud [m]	-	152	24	53	27	65	9
H_2 concentration at dew point [%]	9.4	4.5	9.8	4.6	2.6	6.7	7.1
Atmospheric conditions							
Temperature [°C]	30	25	26	19	12.4	15.5	20.5
Pressure [10^2 Pa]	788	787	789	789	785	786	786
Humidity [%]	18	50	27	27	43	29	30
Dew point [°C]	4.0	12.9	2.0	2.9	5.8	-1.7	-0.8
Wind speed [m/s]	3.5	2.0	4.7	3.4	5.9	1.8	4.2
Stability class	unstable	extremely unstable	unstable	unstable	neutral, slightly stable	unstable	neutral

The developing hydrogen gas cloud and the visible cloud, respectively, could be observed over several hundreds of meters, when the ground was able to sufficiently cool down. The visible cloud was initially steeply rising, before it later remained longer near the ground (Fig. 8-9). This behavior was explained with the high impulse when opening the valve showing a high sensitivity of the type of release for LH_2. Unlike LH_2 pool vaporization with typical vaporization rates of 0.4 - 0.8 mm/s, high release rates lead to intensive turbulences with violent cloud formation and rapid mixing with the ambient air.

Fig. 8-10 shows for test 6 the concentration distribution as was derived from the temperature measurements assuming adiabatic mixing of hydrogen with the ambient air [Witcofski 1984].

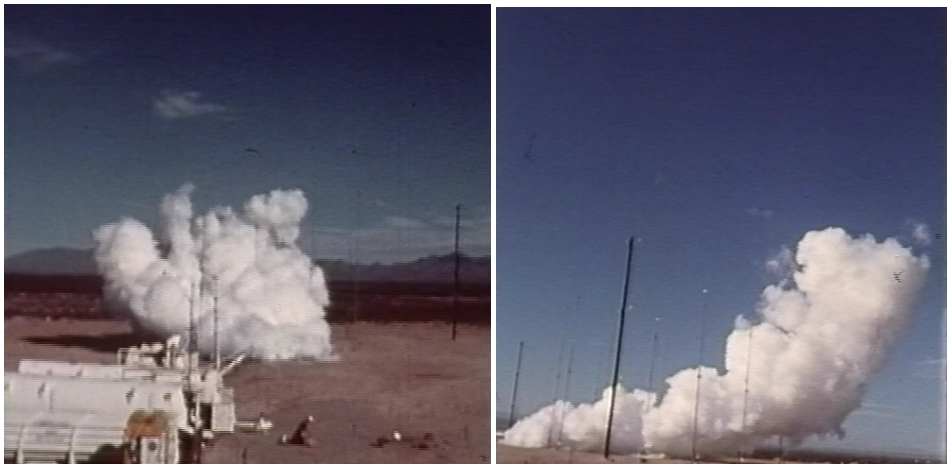

Figure 8-9. Cold hydrogen vapor cloud dispersion during the NASA spill test 6 (Courtesy of NASA)

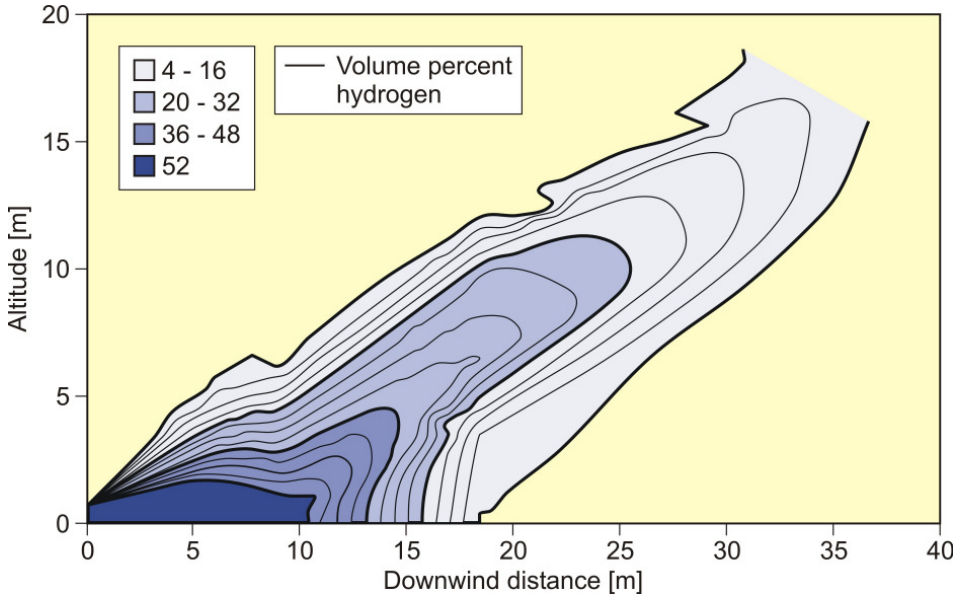

Figure 8-10. Measured concentration distribution after 21 s of test #6 of the NASA spill tests [Witcofski 1984]

8.2.3. FZJ Tests on Liquid Hydrogen Pool Spreading

Before tests with the spillage of LH_2 started, the Research Center Jülich has conducted a systematic series of spill tests with liquid nitrogen in order to investigate the principal phenomena occurring with the spillage of cryogenic liquids. For this purpose, the experimental facility KIWI was designed and constructed. It was a 60° segment of a circle with a side length of 12 m filled with water (depth: 0.5 m) as shown in Fig. 8-11, top left. A tipping device at the (circle's) center allowed both instantaneous (up to 80 l) and continuous release (at a rate of up to 2.5 l/s) of the cryogen onto the water with minimum disturbance of the water surface near the spill point. Measurements of the pool spreading were done by thermocouple arranged closely above the water surface to indicate the presence (or not) of the cold liquid. A total of 40 tests were conducted with quantities spilled of 20 - 80 l of LN_2 and, in the continuous case, with release rates of 1 - 2.5 l/s. Maximum pool radius observed was in the range of 2 - 6 m. The wind was found to have a strong influence on the pool shape. At the end of the tests, ice became visible on the water surface exhibiting various bizarre structures differing according to the type of release. The other photographs in the figure show the spreading pool after an instantaneous spill (top right) and the ice structure formed on the water surface typical for an instantaneous release exhibiting the comb structure of 3D convection cells in the water.

Figure 8-11. LN_2 release test facility KIWI at FZJ (top left) with a spreading pool (top right) and typical ice structure formation on the water surface (bottom) [Dienhart 1995]

The BAM, Germany, conducted in 1994 LH_2 (and LPG) release trials on a much smaller scale compared to the White Sands trials. In four of the six tests with LH_2 (Table 8-3), the Research Center Jülich (FZJ) studied in more detail the pool behavior by measuring the LH_2 pool radius in two directions as a function of time [Dienhart 1995]. The release of LH_2 was made both on a water surface using a circular swimming pool with 3.5 m diameter (two tests) as depicted in Fig. 8-12, top, and on a solid ground represented by a square aluminum sheet with 2 m side length and 20 mm thickness. By means of a diffuser and a catching pot (Fig. 8-12, bottom), the initial momentum of the exiting liquid was to be minimized. A cross-shaped trestle was constructed to be arranged above the respective ground. On two perpendicular branches of the trestle, a total of 18 thermocouples were fixed every 0.1 and 0.2 m, respectively, in radial direction. They were adjusted approximately 1 mm above the surface of the ground and served as indicator for presence of the spreading cryogen.

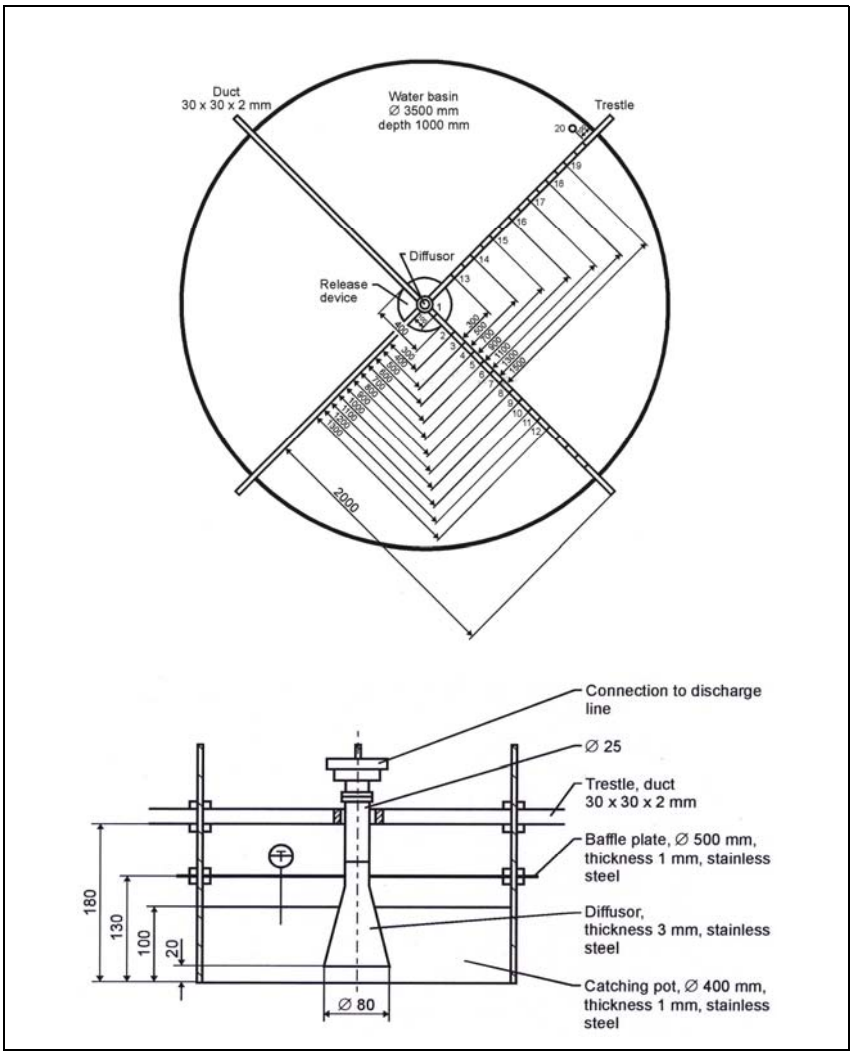

Figure 8-12. Experimental arrangement of LH_2 pool spreading on water [Dienhart 1995]

The spill tests on water were performed over a time period of 62 s each at an estimated rate of 5 l/s of LH_2, a value which is already corrected by the flash-vaporized fraction of at least 30 %. After contact of the LH_2 with the water surface, a clearly visible closed pool was formed. The equilibrium pool radius did not remain constant, but moved forward and backward within the radial range of 0.4 - 0.6 m. This pulsation-like behavior, which was also observed by the NASA experimenters in their tests, is probably caused by the irregular efflux due to the violent bubbling of the liquid and release-induced turbulences. Single small floes of ice escaped the pool front and moved outwards as can be seen from Fig. 8-13. After cutting off the source, a massive ice layer was identified where the pool was boiling. Also long-shaped ice tracks leading radially away could be observed.

Table 8-3. Characteristic parameter of the LH_2 pool spreading trials by FZJ conducted on May 19, 1994 [Dienhart 1995]

Parameter	Test 1	Test 2	Test 3	Test 4	Test 5	Test 6
Ground	Al sheet (0.5 m^2)	Al sheet (0.5 m^2)	water (9.6 m^2)	water (9.6 m^2)	Al sheet (4 m^2)	Al sheet (4 m^2)
Release time GH_2 [s]	90	30	90	60	60	55
Release time LH_2 [s]	50	61	62	62	62	62
Mass flow [kg/s]	0.315	0.315	0.350	0.350	0.450	0.450
Volume flow [l/s]	4.5	4.5	5	5	6	6
Atmospheric conditions						
Temperature [°C]	12	12	12	12	11	10
Pressure [10^2 Pa]	983	983	985	985	986	986
Humidity [%]	96.5	96.5	96.7	96.7	97.0	97.0
Wind speed [m/s]	0-1	0-1	0-1	0-1	0-1	0-1

In the two tests on the aluminum sheet, conducted at an LH_2 release rate of (corrected) 6 l/s over 62 s each, the pool front was also observed to pulsate showing a maximum radius in the range between 0.3 and 0.5 m. Pieces of the cryogenic pool were observed to move even beyond the edge of the sheet. Not always all thermocouples within the pool range had permanent contact to the cold liquid indicating non-symmetrical spreading or ice floes which passed the indicator. The very low kinematic viscosity of hydrogen certainly has an influence on the stability of the pool front, its breakup, and its pulsation behavior. Also wind probably had an effect, which may explain the irregularities in the measured pool front.

Figure 8-13. LH_2 pool spreading on water during BAM tests in 1996 with ice layer visible at test end (Courtesy of BAM)

8.2.4. Japan Tests on Liquid Hydrogen Pool Spreading

In 1993, lab-scale spill experiments with LH_2 and LOX were conducted to examine the cryogen behavior on solid grounds like concrete and dry/wet sand and heat transport phenomena influenced by the moisture in the ground [Takeno 1994]. A new series of LH_2 spills, still on lab-scale, was made in 2000 investigating the pool spreading and vaporization behavior in a 0.7 x 2.5 m^2 open basin (Fig. 8-14). Phenomena such as the transition from film to nucleate boiling and the heat transfer from the ground were examined in detail to be applied to the CHAMPAGNE computer model [Chitose 2002].

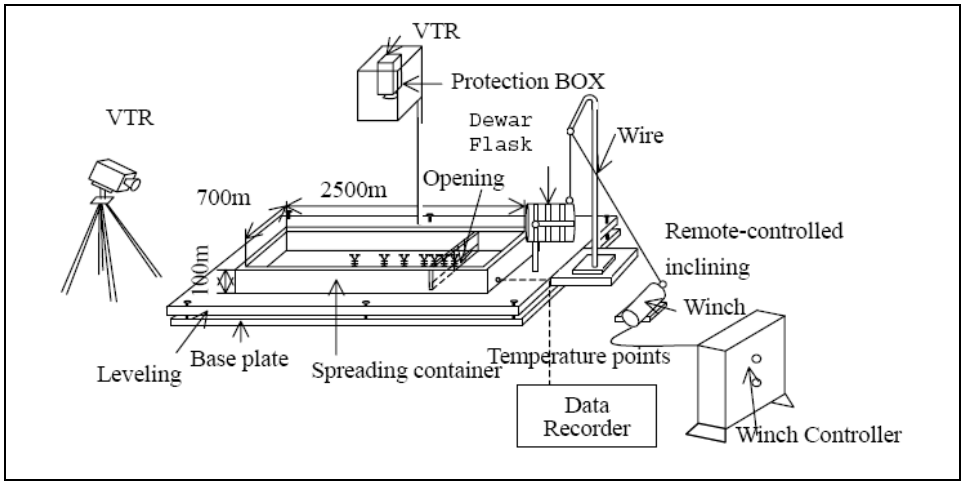

Figure 8-14. Experimental setup of Japanese lab-scale LH_2 spill testing [Chitose 2002]

CHAMPAGNE is a multi-phase, multi-component thermodynamics model originally created for the assessment of severe accidents in fast breeder nuclear reactors. It has been modified to also treat the formation and atmospheric dispersion of hydrogen-air vapor clouds resulting from LH_2 spills. The code was successfully applied to the NASA LH_2 spill experiments of 1980 [Chitose 1996].

8.2.5. Experimental Work on Pool Fires

In the late 1950s, experiments with the release of liquid hydrogen and subsequent ignition were conducted by Arthur D. Little Inc. [ADL 1960, Cassut 1960], the Lockheed Skunk Works [Rich 1973], and the US Federal Bureau of Mines [Zabetakis 1961]. First tests to burn 1 l of LH_2 using in an open dewar showed that there was a quiet flame of the vaporizing H_2 gas, but a violent explosion when the H_2 contained 10 % of solid air.

At the Lockheed Skunk Works site in California, it was tried to create controlled explosions by rupturing tanks filled with LH_2 under pressure. These tests, however, were not successful; the hydrogen was simply disappearing into the atmosphere. Ignition was leading to quickly dissipating fire balls. The only experiments creating a major shock wave was when equal amounts of LH_2 and LOX were brought together [Rich 1995].

Main objective of the burning tests was the derivation of empirical relationships between the amount of spilled LH_2 and flame height/width to be used for setting standards for the definition of safety distances. Fig. 8-15 shows the measurements of maximum height and width of the flames from rapid spillage and ignition with quantities of up to 89 l of LH_2 [Zabetakis 1960]. The fire ball was initially mushroom-shaped, later hemispherically shaped and detaching from the ground. An empirical correlation between maximum flame height/ width and the spilled volume was derived as

$$H_{max} \approx W_{max} \approx 2.1 * \sqrt{V_l} \quad [m] \tag{8-9}$$

where H_{max}, W_{max} – maximum flame height/width, m; V_l – spilled LH_2 volume, liter.

Ignition of the vapor above the pool (depth: 50 - 300 mm) was by either spark or flame source in the range of up to 8 s after spillage. The later the ignition, the larger was the fire ball.

For the LH_2 spill and ignition tests, with quantities of 54 - 90 l given onto a steel plate or loose gravel, the overpressures were measured at a distance of ~50 m. The results shown in Fig. 8-16 as a function of the ignition time after spillage are given in decibel, dB, (scale on the left-hand ordinate) and in Pa (right-hand ordinate). The blast pressures produced were relatively small and were depending on the time delay for ignition [Zabetakis 1960]. They were found to increase with delay time, until after more than 5 - 6 s of delay, they were decreasing again as soon as the H_2 concentration in the rising and diffusing vapor clouds became smaller.

In pool fires, the hydrogen flames principally remained limited to the pool size, but were largely extended, up to 50 m, in vertical direction. They were even able to ignite separated flammable gas pockets creating a new fire ball. The hydrogen vapor clouds evolving from LH_2 pools into the open atmosphere appeared to be inhomogeneously composed with a stoichiometric mixture being highly unlikely [ADL 1960].

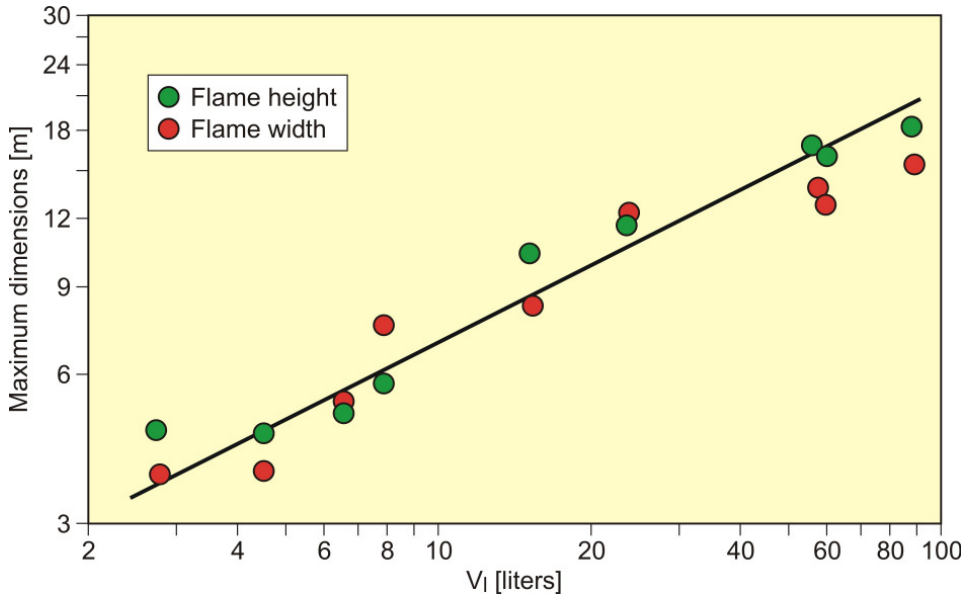

Figure 8-15. Maximum flame height and width upon release and ignition of LH_2 [Zabetakis 1960]

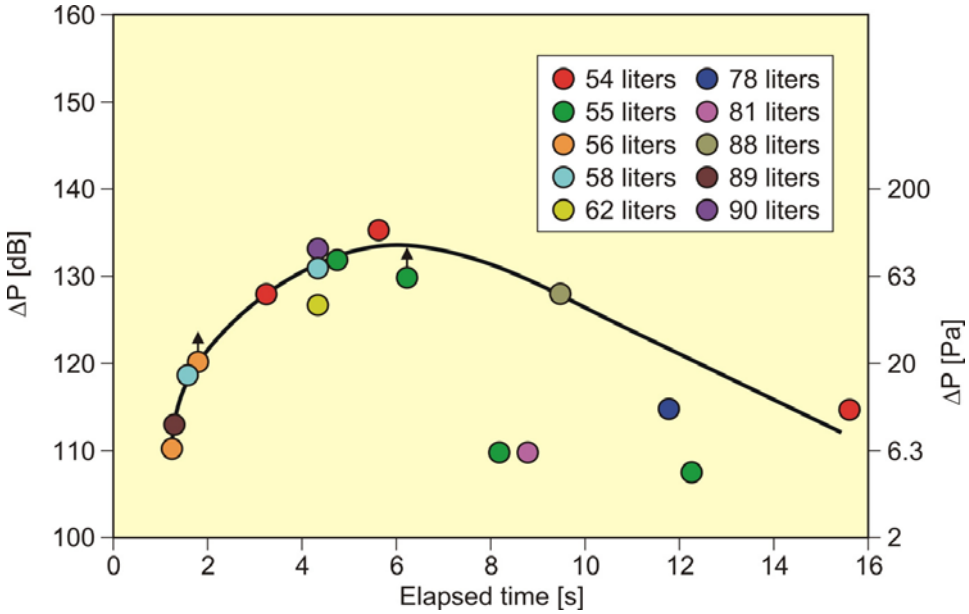

Figure 8-16. Overpressures measured at 49 m distance after ignition of vapor cloud above LH_2 pools vs. time of ignition after spillage [Zabetakis 1960]

Results from the experiments showed that regression rates of burning LH_2 pools were comparable to those obtained from un-ignited, simply vaporizing pools. It was concluded that the radiation heat input into the pool was about the same as the heat introduced by condensation of air into the pool [ADL 1960].

Another important result was that neither detonation nor the tendency towards a detonation was observed. Detonation hazards from an open LH_2 pool appeared relatively slight, when in contact with solid air, severest if oxygen was accumulating [Cassut 1960]. Partial obstruction near the pool was observed to lead to higher pressure pulses making it adviceable not to have any barricading structures around LH_2 storage vessels. A detonation in a free H_2-air mixture, however, was found to be highly unlikely. Only when using strong igniters or by the initiation of a shock wave was it possible to detonate the H_2-air-mixture following the spillage of small LH_2 amounts [Brewer 1981].

Fig. 8-17 shows a comparison between liquid hydrogen and liquefied natural gas burning rates under steady-state conditions which are expected to be higher in the beginning, if pools were ignited soon after having been released [Zabetakis 1960]. The LH_2 curve corresponds to a regression rate of 11.1 mm/min compared to only 2.4 mm/min for LNG. In [Edeskuty 1978], a range of the LH_2 regression rate between 30 and 66 mm/min is given. Zabetakis measured the regression rates of burning pools in 150 mm dewars.

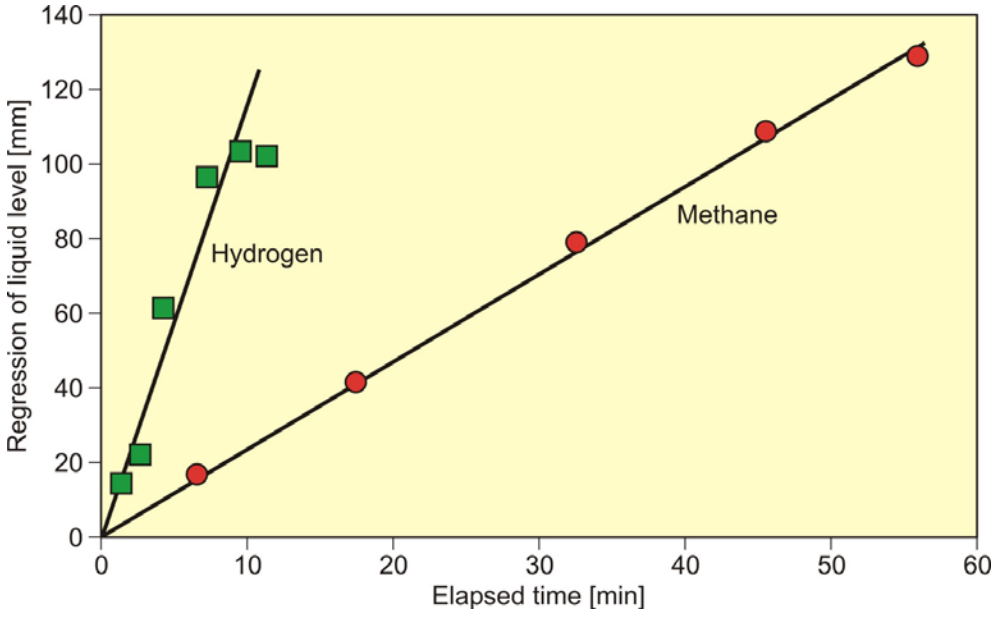

Figure 8-17. Regression rate of burning LH_2 and LNG pools in 150 mm dewars [Zabetakis 1960]

In Japan, experimental work on H_2 safety began in the early 1980s [AIST 1982], when tests with ignition of LH_2 in a 0.3 m diameter open dewar were conducted to investigate LH_2 flame behavior in comparison to gasoline flames. Burning rates expressed as liquid level regression were measured to be 0.4 mm/s, which was six times larger than for gasoline. In other tests on directly burning LH_2 pools conducted in a cylindrical vessel of 300 mm diameter and 0.21 m height, the measured burning rate was 22 mm/min [Urano 1986]. The generated flames reached a length of 2 - 3 m with widths between 0.8 and 1.1 m. Both "normal" and the much more violent "abnormal" burning with very high flames was observed, when the burning LH_2 came into contact with solidified oxygen from the air [Urano 1986]. Regression rates of burning LH_2 pools can even be enhanced up to 1000 mm/min, if solid oxygen formed at the surface to the open atmosphere and falling into the pool reacts with the hydrogen in a violent, unstable burning with flames lengths of more than 5 m and widths of more than 3 m. The heat flux from burning cloud above LH_2 pool was measured at 11.9 kW/m^2 [Urano 1986].

The tests in Japan with burning LH_2 were also used to examine different methods of extinguishing pool fires. Minimum quantities required were found to be 8.1 kg/(m^2 s) of CO_2 or 5.2 kg/(m^2 s) of $NH_4H_2PO_4$ powder, respectively [Horiguchi 1986].

Radiation measurements from the flames above the LH_2 pool revealed values for the peak source brightness of up to 144 kW/m^2. The deduced emissivity factor was 0.085 based on a flame temperature of 2050°C [ADL 1960]. Strong variations were due to the fact that flames were very wind-sensitive. In extended vapor clouds from continuous spills, flames were observed to travel downwind for several tens of meters. Radiation impact was definitely much lower compared to hydrocarbon fires allowing a reduced spacing for LH_2 storage vessels. From the radiation and flame size measurements, it was concluded that with regard to unprotected personnel, a safe distance to a large-scale burning LH_2 pool is recommended to be about 60 m; a respective distance for a JP-4 fuel fire would be at least 220 m [Cassut 1960].

8.3. State-of-the-Art Modeling of Cryogenic Pool Behavior

8.3.1. Historical Overview on Models

Parallel to all experimental work on cryogenic pool behavior, calculation models have been developed for assessment and simulation purposes. All are based on the radial spreading of a pool. Differences refer to the type of release or the ground considered. At the beginning, purely empirical relationships were derived to correlate the spilled volume/mass with pool size and vaporization time. Such equations, however, were according to their nature strongly case-dependent.

A more physical approach is given in mechanistic models. Here the pool is assumed to be of cylindrical shape with initial conditions for height and diameter, and the conservation equations for mass and energy are applied [e.g., Fay 1978, Briscoe 1980]. Gravitation is the driving force for the spreading of the pool transforming all potential energy into kinetic energy. Drawbacks of these models are given in that the calculation is terminated when the minimum thickness is reached, that only the leading edge of the pool is considered, and that a receding pool cannot be simulated.

State-of-the-art modeling applies the so-called shallow-layer equations, a set of non-linear differential equations based on the conservation laws of mass and momentum. It allows the description of the transient behavior of the cryogenic pool and its vaporization. Three phases are distinguished depending on the acting forces which dominate the spreading:

- gravitational flow determined by the inertia of the cryogen and characterized by a hydraulic gradient at the front edge;
- gravitational viscous flow after pool height and spreading velocity have decreased making sheer forces at the boundary dominant;
- equilibrium between surface tension and viscous forces with gravitation being negligible.

During spreading, the pool passes all three phases, whereby its velocity is steadily decreasing. For cryogens, these models need to be modified with respect to the consideration of a continuously decreasing volume due to vaporization. Also film boiling has the effect of reducing sheer forces at the boundary layer.

Based on the above principles, the AEA code GASP (Gas Accumulation over Spreading Pools) has been created [Webber 1991] as a further development of the Brandeis model [Brandeis 1983]. It was tested mainly for LNG and slowly evaporating pools, but not for liquid hydrogen. Brewer also tried to establish a shallow-layer model to simulate LH_2 pool spreading. But his version was plagued by severe numerical instabilities allowing to conduct only two successful predictive calculations for LH_2 aircraft accident scenarios [Brewer 1981].

8.3.2. LAUV Model Description

FZJ has developed the computer code LAUV [Dienhart 1995] based on the shallow-layer equations which allow for the description of cryogenic pool height and velocity as a function of time and location. The code addresses the relevant physical phenomena in both instantaneous and continuous (at a constant or transient rate) type releases onto either solid or liquid ground. Heat conduction from the ground is deemed the dominant heat source for vaporizing the cryogen, determined by solving the 1D or optionally 2D Fourier equation. Other heat fluxes are neglected.

Considering the volume of an incremental pool element, the mass conservation equation is given by balancing the volume change in time with the sum of all volume fluxes passing the element's boundaries. For a pool with cylindrical geometry, it is

$$\frac{\partial(rh)}{\partial t} + \frac{\partial(urh)}{\partial r} + r(v-w) = 0\,, \tag{8-10}$$

where $h=h(r,t)$ – pool height, m; r – radius, m; t – time, s; $u=u(r,t)$ – horizontal (depth-averaged) pool spreading velocity, m/s; w – liquid fuel source rate, m/s; v – liquid fuel vaporization rate, m/s.

From the simple 1D analytical solution of the Fourier equation, the vaporization rate per unit surface can be derived as

$$v = \frac{\lambda \Delta T}{\rho_l \Delta H_v \sqrt{\pi a} \sqrt{t - t'}}, \tag{8-11}$$

where λ – thermal conductivity of ground, W/(m K); ΔT – temperature difference between liquid and ground, K; ρ_l – density of liquid, kg/m^3; ΔH_v – vaporization enthalpy, J/kg; a – thermal diffusivity, m^2/s; t' – time moment from which surface element gets into contact with pool, s.

The code includes optionally a 2D numerical solution which is able to consider also the effect of temperature increase during intermittent times of no coverage with the cryogen.

The momentum conservation equation is determined by the balance of forces acting on the incremental pool volume taking account of buoyancy and friction forces:

$$\frac{\partial u}{\partial t} + \frac{\partial}{\partial r}\left(\frac{u^2}{2} + \delta g h\right) + \frac{F}{h} = 0, \tag{8-12}$$

where g – acceleration of gravity, m/s^2; $F=F(u,h)$ – friction force per mass unit, kg; δ – reduction factor which is 1 for solid ground (equation (8-8)). The friction force is chosen according to the approach in GASP considering distinct contributions from laminar and turbulent flux.

The above shallow-layer differential equation system (8-10) and (8-12) is solved by applying an explicit finite-difference scheme. It is valid under the following initial and boundary conditions:

- Spreading is horizontal in radial direction (1D) in unobstructed terrain.
- For instantaneous release, the pool is initially at rest (zero momentum), i.e., purely gravitational spreading. The initial pool height h(r) is assumed to be a (negative) square function of the radius.
- For continuous release, the source is a volume flow per unit surface downwards and perpendicular to the spreading. Source is always in the center.
- Vaporization is a volume loss per unit surface upwards through the pool surface.
- There is no vertical velocity profile within the pool (which is realistic for shallow layers and low friction).
- Densities of ground and cryogen remain constant, i.e., no influence by bubble formation.

Furthermore the LAUV model includes the possibility to simulate moisture in a solid ground connected with an extension of the heat balance by a term describing the water/ice phase transition (liberation of solidification enthalpy), and with a change of material properties when water turns to ice. For a water ground, LAUV contains, as an option, a finite-differences

submodel to simulate ice layer formation and growth into the depth. Assumptions are a plane ice layer neglecting effects like convective flow in the water, development of waves, or pool acceleration due to buoyancy of the ice layer.

8.3.3. Validation of the LAUV Code

British Gas LNG Pool Spreading Experiment

One of the experiments conducted by British Gas with the release of LNG has been used to compare the measurements with the prediction by respective computer models which have been developed to simulate such accidental cryogen spill events, the British code GASP and the German code LAUV [Dienhart 1995].

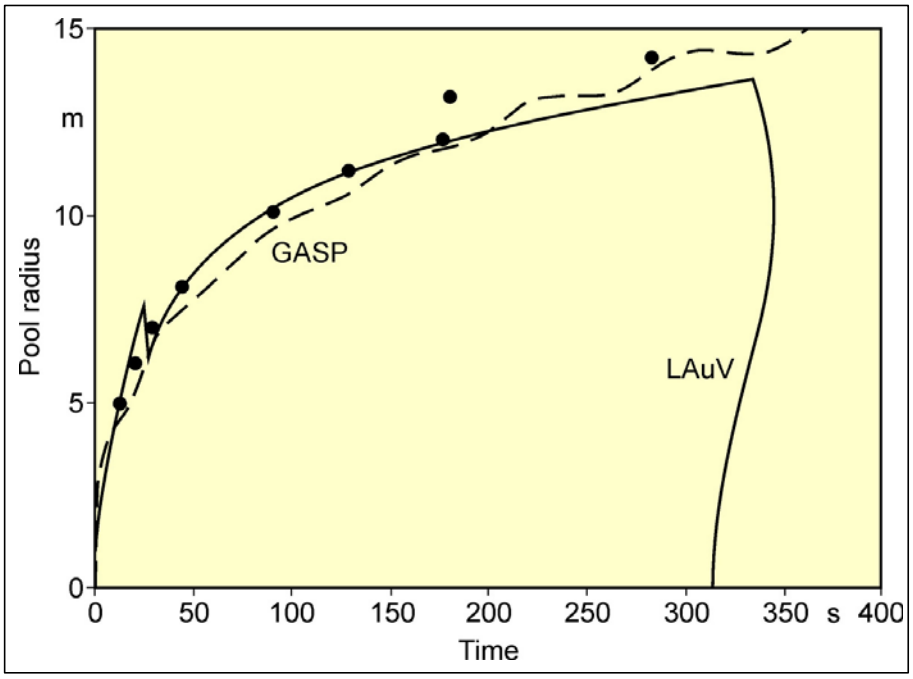

Figure 8-18. Comparison of postcalculation of an LNG spill experiment on dry concrete with the German LAUV code and the British GASP code [Dienhart 1995]

The boundary conditions of the test considered were dry concrete as ground, a spill time of 300 s, and a released quantity of 2.5 m^3 of LNG with a gradually decreasing release rate between 47 and 37 l/s. Measurements and calculational results given in Fig. 8-18 show the maximum radius of the LNG pool develop to approximately 13 m. About 10 s after spill termination, at t = 310 s, the pool is predicted to break up from the central spill point. A ring-shaped pool is formed which recedes from both inside and outside, until at t = 350 s, it has

completely died away. The measurements refer to the front edge of the pool, no experimental evidence is available for the trailing edge. The experimental data are in good agreement with both model calculations.

NASA LH_2 Spill Experiments

Trial #6 of the NASA test series was also subject of a postcalculation with the LAUV model. The nominal release rate of 134 l/s of LH_2 reduced by the flash-vaporized fraction leads to an estimated 87 l/s rate over 38 s contributing to pool spreading. The maximum pool radius was calculated to be about 6.5 m (Fig. 8-19), more than twice the measurement range for the radius observed in the test (Fig. 8-19). The calculated pool lifetime is 43.5 s which is about the figure of 43 s estimated by the NASA experimenters. The discrepancy in pool size is most certainly due to percolation of the liquid into the sand and furrows developing on the test site enlarging the surface area. Also the release process itself with the LH_2 first splashing on a deflection plate before hitting the ground certainly increased the vaporization rate. These all are aspects which were not simulated in the calculation and which may have significantly reduced the pool size [Verfondern 1997].

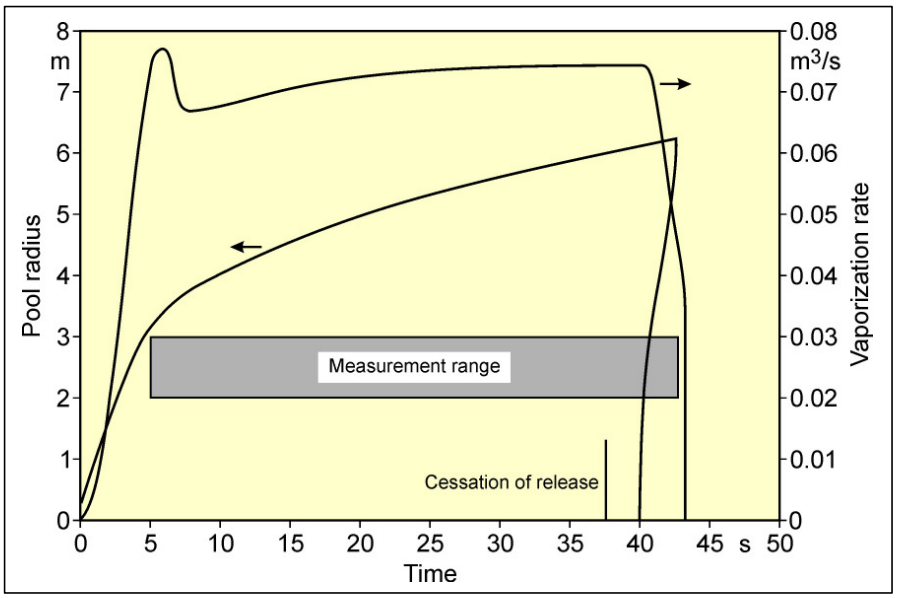

Figure 8-19. Postcalculation of the NASA LH_2 spill experiment #6 on compacted sand with the LAUV code [Dienhart 1995]

FZJ LN_2 Pool Spreading Experiments

An important part of the LAUV code validation process was the simulation of the LN_2 release experiments on water with the KIWI test facility at FZJ [Dienhart 1995]. Fig. 8-20 shows two examples of a comparison between measurements and postcalculation, an instantaneous release of 40 l of LN_2 on water (top) and a continuous release at a varying rate of 2.5 l/s over 73 s followed by a linearly decrease to zero at t = 121 s (bottom).

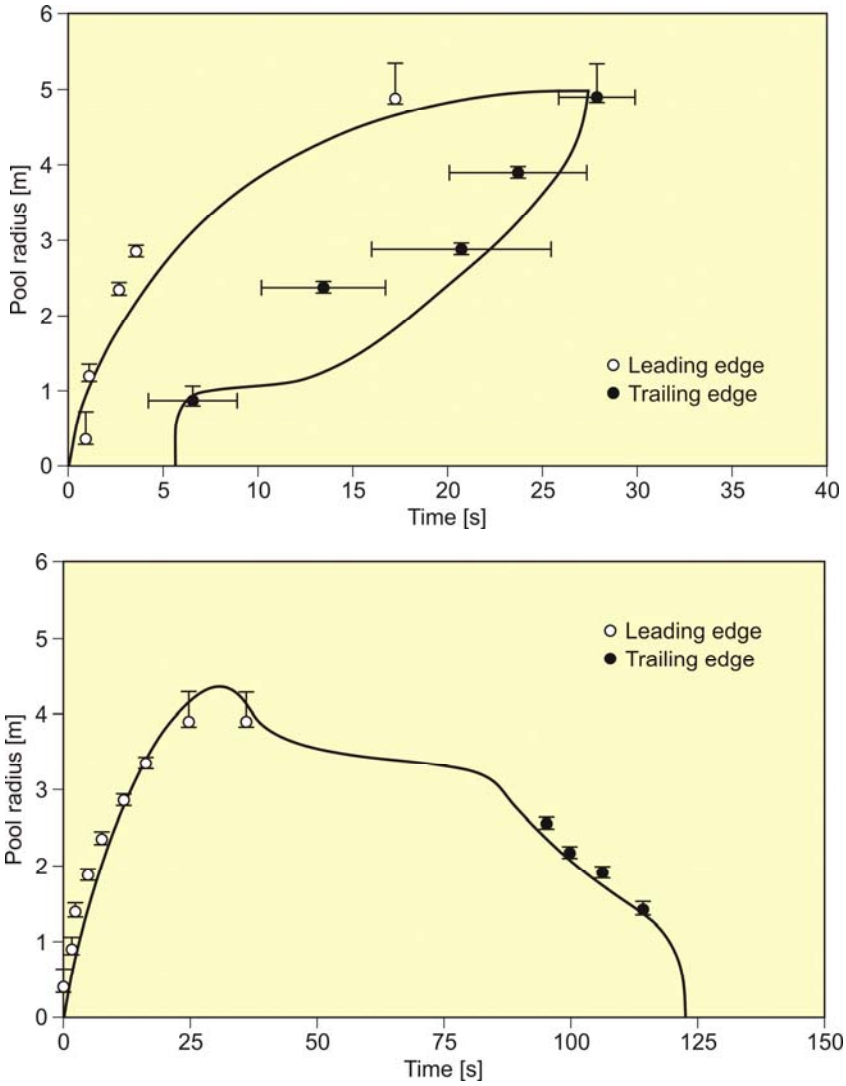

Figure 8-20. Comparison of LN_2 pool measurements with respective LAUV postcalculations of an instantaneous release of 40 l (top) and a continuous release at a varying rate (bottom) [Dienhart 1995]

FZJ LH_2 Pool Spreading Experiments

Calculation results of the FZJ experiments of LH_2 pool spreading with the LAUV model are shown in Fig. 8-21. The symbols represent the outermost positions which had definite contact with the cryogen, meaning that the principal uncertainty for the pool radius is given by the distance to the next measuring position (see error bars in figures). The shaded area describes the pulsation range according to what was observed from the video recording.

For the spill tests on water (Fig. 8-21, top), both measurement and calculation reveal the pool front at the beginning to have shortly propagated beyond the steady state presumably indicating the phenomenon of a detaching pool ring typical for continuous releases. The radius was then calculated to slowly increase due to the gradual temperature decrease of the ice layer formed on the water surface. Equilibrium is reached approximately after 10 s into the test. At time 62.9 s, i.e., about a second after termination of the spillage, the pool has completely vaporized. Despite the given uncertainties, the calculated curve for the maximum pool radius is still well within the measurement range. The ice layer thickness could not be measured during or after the test. According to the calculation, it has grown to a thickness of 7 mm at the center with the longest contact to the cryogen.

The spill tests on the aluminum ground (Fig. 8-21, bottom) conducted with a somewhat higher release rate is characterized by a steadily increasing pool radius. Here is no sign of a detaching ring as slightly indicated by the first measurement points due to the (calculated) high heat flux which makes the ring immediately decay away. The fact that the attained pool size here is smaller than on the water surface is due to the rapid cooling of the ground leading soon to the nucleate boiling regime and enhanced vaporization, whereas in the case of water, a longer film boiling phase on the ice layer does not allow for a high heat flux into the pool. This effect was well reproduced by the LAUV calculation.

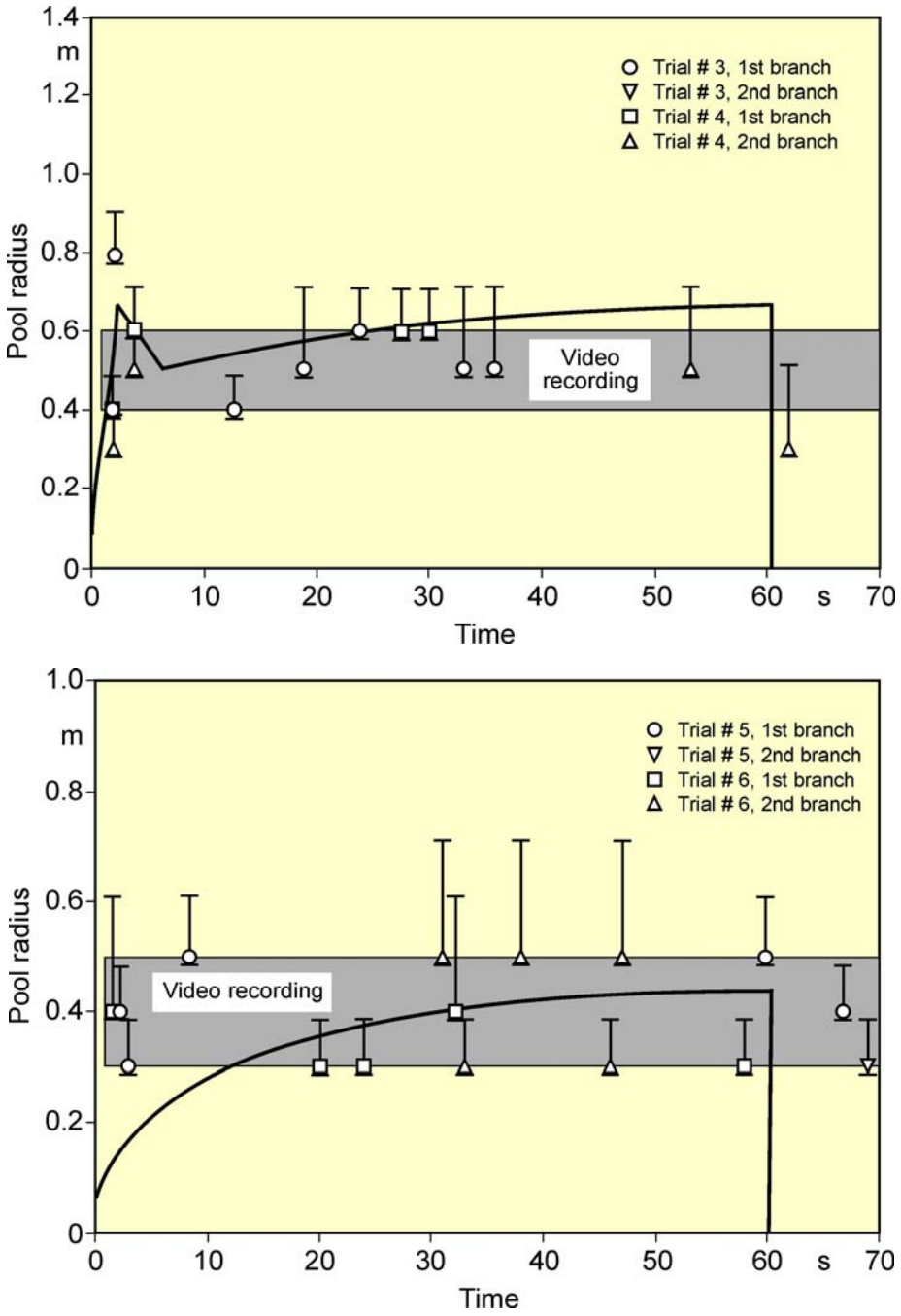

Figure 8-21. Comparison of LH_2 pool measurements with respective LAUV calculations of a continuous release over 62 s at 5 l/s on water (top) and at 6 l/s on a solid surface (bottom) [Dienhart 1995]

8.4. Prediction of LH_2 Pool Behavior in Accidental Spill Scenarios

8.4.1. CRYOPLANE Fuel Tank

The first example of a predictive calculation with the LAUV model refers to the CRYOPLANE project considering a hydrogen propelled aircraft of the type Airbus A310 (see section 7.2.3.). This aircraft has been designed to contain its total fuel of 240 m^3 of LH_2 in two 40 m^3 capacity active tanks plus two 80 m^3 capacity reserve tanks, all arranged above the passengers' section. The accidental event of an LH_2 tank rupture associated with a complete spill of the contents was subjected to a simulation with the LAUV code [Dienhart 1995].

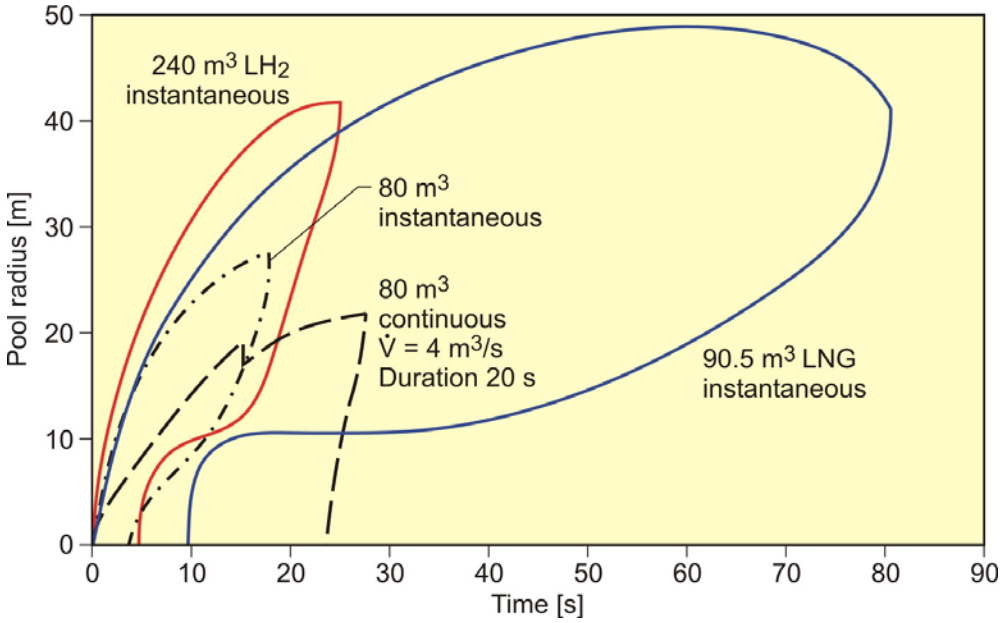

Figure 8-22. Instantaneous and continuous LH_2 release from a CRYOPLANE fuel tank on dry concrete and comparison with an LNG release of the same energy contents [Dienhart 1995]

The results (no flash-vaporization assumed) are given in Fig. 8-22. The LH_2 released in an instantaneous spill of all four tanks, 240 m^3 of LH_2, (assuming one central release spot) leads to a 42 m radius pool and a 25 s lifetime (red curve). The pool breaks up at the center after a few seconds forming an inner radius of the – then – annular-shaped pool. For the case of only one large tank to spill its contents of 80 m^3, the liquid hydrogen is estimated to spread in a pool with a maximum radius of 27 m and with a lifetime of 18 s (black dash-dotted curve). A spillage of the same amount continuously over a period of 20 s leads to a somewhat less extended pool with a total lifetime of 27 s (black dashed curve).

The comparison with an LNG fuel tank of the same energy contents as the 240 m^3 of LH_2, translating into 90.5 m^3 of LNG, shows that the developing LNG pool exhibits, despite a smaller volume, a larger maximum radius. The outwards spreading LNG ring pool reaches a maximum radius of almost 50 m after about 60 s. The pool breaks up already very soon (after 9 s) and continues to spread as a ring until after 60 s, it starts to recede from the outside (blue curve). Outer and inner radius meet after the total pool's lifetime of 82 s.

8.4.2. Comparison of Different Cryogen Cargos of a Tank Truck

Another predictive study with the LAUV code was made to analyze the differences in the spreading behavior of the cryogens LH_2, LOX, LNG, and LN_2 on solid ground (macadam) for the case of a 40 m^3 volume representative of a road tank truck load [Verfondern 1997]. Due to the different properties of these four cryogens (Table 8-4), their pool spreading and vaporization behavior is also very different. As can be deduced from equation (8-11), the vaporization rate increases with decreasing density and decreasing heat of vaporization. Results are shown in Table 8-5 and in Fig. 8-23 for an instantaneous spill (top) and a continuous spill at a rate of 1 m^3/s (bottom).

Table 8-4. Comparison of properties of different cyrogens

Cryogen	LH_2	LN_2	LOX	LNG (LCH_4)
Molecular weight [g/mol]	2.02	28.01	32.00	16.04
Boiling Point [K]	20.3	77.4	90.2	111.6
Density at BP	71	808	1141	423
Heat of vaporization [kJ/kg]	446	199	255	510
Heat of vaporization [kJ/mol]	0.90	5.59	8.16	8.18
Heat flux density [kW/(m^2]	100	25	22	95
Specific heat capacity [kJ/(kg K)]	9.7	2.0	1.5	3.5
Thermal conductivity [W/(m K)]	0.099	0.137	0.150	0.208
Dynamic viscosity [10^{-4} N s/m^2]	0.13	1.65	1.89	1.07
Surface tension [10^{-3} N/m]	1.92	8.5	13.2	12.94

A remarkable difference for both release modes is the small size and the short lifetime of the LH_2 pool compared to all other pools. The LH_2 lifetime of about 13 s for the instantaneous spill and maximum distance from the (central) spill point of about 20 m are much lower than the respective LN_2, LNG, or LOX data. The LNG pool exhibits with 94 s the longest lifetime. In terms of mass vaporization, rates are highest for the heavy cryogens LN_2 and LOX compared to the light cryogens LH_2 and LNG.

For the more realistic case of a continuous release over 40 s at a constant rate, the maximum LH_2 pool radius will be reduced down to 12 m. Also the mass vaporization rate of LH_2 has decreased from 280 to 70 kg/s. When the release is terminated after 40 s, the LH_2 will have disappeared after 5 more seconds. All other pools are only slightly reduced in size compared to the instantaneous release case. The maximum radius of the LNG pool is reduced from 38 to 33 m and also, although not quite as large in size as LOX, will survive longest with 94 seconds.

Table 8-5. Predicted pool radius, vaporization time, and vaporization rate after a 40m³ instantaneous / continuous spill on solid ground

Cryogen	LH_2	LN_2	LOX	LNG
Instantaneous release of 40 m³				
Maximum pool radius [m]	20	32	38	38
Vaporization time [s]	13	48	63	65
Maximum vaporization rate [m³/s]	4.0	1.2	0.9	0.8
Maximum vaporization rate [kg/s]	280	970	910	340
Continuous release of 40 m³ at a constant rate, spill time 40 s				
Maximum pool radius [m]	12	26	37	33
Vaporization time [s]	45	84	55	94
Maximum vaporization rate [m³/s]	1.0	0.6	1.0	0.5
Maximum vaporization rate [kg/s]	70	480	1140	220

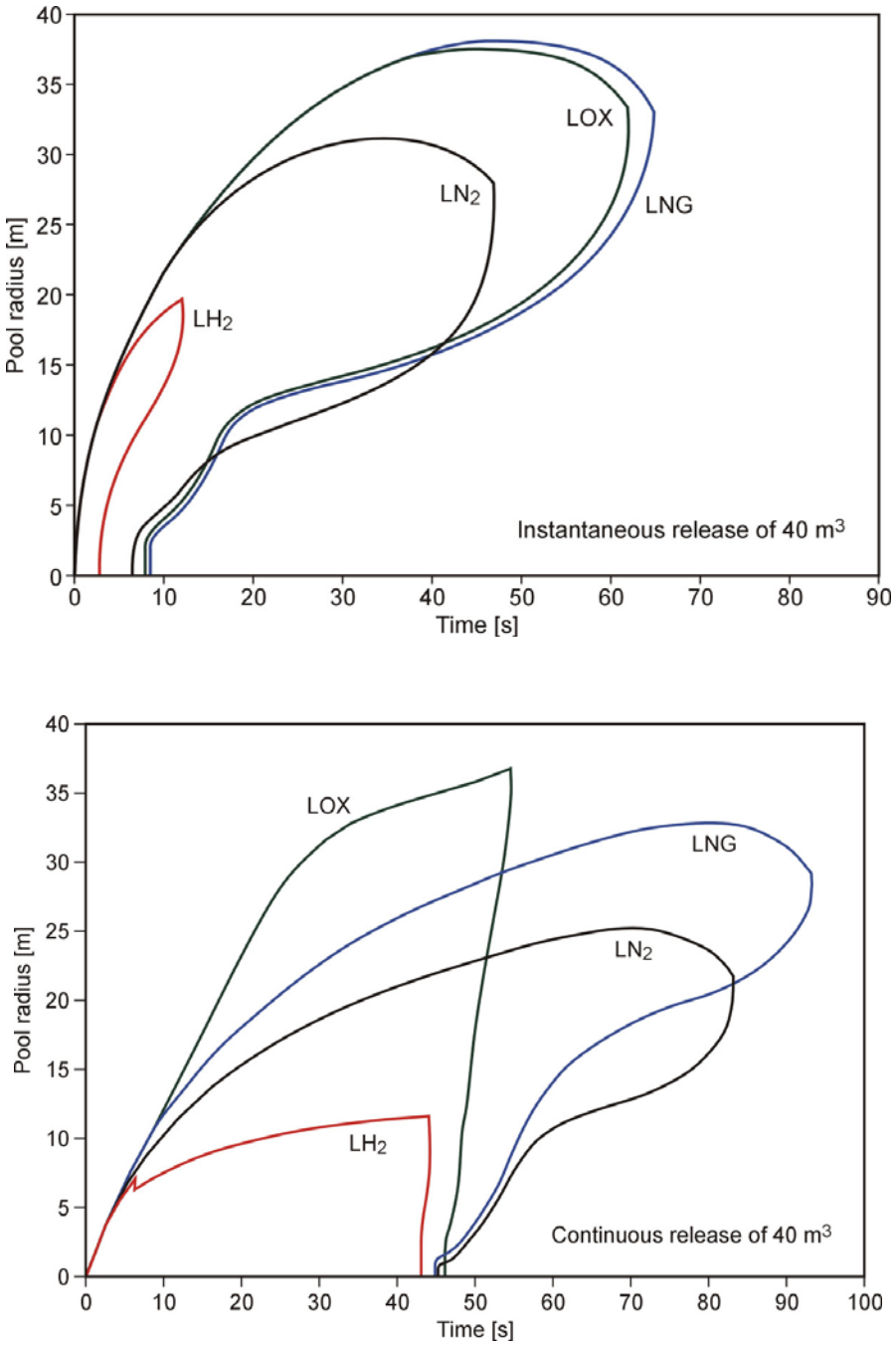

Figure 8-23. LAUV prediction of the spreading behavior of an LH_2, LN_2, LNG, and LOX pool, respectively, after a 40 m^3 spill onto solid ground (macadam) instantaneous release (top) and continuous release over 40 s (bottom)

8.4.3. Simulation of Passive Catalytic Recombiner Operation in a Garage

Passive autocatalytic recombiners, PAR, (Fig. 8-24) have become part of the safety concept for the nuclear containment of many nuclear power plants in Europe. In case of severe accidents with core melting, hydrogen can be generated evolving from the zirconium-steam interaction in the cladding at high temperatures. For a typical pressurized light water reactor (reference plant: Biblis B, Germany) with a Zr contents in the fuel cladding of some 40 t, the maximum amount of H_2 liberated into the containment could be 20,000 Nm^3. The employment of PARs is expected to reduce the amount of hydrogen and mitigate the hazard of an explosion inside the nuclear containment. A PAR makes use of the exothermal reaction of hydrogen and oxygen on catalytic surfaces generating steam and heat [IAEA 2001].

Figure 8-24. Principle of a passive catalytic recombiner

A PAR is a fully passively acting system, i.e., no additional external power supply or operational action is necessary in order to start and support the operation. The proper location of a sufficient number of PARs allows for prevention of the formation of flammable mixtures inside the enclosure without additional venting devices. In general, however, the PAR represents a safety measure that may be used complementary to other techniques, e.g., venting or inerting, as the demands on PAR for non-nuclear applications can be quite different. With an increasing number of hydrogen applications, numerous scenarios with regard to possible release amount and rates, flow and process conditions etc. have to be considered. PAR designs will have to reflect the respective boundary conditions.

A significant drawback of today's recombiners hindering the introduction as safety device in many applications is the risk of catalyst overheating in cases of high concentrations of hydrogen. For advanced designs, the recombiner is combined with passive cooling elements in order to enhance the removal of the reaction heat from the catalyst [Reinecke 2007].

In a theoretical study, it was examined whether and to what extend such a device for reducing the amount of undesired hydrogen is also applicable to a garage for H_2 driven vehicles in cases where hydrogen is leaking from the storage tank [Verfondern 2004]. The simulation of the operation of a passive recombiner in a garage was performed with the CFD code CFX [CFX 2001] which allows the detailed analysis of a multi-component gas flow in a complex confined or partially confined 3D geometrical structure taking into account all relevant physical phenomena which occur in cases as considered here.

The principal task to be solved starts from a partially confined space, in which a hydrogen containing system is placed. The dimensions of the room structure selected for this study were 6 x 6 m^2 ground surface and a height of 3.2 m. Room atmosphere is air at ambient conditions. As part of a safety concept for the H_2 system – and topic of investigation in this study – a catalytic recombiner is employed in the upper part of the space close to the ceiling. Its geometrical shape is ideally flat and wide, particularly if the position of the H_2 source is variable. In the calculation grid, the PAR is represented by a 0.2 m thick box-shaped component with a horizontal cross section of 3 x 3 m^2 in central position and with a distance of 0.5 m hanging below the ceiling. The room must have an opening (or active venting system), in order to avoid – in case of PAR operation – a pressure buildup resulting from the liberated product gases of the conversion reaction. The opening also serves as a means for passive heat removal. The opening with a 1.5 x 1.5 m^2 extension is centrally arranged in the ceiling above the PAR. (All dimension figures are valid for the total room.)

Due to the symmetry of the arrangement, it is sufficient to model a quarter section of the room only (Fig. 8-25). Boundary conditions are then reflecting at the symmetry axes. The opening at the top represents a "pressure" boundary condition. All other boundaries are solid walls.

The source is simply simulated by a small 2D inlet patch of the dimensions 0.2 x 0.2 m^2 on the ground in central position. It releases gaseous hydrogen at a given temperature, release rate, release duration, and release direction. For the present study, a release rate of 0.5 kg/h (total room) at ambient (case 1) or cryogenic temperature (case 2) has been chosen.

The PAR component simulated in the model by a box-shaped space near the ceiling represents a (partial) sink for the incoming hydrogen and at the same time a source for steam and heat. The effectiveness of conversion as a function of H_2 concentration is assumed according to a characteristic curve which is given as boundary condition. The exiting gas mixture consists of the product gas (assumed water vapor only) and still unconverted H_2 at a temperature of 910 K. The modeling of the conversion reaction is directly linked with the oxygen contents in the room atmosphere.

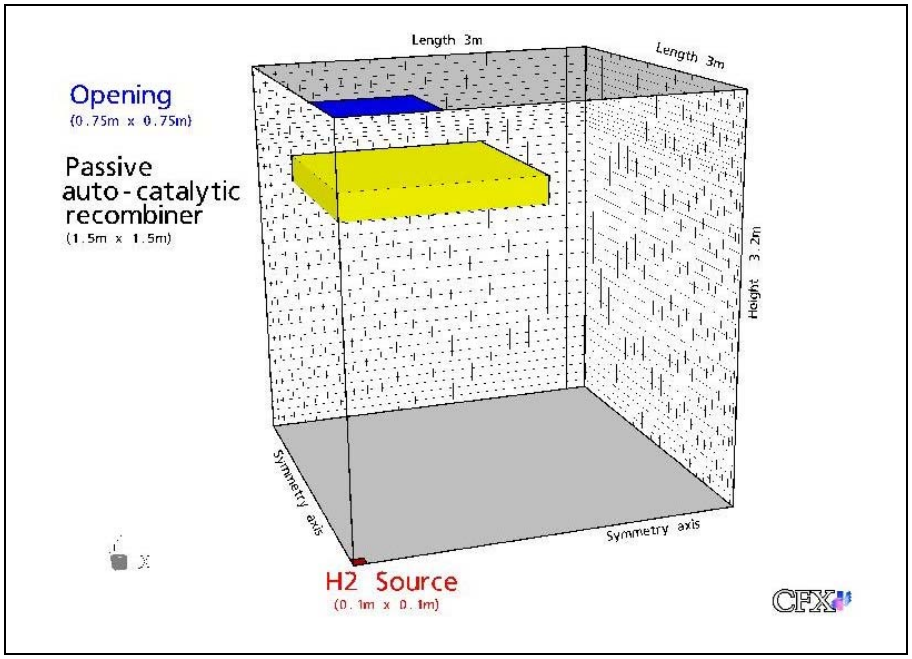

Figure 8-25. Calculation grid for reference case

For the given structure, the initial (total) room atmosphere contains a mass of 34.5 kg of O_2 allowing ideally the conversion of 4.3 kg of H_2 in a stoichiometric reaction, before the PAR stops being active due to lack of oxygen (unless there are other O_2 sources like from air ingress through the opening in the ceiling).

In Fig. 8-26, left-hand side, the concentration distribution of the gaseous H_2 released at ambient temperature (case 1) is plotted showing the upwards flow in a column-like shape, outside of which no H_2 is found. The column broadens with height resulting from the admixing of air, but still has at its center an H_2 concentration of around 30 vol%. The column is quenched as soon as it reaches the conversion area of the recombiner, where both H_2 and O_2 concentrations are reduced.

As can be seen from the temperature distribution on the right-hand side of Fig. 8-26, only a limited part of the catalytic recombiner is actively involved in the conversion process. Correspondingly the water vapor production is limited and thus the temperature increase exhibiting a maximum of about 780°C. The conversion rate is about 7 g/(m^2 s) of H_2 which means that the gas mixture leaving the recombiner still has a hydrogen concentration of 25 vol%. Although the calculation is transient, the state as shown in the plot was found to be stationary after a short time.

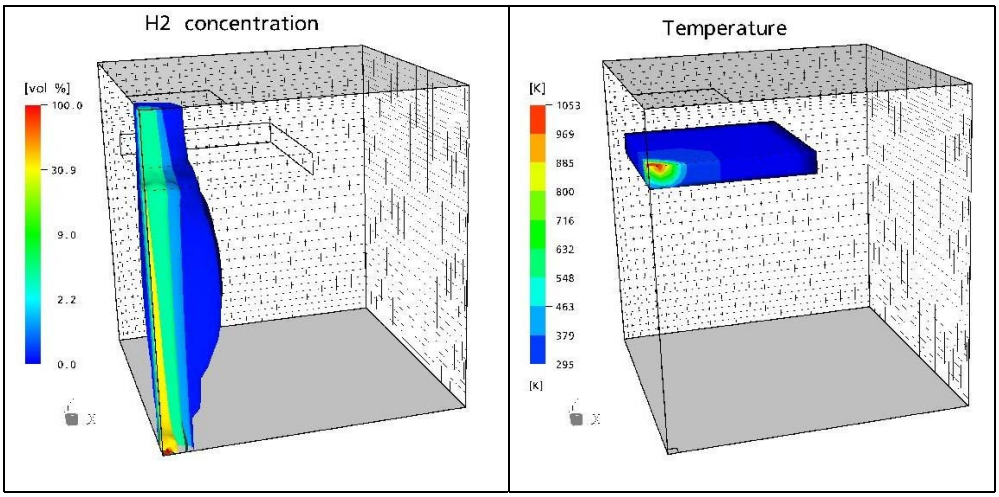

Figure 8-26. H_2 concentration (left) and temperature distribution for reference case

In the calculation with hydrogen gas at cryogenic temperature (case 2) escaping from the source, the upwards flow of the H_2 remains restrained to an even more narrow range compared to the ambient temperature case as is shown in Fig. 8-27. Due to a weaker buoyancy of the cold gas, the admixing of air is obviously smaller. Also H_2 concentrations remain lower near the column center compared to the previous case. The maximum temperature of ~690°C attained in the PAR is lower by about 100 degrees than in case 1.

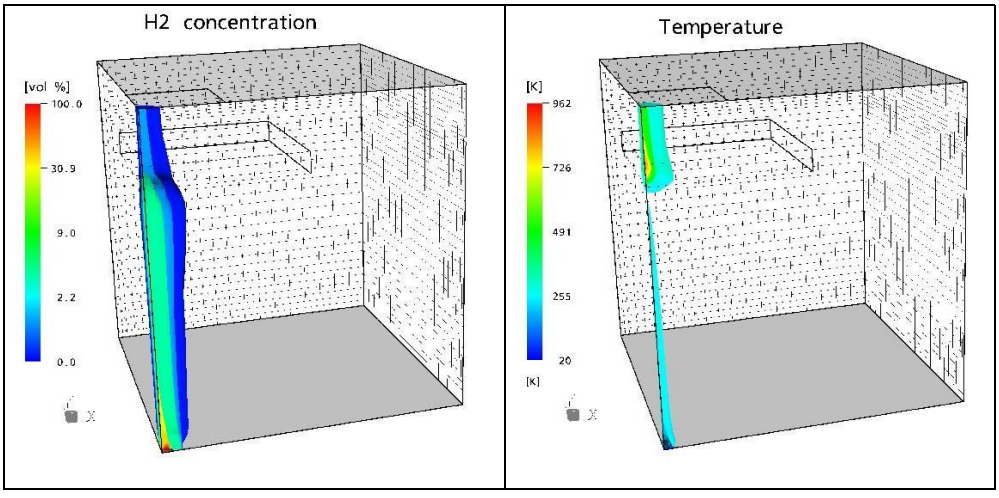

Figure 8-27. H_2 concentration (left) and temperature distribution for case with cryogenic gaseous hydrogen escaping the source

For the case of an opening above the PAR with reduced size, the calculation has shown that less gas and thus less heat is leaving the room. The heated gas is rather recirculated outside along the side walls steadily re-entering the recombiner, where the gas is continuously heated up as long as still H_2 and O_2 is available, even to unacceptable values.

Increasing the size of the source area (and leaving the mass escape rate constant), increases as expected the PAR area affected by the conversion process, but on the other hand appears to create a complex transient flow pattern, which requires further analysis.

The CFD model calculations have shown that it is reasonably possible to simulate the operation of a catalytic recombining device in partially confined areas, thus allowing the designing of appropriate safety concepts for rooms with H_2 containing systems. The design of the garage selected here as an example is certainly neither ideal nor representative for a future H_2-driven vehicle garage. Accident conditions with small leakage rates appear to be controllable with no major problem, whereas in case of larger release rates, e.g., the spontaneous escape of the entire inventory of a vehicle tank, additional safety measures like active cooling systems would be required.

8.5. Pool Fire Modeling

Also with regard to pool fires, model development has been conducted since a long time. Starting with simple models to describe empirical relationships between flame dimensions and spilled fuel mass, the development of more and more sophisticated models has been following to simulate large-scale effects such as plume characteristics, dispersion of combustion products, or heat radiation.

Various state-of-the-art CFD codes are available that allow the assessment of pool fire behavior, e.g., CFX, FLUENT, PHOENICS offering submodels to describe more complex situations such as object/flame interaction. Due to the turbulent character, turbulence models, e.g., the k-ε model, are used. Radiative heat transfer equations are applied to model thermal radiation.

The first systematic studies of pool fires were conducted in the 1950s [Hottel 1958]. In industrial practice, the larger pool fires are of most concern, where “large” means a pool diameter of 0.2 m and greater. A 0.2 m diameter pool on fire typically produces about 100 kW [Babrauskas 1983]. The energy balance for a burning pool is:

$$\dot{m} * \Delta H_v = \dot{q}_r + \dot{q}_c \qquad (8\text{-}13)$$

where $\dot{m}$ – mass loss or burning rate, kg/(m^2 s); J; ΔH_g – total heat of vaporization (heat to bring liquid to boiling point plus heat to vaporize), J; $\dot{q}_r$ – radiant heat flux absorbed by the pool, kJ/kg; $\dot{q}_c$ – heat received convectively, kJ/kg, and with other minor contributions neglected.

Two regimes for the regression rate have been identified depending on the pool dimension. For small diameters (D < 0.2 m), heat transport by conduction is dominant. The regression rate decreases with increasing radius indicated by the following functional relationship:

$$\dot{m} = \frac{\dot{q}_c}{\Delta H_v} = a * D^{-n} + b \tag{8-14}$$

where a, b are constants and n is in the range between 0.5 and 1.5 for the laminar burning mode with pool diameters below 50 mm. For the turbulent convective mode, $\dot{m}$ becomes independent of the pool diameter.

For large diameters (D > 0.2 m), heat radiation is dominant resulting in increasing regression rates for increasing radius:

$$\dot{m} = \frac{\sigma T_f^{\,4} \left(1 - \exp\{-k\beta D\}\right)}{\Delta H_v} = \dot{m}_\infty \left(1 - \exp\{-k\beta D\}\right) \tag{8-15}$$

where σ – Stefan-Boltzmann constant, = $5.67*10^{-11}$ kW/(m^2 K^4); T_f – effective equivalent grey gas flame temperature, K; $\left(1 - \exp\{-k\beta D\}\right)$ – effective flame volume emissivity; k – absorption-extinction coefficient of flame; β – mean beam length corrector. In most cases, the parameters T_f, k, β are not measured directly. For many fuels, reliable measurements exist only for $\dot{m}$ as a function of pool diameter D.

In [Zabetakis 1967], the regression rate $\dot{v}$ of a pool burning in air under wind-free conditions is given as:

$$\dot{v} = \dot{v}_\infty * \left(1 - \exp\{-k\beta D\}\right) \tag{8-16}$$

with the two empirical factors (k*β) – opacity coefficient, m^{-1}, (0.18 - 0.27 for hydrocarbons) and $\dot{v}_\infty$ – mass loss rate for an infinite, i.e., radiation-dominated pool, mm/min, and

$$\dot{v}_\infty = 0.076 * \frac{\Delta H_c}{\Delta H_v} \; mm/\min \tag{8-17}$$

where ΔH_c – net heat of combustion, J/kg. $\dot{v}$ corresponds to $\dot{m}$ except that its unit is a "speed". Multiplied with the density yields then the unit of $\dot{m}$ of kg/(m^2 s).

The data for some cryogens and for gasoline to calculate regression rates of burning pools are listed in Table 8-6. The data for $\dot{m}_\infty$ and (k*β) were taken from [Babrauskas 1983].

If looking at the results from equation (8-17) listed in the last column of the table, a particularly large discrepancy can be recognized for liquid hydrogen which are probably due to uncertainties in the experimental determination of the respective parameters. For liquid hydrogen, the limit according to equation (8-17) is $\dot{v}_\infty$ = 20.5 mm/min. Also for gasoline pool fires, there is a major difference, whereas data for LNG and LPG are in satisfactory agreement.

Table 8-6. Data for large pool burning rate estimates

Fluid	Density [kg/m^3]	ΔH_v [kJ/kg]	ΔH_c [MJ/kg]	k β (1) [m^{-1}]	T_f (1) [K]	$\dot{m}_\infty$ (2) [mm/min]	$\dot{v}_\infty$ (3) [mm/min]
LH_2	71	446	120	6.1	1600	142.2	20.5
LNG	422	510	61	1.1	1500	11.1	9.1
LPG	544	428	46	1.4		10.9	8.2
Gasoline	737	330	44	2.1	1450	4.5	11.3

(1) taken from [Babrauskas 1983]
(2) according to equation (8-15) [Babrauskas 1983] converted to mm/min
(3) according to equation (8-17) [Zabetakis 1967]

Fig. 8-28 shows the largely scattering measurements for a cryogenic liquid, LNG, under steady-state burning condition in a wind-free environment in comparison with the calculated curves for LNG, LH_2, and gasoline determined according to equation (8-15).

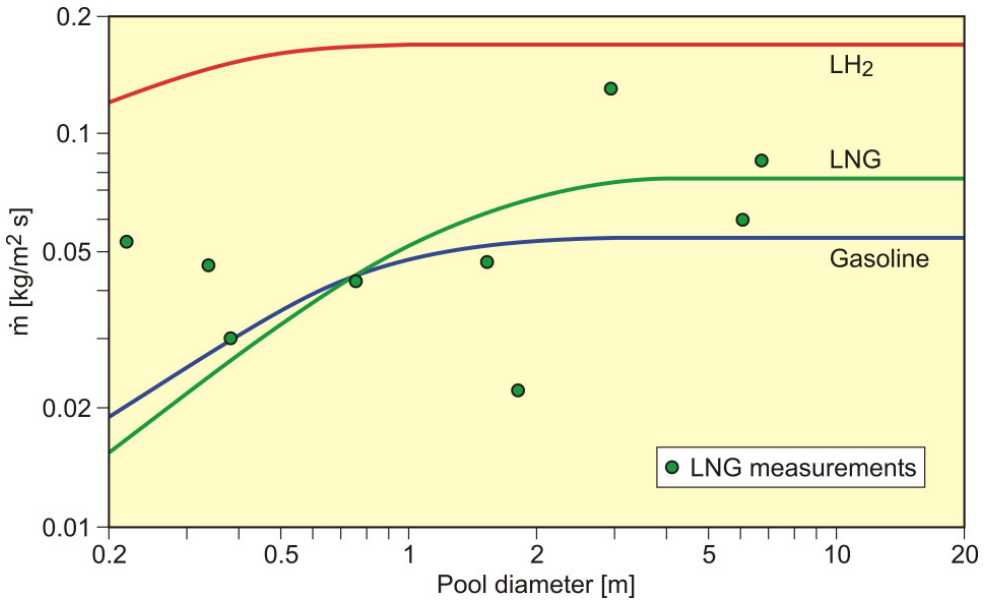

Figure 8-28. Steady-state pool burning rates [Babrauskas 1983]
(Note logarithm scales)

Correlations for the flame height of a pool fire that are widely used are [Iqbal 2004]

$$H_f = 0.235 * \dot{Q}^{0.67} - 1.02 * D \tag{8-18}$$

where H_f – height of flame, m; J; $\dot{Q}$ – heat release rate of the fire, kW.

and

$$H_f = 42 * D * \left(\frac{\dot{m}}{\rho_a \sqrt{g\, D}} \right)^{0.61} \tag{8-19}$$

where ρ_a – density of ambient air, kg/m^3; J; g – gravitational acceleration, m/s^2.

These equations can also be applied for the determination of the radiative heat transfer.

9. SUMMARY AND CONCLUSIONS

The production, storage, and transportation facilities for generating and handling liquid hydrogen are well developed and widely applied large-scale technologies at a high safety level. With regard to the large hazardous potential of the hydrogen, the consideration of safety aspects when dealing with liquid hydrogen is of utmost importance. The aim of this report was to introduce the particular properties of liquid hydrogen and to identify the safety concerns in connection with the cryogenic liquid. Furthermore it described the safety-related experimental activities, whose objectives were to understand the physical phenomena associated with the inadvertent release of LH_2 and demonstrate its behavior under accidental conditions. Finally approaches were pointed out to simulate the behavior of the cryogen by theoretical models, which allow the assessment of the consequences of an accidental LH_2 spillage as a part of probabilistic safety and risk assessments. The following conclusions can be drawn:

- There is already a worldwide hydrogen market existing which is expected to grow further. In particular, there will be an increasing need for hydrogen used as a clean and environmentally friendly fuel. Also the use of hydrogen in its liquefied state will further increase representing an efficient and economic option for storage and transportation of hydrogen.

- In the transportation sector, liquid hydrogen is presently only well established in the space industries as a rocket fuel, while it will presumably play an increasingly important role in additional transportation applications. Currently in progress is its utilization as vehicle fuel connected with the respective establishment of an appropriate infrastructure, e.g., LH_2 refueling stations. Despite still open technological and economic questions, a significant progress has been achieved such that the introduction of gaseous and liquid H_2 driven vehicles into the market is foreseen within a decade from now.

- Experience from experiments simulating accident scenarios with gaseous and liquid hydrogen and the lessons learnt from accidents have led to a set of codes, standards, regulations, and guidelines, which resulted in the high level of safety achieved by today. It remains, however, still the permanent need for revision and development of the actual legislation with the goal of further improvement.

- With regard to separation distances, the selection of criteria and the definition of threshold values to cut off the negligible risk will be country-specific and depend on its established set of rules and guidelines. With increasing number of hydrogen systems emerging worldwide, harmonization of the sets of rules, standards, and guidelines is needed. Comparing liquid versus gaseous hydrogen, there are guidelines which acknowledge the principally lower hazardous potential of the LH_2 by means of shorter safety distances.

- Despite numerous experiments in the past to investigate the liquid hydrogen behavior following an accidental spillage, there are still open questions which require further efforts to extent the still poor experimental data basis. These efforts should include the determination of vaporization rates from large spills of LH_2 and the examination of the pool propagation on different grounds, but also the dispersion behavior of cold vapor clouds evolving from the vaporization of the

cryogenic liquid (near-field and far-field), and the behavior of pool fires and the effect of water vapor and condensed fog on flame travel.

- The physical phenomena of cryogenic pool spreading and vaporization are principally understood providing the basis for modeling efforts to simulate LH_2 behavior in all situations of interest. Starting with simple empirical relationships, the development of calculation models has eventually resulted in computer codes based on the "shallow layer" differential equation system currently representing the state of the art.

- At present, all existing cryogenic pool spreading models assume a central spill point and radial spreading of the liquid. Next stage in modeling should incorporate additional effects such as obstacles to the spreading in the vicinity, inclining terrain, channel flow, which would all result in differently shaped vapor clouds. Such models should then ideally be coupled to CFD codes capable of describing the atmospheric dispersion of both negatively and positively buoyant vapor clouds.

REFERENCES

Abe A., et al. Studies of the Large-Scale Sea Transportation of Liquid Hydrogen. *International Journal of Hydrogen Energy,* **23:**115-121, 1998.

Aceves S.M., et al. Certification Testing and Demonstration of Insulated Pressure Vessels for Vehicular Hydrogen Storage. U.S. DOE Hydrogen Program Review, Report NREL/CP-610-32405, National Renewable Energy Laboratory, Golden, USA, 2002.

Aceves S.M., et al. Advanced Concepts for Vehicular Containment of Compressed and Cryogenic Hydrogen. In *Proc. 16th World Hydrogen Energy Conference WHEC'16,* paper 420, Lyon, France, 2006.

ADL. Final Report on an Investigation of Hazards Associated with the Storage and Handling of Liquid Hydrogen. Report C-61092, Arthur D. Little Inc., Cambridge, USA, 1960.

AIST. Japan's Sunshine Project – Summary of Hydrogen Energy R&D 1982. Agency of Industrial Science and Technology, Ministry of International Trade and Industry, Tokyo, Japan, 1982.

Arnold G. and Wolf J. Liquid Hydrogen for Automotive Application, Next Generation Fuel for FC and ICE Vehicles. *Teion Kogaku (J. Cryo. Soc. Japan),* **40**:221-230, No. 6, 2005.

Astbury G.R. and Hawksworth S.J. Spontaneous Ignition of Hydrogen Leaks: A Review of Postulated Mechanisms. In *Proc. 1st International Conference on Hydrogen Safety ICHS-2,* Pisa, Italy, 2005.

Babrauskas V. Estimating Large Pool Fire Burning Rates. *Fire Technology,* **19**:251-261, 1983.

Bainbridge P. LNG in North America and the Global Context. *IELE/AIPN Meeting,* Houston, USA, October 2002.

Baines A. and Schmidtchen U. Afterglow of a Myth – Why and How the „Hindenburg" Burnt. DWV Statement #4, http://dwv-info.de/e/publications/2000/hbe.pdf, German Hydrogen Association, Berlin, Germany, 2000.

BAM. Sicherheitsgutachten zur Vorprüfung einer Tank- und Verdampferanlage für verflüssigten Wasserstoff (LH_2) im Rahmen eines öffentlichen Zulassungsverfahrens nach Bundes-Immissionsschutz-Gesetz (BImSchG). Bundesanstalt für Materialforschung und -prüfung, Berlin, Germany (1994).

Behrend E., et al. Folgenschwere Explosion – Bericht über Ursachen und Hergang des Berstens eines Wasserstofftanks in Hanau - Teil 1. *TÜ,* **34:**176-179 and Teil 2. *TÜ,* **34:**225-229, 1993.

Bevilaqua Knight Inc. Bringing Fuel Cell Vehicles to Market, Scenarios and Challenges with Fuel Alternatives. Consultant Study Report, Hayward, USA, 2001.

BMBF. Project V3MVT100. http://www.icefuel.de , 2006.

BMI. Bekanntmachung der Richtlinie für den Schutz von Kernkraftwerken gegen Druckwellen aus chemischen Reaktionen durch Auslegung der Kernkraftwerke hinsichtlich ihrer Festigkeit und induzierter Schwingungen sowie durch Sicherheitsabstände. Bundesministerium des Innern, Bonn, Germany, 1976.

Boeing. An Exploratory Study to Determine the Integrated Technological Air Transportation System Ground Requirements of Liquid-Hydrogen-Fueled Subsonic Long-Haul Civil Air Transports. Report NASA-CR-2699, National Aeronautics and Space Administration, Washington D.C., USA, 1976.

Boeing. Boeing Tests HALE Hydrogen Propulsion System Using Ford-Developed Engine. News Release, October 24, 2007, http://www.boeing.com/news/releases/2007/q4/071024b_nr.html , Boeing Integrated Defense Systems, St. Louis, USA, 2007.

Bowman M. The Big Chill. http://www.external.ameslab.gov/news/Inquiry/fall97/bigchill.html , 1998.

Bracha M., et al. Large-Scale Hydrogen Liquefaction in Germany. *International Journal of Hydrogen Energy,* **19:**53-59, 1994.

Brandeis J. and Ermak D.L. Numerical Simulation of Liquefied Fuel Spills – I. Instantaneous Release into a Confined Area. *International Journal of Numerical Methods in Fluids*, **3:**333-345, 1983, and II. Instantaneous and Continuous LNG Spills on an Unconfined Water Surface. *International Journal of Numerical Methods in Fluids*, **3:**347-361, 1983.

Breitung W. and Redlinger R. A Model for Structural Response to Hydrogen Combustion Loads in Severe Accidents. *Nuclear Technology,* **111:**420-425, 1995.

Brentari E.G. and Smith R.V. Nucleate and Film Pool Boiling Design Correlations for O_2, N_2, H_2, and He. In *International Advances in Cryogenic Engineering,* paper T-1, Plenum Press, New York, USA, 1965.

Brewer G.D., et al. Assessment of Crash Fire Hazard of LH_2-Fueled Aircraft. Final Report No. NASA-CR-165525, NASA Lewis Research Center, Cleveland, USA, 1981.

Briscoe F. and Shaw P. Spread and Evaporation of Liquid. *Progress in Energy and Combustion Science,* **6:**127-140, 1980.

Carslaw H.S. and Jaeger J.C. *Conduction of Heat in Solids.* Clarendon Press, Oxford, United Kingdom, 1959.

Cassut L.H., et al. A Study of the Hazards in the Storage and Handling of Liquid Hydrogen. *Advances in Cryogenic Engineering,* **5:**55-61, 1960.

CFX. *CFX-4.4 User Documentation.* CFX International, AEA Technology, Harwell, United Kingdom, 2001.

Chirivella J.E. and Witcofski R.D. Experimental Results from Fast 1500-Gallon LH_2 Spills. *American Institute of Chemical Engineers Symposium Series,* **82:**120-140, 1986.

Chirivella J.E. Analysis of the "Phantom" Fires on the Space Shuttle External Tank Base and the Nature of the Space Shuttle "Phantom" Fires: LH_2 Leaks. In *Proc. 34th Combustion*

Systems Hazards Subcommittee and Airbreathing Propulsion Subcommittee Joint Meetings JANNAF, Palm Beach, USA, 1997.

Chitose K., et al. Analysis of a Large-Scale Liquid Hydrogen Spill Experiment Using the Multi-Phase Hydrodynamics Analysis Code (Champagne). In *Proc. 11th World Hydrogen Energy Conference WHEC'11,* pages 2203-2211, Stuttgart, Germany, 1996.

Chitose K., et al. Activities on Hydrogen Safety for the WE-NET Project – Experiment and Simulation of the Hydrogen Dispersion. In *Proc. 14th World Hydrogen Energy Conference WHEC'14*, Montreal, Canada, 2002.

Danieli E. Personal Communication. Praxair, Danbury, USA, 1997.

DASA. CRYOPLANE – Deutsch-Russisches Gemeinschaftsprojekt zum Einsatz kryogener Treibstoffe in der zivilen Luftfahrt – Realisierbarkeitsstudie 1990/91/92. Report, Deutsche Aerospace Airbus GmbH, Hamburg, Germany, 1992.

Dawson V.P. and Bowles M.D. Taming Liquid Hydrogen: The Centaur Upper Stage Rocket 1958-2002. The NASA History Series, Report NASA SP-2004-4230. National Aeronautics and Space Administration, Washington D.C., USA, 2004.

Dechema. A Study for the Generation, Inter-Continental Transport, and Use of Hydrogen as a Source of Clean Energy on the Basis of Large-Scale and Cheap Hydro-Electricity. Final Report on Contract No. EN3S-0024-D(B), Deutsche Gesellschaft für Chemisches Apparatewesen, Frankfurt, Germany, 1987.

Dienhart B. Ausbreitung und Verdampfung von flüssigem Wasserstoff auf Wasser und festem Untergrund. Report Jül-3155, Research Center Jülich, Germany, 1995.

Drnevich R. Hydrogen Delivery Liquefaction and Compression. *Workshop on Strategic Initiatives for Hydrogen Delivery,* Washington D.C., USA, 2003.

Duijm N.J. and Markert F. Safety-Barrier Diagrams for Documenting Safety of Hydrogen Applications. In *Proc. 2nd International Conference on Hydrogen Safety ICHS-2,* San Sebastian, Spain, 2007.

EC. Hydrogen Energy and Fuel Cells – A Vision of Our Future. High Level Group Summary Report, European Commission, Brussels, Belgium, 2003.

Edeskuty F.J. and Williamson K.D. Storage and Handling of Cryogens. *Advances in Cryogenic Engineering*, **17:**56-68, 1972.

Edeskuty F.J. Critical Review and Assessment of Problems in Hydrogen Energy Delivery Systems. Report LA-7405-PR, Los Alamos Scientific Laboratory, USA, 1978.

Edeskuty F.J. and Stewart W.F. *Safety in the Handling of Cryogenic Fluids.* The International Cryogenics Monograph Series, Plenum Press, New York, USA, 1996.

Eichert H., et al. Gefährdungspotential bei einem verstärkten Wasserstoffeinsatz. Study for the Büro für Technikfolgenabschätzung des Deutschen Bundestags, Deutsches Zentrum für Luft- und Raumfahrt (DLR), Stuttgart, Germany, 1992.

EIGA. Safety in Storage, Handling and Distribution of Liquid Hydrogen. Report DOC 06/02/E, http://www.eiga.org/pdf/ Doc%2006%2002%20E.pdf , 2002.

ESS. The ESS Project Volume III Update. European Spallation Source Technical Report, Status 27.05.04. http://neutron.neutron-eu.net/n_documentation/n_reports/n_ess_reports_and_more/106 , European Industrial Gases Association, Brussels, Belgium, 2004.

Ewald R. Kryogene Speichertechnik für Flüssigwasserstoff. In *Wasserstoff-Energietechnik, Bilanz – Konzepte – Perspektiven,* VDI Berichte 602, pages 101-117, Verein Deutscher Ingenieure, Düsseldorf, Germany, 1987.

Fay J.A. A Preliminary Analysis of the Effect of Spill Size on the Level of Hazard from LNG Spills on Land and Water. Report No. DOE/EV-0002, US Department of Energy, USA, 1978.

Foldeaki M., et al. Material Selection for Magnetic Refrigerator Design. In *Proc. 7th Canadian Hydrogen Workshop,* pages 439-453, Quebec City, Canada, 1995.

Fukushima Y. and Matsui A. Development of Liquid Rocket Engines for H-II Rocket. In *Proc. International Hydrogen and Clean Energy Symposium IHCE'95*, pages 361-364, Tokyo, Japan, 1995.

Giacomazzi G. and Gretz G. Euro-Quebec Hydro-Hydrogen Project (EQHHPP): A Challenge to Cryogenic Technology. *Cryogenics*, **33:**767-771, 1993.

GM. Fuel Cell Technology for Sustainable Mobility. Company's Brochure, Adam Opel AG, Rüsselsheim, Germany, 2007.

GQ-CEC. Euro-Quebec Hydro-Hydrogen Pilot Project – Phase II, Feasibility Study. Final Report, Vol. I-V, Government of Quebec, Commission of the European Communities, 1991.

Gu L.X., et al. *LH_2 Storage Tanks at KSC.* Project at Florida Solar Energy Center, Cocoa, USA, 2005.

Gugan K. *Unconfined Vapour Cloud Explosions.* The Institution of Chemical Engineers, Rugby, United Kingdom, 1978.

Guthrie E., et al. Infrastructure Developments for Hydrogen, In *Proc. 16th World Hydrogen Energy Conference WHEC'16*, Lyon, France, 2006.

Haidn O.J., et al. Improved Combustion Efficiency of a H_2/O_2 Steam Generator for Spinning Reserve Application. In *Proc. 11th World Hydrogen Energy Conference WHEC'11,* pages 1418-1427, Stuttgart, Germany, 1996.

Hijikata T. Research and Development of International Clean Energy Network Using Hydrogen Energy (WE-NET). *International Journal of Hydrogen Energy,* **27:**115-129, 2002.

Hiraoka K., et al. Energy Analysis and CO_2 Emission Evaluation of a Solar Hydrogen Energy System for the Transportation System in Japan – I. Conceptual Design of the System. *International Journal of Hydrogen Energy,* **16:**631-638, 1991.

Hord J. How Safe is Hydrogen. In *Symposium on Hydrogen for Energy Distribution,* Chicago, USA, 1978.

Horiguchi S., et al. Fire Extinguishment for Liquefied Hydrogen. *Journal of National Chemical Laboratory Industry,* **81**:421-425, 1986

Hottel H.C. Review – Certain Laws Governing Diffusive Burning of Liquids. In Blinov V.I. and Khudiakov G.N. *Fire Research Abstracts and Reviews,* **1**:41-44, 1958.

IAEA. *External Man-Induced Events in Relation to Nuclear Power Plant Siting – A Safety Guide.* Safety Series No. 50-SG-S5, International Atomic Energy Agency, Vienna, Austria, 1981.

IAEA. Mitigation of Hydrogen Hazards in Water-Cooled Power Reactors. Report IAEA-TECDOC-1196, International Atomic Energy Agency, Vienna, Austria, 2001.

Iqbal N. and Salley M.H. Fire Dynamics Tools (FDT^s) Quantitative Fire Hazard Analysis Methods for the U.S. Nuclear Regulatory Commission Fire Protection Inspection Program. Final Report NUREG-1805, Division of System Safety and Analysis, Office of Nuclear Reactor Regulation, U.S. Nuclear Regulatory Commission, Washington DC, USA, 2004.

Iwasaki W. A Consideration of Power Density and Hydrogen Production and Utilization Technologies. *International Journal of Hydrogen Energy,* **28:**1325-1332, 2003.

Krainz G., et al. Development of Automotive Liquid Hydrogen Storage Systems. In *Proc. Cryogenic Engineering Conference and International Cryogenic Materials Conference CEC-ICMC,* Anchorage, USA, 2003.

Krainz G., et al. Anwendungsorientierte Entwicklung von Wasserstoff-Speichersystemen für den automotiven Einsatz. In *Proc. 4th German Hydrogen Congress*, pages 164-168, Essen, Germany, 2008.

Kreiser A.M, et al. Analyse von Störfällen mit Wasserstoff in bisherigen Anwendungs-bereichen mit besonderer Berücksichtigung von LH_2. Report IKE 2-116, Institut für Kernenergetik und Energiesysteme der Universität Stuttgart, Germany, 1994.

Kurioka H., et al. Fire Properties in Near Field of Square Fire Source with Longitudinal Ventilation in Tunnels. *Fire Safety Journal*, **38**:319-340, 2003.

Kusterer H. and Scherf H. HYDROSS – Einsatz von Wasserstoff zur Sofortreservebereit-stellung. In *Proc. Status Seminar Wasserstoff als Energieträger,* pages 95-128, Projektträger Biologie, Energie, Ökologie, Research Center Jülich, Germany, 1995.

LBST. http://www.h2mobility.org/, Ludwig-Bölkow-Systemtechnik, Ottobrunn, Germany, 2008a.

LBST. http://www.h2stations.org/, Ludwig-Bölkow-Systemtechnik, Ottobrunn, Germany, 2008b.

Lind C.D. What Causes Unconfined Vapor Cloud Explosions. *Loss Prevention*, **9:**101-105, 1975.

Lipman T.E. and Delucchi M.A. Hydrogen-Fuelled Vehicles. *International Journal of Vehicle Design,* **17**:562-589, 1996.

Lodhi M.A.K. and Mires R.W. How Safe is the Storage of Liquid Hydrogen? *International Journal of Hydrogen Energy,* **14**:35-43, 1989.

Luketa-Hanlin A. A Review of Large-Scale LNG Spills: Experiments and Modeling. *Journal of Hazardous Materials,* **A132:**119-140, 2006.

Malkov M.P. Industrial Production of Heavy Water. *Atomnaya Energiya,* **7:**101-109, No. 2, 1958.

Marangon A., et al. Safety Distances: Definition and Values. *International Journal of Hydrogen Energy*, **32:**2192-2197, 2007.

Marsh Property Risk Consulting. *The 100 Largest Losses 1972-2001.* 20th Edition, Report OAM-PRC-19-03.01-10M, http://www.marshriskconsulting.com/Load/article_452602.pdf, New York, USA, 2003.

Mei R.W. and Klausner J. Project Title: Chill Down Processes of Hydrogen Transport Pipelines. Report NASA/CR-2006-214091, National Aeronautics and Space Administration, Washington D.C., USA, 2006.

Meratla Z. Large Scale Liquid Hydrogen Transport by Air. In *Proc. 11th World Hydrogen Energy Conference WHEC'11,* pages 1347-1353, Stuttgart, Germany, 1996.

Michel F., et al. Liquid Hydrogen Technologies for Mobile Use. In *Proc. 16th World Hydrogen Energy Conference WHEC'16,* paper 160, Lyon, France, 2006.

Miller A. Heavy Water: A Manufacturers' Guide for the Hydrogen Century. *Canadian Nuclear Society Bulletin,* **22**:1-14, No. 1, 2001.

Miyake H., et al. Studies of Slush Hydrogen. In *Proc. International Hydrogen and Clean Energy Symposium IHCE'95,* pages 223-226, Tokyo, Japan, 1995.

Moorhouse J. and Carpenter R.J. Factors Affecting Vapour Evolution Rates from Liquefied Gas Spills. Report MRS E 460, British Gas, Solihull, United Kingdom, 1986.

Moorhouse J. and Roberts P. Cryogenic Spill Protection and Mitigation. *Cryogenics,* **28:**838-846, 1988.

Müller D. Hydrogen 7: BMW bringt Luxuslimousine mit Wasserstoff-Antrieb. http://www.zdnet.de/enterprise/tech/auto/0,39026506,39147426,00.htm, ZDNet Deutschland Test & Technik, 2006.

Mulready D. *Advanced Engine Development at Pratt & Whitney – The Inside Story of Eight Special Projects 1946-1971.* SAE International, Society of Automotive Engineers, Inc., Warrendale, USA, 2001.

Murase M. R&D Plans for WE-NET (World Energy Network) – Hydrogen and Clean Energy. In *Proc. NEDO International Symposium,* pages 55-64, Tokyo, Japan, 1995.

NASA. Report of the Presidential Commission on the Space Shuttle Challenger Accident (1986). http://science.ksc.nasa.gov/shuttle/missions/51-l/docs/rogers-commission/table-of-contents.html , 1997.

NASA. *NASA Facts.* FS-2001-09-015-KSC, Revised 2006, Kennedy Space Center, USA (2006).

NEDO. International Clean Energy Network Using Hydrogen Conversion (WE-NET). 1995 Annual Summary Report on Results, NEDO-WE-NET, Tokyo, Japan, 1996.

Nellis W. *Jumpin' Jupiter! Metallic Hydrogen.* https://www.llnl.gov/str/Nellis.html, Lawrence Livermore National Laboratory, USA, 1996.

Newi G. and Wienberg G. CH_4 / H_2 Brennstoffzellen in Wohngebieten. In *Wasserstoff-Energietechnik IV,* VDI Berichte No. 1201, pages 73-85, Verein Deutscher Ingenieure, Düsseldorf, Germany, 1995.

NFPA. *NFPA News,* **9**:1-3, December, 2005.

NIST. *Chemistry WebBook.* NIST Standard Reference Database Number 69, June 2005 Release. http://webbook.nist.gov/chemistry/, National Institute of Standards and Technology, Gaithersburg, USA, 2005.

Ogden J. Hydrogen as an Energy Carrier. Presentation at UC Berkeley on November 5, 2004, http://www.its.berkeley.edu/itsreview/ITSReviewonline/winter20042005/ogdenhydrogenppt.pdf , 2004.

Ordin P.M. Review of Hydrogen Accidents and Incidents in NASA Operations. Technical Memorandum NASA TM X-71565, Lewis Research Center, Cleveland, USA, 1974.

Pehr K. Experimentelle Untersuchungen zum Worst-Case-Verhaltenvon LH_2-Tanks für PKW. In *Wasserstoff-Energietechnik IV*, VDI Berichte 1201, pages 57-71, Verein Deutscher Ingenieure, Düsseldorf, Germany, 1995.

Pehr K. Experimental Investigations on the Worst Case Behavior of LH_2/LNG Tanks for Passenger Cars. In *Proc. 11th World Hydrogen Energy Conference WHEC'11,* pages 2169-2186, Stuttgart, Germany, 1996.

Peschka W. *Liquid Hydrogen: Fuel of the Future.* Springer-Verlag Wien New York, 1992.

Petersen U., et al. Design and Safety Considerations for Large-Scale Sea-Borne Hydrogen Transport. *International Journal of Hydrogen Energy,* **19:**597-604, 1994.

Pohl H.-W. and Wildner D. Hydrogen Demonstrator Aircraft. In *Proc. 11th World Hydrogen Energy Conference WHEC'11,* pages 1779-1786, Stuttgart, Germany, 1996.

Prince A.J. Details and Results of Spill Experiments of Cryogenic Liquids onto Land and Water. Report SRD R324, UKAEA, Safety and Reliability Directorate, Culcheth, United Kingdom, 1985.

Quack H. Die Schlüsselrolle der Kryotechnik in der Wasserstoff-Energiewirtschaft. http://www.tu-dresden.de/mwiem/kkt/mitarbeiter/lib/Wasserstoff/wassertech.html, *Klima Luft- und Kältetechnik*, **3:**157-161, 2002.

Regar K.-N., et al. Der neue BMW 735i mit Wasserstoffantrieb. In *Wasserstoff-Energietechnik,* VDI Berichte 725, pages 187-196, Verein Deutscher Ingenieure, Düsseldorf, Germany, 1989.

Reinecke E.-A., et al. Design of Catalytic Recombiners for Safe Removal of Hydrogen from Flammable Gas Mixtures. In *Proc. 2nd International Conference on Hydrogen Safety ICHS-2,* San Sebastian, Spain, 2007.

Rew P.J. and Hulbert W.G. Development of Pool Fire Thermal Radiation Model. HSE Contractor Report WSA/RSU8000/018, Epsom, United Kingdom, 1995.

Rich B.R. Lockheed CL-400 Liquid Hydrogen Fueld Mach 2.5 Reconnaissance Vehicle. *Working Symposium on LH_2 Fueld Aircraft,* NASA Langley Research Center, Hampton, USA, 1973.

Rich B.R. and Janos L. *Skunk Works – A Personal Memoir of my Years at Lockheed.* Warner Books, London, United Kingdom, 1995.

Ringland J.T. Safety Issues for Hydrogen-Powered Vehicles. Report SAND94-8226, Sandia National Laboratory, Albuquerque, USA, 1994.

Schödel J.P. Hydrogen – A Safety Risk? In *Proc. CEC Seminar on Hydrogen as an Energy Vector: Its Production, Use and Transportation,* Report EUR 6085, pages 567-581, Commission of the European Communities, Brussels, Belgium, 1978.

Sherif S.A. Onboard Spacecraft under Normal and Reduced Gravity. Presentation August 12-15, 2003.

Simbeck D. and Chang E. Hydrogen Supply: Cost Estimate for Hydrogen Pathways – Scoping Analysis. Report NREL/SR-540-32525, National Renewable Energy Laboratory, Golden, USA, 2002.

Sittig M. *Cryogenics Research and Applications.* D. van Nostrand Company, Inc., Princeton, USA, 1963.

Sloop J.L. Liquid Hydrogen as a Propulsion Fuel – 1945-1959. NASA History Office, Report NASA SP-4404, National Aeronautics and Space Administration, Washington D.C., USA, 1978.

Specht M, et al. Regenerativer Wasserstoff – Erzeugung, Nutzung und Syntheserohstoff. In *Wasserstoff und Brennstoffzellen – Energieforschung im Verbund*, Themen 2004, pages 33-40, ForschungsVerbund Sonnenenergie, Berlin, Germany, 2004.

SRI. Liquid Hydrogen Production and Commercial Demand in the United States. SRI Project 8562 Final Report. http://ntrs.nasa.gov/archive/nasa/casi.ntrs.nasa.gov/19910006853_1991006853.pdf , SRI International, Menlo Park, USA, 1990.

Stang J., et al. On the Design of an Efficient Hydrogen Liquefaction Plant. In *Proc. 16th World Hydrogen Energy Conference WHEC'16,* paper 324, Lyon, France, 2006.

Stewart W.F. Liquid Hydrogen as an Automotive Fuel. *Advances in Cryogenic Engineering,* paper O-2, Plenum Press, New York, USA, 1980.

Stewart W.F. Operating Experience with a Liquid-Hydrogen Fueled Buick and Refueling System. *International Journal of Hydrogen Energy,* **9:**525-538, 1984.

Stolper A. Erste Erfahrungen aus dem ZEMShips Projekt. In *Proc. 4th German Hydrogen Congress*, pages 153-157, Essen, Germany, 2008.

Takeno K., et al. Evaporation Rates of Liquid Hydrogen and Liquid Oxygen Spilled onto the Ground. *Journal of Loss Prevention in the Process Industries,* **7:**425-431, 1994.

Taylor J.B. Technical and Economical Assessment of Methods for the Storage of Large Quantities of Hydrogen. *International Journal of Hydrogen Energy,* **11:**5-22, 1986.

Trill R. Personal Communication, Linde AG, Höllriegelskreuth, Germany, 1997.

Tupolev. Development of Cryogenic Fuel Aircraft. http://www.tupolev.ru/English/Show.asp?SectionID=82 , Tupolev PSC, Moscow, Russia, 2008.

Tzimas E., et al. Hydrogen Storage: State-of-the-Art and Future Perspective. Report EUR 20995 EN, http://ie.jrc.cec.eu.int/publications/scientific_publications/2003/P2003-81=EUR20995EN.pdf , European Commission, JRC Petten, The Netherlands, 2003.

Urano Y., et al. Hazards of Burning Liquefied Hydrogen – Part 1: Flame of Stable Burning – Part 2: Flame of Abnormal Burning. *National Chemical Laboratory for Industry*, **81:**143-157, 1986. (In Japanese).

US-DOT. Clean Air Programm – Use of Hydrogen to Power the Advanced Technology Transit Bus (ATTB): An Assessment. Report DOT-FTA-MA-26-0001-97-1, US-Department of Transportation, Washington D.C., USA, 1997.

US-NRC. Evaluations of Explosions Postulated to Occur on Transportation Routes Near Nuclear Power Plants. Regulatory Guide 1.91, Revision 1, U.S. Nuclear Regulatory Commission, Rockville, USA, 1978.

Vander Arend P.C. et al. The Liquefaction of Hydrogen. In *Scott R.B. et al. (Eds.). Technology and Uses of Liquid Hydrogen.* Pages 38-105, Pergamon Press Ltd, Oxford, United Kingdom, 1964.

Verfondern K. and Dienhart B. Pool Spreading and Vaporization of Liquid Hydrogen. *International Journal of Hydrogen Energy*, **32:**2106-2117, 2007.

Verfondern K. Hydrogen as an Energy Carrier and its Production by Nuclear Power. Report IAEA-TECDOC-1085, International Atomic Energy Agency, Vienna, Austria, 1999.

Verfondern K., et al. Experimental Investigations and Numerical Modeling on Hydrogen Recombining Devices in Closed Areas. In *Proc. 15th World Hydrogen Energy Conference WHEC'15,* paper 1369, Yokohama, Japan, 2004.

Verfondern K (Ed.). *Nuclear Energy for Hydrogen Production.* Schriftenreihe des Forschungszentrums Jülich, Energy Technology Vol. 58, Jülich, Germany, 2007.

Webber D.M. Source Terms. *Journal of Loss Prevention in the Process Industries,* **4:**5-15, 1991.

WEC. Deciding the Future: Energy Policy Scenarios to 2050 – Executive Summary. *World Energy Council,* London, United Kingdom, 2007.

Wikipedia. Equation of State. http://en.wikipedia.org/wiki/Equation_of_state, 2007.

Wikipedia. Magnetic Refrigeration. http://en.wikipedia.org/wiki/Magnetic_refrigeration, 2008.

Witcofski R.D. and Chirivella J.E. Experimental and Analytical Analyses of the Mechanisms Govering the Dispersion of Flammable Clouds Formed by Liquid Hydrogen Spills. *International Journal of Hydrogen Energy*, **9:**425-435, 1984.

Wolf J. Die neuen Entwicklungen der Technik – Elemente der Wasserstoff-Infrastruktur von der Herstellung bis zum Tank. *Medienforum Deutscher Wasserstoff-Tag,* München, Germany, 2003.

Zabetakis M.G. and Burgess D.S. Research on the Hazards Associated with the Production and Handling of Liquid Hydrogen. Report WADD TR 60-141, Wright Air Development Division, USA, 1960.

Zabetakis M.G., et al. Explosion Hazards of Liquid Hydrogen. *Advances in Cryogenic Engineering*, **6:**185-194, 1961.

Zabetakis M.G. *Safety with Cryogenic Fluids.* Plenum Press, New York, USA 1967.

Zalosh R.G., et al. Compilation and Analysis of Hydrogen Accident Reports. Final Technical Report COO-4442-4, Factory Mutual Research Corporation, Norwood, USA, 1978.

Zuber N. *Hydrodynamic Aspects of Boiling Heat Transfer.* US Atomic Energy Commission, Research Laboratory Los Angeles and Ramo-Wooldridge Corporation, University of California, USA, 1959.

APPENDIX: PHYSICAL AND CHEMICAL PROPERTIES OF HYDROGEN

Parameter		Value	Unit
Molecular weight		2.01594	g/mol
Stoichiometric fraction in air		29.53	vol%
Boiling point (BP)		20.369	K
Melting point (MP)		14.01	K
Triple point (TP)	temperature	13.8	K
	pressure	7.2	kPa
Critical point	temperature	33.145	K
	pressure	1.2964	MPa
	density	31.263	kg/m^3
Electronegativity		2.20	Pauling scale
Density	gas @ NTP [1]	0.08376	kg/m^3
	gas @ STP [2]	0.08990	
	gas @ BP	1.338	
	para liquid @ BP	70.78	
	normal[8] liquid @ BP	70.96	
	slush with 50 mass% solid @ TP	81.48	
	para solid @ MP	86.50	
	solid @ 4 K	88.0	
Expansion ratio liquid/ambient		845	-
Diffusion coefficient @ NTP [1]		$0.61*10^{-4}$	m^2/s
Diffusion velocity @ NTP [1]		< 0.02	m/s
Buoyant velocity		1.2 - 9.1	m/s
Gas constant		4124.3	J/(kg K)
Specific heat (constant p)	gas @ NTP [1]	14.89	kJ/(kg K)
	gas @ STP [2]	14.304	
	gas @ BP	12.15	
	liquid @ BP	9.69	
	slush with 50 mass% solid @ TP	11.4	
Ratio of specific heats c_p/c_v @ NTP		1.308	-
Thermal conductivity	gas @ NTP [1]	0.1897	W/(m K)
	gas @ BP	0.01694	
	liquid @ BP	0.09892	
	solid @ TP	0.90	
Viscosity	gas @ NTP [1]	8.948	µPa s
	gas @ BP	1.079	
	liquid @ BP	13.32	

Parameter	Value	Unit
Surface tension @ BP	$1.92*10^{-3}$	N/m
Vapor pressure normal[8] @ TP para @ TP solid @ 10 K	7200 7040 257	Pa
Para/ortho ratio @ STP @ BP	25 / 75 99.79 / 0.21	%
Inversion temperature @ 0.1 MPa	193	K
Heat of conversion from ortho to para @ BP from normal[8] to para	703[6] 527 - 670[7]	kJ/kg
Heat of melting (fusion) @ MP	58.8	kJ/kg
Heat of vaporization @ BP	445.6	kJ/kg
Vaporization index [3]	8.9	K cm^3/J
Vaporization rate (steady state) of LH_2 pool	4.2 - 8.3 25 - 50[6]	mm/s
Heat of sublimation	379.6	kJ/kg
Speed of sound gas @ NTP [2] in stoichiometric H_2-air mixture in gas @ BP in liquid @ BP	1294 404 355 1093	m/s
Inversion (Joule Thomson) temperature	193	K
Flammability limits in air	4.0 - 75.0 [4]	vol%
Detonability limits in air	13 - 70 [5]	vol%
Minimum ignition energy for detonation	$1.9*10^{-5}$ ~ 10,000	J
Auto-ignition temperature in air	793 - 1023 (858)	K
Hot air jet ignition temperature	943	K
Gross heat of combustion or Higher Heating Value (HHV) @ NTP[1]	141.86 12.75	MJ/kg MJ/m^3
Net heat of combustion or Lower Heating Value (LHV) @ NTP[1]	119.93 10.8	MJ/kg MJ/m^3
Flame temperature (theoretical)	2318	K
Laminar burning velocity air @ stoich. maximum @ 42.5 vol%	2.65 3.46	m/s
Visible laminar flame front velocity	18.6	m/s
Burning rate of LH_2 pool	0.5 - 1.1[6]	mm/s
Deflagration pressure ratio	8.15	-

Parameter	Value	Unit
Quenching distance @ NTP (1)	0.64	mm
Maximum experimental safe gap @ NTP(1)	0.08	mm
Adiabatic flame temperature	2318	K
Emission coefficient	< 0.1	-
Detonation velocity	1480 - 2150	m/s
Chapman-Jouguet (CJ) velocity	1968	m/s
CJ detonation pressure ratio p_{CJ}/p_0	15.6	-
Energy release	2.82	MJ/kg mixture
Detonation cell size	15	mm
Critical tube diameter	0.2	m
Detonation initiation energy	1.1	g tetryl(9)
Detonation induction distance @ NTP (1)	length/diameter ~ 100	
TNT equivalent	26.5	kg TNT/kg

(1) NTP (Normal temperature and pressure): 293 K, 101325 Pa.
(2) STP (Standard temperature and pressure): 273 K, 101325 Pa.
(3) Indicates the relative ease of a substance to vaporize.
(4) LFL is valid for upward propagation of flame. For downward propagation, LFL is 5.3 vol%.
(5) Valid for weak ignition. For a high-energy igniter, a range of 11.6 - 74.9 was quoted.
(6) according to [NASA 1997]
(7) according to [Tzimas 2003]
(8) "normal" hydrogen = 75 % ortho + 25 % para
(9) Formula: $C_7H_5N_5O_8$; IUPAC name: 2,4,6-trinitrophenyl-N-methylnitramine

ACKNOWLEDGEMENT

The author wishes to express his gratitude to valuable comments by

Frank Markert
Ernie Reinecke
Ulrich Schmidtchen
Michael Stöcklin

and to excellent drawings by

Sigrid Reiche-Begemann

1. **Einsatz von multispektralen Satellitenbilddaten in der Wasserhaushalts- und Stoffstrommodellierung – dargestellt am Beispiel des Rureinzugsgebietes**
   von C. Montzka (2008), XX, 238 Seiten
   ISBN: 978-3-89336-508-1

2. **Ozone Production in the Atmosphere Simulation Chamber SAPHIR**
   by C. A. Richter (2008), XIV, 147 pages
   ISBN: 978-3-89336-513-5

3. **Entwicklung neuer Schutz- und Kontaktierungsschichten für Hochtemperatur-Brennstoffzellen**
   von T. Kiefer (2008), 138 Seiten
   ISBN: 978-3-89336-514-2

4. **Optimierung der Reflektivität keramischer Wärmedämmschichten aus Yttrium-teilstabilisiertem Zirkoniumdioxid für den Einsatz auf metallischen Komponenten in Gasturbinen**
   von A. Stuke (2008), X, 201 Seiten
   ISBN: 978-3-89336-515-9

5. **Lichtstreuende Oberflächen, Schichten und Schichtsysteme zur Verbesserung der Lichteinkopplung in Silizium-Dünnschichtsolarzellen**
   von M. Berginski (2008), XV, 171 Seiten
   ISBN: 978-3-89336-516-6

6. **Politikszenarien für den Klimaschutz IV – Szenarien bis 2030**
   hrsg.von P. Markewitz, F. Chr. Matthes (2008), 376 Seiten
   ISBN 978-3-89336-518-0

7. **Untersuchungen zum Verschmutzungsverhalten rheinischer Braunkohlen in Kohledampferzeugern**
   von A. Schlüter (2008), 164 Seiten
   ISBN 978-3-89336-524-1

8. **Inorganic Microporous Membranes for Gas Separation in Fossil Fuel Power Plants**
   by G. van der Donk (2008), VI, 120 pages
   ISBN: 978-3-89336-525-8

9. **Sinterung von Zirkoniumdioxid-Elektrolyten im Mehrlagenverbund der oxidkeramischen Brennstoffzelle (SOFC)**
   von R. Mücke (2008), VI, 165 Seiten
   ISBN: 978-3-89336-529-6

10. **Safety Considerations on Liquid Hydrogen**
    by K. Verfondern (2008), VIII, 167 pages
    ISBN: 978-3-89336-530-2

Band | Volume 10
ISBN 978-3-89336-530-2

JÜLICH
FORSCHUNGSZENTRUM